# *IN VITRO* AND PRE-CLINICAL EVALUATION OF ANTI-METASTATIC ACTIVITY OF PHLORIDZIN DOCOSAHEXAENOATE (PZ-DHA) VERSUS TRIPLE-NEGATIVE BREAST CANCER

by

T R G Wasundara Fernando

Submitted in partial fulfilment of the requirements
for the degree of Doctor of Philosophy

at
Dalhousie University
Halifax, Nova Scotia
August 2018

***For my Amma and Thaththa with love..***

***"There's a way to do it better – find it."***

*-Thomas A. Edison*

## TABLE OF CONTENTS

## LIST OF TABLES

## LIST OF FIGURES

## ABSTRACT

The World Health Organization identifies breast cancer as the most common cancer among women worldwide. Triple-negative breast cancer (TNBC) lacks receptors for estrogen (ER), progesterone (PR), and human epidermal growth factor 2 (HER2); therefore, TNBC does not respond to hormone- or HER2-targeted therapy. Even though TNBC responds initially to chemotherapy, these cells eventually develop resistance to chemotherapy and metastasize to distant organs. Therefore, research is continued to identify novel remedies to treat TNBC more effectively. Phloridzin docosahexaenoate (PZ-DHA) is a novel polyphenol fatty acid ester derivative that combines a flavonoid precursor compound known as phloridzin (PZ) with an omega-3 fatty acid known as docosahexaenoic acid (DHA) through an acylation reaction catalyzed by lipase B enzyme extracted from *Candida antarctica*. The current project was designed to investigate the pharmacokinetic parameters, anti-proliferative, anti-metastatic, and anti-angiogenic activities of PZ-DHA using *in vitro*, *ex-vivo* and *in vivo* models of breast cancer. PZ-DHA improved the cellular uptake of PZ and intracellular stability of DHA. PZ-DHA was absorbed following intraperitoneal administration into Balb/c female mice and underwent phase I and II metabolism. PZ-DHA and its metabolites were readily distributed throughout the body. PZ-DHA was selectively cytotoxic to mammary carcinoma cells, including TNBC cells (MDA-MB-231, MDA-MB-468, 4T1), and showed minimum cytotoxic activity against non-malignant cells (MCF-10A mammary epithelial cells and human dermal fibroblasts). Sub-cytotoxic concentrations of PZ-DHA attenuated the proliferation of MDA-MB-231 cells by arresting the cell cycle at $G_2$/M, and inhibiting protein kinase B (Akt) and mitogen activated protein kinase signaling. PZ-DHA inhibited the migration, invasion, TGF-β-induced small molecular Rho GTPase signaling, and expression of transcription factors (β-catenin, Slug and ZEB1) involved in epithelial-to-mesenchymal transition. Furthermore, PZ-DHA inhibited the expression of MMP2 and increased E-cadherin levels in MDA-MB-231 cells. Intraperitoneal administration of PZ-DHA inhibited the growth and metastasis of orthotopically implanted 4T1 and MDA-MB-231 cells to the lungs of Balb/c and NOD-SCID female mice, respectively, as well as suppressing the expression of Ki67, MMP2 and CD31in primary tumors. Sub-cytotoxic concentrations of PZ-DHA suppressed the proliferation of human umbilical vein endothelial cells (HUVEC) and human microvascular endothelial cells (HMVEC), and arrested HUVECs at $G_0/G_1$. Furthermore, PZ-DHA blocked tube formation by HUVECs and HMVECs *in vitro*, and vessel sprouting by thoracic aortic sections harvested from Wistar rats. PZ-DHA-induced inhibitory effects on Akt and vascular endothelial growth factor ($VEGF_{165}$)-stimulated Rho GTPase signaling in HUVECs was also documented. Intraperitoneal administration of PZ-DHA inhibited angiogenesis within $VEGF_{165}$- and basic fibroblast growth factor (bFGF)-containing Matrigel plugs implanted into Balb/c female mice, confirming anti-angiogenic activity of PZ-DHA. These findings provide strong evidence for PZ-DHA-mediated inhibition of TNBC cell metastasis by inhibiting multiple aspect of the process; therefore, PZ-DHA shows promise as a therapeutic agent to inhibit the progression of TNBC in patients.

## LIST OF ABBREVIATIONS AND SYMBOLS USED

| | |
|---|---|
| × g | gravity |
| 7-AAD | 7-Aminoactinomycin |
| Ab | Antobodies |
| ABC | ATP binding cassette |
| ADME | Absorption, Distribution, Metabolism and Excretion |
| AGS | Angiostatin |
| Akt | Protein kinase B |
| ALT | Alanine transaminase |
| ANOVA | Analysis of variance |
| AP | Activator protein |
| ATCC | American Type Culture Collection |
| ATP | Adenosine triphosphate |
| AUC | Area under the curve |
| Bcl-2 | B-cell lymphoma 2 |
| BCRP | Breast cancer resistant protein |
| bFGF | basic-Fibroblast growth factor |
| BRCA | Breast cancer gene |
| BSA | Bovine serum albumin |
| CA-LB | *Candida antarctica* lipase B |
| Caspase | Cysteine-dependent aspartate-directed proteases |
| CD | Cluster of differentiation |
| Cdc | Cell division cycle |
| CDK | Cyclin-dependent kinase |
| $C_{max}$ | Maximum serum concentration |
| CREB | cAMP response element-binding protein |
| CRE | cAMP response elements |
| CTC | Circulating tumor cells |
| CYP | Cytochrome P |
| DCIS | Ductal carcinoma insitu |
| DDC | DNA diagnostic center |

| | |
|---|---|
| DHA | Docosahexaenoic acid |
| DMEM | Dulbecco’s Modified Eagle’s Medium |
| DMSO | Dimethylsulfoxide |
| DNA | Deoxyribonucleic acid |
| E-cadherin | E type calcium-dependent adhesion |
| EDTA | Ethylenediaminetetraacetic acid |
| EGCG | Epigallocatechin gallate |
| EGF | Epidermal growth factor |
| EGFR | Epidermal growth factor receptor |
| EGM | Endothelial growth medium |
| EGTA | Ethylene glycol-bis(β-aminoethyl ether)-N,N,N',N'-tetraacetic acid |
| ELK | ETS domain-containing protein |
| ECM | Extracellular matrix |
| EMT | Epithelial-to-mesenchymal transition |
| ER | Estrogen receptor |
| ERK | Extracellular signal–regulated kinase |
| ESI | Electrospray ionization |
| FACS | Fluorescence-activated cell sorting |
| FANCM | Fanconi anemia complementation group M |
| FBS | Fetal bovine serum |
| FL | Filter |
| FLT | Fms-like tyrosine kinase |
| FSC-H | forward scatter |
| $G_0/G_1$ | $Gap_0/Gap_1$ phase |
| $G_2$/M | $Gap_2$/mitosis phase |
| GLUT | Glucose transporters |
| GRB2 | Growth factor receptor-bound protein 2 |
| GSK3β | Glycogen synthase kinase 3 β |
| GST | Glutathione S-transferases |
| GTP | Guanosine-5'-triphosphate |
| h | hour/hours |
| HBSS | Hanks' Balanced Salt Solution |

| | |
|---|---|
| HDF | Human dermal fibroblasts |
| HEPES | 4-(2-hydroxyethyl)-1-piperazineethanesulfonic acid |
| HER2 | Human epidermal growth factor receptor 2 |
| HIF | Hypoxia-inducible factor |
| HMVEC | Human microvascular endothelial cells |
| HPLC | High performance liquid chromatography |
| HRE | Hypoxia response element |
| HRP | Horse radish peroxidase |
| HUVEC | Human umbilical vein endothelial cells |
| IGF | Insulin growth factor |
| IL | Interleukin |
| JAK | Janus kinase |
| KDR | Kinase insert domain receptor |
| $K_e$ | Elimination constant |
| LCIS | Luminal carcinoma insitu |
| LDH | Lactic Acid Dehydrogenase |
| LPH | Lactase-phlorizin hydrolase |
| M | Molar |
| MAPK | Mitogen-activated protein kinase |
| MAPKK | Mitogen-activated protein kinase kinase |
| MAPKKK | Mitogen-activated protein kinase kinase kinase |
| MEK | MAPK/ERK kinase |
| MET | Mesenchymal-to-epithelial transition |
| min | minute/minutes |
| MMP | Matrix metalloproteinases |
| MS | Mass spectrometry |
| MT | Methyltransferases |
| mTOR | Mammalian target of rapamycin |
| MTS | Inner salt of 3-(4,5-dimethylthiazol-2-yl)-2,5-diphenyltetrazolium bromide |
| MTT | 3-(4,5-dimethylthiazol-2-yl)-2,5-diphenyltetrazolium bromide |
| MW | Molecular weight |
| NADH | Nicotinamide adenine dinucleotide |

| | |
|---|---|
| NAT | N-acetyltransferases |
| N-cadherin | N type calcium-dependent adhesion |
| NF-κB | Nuclear factor kappa-light-chain-enhancer of activated B cells |
| NMR | Nuclear magnetic resonance |
| NOD-SCID | Non-obese diabetic severe combined immune-deficient |
| OD | Optical density |
| PALB2 | Partner and localizer of BRCA2 |
| PAPS | 3'-phosphoadenosine-5'-phosphosulfate |
| PBS | Phosphate buffered saline |
| PDGF | Platelet-derived endothelial growth factor |
| PDK1 | Phosphoinositide-dependent kinase-1 |
| PFA | Paraformaldehyde |
| Pgp | P-glycoprotein |
| PI | Propidium iodide |
| PI3K | Phosphoinositide 3-kinase |
| PIP2 | Phosphatidylinositol 4,5-bisphosphate |
| PIP3 | Phosphatidylinositol (3,4,5)-trisphosphate |
| PMS | Phenazine methosulfate |
| PPB | Potassium phosphate buffer |
| PR | Progesterone receptor |
| PT | Phloretin |
| PTEN | Phosphatase and Tensin Homolog |
| PZ | Phloridzin |
| PZ-DHA | Phloridzin docosahexaenoate |
| Rb | Retinoblastoma |
| RNA | Ribonucleic acid |
| ROCK | Rho-associated protein kinase |
| ROS | Reactive oxygen species |
| RT | Retention time |
| RTK | Receptor tyrosine kinase |
| S | Synthesis phase |
| SAM | S-adenosylmethionine |

| | |
|---|---|
| SDS | Sodium dodecyl sulfate |
| Sec | Second/seconds |
| SEM | Standard error mean |
| Ser | Serine |
| SGLT | Sodium/glucose co-transporter |
| SIM | Single ion monitoring |
| SOS | Sons of sevenless |
| SSC-H | Side scatter |
| STAT | Signal transducer and activator of transcription |
| SULT | Sulfotransferases |
| $T_{1/2}$ | Time to reduce serum drug concentration by half |
| TEMED | Tetramethylethylenediamine |
| TGF-β | Transforming growth factor β |
| TGF-βR | Transforming growth factor β receptor |
| Thr | Threonine |
| TIE | Angiopoietin receptor |
| $T_{max}$ | Time to reach the highest serum drug concentration |
| TNBC | Triple-negative breast cancer |
| TNF-α | Tumor necrosis factor α |
| TSP | Thrombospodin |
| TXL | Paclitaxel |
| Tyr | Tyrosine |
| UDPGA | UDP-glucuronic acid |
| UGT | UDP-glucuronosyltransferases |
| UPLC | Ultra Performance Liquid Chromatography |
| v/v | Volume by volume |
| v/w | Volume by weight |
| VE-cadherin | Vascular endothelial type calcium-dependent adhesion |
| VEGF | Vascular endothelial growth factor |
| ZEB | Zinc Finger E-Box Binding Homeobox |

## ACKNOWLEDGEMENTS

I distinctly remember the very first day I learned about "research", during one of my Grade-six science classes. Later that day in the afternoon, my mother tried her best to help me to understand more about it, even though she was not a scientist. I was extremely fascinated by her words and I believe in that afternoon she planted the first seed in my mind, which later grew into a huge tree that inspired me to become a researcher. I found my strong interest in cancer research when I was 17 years-old, and ever since an enormous number of people have helped me to reach my goals. Today, in my doctoral thesis, I want to thank all of them for their kindness and love.

I would like to recognize the pain that cancer patients have been through and are still going through. I also want to recognize the pain suffered by their families/friends due to the loss of loved-ones including me and my family who grieved in the pain of losing one of our family members while I was writing this thesis. I believe in a cancer-free future and I hope research will continue to meet that goal.

This thesis would not have been possible without the help, support and guidance that came at the perfect time from many valuable individuals. First, my supervisor, Dr. David Hoskin, it is not just science and research that I learned from you, but many more life lessons that I will take with me where ever life takes me. Thank you for giving me many opportunities to learn more. I have definitely become a better person and a better researcher under your supervision. A huge thank to you for teaching me to think critically and see the bright side of everything. You always had something good to say to me, even when I brought you the worst news about an experiment such as, "*Dr. Hoskin, my animal experiment didn't work!* :(". Your immense knowledge, critical thinking, patience, understanding, friendly and calm personality made the perfect environment for me to complete this project with success.

Second, my co-supervisor Dr. Vasantha Rupasinghe. I can not thank you enough for introducing me to cancer research during my MSc program which was a dream coming true for me and I wanted to use it as an opportunity to build a strong foundation for this PhD project. Thank you very much for putting up with my strange hours in the Truro lab with late nights and week-ends. Your thoughtfulness, patience, guidance, vast knowledge and willingness to experiment new research aspects made it extremely easy to progress smoothly with everything I wanted to do during this project.

I would like to extend my sincere gratitude to my supervisory committee members, Dr. Paola Marcato, Dr. Kerry Goralski and Dr. David Waisman. Thank you for being

available whenever I needed your support and sometimes offering it even before I ask. Your continuous and constructive inputs have made my project a successful and exciting story. I have enjoyed working with you.

I owe a huge thank you to all past and present Hoskinites! It has been a wonderful journey! No words can express how much I value all of you. You have made every single day, an exciting day to come to the lab and work with full of energy. Thank you for warmly welcoming me to the lab and offering your support and help when I needed it the most! Thank you for laughing with me, crying with me and for being there for me. I want to thank my mentor, Dr. Melanie Coombs for setting up the perfect role-model for me in the lab. Sometimes, I tried to be like you! Thank you for teaching me cell culture, animal experiments, helping me with my writing, and for being patient to answer my questions. Thank you, Dr. Anna Greenshields, for everything you have done. Anna, you have been a caring friend, a sister and a teacher to me and I always enjoyed your company. Thank you for holding my hand whenever I felt insecure and helping me to gain my confidence and stay strong! Thank you, Javad Ghassemi-Rad for helping me with my assays and staying in late nights to help me to finish my animal experiments. I am sure the pictures you took made some of my *in vivo* thesis figures amazing! Thank you, Dr. Carolyn Doucette, Dr. Laurence Madera, Leanne Delaney, Alicia Malone, Andrea Rasmussen, Joe Loung, Emma MacLean, Mary Foley, Taylor Thorburn, Nathan Farias, Dr. Jordan Warford, Dan Arsenault, and Allison Knickle for helping with my project and making our lab a pleasant and nice place to work.

A big thank to all the past and present members in the Rupasinghe lab! Thank you Dr. Ziaullah for your amazing work in synthesizing PZ-DHA and I also want to thank Dr. Sandhya Nair for helping me with getting started with cancer research. Thank you for warmly welcoming (back) whenever I was in the Truro lab to try my new experiments. Thank you Niroshaathevi Arumuggam, Niluni Wijesundara, Madumani Amararathna, Wasitha Thilakarathna, Kithma de Silva, Tennille Crossman and Satvir Sekhon-Loodu for your support and help when I was in Truro. Your smiles made long days less tiring. Thank you, Niro, Dushanthi Sampath, Chamara Jayasinghe, Marco Medina, Jyoti Joshi, Madumani and Niluni for delicious food.

I want to thank Cancer Research Training Program (CRTP) of Beatrice Hunter Cancer Research Institute (BHCRI) for awarding me with a CRTP trainee award and funding my doctoral program through funds from the Terry Fox Research Institute, Canadian Breast Cancer Society, Dalhousie Medical Research Foundation and Canadian Imperial Bank of Commerce. I also would like to thank BHCRI for all the opportunities I was given to

learn more about cancer research. Many thanks to Canadian Breast Cancer Foundation, Canadian Cancer Society and Natural Sciences and Engineering Research Council for providing operating funding for my project. A huge thank to the Department of Pathology and Department of Microbiology and Immunology at Dalhousie University for your support during past few years.

I want to thank Eva Rogerson, Pat Colp, Dr. Dharini Bharadwaj, Nick Relja, Mary Ann Trevors, Stephen Whitefield, Dr. Krysta Coyle and the staff in the Carlton Animal Care Facility for technical support and advice during several experiments of my project. Life in Tupper was amazing and thanks to everyone for the laughs and giggles that we shared. Special thanks to Dr. Jason McDougall, Holly and Anusha for providing rat aortas for my experiments.

Thank you, Louise Primeau and Tyler Leblanc, for your care and support at home. I am sorry if I disturbed you with late night cooking and studying. You made a wonderful home for me for the past few years. I thank you so much, Faye Bradley (Faye mom) for being my mother since I came to Canada. Your love, caring words and hugs gave me feelings of home and you are one of the strongest people I have ever met in my life. Thank you for welcoming me into your family and making me a part of it. Thank you, Gwen Gero, Sterling Gero, Shirley Bradley (my secret sister), Judy Nelson, Keith Bradley and Katherine Bradley for being the sisters and brothers of my new home. A huge thank to all my friends who helped me in countless different ways; you all mean a lot to me.

Last, but most certainly not least, my family ♥; Amma, Thaththa, sister-Narmada, brother-Deeghayu and brother-in-law-Kapil. You are my EVERYTHING! It is nothing, but your love that kept me going through thick and thin. Honestly, this thesis would not have been possible had it not been for your eternal, unconditional love and care. Thank you for believing in me and patiently waiting for me. I faced many devastating life experiences during my doctoral studies; but you held my hand and gave me strength and courage to complete my work. A very special thank to my mother and father for teaching me the best lesson that I have learned in my life; "*Stay strong despite the difficulties and be determined until you reach your goals*".

# CHAPTER 1 : INTRODUCTION

## 1.1 Cancer

According to World Health Organization, cancer is the second leading cause of deaths worldwide and the global cancer burden is expected to rise to 21.7 million new cancer cases and 13 million cancer-caused deaths by the year 2030 (WHO, 2018). Cancer is a collection of diseases driven by wide genomic abnormalities such as aberrant and constitutive signaling of cell proliferation, growth and survival. Therefore, cancers are often self-sufficient and characterized by uncontrolled-cell division and potential to spread to other parts of the body (Hanahan and Weinberg, 2000). Cancer is a leading cause of deaths in Canada; it was estimated 80,800 cancer-related deaths would occur in the year 2017 (Canadian Cancer Statistics, 2017a). Cancer statistics are continuously growing, and 206,200 new cancer cases were expected in Canada in 2017. Lung, breast, colorectal and prostate are the most common cancers in Canada; these cancers account for 50% of all new cancer cases (Canadian Cancer Statistics, 2017a).

In the year 2000, Hanahan and Weinberg detailed six biological capabilities that a cancer acquires during its development (Hanahan and Weinberg, 2000). The scope of this concept was expanded by introducing 2 emerging and 2 enabling additional capabilities in 2011 (Hanahan and Weinberg, 2011). Currently, these are recognized as “Ten hallmarks of cancer”; namely, sustained proliferative signaling, evasion of growth suppressors, invasion and metastasis, replicative immortality, angiogenesis, resistance to cell death, avoidance of immune destruction, tumor-promoting inflammation, genome instability and mutation, and deregulation of cellular energetics (Hanahan and Weinberg, 2000, 2011). The history of cancer research includes many discoveries over the past century; however, during the past two decades, remarkable contributions have been made in light of the influence of cancer hallmark identification on recent advances in cancer research (Burney and Al-Moundhri, 2008; Chap and Patel, 2011; Weinstein and Case, 2008).

## 1.2 Breast cancer

Breast cancer is a malignancy that originates from the epithelial cells of mammary ducts (Polyak, 2011). It is the leading type of cancer among women worldwide and the leading disability-adjusted life-years as well (Fitzmaurice et al., 2015). Breast cancer also affects men (Yalaza et al., 2016); however, the female gender is one of the top-established breast cancer risk factors (Anothaisintawee et al., 2013). Breast cancer is responsible for 13% of cancer-associated deaths among Canadian women; it was estimated that 26,300 Canadian women would be diagnosed with breast cancer and 5,000 would die from the disease in 2017 (Canadian Cancer Statistics, 2017a).

Breast cancer is an extremely heterogenous disease (Polyak, 2011; Rivenbark et al., 2013; Song et al., 2016; Turashvili and Brogi, 2017). This heterogeneity is the result of multiple clinical and histopathological forms. Heterogeneity is observed among patients (inter-tumor heterogeneity), as well as within a patient (intra-tumor heterogeneity). Clinically, breast cancer is categorized into stages I-IV. Stage I is benign and restricted to breast tissue while stage IV represents the most advanced and aggressive metastatic stage. Biomarker heterogeneity of breast cancers is based on the expression of estrogen receptor (ER), progesterone receptor (PR) and human epidermal growth factor receptor 2 (HER2) (Rivenbark et al., 2013; Turashvili and Brogi, 2017). Differential expression of these biomarkers provides the base for molecular subtype classification of breast cancers (Cancer Genome Atlas Network, 2012; Eroles et al., 2012).

### 1.2.1 Breast cancer sub-types

Breast cancer is divided into 6 different subtypes (luminal A, luminal B, HER2-enriched, basal-like, claudin-low and normal breast-like) based on the expression patterns of molecular markers such as ER, PR, HER2, p53 and the proliferation marker Ki67 (Eroles et al., 2012; Goldhirsch et al., 2011; Voduc et al., 2010). In addition to different gene expression profiles, breast cancer subtypes demonstrate substantial differences in the regulation of cell cycle checkpoints, responses to chemotherapy, and metastatic patterns. Bower et al. (2017) suggest that breast cancer cells grown in culture show defects in DNA synthesis and subsequent $G_2$/M transition, regardless of the subtype. Luminal B breast cancer cells show impairment of the decatenation $G_2$ checkpoint while basal-like

breast cancer cells show defects in the spindle assembly checkpoint. Both of these defects are related to the $G_2$/M checkpoint, even though distinct from each other at the molecular level (Bower et al., 2017). Claudin-low breast cancer cells and basal-like breast cancer cells show chromatin cohesion defects (Bower et al., 2017). Carey et al. (2007) suggest that patients suffering from HER2-enriched and basal-like (ER-, PR- and HER2-) breast cancers show the greatest initial clinical response to anthracycline-based chemotherapy when compared to luminal breast cancer; however, these two subtypes show the worst distant disease-free survival and overall survival. The poor prognosis of HER2-enriched and basal-like breast cancers is due to relapse with residual disease (Carey et al., 2007). The metastatic pattern and local relapse vary considerably among breast cancer subtypes. The luminal A subtype has the best prognosis and lowest rate of regional relapse and metastasis. With the breast conservation therapy, HER2-enriched and basal-like tumors show an increased risk of regional recurrence. Luminal B, HER2-enriched and basal-like breast caners exhibit an elevated risk of local and regional relapse following mastectomy (Voduc et al., 2010). A study conducted by Kennecke et al., (2010) using archived data of breast cancer patients between 1986-1992 suggests that breast cancer for the most part spreads to the bones, regardless of disease subtype. Luminal A and HER2-enriched breast cancers are associated with brain, liver and lung metastases. Basal-like breast cancers show a significantly higher rate of secondary metastasis to the brain and lungs and reduced metastasis to the liver and bones (Kennecke et al., 2010).

### 1.2.2 Triple-negative breast cancer

Triple-negative breast cancer (TNBC) is an aggressive type of breast cancer with poor prognosis which accounts for 15-20% of all invasive breast cancers (Khalifa et al., 2016; Pistelli et al., 2013). TNBC cells show a negative pattern for ER, PR and HER2 (similar to basal-like subtype) staining in immunohistochemistry; therefore, TNBC patients do not benefit from endocrine therapy or HER2-targeted therapy. This lack of targets leaves TNBC patients who relapse following chemotherapy with only limited treatment options (Hudis and Gianni, 2011; Rampurwala et al., 2016; Santuario-Facio et al., 2017). Recurrent TNBC is often associated with aggressive metastasis and death. In addition, TNBC patients experience early onset of the disease and typically have a family history

of breast cancer, suggesting a possible linkage to multiple genetic mutations (Hahnen et al., 2017). The many genetic susceptibilities to TNBC include highly penetrant, germline mutations in breast cancer susceptibility gene 1 and 2 (BRCA1 and BRCA2). In fact, 70% and 20% of women who carry mutations in BRCA1 and BRCA2, respectively, develop breast cancers showing triple negative phenotype (Foulkes et al., 2010). TNBC is also associated with rarely mutated breast cancer predisposition genes such as partner and localizer of BRCA2 (PALB2) and Fanconi anemia complementation group M (FANCM) (Cybulski et al., 2015; Easton et al., 2015; Kiiski et al., 2014).

### 1.3 TNBC chemotherapy

Although the treatment of early-diagnosed cancers is associated with a better outcome, the cost of cancer treatment is extremely high regardless of the disease stage. A survey conducted by de Oliveira and colleagues suggest that the cost of cancer care in Canada was $ 2.9 billion in 2005 and it rose steadily, leading to a cost of $ 7.5 billion in 2012. Most of the expenses are associated with chemotherapy and radiation therapy (de Oliveira et al., 2018). The prognosis of hormone receptor-positive breast cancers and HER2-positive breast cancer is satisfactory, as these two types of cancers respond to ER- and HER2-targated therapies, respectively (Callahan and Hurvitz, 2011; Lumachi et al., 2013). However, treatment of TNBC still relies on surgical procedures and non-specific chemotherapeutic strategies such as anthracyclines or taxanes (André and Zielinski, 2012) and/or a combination of all these approaches along with radiation therapy (Yagata et al., 2011). Although TNBC cells lack the therapeutic targets of ER or HER2, the suitability of other potential targets has been evaluated. In fact, anti-vascular endothelial growth factor (VEGF) therapy, anti-transforming growth factor (TGF)-β treatment, TGF-βRIII-targeted therapy, fibroblast growth factor (FGF)-targeted therapy, and poly(ADP-ribosyl)ation polymerase (PARP)-targeted therapy have been investigated (Bhola et al., 2013; Dent, 2009; Jovanović et al., 2014; Pal and Mortimer, 2009; Sharpe et al., 2011). Taking a different approach, another study shows that targeting DNA double strand repair mechanisms may be a promising approach to the treatment of TNBC (Song et al., 2013). In the search for novel treatment targets in TNBC, the phosphoinositide 3-kinase (PI3K)/ protein kinase B (Akt)/ mammalian target of rapamycin (mTOR) signaling pathway has received distinct attention. PI3K/Akt/mTOR-targeted therapies have now

progressed to phase II clinical trials and show promise as a treatment modality for TNBC (Dey et al., 2017). p53 mutations are frequently observed in TNBC (Dang and Peng, 2013; Davion et al., 2012). Another growing area of research relating to therapy for TNBC is p53-targeted treatment (Synnott et al., 2017). The combination of afore-mentioned therapies is also being developed as treatment for metastatic TNBC (Turner et al., 2013).

## 1.4 Phytochemicals

Plant secondary metabolites (also known as phytochemicals) are not essential for plant cell metabolism and basic physiological functions such as growth, respiration and reproduction (Campos-Vega and Oomah, 2013; Jenzer Bern and Sadeghi Bern, 2016; Zhao et al., 2005). Phytochemicals form an extremely heterogenous group and are found in relatively low abundance compared to primary substances that are necessary for plant cell metabolism and function (Bourgaud et al., 2001). The majority of phytochemicals exhibit strong colors and/or fragrances. Multiple functions of phytochemicals have been identified. For example, they serve as a defense against pathogens, insects and herbivores, and function as metal transporting agents, agents of symbiosis, sexual hormones and differentiation effectors (Bennett and Wallsgrove, 1994; Bourgaud et al., 2001; Waterman, 2007; Zhao et al., 2005). The wide-ranging roles of phytochemicals in plants have fueled an interest in investigating them for potential benefits for human health. Phytochemicals are categorized into many sub-groups that include alkaloids, polyphenols, saponins, tannins, terpenoids and thiols (Campos-Vega and Oomah, 2013; Jenzer Bern and Sadeghi Bern, 2016).

Beneficial effects and mechanisms of action of phytochemicals in the prevention and treatment of chronic diseases such as cancer, cardiovascular disease, diabetes and neurodegenerative diseases have been extensively studied (George et al., 2017; Guhr and Lachance; Heneman, 2008; Kumar Mukhopadhyay et al., 2012; Leitzmann, 2016; Liu, 2003; Rao and Ali, 2007; Zhang et al., 2015a). Phytochemicals mediate their biological activities by modulating oxidative stress, gene function regulation, gap-junction communication, hormone and immune modulation, carcinogen metabolism, and alteration of metabolic pathways by inducing phase II enzymes (Rao and Ali, 2007). In

spite of the fact that phytochemicals are increasingly being accepted as health-promoting agents, their clinical applications are limited due to reduced bioavailability resulting from poor cellular uptake and interactions with other food components at the absorption site (Abourashed, 2013; Epriliati and Ginjom, 2012; Holst and Williamson, 2008; Phan et al., 2016). Therefore, much recent phytochemical-related research is focused on increasing phytochemical bioavailability and/or phytochemical delivery to target tissues (Aqil et al., 2013; Wang et al., 2014a).

## 1.5 Flavonoids and ω-3 fatty acids

### 1.5.1 Flavonoids

Even though flavonoids show potent activity against many types of cancer *in vitro* and *in vivo*, a major limitation to their clinical application is their poor penetration through biological barriers. Three different approaches that have been used to improve the cellular uptake and bioavailability of flavonoids are discussed in the subsequent sections of this chapter.

#### 1.5.1.1 Methylation of flavonoids

Methylation of flavonoids has been reported by many research groups to improve bioavailability and/or bioactivity (Koirala et al., 2016; Wen and Walle, 2006). For example, *O*-methylation at the free hydroxyl groups and *C*-methylation at the carbon skeleton dramatically increases the metabolic stability of flavonoids and chalcones (Koirala et al., 2016) (Figure 1.1). Methylation improves the bioavailability of flavonoids by increasing their lipophilicity and, interestingly, in some cases the pharmacological activities remain unchanged following methylation. For example, 7-*O*-methylation of genistein does not alter the anti-cancer and anti-angiogenic activities of genistein; however, daidzein shows better anti-cancer activity following similar methylation (Koirala et al., 2015). Methylated-derivatives of 7,8-dihysroxyflavone and 7-hydroxy-8-methoxyflavone show improved and prolonged anti-oxidant and cytoprotective activities in human umbilical vein endothelial cells (HUVECs) when compared to the parent flavone (Koirala et al., 2014). Similarly, 3'-*O*-methylquercetin shows increased antioxidant activity by increasing quercetin retention in human plasma (Manach et al., 1998). Methylation causes the hydroxyl groups of flavonoids to become unavailable for

any further phase II conjugation reactions (i.e., glucuronidation and sulphation). This increases their metabolic stability and improves intestinal absorption as well (Walle, 2009). Wen and Walle, (2006) report that the depletion of 7-hydroxyflavone, chrysin, and apigenin as glucuronides and sulphides is significantly greater than their respective methylated-derivatives, 7-methoxyflavone, 5,7-dimethoxyflavone and 5,7,4'-trimethoxyflavone, in the presence of pooled human liver S9 fractions (Wen and Walle, 2006). Furthermore, methylation also increases the transport of 7-hydroxyflavone, chrysin, and apigenin across Caco-2 intestinal cells, suggesting enhanced potential for intestinal absorption (Wen and Walle, 2006).

#### 1.5.1.2 Incorporation of flavonoids into emulsions

Another method of improving the bioavailability and the shelf life of flavonoids is their incorporation into emulsions (Munin and Edwards-Lévy, 2011), which improves their bioavailability without making modifications to the chemical structure of flavonoids. Studies show that encapsulation of flavonoids into micro/nano-emulsions improves their stability and bioavailability as a topical application. For example, when incorporated into emulsions, quercetin and 3-*O*-methylquercetin show similar absorption through pig ear skin; interestingly, permeation through the skin is higher when the emulsion surface is positively-charged (Fasolo et al., 2009). Akhtar et al. (2014) noted that rutin (quercetin-3-rutinoside) is successfully incorporated into the internal aqueous phase of a water-in-oil-in-water (W/O/W) emulsion, resulting in improved droplet size of the emulsion. Incorporation of flavonoids into emulsions has been performed using pure flavonoid compounds, as well as plant extracts containing flavonoids. O/W emulsion of an extract containing polyphenols from *Hippophae rhamnoides* and *Cassia fistula* shows satisfactory anti-oxidant activity and improved shelf life, suggesting its suitability for topical application (Khan et al., 2013a). In addition, the incorporation of quercetin alone, as well a quercetin-rich ethanolic extract of *Achyrocline satureioides*, into an emulsion preserves the anti-oxidant activity quercetin, and results in a higher accumulation in pig skin when applied as an emulsion of extract compared to an emulsion of pure quercetin (Zorzi et al., 2016). Since the antioxidant activity of flavonoids is preserved and improved in emulsions, this method is used as an alternative method of enhancing the

emulsion system stability by preventing lipid oxidation (Luo et al., 2011; Rupasinghe and Yasmin, 2010; Yang et al., 2015a; Zorzi et al., 2016).

#### 1.5.1.3 Enzyme-catalyzed acylation of flavonoids

Enzyme-catalyzed acylation is a well practiced approach to improving the physicochemical properties of flavonoids. However, it is important to assure that the biological activities of the flavonoids are not compromised by the structural modification introduced by acylation. This is achieved by preserving regioselectivity during the transformation (Chebil et al., 2006; De Oliveira et al., 2009). The acylation of flavonoids is catalyzed by various enzymes. Lipase B enzyme from *Candida antarctica* (CA-LB) is an excellent biocatalyst that is associated with higher regioselectivity (Katsoura et al., 2006; Poojari and Clarson, 2009; Ziaullah et al., 2013). Acylation of flavonoid glycosides occurs with all lipases and subtilisin; however, flavonoid aglycone acylation is possible only with *Pseudomons cepacia* lipase and carboxylesterase (Chebil et al., 2006). Further mechanisms and details on the acylation of flavonoids using fatty acids as acyl donors will be detailed in Section 1.10.

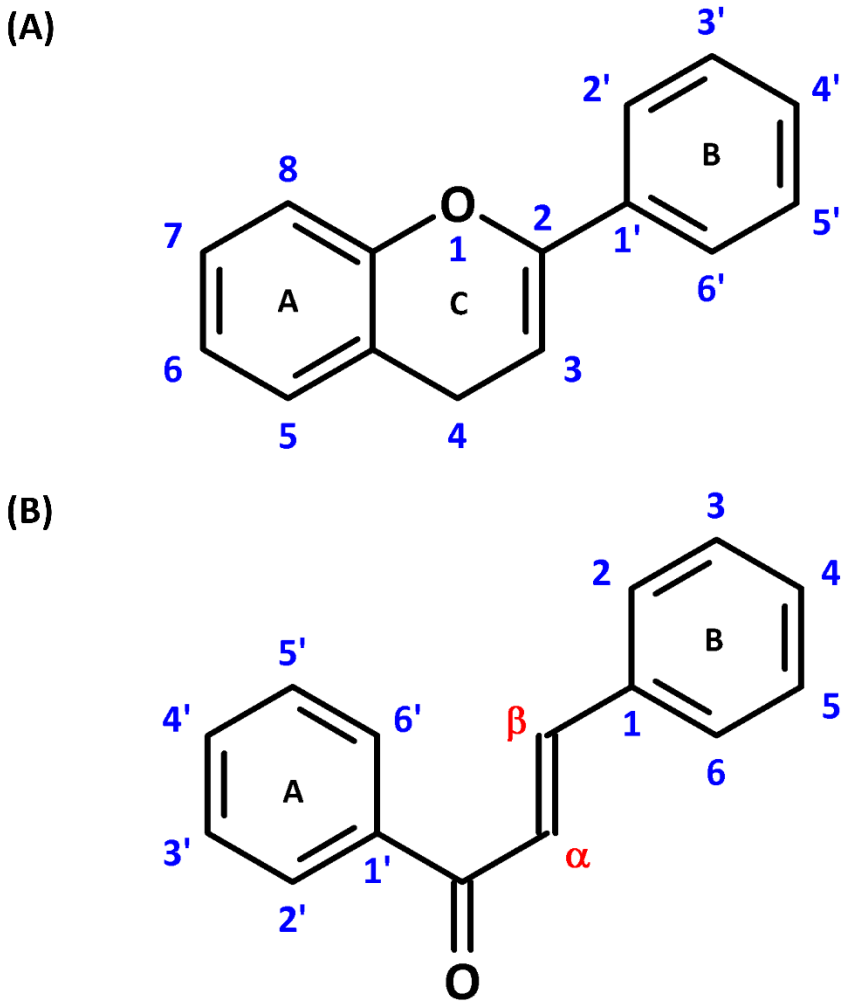


**Figure 1.1. Basic carbon skeleton of flavonoids and chalcones**
**(A)** The basic carbon skeleton of flavonoids is composed of the ring A, ring B and the three-carbon bridge at the middle forming ring C. **(B)** The middle ring C is partially closed with or without the $C_{\alpha}$-$C_{\beta}$ double bond in chalcones. $C_3$, $C_4$, $C_{2'}$, $C_{4'}$ and $C_{6'}$ are considered as the most potential sites to undergo conjugation reactions in chalcones.

## 1.6 Pharmacokinetics

Pharmacokinetics is a distinct branch of pharmacology that is dedicated to understanding absorption, distribution, metabolism and excretion (ADME) of drugs and xenobiotics (Benet, 1993). The importance of pharmacokinetics in relation to flavonoids and ω-3 fatty acids are discussed below.

### 1.6.1 Bioavailability

Bioavailability is one of the principle pharmacokinetic parameters that refers to the fraction of administered drug dose available in the systemic circulation in its un-changed form (Griffin et al., 2013). Flavonoids mainly exist as glucosides in plants; their bioavailability following oral administration has been studied extensively (Pikulski and Brodbelt, 2003; Xiao, 2017). The bioavailability of dietary flavonoids is not impressive, mainly due to their rapid metabolism and poor cellular uptake (Jiang and Hu, 2012). Orally administered flavonoid glycosides are readily hydrolysed by lactase phloridzin hydrolase (LPH) enzyme in the brush-border of the small intestine (Day et al., 2000a) or by other lipases produced by gut microflora (Bokkenheuser et al., 1987). This initial hydrolysis favors the intestinal uptake of flavonoids by decreasing their hydrophilicity; however, free-flavonoids are highly susceptible to phase II conjugation reactions when compared to glycosides (Nemeth et al., 2003). Dietary intake of different flavonoid subgroups shows varying degrees of absorption and bioavailability. In general, the bioavailability of isoflavones is the greatest among all flavonoid subfamilies. Flavanols and flavanones show intermediate bioavailability while the absorption and bioavailability of anthocyanins and proanthocyanidins is extremely poor (Viskupičová et al., 2008). Another parameter that affects the bioavailability of flavonoids is related to efflux transporters. Studies suggest that flavonoids serve as substrates for ATP-binding cassette (ABC) transporters such as P-glycoprotein (Pgp), multi-drug resistant protein2 (MRP2) and breast cancer resistant protein (BCRP) (An et al., 2011; Jiang and Hu, 2012; Liu et al., 2002; Petri et al., 2003). Efflux of flavonoids thorough these transporters further reduces their bioavailability.

### 1.6.2 Phase I metabolism

The metabolism of most drugs/xenobiotics begins with phase I biotransformation (often referred as intermediary metabolism). Phase I reactions include *de novo* formation or exposure of functional groups on drugs/xenobiotics, resulting in increased hydrophilicity and/or polarity. These reactions are governed by cytochrome-p450 (CYP450) acting as monooxygenases, dioxygenases and hydrolases (Omiecinski et al., 2011; Zanger and Schwab, 2013). There are 18 mammalian CYP450 families that encode 57 genes in human genome (Nebert et al., 2013; Zanger and Schwab, 2013). Despite of the existence of many CYP450 families, only CYP1, CYP2, CYP3 and CYP4 family genes are responsible for encoding enzymes involved in drugs/xenobiotics metabolism, hence other 14 gene families are involved in the metabolism of endogenous compounds such as amino acids, steroids, and bile acids (Lewis, 2003; Nebert et al., 2013; Zanger et al., 2008). CYP450 enzymes catalyze either detoxification and/or bioactivation of drugs/xenobiotics by hydrolysis, reduction, *N*- and *O*-dealkylation, aliphatic and aromatic hydroxylation, *N*- and *S*-oxidation, and deamination (Matsuo et al., 2008; Omiecinski et al., 2011). CYP450 enzymes are mainly located in the endoplasmic reticulum of hepatocytes; however, they are widely distributed in other tissues such as intestine and kidneys (Omiecinski et al., 2011). The metabolism of drugs/xenobiotics by hepatic microsomal CYP450 enzymes is coupled with an electron donor enzyme known as NADPH–cytochrome P450 oxidoreductase; hence, phase I biotransformation reactions are NADPH-dependent (Riddick et al., 2013).

### 1.6.3 Phase II metabolism

Phase II metabolism processes drugs/xenobiotics into easily excretable forms; therefore, phase II reactions (also known as conjugation reactions) play a leading role in detoxifying transformations (Jancova and Siller, 2012; Jancova et al., 2010). However, the resulting conjugates of phase II metabolism may also be more toxic metabolites or more potent forms of the parent drug. Phase II metabolizing enzymes are mostly transferases such as methyltransferases (MTs), UDP-glucuronosyltransferases (UGTs), sulfotransferases (SULTs), N-acetyltransferases (NATs) and glutathione S-transferases (GSTs) (Jancova and Siller, 2012).

### 1.6.4 Pharmacokinetics of flavonoids and their derivatives

Pharmacokinetics of flavonoids is a complex field of study. There are well-established and widely-accepted principles related to the pharmacokinetics of flavonoids; nevertheless, significant controversy exits regarding flavonoid metabolism and absorption.

CYP450 enzymes induce the oxidation and hydroxylation of drugs/xenobiotics; thus, phase-I reactions increase the hydrophilicity of substances. Therefore, phase I reactions are considered as essential transformations prior to phase II reactions. However, it is well recognized that flavonoids are capable of directly undergoing phase II conjugation reactions without the need for CYP450-mediated pre-preparation (Jiang and Hu, 2012). Oliveira et al. (2002) report that quercetin and kaempferol undergo UGT isoform, UGT1A9-mediated phase II glucuronidation reactions, and absorption through the intestinal epithelium in the glycoside form (Oliveira et al., 2002). Quercetin and luteolin undergo regioselective phase II glucuronidation in the presence of rat and human liver and intestinal microsomes (Boersma et al., 2002); however, Day et al. (2000) suggest that the site of glucuronidation largely affects the biological activity of the resulting conjugates. Phloretin (PT), a flavonoid found in apples and apple-derived products, undergoes phase II glucuronidation and sulphation reactions and excreted in the urine of male Wistar rats. In contrast, the absence of unchanged, or conjugated metabolites of its glucoside, phloridzin (PZ), in the plasma following oral administration suggests rapid hydrolysis of PZ, resulting in PT (Crespy et al., 2001). A sub-group of flavonoids, epicatechins and catechins produce *O*-methylated- and glucuronidated- metabolites following perfusion into rat intestinal tissues (Kuhnle et al., 2000). Donovan et al. (2001) suggest that such methylation is also possible in the rat liver. Walle (2009) suggests that methylated-flavonoids are metabolically stable and do not undergo further conjugation reactions. In contrast, three isoforms of *O*-methylated chalcones, flavokawains (flavokawain A, B and C) continue to produce metabolites through phase I hydroxylation and phase II glucuronidation in the presence of human liver microsomes, suggesting that further conjugation may be possible when additional hydroxyl groups are introduced (Zenger et al., 2015). The pharmacokinetics and metabolism of flavonoids has been

studied widely; however, to the best of my knowledge, the pharmacokinetics or the metabolism of novel flavonoid derivatives is not reported in the literature.

### 1.6.5 Pharmacokinetics of ω-3 fatty acids

In this section, the pharmacokinetics of ω-3 fatty acid is outlined, giving specific attention to docosahexaenoic acid (DHA). ω-3 fatty acids possess many health benefits, including anti-cancer activities, and play a role in growth and development of crucial tissues in the brain, retina, testis and ovaries (Esmaeili et al., 2015; Innis, 2007; Nehra et al., 2012; Querques et al., 2011). DHA, an ω-3 fatty acid, is readily absorbed by cells (D'Eliseo and Velotti, 2016; Glatz and van der Vusse, 1996); however, little is known about its stability in cells. Park et al. (2016) showed that DHA is available in MCF-7, human breast cancer cells and HepG2, human liver cancer cells at 24h post-treatment (Park et al., 2016). A phase I randomized clinical trial conducted including 42 adult males showed that the area under the curve ($AUC_{0-72}$) for DHA is lower in the before meal condition in comparison to the after meal condition, suggesting that the absorption of DHA is dependent on the timing of its administration relative to food intake (Shimada et al., 2017). ω-3 fatty acids serve as substrates for CYP450 enzymes (phase I metabolism); therefore, the metabolism (hydroxylation and epoxidation) of ω-fatty acids, including DHA, is mainly mediated through several isoforms of CYP450 (Arnold et al., 2010). Fer et al. (2008) reported that DHA functions as an alternative substrate in arachidonic acid metabolism by two isoforms of CYP family 4 enzymes, CYP4F2 and CYP4F3B. These authors suggest that the physiological activities of DHA may be attributed to the synthesis of active hydroxylated metabolites (Fer et al., 2008a). Another study from the same group shows that DHA is effectively epoxidised by CYP2C9, CYP2C19 and CYP1A2 (Fer et al., 2008b). Furthermore, an early study conducted by VanRollins and co-workers shows that in the presence of rat liver microsomes, DHA undergoes hydroxylation, epoxidation and lipoxygenase-like hydroxylation, suggesting the involvement of CYP450 monooxygenases in the phase I metabolism of DHA (VanRollins et al., 1984). The excretion patterns of DHA are not well discussed in literature. One study suggests that the lipid peroxidation-derived products produced following administration of DHA to osteogenic disorder shionogi rats undergoes

conjugation with glutathione in the liver and is excreted as mercapturic acid in urine (Sekine et al., 2007).

## 1.7 Cell proliferation and cytotoxicity

### 1.7.1 Breast cancer cell proliferation

Like any other malignant cell type, breast cancer cells multiply uncontrollably. The uncontrolled division of cancer cells is explained by the collective contribution of four hallmarks outlined by Hanahan and Weinberg (2000). Firstly, the self sufficiency in growth signals or sustained proliferation signals within the tumor cells leads to continuous cell proliferation. Secondly, cancer cells evade growth suppressors by being refractory to anti-growth signals. Thirdly, the replicative immortality of cancer cells, allows them to proliferate limitlessly. Finally, cancer cells evade apoptosis by resisting cell death signals.

Production of new daughter cells by cell division is strictly controlled by the kinases which regulate the progression of a cell through the cell cycle. Therefore, the major events of the cell cycle, DNA replication, mitosis and mitotic exit, take place once per cycle. The cell cycle is composed of 4 phases, gap 0 ($G_0$), gap 1 ($G_1$), synthesis (S), gap 2 ($G_2$) and mitosis (M) (Israels and Israels, 2000). A cell in $G_0$, the resting phase of the cell cycle, enters the $G_1$ phase when it is ready to undergo cell division. The transition of a cell through the cell cycle is mediated through the action of cyclins and cyclin-dependent kinases (CDKs) specific to each phase; the activation of the CDK cascade is regulated by transcriptional and non-transcriptional mechanisms (Cho et al., 2001; Dominguez-Sola et al., 2007; Mester and Redeuilh, 2008; Romanel et al., 2012). Type D cyclin-activated CDK4 and CDK6 initiate the formation of Cyclin D-CDK4 and/or cyclin D-CDK6 complexes, leading to the completion of $G_1$ phase by a cell. Cyclin D1 and E serve as the early response proteins to treatment which regulate the proliferation of breast cancer cells (Caldon et al., 2006). Recent studies show that the inhibition of CDK4/6 is an attractive target to control the growth of ER+ breast cancer cells (Finn et al., 2009, 2015; Mayer, 2015). The irreversible transition of cells from one phase to the next is controlled by positive-feedback loops; this concept is explained as *"all-or-nothing switch into mitosis"* by O'Farrell in 2001 (O'Farrell, 2001). As such, CDK-induced post translational

inhibition of its inhibitors (e.g., Wee1) and stimulation of stimulators (e.g., Cdc25) leads to the activation of cyclin-CDK complexes and fuels the progression of the cell through the entire cell cycle (O'Farrell, 2001; Romanel et al., 2012). Preparation of a cell for S phase DNA synthesis begins at the end of the $G_1$ phase; the cyclinA-CDK2 and/or cyclinE-CDK2 complex mediates DNA replication machinery of the cell following S-phase entry (Woo and Poon, 2003). Bi et al. (2015) demonstrated that the inhibition of cyclinE-CDK2 and cyclinA-CDK2 complex formation controls the proliferation of ER+ MCF-7 and T-47D breast cancer cells (Bi et al., 2015). In addition, loss or deletions of endogenous CDK inhibitors such as retinoblastoma (Rb), $p16^{INK4}$, $p21^{WAF1}$, and $p27^{KIP1}$ are commonly seen in breast cancer cells, suggesting an uncontrolled $G_2$ entry of these cells and activation of cyclinB-CDK1 complex (Fernández et al., 1998). The proliferation of ER+ breast cancer cells is mainly regulated through the phosphorylation of hormone receptors following binding of estrogen (Gross and Yee, 2002). Insulin-like growth factor (IGF)-driven proliferation is observed in most of the breast cancer cells, regardless of the molecular subtype (Christopoulos et al., 2015; Mester and Redeuilh, 2008; Yang and Yee, 2012; Yerushalmi et al., 2012). Therefore, IGF receptor-mediated activation of downstream PI3K/Akt/mTOR and mitogen-activated protein kinase (MAPK) signaling pathways is responsible for the proliferation of many breast cancer subtypes (Elumalai et al., 2014; Gooch et al., 1999; Voudouri et al., 2015).

### 1.7.2 Signaling pathways involved in breast cancer cell proliferation and survival

#### 1.7.2.1 PI3K/Akt/mTOR pathway

Among the many pathways that are actively involved in breast cancer cell proliferation, PI3K/Akt/mTOR signaling receives special attention as a potential target for novel therapies. The PI3K/Akt/mTOR pathway also plays an important role in endocrine resistance of breast cancers (Araki and Miyoshi, 2018; Hasson et al., 2013; Nicolini et al., 2015). Activation of PI3K/Akt/mTOR signaling pathway induces cell proliferation, survival and protein synthesis (Figure 1.2); therefore, over activation of this pathway is observed in many cancer types (Khan et al., 2013b; Pópulo et al., 2012). The PI3K/Akt/mTOR pathway is activated *via* trans-membrane receptors such as integrins, cytokine receptors, G-protein coupled receptors, and B and T cell antigen receptors;

however, aberrant Akt signaling in cancer cells is mainly mediated through receptor tyrosine kinases (RTK) (Arcaro and Guerreiro, 2007; Fruman et al., 2017; Juntilla and Koretzky, 2008; New et al., 2007; Wu et al., 2016a). The binding of a growth factor molecule to the extracellular domain of the RTK induces receptor dimerization and sends signals to the intracellular domain. Following heterogeneous auto-phosphorylation of receptor monomers at the intracellular domain, the intracellular docking site is activated and PI3K is recruited to the docking site (Hubbard and Miller, 2007; Ullrich and Schlessinger, 1990). Binding of PI3K to phosphorylated RTK *via* p85 regulatory subunit activates PI3K-mediated synthesis of phosphatidylinositol-3,4,5-trisphosphate (PIP3) from phosphatidylinositol-4,5-bisphosphate (PIP2) (Fruman, 2010; Jimenez et al., 2002). PIP3 functions as a membrane-bound docking site for proteins such as Akt that contain a pleckstrin-homology (PH)-domain. Akt is then translocated to the plasma membrane and phosphorylated by phosphoinositide-dependent kinase-1 (PDK1) (Blind et al., 2014; Hay and Sonenberg, 2004; Khan et al., 2013b). Following phosphorylation of Akt at Ser473 and Thr308, several downstream signaling molecules are activated, one of which is mTOR. Phosphorylation of mTOR at Ser2448 induces the proliferation and survival of cells *via* p70S6 (Chiang and Abraham, 2005). PTEN (Phosphatase and Tensin homolog) acts as a negative regulator of PI3K/Akt/mTOR signaling by buffering PI3K-induced PIP3 production; therefore, PTEN is lost in many cancers. PTEN reverses the conversion of PIP2 to PIP3 and thereby inhibits the progression of Akt signaling (Chalhoub and Baker, 2009; Georgescu, 2010).

#### 1.7.2.2 MAPK pathway

The MAPK pathway is another well-characterized pathway that regulates mammalian cell proliferation. There are three major MAPK signaling cascades; extracellular signal-regulated kinase (ERK), p38 MAPK and Jun N-terminal kinase (JNK) (Widmann et al., 1999; Zhang and Liu, 2002). All three MAPK are activated by growth factors and cytokines; p38 MAPK and JNK also mediate stress-induced cellular responses (León-González et al., 2015). MAPK cascades are composed of at least three proteins (MAPKKK: MAPK kinase kinase, MAPKK: MAPK kinase and MAPK); the successive activation of these proteins leads to critical cellular events such as cell proliferation, differentiation, inflammation, stress response and apoptosis (Zhang and Liu, 2002). In

general, activation of ERK1/2 sends mitogenic signals to induce cell proliferation and survival. However, some studies show that the activation of ERK results in apoptosis signals that induce cell death (Mebratu and Tesfaigzi, 2009). Tang et al. (2002) suggest that the activation of ERK1/2 following minor damage to DNA causes cell cycle arrest in order to promote DNA repair whereas extensive DNA damage-induced ERK1/2 activation stimulates apoptosis (Tang et al., 2002). Since the scope of the current project is to evaluate the anti-proliferative effects of test compounds at a sub-cytotoxic concentration at which only minor DNA damage is likely, the role of ERK on cell proliferation is discussed. Activation of ERK signaling is initiated by binding of a growth factor to the extracellular domain of RTK. Activated RTK undergoes receptor dimerization and membrane-bound GTPase (RAS) protein communicates with the intracellular domain of RTK *via* growth factor receptor-bound protein 2 (GRB2) and son of sevenless protein (SOS). Activated RAS acts on downstream signaling molecules that activate the three proteins of the ERK cascade; MAPKKK: rapidly accelerated fibrosarcoma protein 1 (RAF1), MAPKK: MAPK/ERK kinase (MEK) and MAPK: ERK1/2. All three of these proteins interact with the scaffolding protein, kinase suppressor of RAS (KSR) (Mebratu and Tesfaigzi, 2009; Morrison, 2001; Raabe and Rapp, 2002). Activated ERK1/2 then translocates into the nucleus; in the nucleus, the transcription factor ELK is activated, leading to cell proliferation (Mebratu and Tesfaigzi, 2009). Persistent activity of ERK1/2 is essential for the progression of cells through $G_1$; however, rapid inactivation of ERK1/2 is required at the $G_1$/S transition (Meloche, 1995; Yamamoto et al., 2006).

### 1.7.3 *In vitro* and *in vivo* anti-proliferative and cytotoxic activity of flavonoids and their derivatives

Anti-proliferative activity of flavonoids as well as flavonoid-rich plant extracts is a widely studied topic. Flavonoid-induced growth inhibitory effects have been demonstrated using *in vitro* cell cultures as well as animal models of various cancers. Flavonoids exert these anti-proliferative activities through several mechanisms, including inhibition of the kinase activity of cell proliferation and survival pathway proteins and/or stimulation of signaling pathways involved in cell death and apoptosis (Amawi et al., 2017; Batra and Sharma, 2013; Brownson et al., 2002; Zhu et al., 2015). Interestingly,

some flavonoid-induced cytotoxic and anti-proliferative effects are selective toward malignant cells (Chiang et al., 2006). These aspects are detailed in this section.

Quercetin, a well-known plant flavanol, inhibits the proliferation of HA22T and VGH human hepatocellular carcinoma cells by arresting cell cycle progression at S phase (Chang et al., 2009). Furthermore, reactive oxygen species are involved in the quercetin-induced death of hepatocellular carcinoma cells and a potential synergistic activity of quercetin during its concurrent use with paclitaxel (Chang et al., 2009). Quercetin suppresses the proliferation of MDA-MB-231 human TNBC cells by arresting the cell cycle at $G_0/G_1$ phase through the JNK/FoxO3a axis (Nguyen et al., 2017). Triantafyllou et al. (2007) reported that quercetin stabilizes hypoxia inducible factor-1 α (HIF1α) in HeLa human cervical cancer cells, although cell proliferation is inhibited *via* ion-chelation (Triantafyllou et al., 2007). Quercetin also increases HIF1α expression in HepG2 cells and decreases cell proliferation by increasing the expression of CDK inhibitor $p21^{WAF}$ in a HIF1α-dependent manner (Bach et al., 2010). PT selectively inhibits the proliferation of MDA-MB-231 breast cancer cells without causing cytotoxic effects to MCF-10A non-malignant mammary epithelial cells. PT-induced inhibition of glucose transporters (GLUT2) in MDA-MB-231 cells stimulates cell cycle arrest. An inhibitory effect of PT on the MDA-MB-231 xenograft growth in Balb/c nude mice has also been reported (Wu et al., 2018). In agreement with these findings, our previous work suggests that intra-tumoral administration of the aglycone of PZ, PT inhibits MDA-MB-231 xenograft growth in non-obese severe-combined immune deficient (NOD-SCID) (Fernando et al., 2016). Apigenin, another dietary flavonoid, selectively inhibits the growth of HepG2, Hep3B, and PLC/PRF/5 human hepatocellular carcinoma cells, but not BNL CL.2 normal mouse hepatocytes, and induces the apoptosis of HepG2 cells and increases accumulation of cells in the $G_2$/M phase through a $p53/p21^{WAF}$ related mechanism (Chiang et al., 2006). Another study suggests that apigenin induces the apoptosis of SW480 human colorectal cancer cells and suppresses the growth of GFP transfected-SW480 xenografts in Balb/c nude male mice (Wang et al., 2011). The cytotoxic effect of apigenin on tamoxifen- and fulvestrant-resistant MCF-7 cells suggests an inhibitory activity against drug-resistant cells (Long et al., 2008). Similar to quercetin, apigenin also acts synergistically with paclitaxel to kill HeLa cervical cancer cells, A549

human lung epithelial carcinoma cells, and Hep3B liver cancer cells (Xu et al., 2011). Quercetin inhibits the growth of MCF-7 breast xenografts in Balb/c nude mice and promotes tumor necrosis (Zhao et al., 2016). Nelson and Falk (1993) report that intraperitoneal administration of PT and PZ inhibits the growth of mouse mammary carcinoma cells grown in Fisher 344 female rats (Nelson and Falk, 1993). Morin, a flavonoid that shows anti-oxidant and anti-cancer activities, inhibits Akt signaling in MDA-MB-231 breast cancer cells and suppresses MDA-MB-231 xenograft growth in athymic nude mice (Jin et al., 2014). Chalcones, a group of flavonoid precursors, inhibit the growth of MCF-7 and MDA-MB-231 breast cancer cells by arresting these cells at $G_2$/M phase of the cell cycle (Hsu et al., 2006). Chalcone compounds have also been widely subjected to chemical modifications to create derivatives that are biologically more potent. A series of chalcone and bis-chalcone derivatives produced by Modzelewska and co-workers by incorporating boronic acid moieties, selectively inhibit the growth of MDA-MB-231 and MCF-7 cells without harming non-malignant MCF-10A and MCF-12A mammary epithelial cells (Modzelewska et al., 2006). Another series of heteroaryl chalcone derivatives show increased-anti-cancer activity toward MDA-MB-231 and MDA-MB-468 TNBC cells; this activity is 3-7-fold higher on cancer cells in comparison to normal cells (Solomon and Lee, 2012).

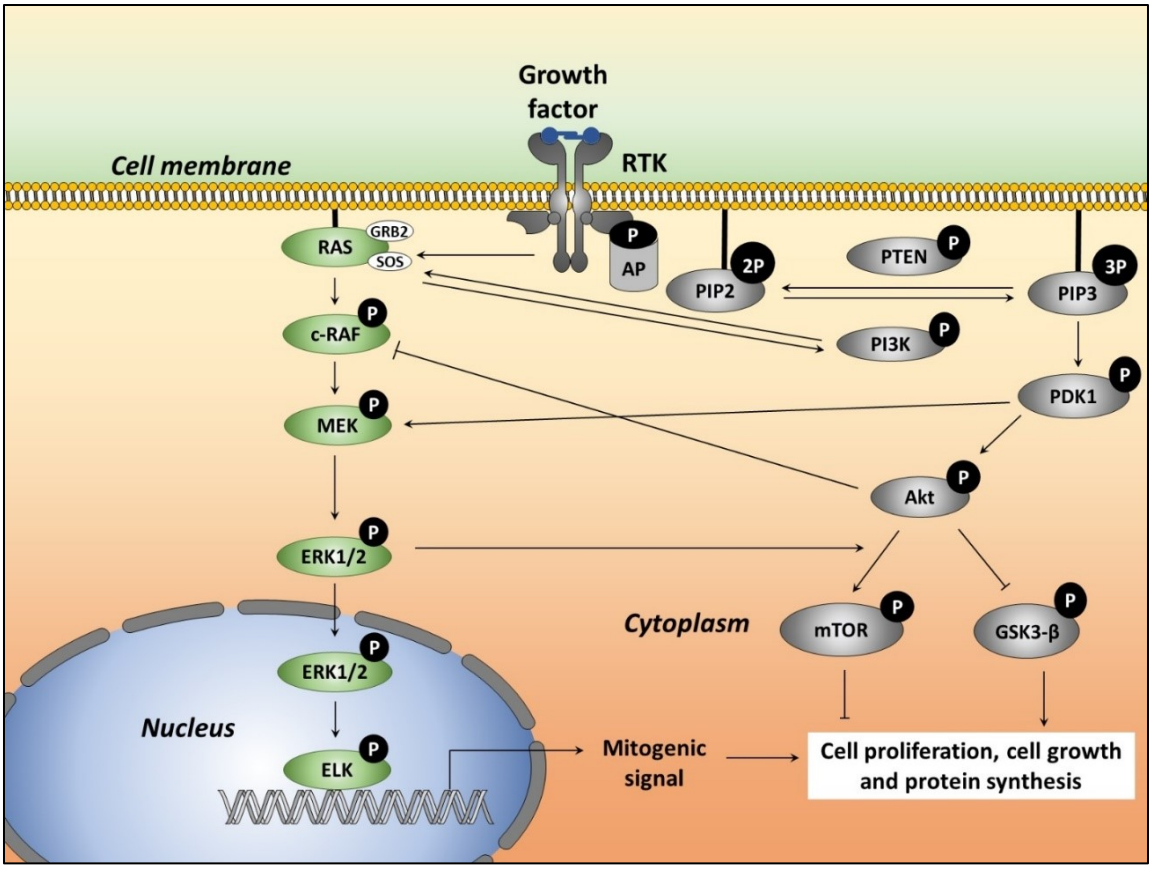


**Figure 1.2. PI3K/Akt/mTOR and MAPK pathways and their crosstalk.**
**Akt**: protein kinase B; **AP**: activator protein; **c-RAF**: proto-oncogene serine/threonine-protein kinase; **ELK**: Ets-like protein-1; **ERK**: extracellular signal-regulated kinase; **GRB2**: growth factor receptor-bound protein 2; **GSK3-β**: glycogen synthase kinase 3-β; **MEK**: mitogen-activated protein kinase kinase; **mTOR**: mammalian target of rapamycin; **PDK1**: phosphoinositide-dependent kinase-1; **PI3K**: phosphoinositide 3-kinase; **PIP2**: phosphatidylinositol-4,5-bisphosphate; **PIP3**: phosphatidylinositol-3,4,5-trisphosphate; **PTEN**: phosphatase and tensin homolog; **RAS**: small molecular GTPase family proteins; **RTK**: receptor tyrosine kinase; **SOS**: son of sevenless.

## 1.8 Metastasis

### 1.8.1 Breast cancer metastasis and signaling pathways involved in breast cancer metastasis

Metastatic disease is the most advanced stage of cancer and it is responsible for about 90% of cancer related-deaths (Chaffer and Weinberg, 2011; Seyfried and Huysentruyt, 2013). Metastasis is a two-phased process and each phase is composed of several interrelated-steps. During the first phase of metastasis, cancer cells become disseminated from a primary cancer site and translocate to a distant site; the second phase begins with the initiation of secondary metastatic lesions by the proliferation of translocated cancer cells (Chaffer and Weinberg, 2011). The breast cancer metastatic cascade is composed of several vital steps; the failure to complete any of these steps blocks metastasis (Figure 1.3). During this process, several changes take place in the cancer cells that allow cancer cells to increase their motility (Olson and Sahai, 2009). One such well-recognized processes is known as epithelial-to-mesenchymal transition (EMT); this process is detailed in Section 1.8.2. The motile breast cancer cells that detach from the primary tumor initiate the metastatic cascade. Migration of detached cells through the basement membrane and the ECM is facilitated by the proteolytic activity of matrix metalloproteinases (MMPs), cathepsins and plasmin secreted by cancer cells, as well as the stromal cells in the tumor microenvironment (Andreasen et al., 2000; Gialeli et al., 2011; Kessenbrock et al., 2010; Rabbani and Mazar, 2001; Tan et al., 2013; Withana et al., 2012). The disseminated cancer cells are carried throughout the body by lymph and blood vessels (Paduch, 2016). Pro-angiogenic factors secreted by cancer cells and stromal cells induce the formation of new blood vessels around the growing tumor; this process is known as angiogenesis. Motile, aggressive cancer cells invade the tumor-associated blood vessels *via* a process known as intravasation (Chiang et al., 2016). Tumor cells in the circulation (circulating tumor cells: CTC) survive by evading anoikis and travel to distant organs to initiate secondary metastases. Breast cancer mainly metastasizes into the bones, lungs, liver and brain (Kimbung et al., 2015; Scully et al., 2012). Studies suggest that the sites of secondary relapse of breast cancer are pre-programmed through distinct mechanisms. These mechanisms involve the communication of CTC-bound ligands with their respective receptors located in the pre-metastatic niches at the secondary site

(Valastyan and Weinberg, 2011). At the secondary site, CTCs undergo extravasation and re-establish the epithelial phenotype through mesenchymal-to-epithelial transition (MET), followed by initiation of cell proliferation to generate micrometastases (Yao et al., 2011a).

Given the complexity of the breast cancer metastatic process, it follows that metastasis involves several different signaling pathways (Figure 1.4). Myc, TGF-β and Src are well known signaling molecules involved in cancer metastasis. Bones are one of the targets of breast cancer metastasis. In addition to the important role of TGF-β in initiating EMT (Beck et al., 2001; Miettinen et al., 1994), TGF-β is critical for breast cancer metastasis to the bone (Kang et al., 2003). The main roles of TGF-β in breast cancer bone metastasis include production of osteoclasts, secretion of IL-11 and increased expression of MMPs (Duivenvoorden et al., 1999; Kang et al., 2005; Roodman, 2004). Another significant site of breast cancer metastasis are the lungs; TNBC cells show a greater tendency to metastasize into lungs (Anders and Carey, 2009). The three main signaling pathways involved in breast cancer metastasis to the lungs involve Notch, Wnt and Hedgehog (Jin et al., 2018). Although the mechanisms by which Notch signaling regulates breast cancer metastasis to the lungs is not yet fully understood, McGovern et al. (2009) suggest that establishment of lung niches for un-transformed stem-cell like cells from a primary breast tumor is mediated through Notch signaling. The role of Wnt/β-catenin signaling in EMT is a well-established concept (Katsuno et al., 2013; Leight et al., 2012). Pre-clinical and clinical studies suggest a link between Wnt/β-catenin activation and lung metastasis in TNBC (Dey et al., 2013; Howe et al., 2003). Hedgehog signaling is highly dysregulated in breast cancer; Arnold et al. (2017) suggest that co-activation of Hedgehog signaling with Wnt/β-catenin is associated with poor clinical outcomes and metastasis in TNBC patients (Arnold et al., 2017). The third most common site of breast cancer metastasis is the liver. Breast cancer metastasis to the liver is also regulated by TGF-β signaling. However, the formation of pre-metastatic niches are mainly governed by MAPK, NF-κB and VEGF signaling during the metastasis of breast cancer cells to the liver (Arnold et al., 2017). Breast cancer metastasis to the brain is mainly driven by epidermal growth factor receptor (EGFR) and HER2 signaling. The overexpression of MMPs and

heparanase through the activation of EGFR and HER2 provides circulating breast cancer cells with the ability to cross the blood-brain-barrier (BBB) (Sirkisoon et al., 2016).

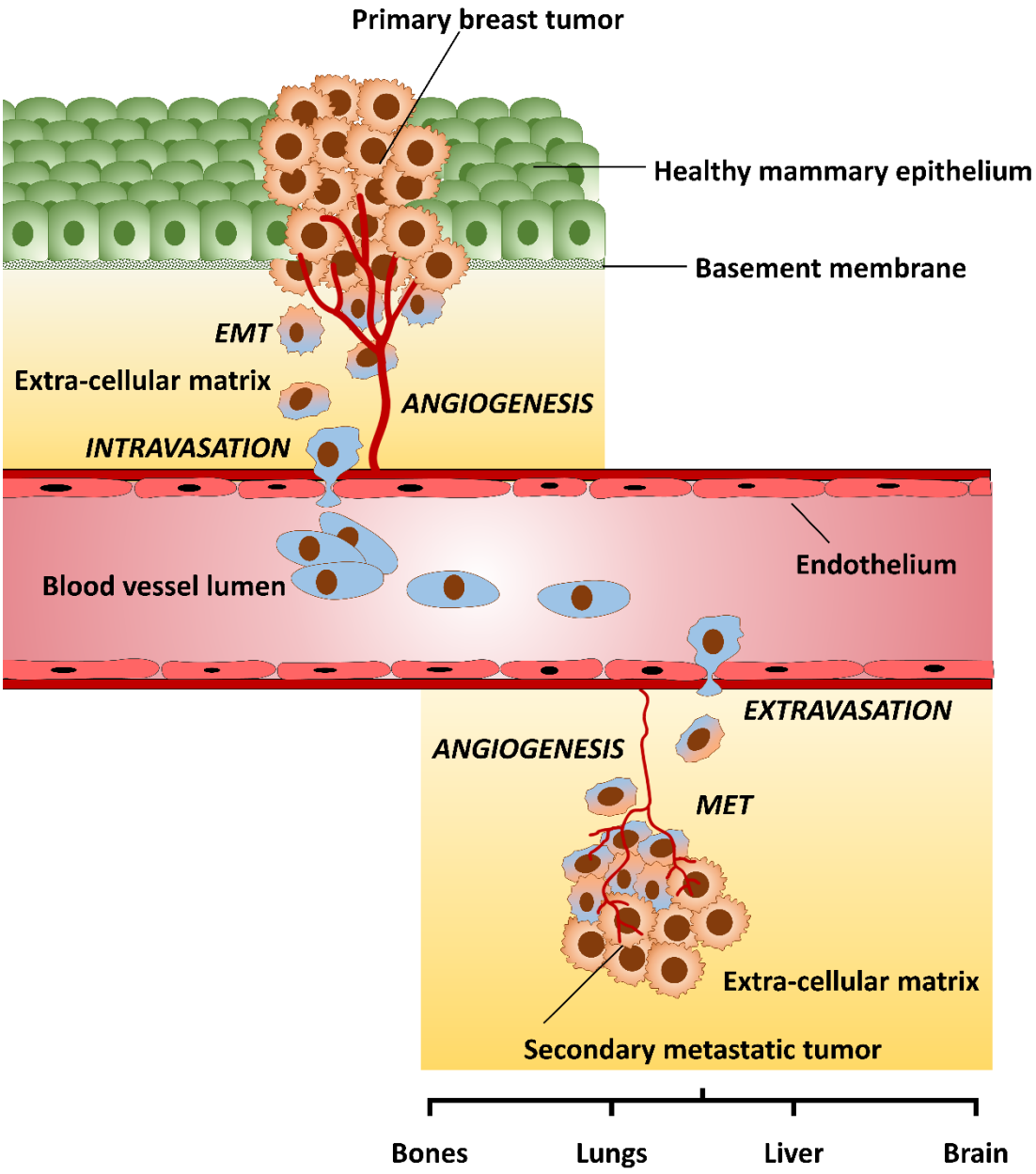


**Figure 1.3. Breast cancer metastatic cascade**
Malignant transformation of the breast epithelium is known as a breast cancer. Breast cancer cells undergo EMT and enter tumor-associated vasculature following invasion through the basement membrane and extra-cellular matrix. The circulating breast cancer cells travel to distant organs such as bones, lungs, liver and brain. At these secondary sites, malignant cells undergo mesenchymal-to-epithelial transformation and form secondary metastatic lesions.
**EMT**, epithelial-to-mesenchymal transformation; **MET**, mesenchymal-to-epithelial transformation

### 1.8.2 Epithelial-to-mesenchymal transition and its relevance to metastasis

As the name implies, EMT refers to the phenotypic transformation of epithelial cells such that they gain a mesenchymal-like phenotype. During this transformation, epithelial makers are gradually lost while more mesenchymal markers are expressed. EMT is not completely a pathological process as type 1 EMT is associated with embryogenesis and organ development; however, this process does not cause pathological conditions such as fibrosis and does not result in an invasive phenotype as in metastasis (Kalluri and Weinberg, 2009; Kim et al., 2014; Zeisberg and Neilson, 2009). Type 2 EMT is activated as a response to tissue trauma and inflammatory injury such as wound healing, tissue regeneration and fibrosis (Tennakoon et al., 2015; Xu and Dai, 2012). Cells undergoing type 3 EMT acquire an invasive phenotype; therefore, this type of transformation is commonly associated with migration and metastasis of malignant cells (Brabletz et al., 2018; Heerboth et al., 2015; Zeisberg and Neilson, 2009). The main focus of this section is type 3 EMT and its relevance to metastasis. The role of EMT in the context of cancer is not restricted to metastasis or the generation of the invasive mesenchymal phenotype. Many researchers suggest that EMT plays a critical role in almost all the phases of tumor progression, including tumor initiation, growth, invasion, dissemination, metastasis, and the development of resistance to chemotherapy (Brabletz et al., 2018; Fischer et al., 2015; Nieto et al., 2016; Zheng et al., 2015). Nieto et al. (2016) explain that the transition of an epithelial cell to a mesenchymal form progresses through two thermodynamically unstable intermediate phenotypes, EM1and EM3, and one stable intermediate phenotype known as EM2 (Nieto et al., 2016). Epithelial cells possess two molecularly distinct domains associated with the cell membrane, namely, apical domain and basolateral domain (Lee and Streuli, 2014). These domains play a significant role in the maintenance of the apical-basal polarity of epithelial cells through the cell-cell, cell-basement membrane and cell-ECM interactions. At the initial steps of EMT, cell surface epithelial markers such as E-cadherin and zonula occludens-1 are downregulated, leading to the loss of tight junctions, adherens junction and desmosomes (Nieto et al., 2016; Zeisberg and Neilson, 2009). The progressive loss of epithelial markers is followed by the increased expression of EMT transcription factors such as Snail, Slug, ZEB1, and Twist

(Ganesan et al., 2016; Lee and Streuli, 2014; Siletz et al., 2013). Stabilization of cytoskeletal markers such as β-catenin and vimentin, together with upregulation of acquired cell surface proteins such as N-cadherin, leads to the establishment of the mesenchymal phenotype, which demonstrates complete loss of apical-basal polarity and acquisition of new front-back polarity (Ganesan et al., 2016; Zeisberg and Neilson, 2009). Recent studies show that the post-translational modifications of EMT transcription factors also play a significant role during tumor metastasis (Chang et al., 2016; Serrano-Gomez et al., 2016). Epithelial cells which complete the entire EMT process become detached from the primary tumor, mostly as single motile cells (Jolly et al., 2017a; Thiery and Lim, 2013). The disseminated tumor cells then invade into the circulation following degradation of the ECM by the proteolytic activity of MMPs (Kessenbrock et al., 2010). In addition to the EMT-mediated phenotypic transformation of epithelial cells, small molecular Rho GTPases (RhoA, Rac1 and Cdc42)-driven cytoskeletal changes play a critical role in cancer cell migration (Edlund et al., 2002; Hou et al., 2013; Raftopoulou and Hall, 2004). At the secondary relapsing site, mesenchymal-like tumor cells undergo reciprocal MET and establish secondary micrometastases (Banyard and Bielenberg, 2015; Tsai and Yang, 2013).

Even though, the critical role of EMT in tumor metastasis is widely accepted, two recent studies conducted using mouse models of pancreatic cancer and breast cancer suggest that EMT is not necessarily required for metastasis (Fischer et al., 2015; Zheng et al., 2015). In a subsequent article, Jolly et al. (2017) note that the extent of the involvement of EMT in metastasis is related to the pattern of cancer cell dissemination and migration. Hence, metastasis is highly dependent on EMT during single cell dissemination whereas EMT is not necessary for collective dissemination and/or cluster-based migration of metastatic cells (Jolly et al., 2017b).

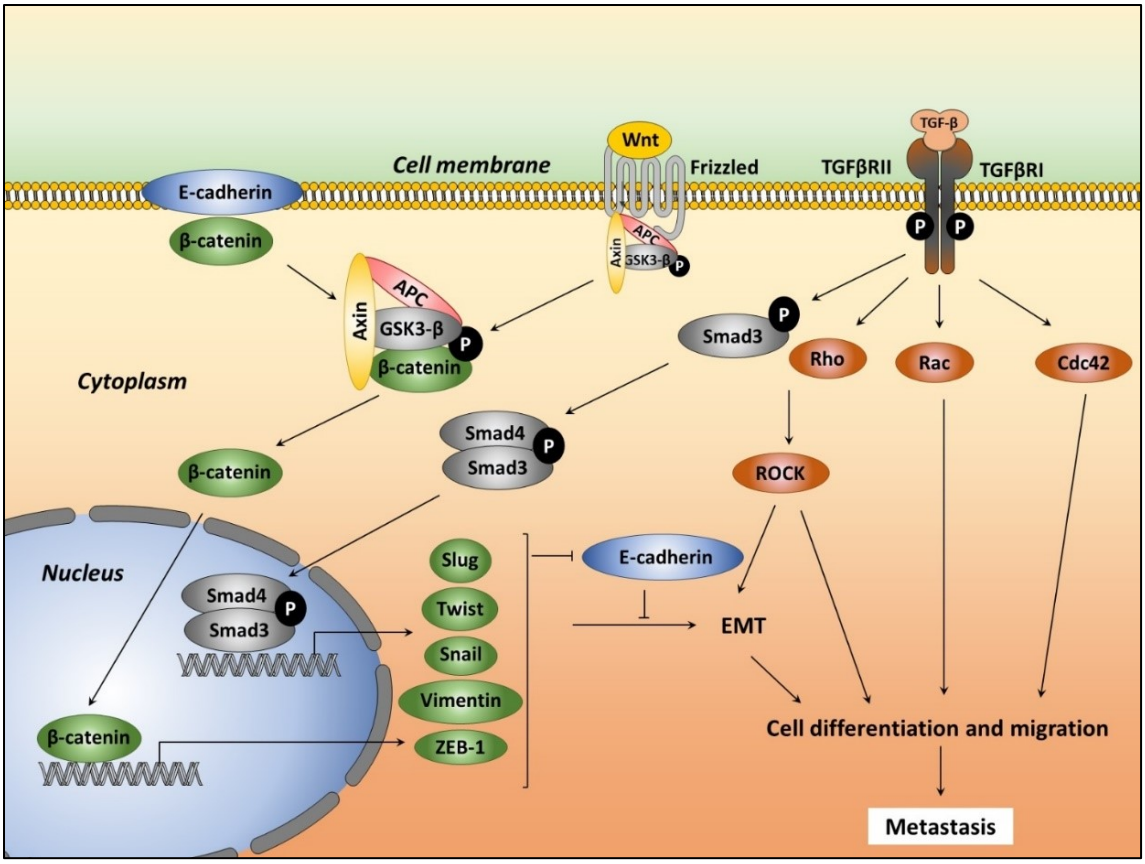


**Figure 1.4. Signal transduction pathways involved in breast cancer cell metastasis.** **APC:** Adenomatous polyposis coli; **E-cadherin**: E-type calcium-dependent adhesion; **GSK3β:** Glycogen synthase kinase 3-β; **Cdc42, Rac1/2/3** and **RhoA:** Small GTPases; **ROCK**: Rho-associated protein kinase; **TGF-β**: Transforming growth factor-β; **TGFβR**: Transforming growth factor-β receptor; **ZEB1:** Zinc finger E-box-binding homeobox 1.

### 1.8.3 *In vitro* and *in vivo* anti-metastatic activity of flavonoids and their derivatives

The ability of flavonoids to act on various signaling pathways and their subsequent convergent activity toward the inhibition of the cellular motility and invasiveness of cancer cells reveals blockade of the metastatic cascade at several levels. In this section, the effect of some flavonoids and their structurally modified derivatives on cancer metastasis and related signaling pathways is presented.

Quercetin and luteolin inhibit invasiveness of aggressive human A431-III epidermal carcinoma cells by down-regulating the expression of EMT transcription factors and reversing the EMT-induced cadherin switch (Lin et al., 2011). In another study, quercetin was found to inhibit the migration and invasion of cultured SAS human oral carcinoma cells by suppressing the expression of MAPK and PI3K-related Rho GTPases, and MMP2 and 9, respectively (Lai et al., 2013). Piantelli et al. (2006) reported that intraperitoneal administration of quercetin and apigenin inhibits the colonization of intravenously injected B16-BL6 metastatic mouse melanoma cells into the lungs of C57BL/6N mice. Furthermore, the inhibition of tumor necrosis factor α (TNF-α)-induced vascular cell adhesion protein 1 (VCAM-1) by HUVECs suggests that flavonoid-mediated anti-metastatic activity is related to the inhibition of cancer cell-endothelium interactions (Piantelli et al., 2006). A dihydroxyflavone know as chrysin attenuates the hypoxia-induced expression of VEGF and signal transducer and activator of transcription 3 (STAT3) without affecting HIF1α protein levels in 4T1 mouse mammary carcinoma cells. Oral administration of chrysin to 4T1 tumor-bearing Balb/c mice causes a significant reduction in lung colonization by 4T1 cells (Lirdprapamongkol et al., 2013). Morin, an anti-cancer flavonoid, inhibits the invasiveness of MDA-MB-231 cells by suppressing MMP2 expression; morin-induced downregulation of N-cadherin in MDA-MB-231 TNBC cells has a negative effect on EMT (Jin et al., 2014). Baicalein, a flavonoid used in Chinese herbal medicine, inhibits the migration and invasion of MDA-MB-231 cells by inhibiting the expression of MMP2 and MMP9 in a concentration-dependent manner (Wang et al., 2010b). Chen et al. 2016 show that 3,6-dihydroxyflavone inhibits the migration and invasion of both ER+ and TNBC cells, and reverses EMT of MDA-MB-231 cells through negative regulation of Notch signaling. Administration of 3,6-dihydroxyflavone suppresses lung colonization by GFP transfected-MDA-MB-231

TNBC cells injected into the tail vain of Balb/c nude female mice (Chen et al., 2016). A novel flavonoid derivative known as VI-14 inhibits the adhesion, migration and invasion of MDA-MB-231 and MDA-MB-435 breast cancer cells by suppressing MMP activity of breast cancer cells. VI-14-induced upregulation of tissue inhibitor of metalloproteinase 1 and 2 together with inhibition of MAPK pathway components (ERK, JNK and p38) and NF-κB activation in MDA-MB-231 cells also has negative regulatory effects on breast cancer metastasis (Li et al., 2012).

## 1.9 Angiogenesis

Angiogenesis, the formation of new blood vessels and capillaries from existing vasculature, is a process that takes place during normal physiological states such as embryogenesis, wound healing and cyclic changes of the female reproductive system (Ferrara, 2001; Góth et al., 2003; Kurz; Mustafa et al., 2012; Seaman et al., 2007). However, angiogenesis also plays a significant role in pathological processes such as diabetic retinopathy, wound healing, and tumor progression and metastasis (Góth et al., 2003; Papetti and Herman, 2002; Seaman et al., 2007). Continuous supply of nutrients and hematogenic dissemination of cancer cells from a primary tumor is dependent on the formation of new capillaries around a growing tumor. The process of angiogenesis is composed of several steps that take place in a progressive order. The basement membrane of existing blood vessels and stromal matrix is degraded as a result of increased protease activity (Lamalice et al., 2007; Nishida et al., 2006). Pro-angiogenic signals promote the migration of the endothelial cells toward an angiogenic stimulus and the proliferation of endothelial cells leads to the formation of solid endothelial cell sprouts in the stromal space (Brooks, 1996; McMahon, 2000; Tahergorabi and Khazaei, 2012). Endothelial cells rearrange and organize into capillary tubes and the formation of tight junctions stabilizes newly formed capillaries. A new basement membrane is formed, completing the angiogenic process (Klagsbrunl and Moses, 1999; Mojzis et al., 2008).

### 1.9.1 Pro-angiogenic and anti-angiogenic factors

Angiogenesis, one of the hallmarks of cancers (Hanahan and Weinberg, 2000, 2011), requires an intricate balance between the molecular mediators of angiogenesis, i.e., pro-angiogenic and anti-angiogenic factors. Pro- and anti-angiogenic factors are secreted by

endothelial cells, cancer cells and surrounding stromal cells (Papetti and Herman, 2002). There are many soluble and membrane-bound pro-angiogenic factors that have distinct contributions to both physiological and pathological angiogenesis.

#### 1.9.1.1 Pro-angiogenic factors

Soluble pro-angiogenic factors such as VEGF, FGF, epidermal growth factor (EGF), platelet-derived endothelial growth factor (PDGF), TGF-α and TGF-β, angiogenin, estrogen, interleukin-8 (IL-8), TNF-α and prostaglandins, as well as membrane-bound pro-angiogenic factors such as integrins, VE-cadherin and ephrins, induce the proliferation, growth and differentiation of endothelial cells (Knoll et al., 2004; Marjon et al., 2004; Papetti and Herman, 2002; Tonini et al., 2003).

VEGF is the most well-defined, soluble pro-angiogenic factor. There are at least 5 members of the human VEGF family identified to date, namely, VEGF-A, VEGF-B, VEGF-C, VEGF-D, and placental growth factor, which is also distantly related to the PDGF family (Christinger et al., 2004; Heloterä and Alitalo, 2007; Holmes and Zachary, 2005). VEGF-A is the most potent pro-angiogenic factor, and is thus considered to be the prototypical VEGF family member, existing in 6 isoforms ($VEGF_{121}$, $VEGF_{145}$, $VEGF_{165}$, $VEGF_{183}$, $VEGF_{189}$ and $VEGF_{206}$,) (Holmes and Zachary, 2005; Papetti and Herman, 2002). $VEGF_{165}$ is the most common isoform secreted into the extracellular environment (Fearnley et al., 2016; Nowak et al., 2010; Papetti and Herman, 2002; Park et al., 1993; Perrot-Applanat, 2012). Pro-angiogenic activities of VEGF are mediated through binding to VEGF receptors (VEGFR1, VEGFR2 and VEGFR3) (Abhinand et al., 2016; Shibuya, 2011). Both VEGFR1 (fms-like tyrosine kinase-1; FLT1) and VEGFR2 (kinase insert domain receptor; KDR/ fetal liver kinase1; FLK1) regulate angiogenesis; however, VEGFR1 is a kinase-impaired RTK whereas VEGFR2 is a receptor with high kinase activity (O'Reilly et al., 1997; Shibuya, 2006; Yancopoulos et al., 2000). VEGFR3 (FLT4) mainly regulates lymphangiogenesis (Jussila and Alitalo, 2002). The VEGFA/VEGFR2 axis functions as the most prominent signaling cascade regulating cellular events related to angiogenesis. VEGFA mediates its pro-angiogenic activities by inducing endothelial cell proliferation, survival, migration, microvascular permeability, and MMP2 secretion (Lohela et al., 2009; Olsson et al., 2006; Smith et al., 2015).

VEGFA-mediated activation of VEGFR2 begins with the autophosphorylation of tyrosine residues in the cytoplasmic domain of VEGFR2 (Tyr801), followed by Tyr1054 and Tyr1059 (Kendall et al., 1999; Shibuya, 2010). Increased kinase activity of VEGFR2 activates downstream signaling pathways, including Akt/mTOR, p38MAPK, ERK and Rho GTPases (Gerber et al., 1998; Gingras et al., 2000; Jopling et al., 2009; Koch and Claesson-Welsh, 2012; dela Paz et al., 2013; Soumya et al., 2016). Activation of these molecular pathways sends mitogenic signals that promote endothelial cell survival and proliferation.

The FGF family is composed of 18 secreted proteins, FGF1–FGF10 and FGF16–FGF23 (Beenken and Mohammadi, 2009). FGFs regulate multiple cellular functions by binding to tyrosine kinase FGF receptors (FGFR; FGFR1-FGFR4) (Ornitz and Itoh, 2015; Zhang et al., 2006). FGF was identified as a growth factor that regulates developmental processes during early vertebrate embryogenesis (Balasubramanian and Zhang, 2016; Ornitz and Itoh, 2015). Cell proliferation, differentiation, and survival are also regulated by FGFs (Beenken and Mohammadi, 2009; Demo et al., 1994; Fukumoto, 2008; Ornitz and Itoh, 2015; Yun et al., 2010). FGF1 and FGF2 (also known as basic FGF; bFGF) are important proangiogenic agents in wound healing; in particular, FGF2 is a highly potent angiogenesis inducer (Broadley et al., 1989; Greenhalgh et al., 1990; Murakami and Simons, 2008; Yang et al., 2015b). Inhibition of VEGF signaling affects the initiation of angiogenesis; in contrast, defects in FGF signaling predominantly impair the maintenance of tumor angiogenesis (Compagni et al., 2000). Binding of FGF to FGFR1 induces receptor dimerization and autophosphorylation of FGFR1. During the first phase of FGFR1 activation, a sequential phosphorylation of 6 tyrosine residues (Tyr653 followed by Tyr583, Tyr 463, Tyr766, Tyr585 and Tyr654) at the kinase domain is required for full kinase activity of FGFR1. Active FGFR1 then activates two downstream pathways, RAS/RAF and PI3K/Akt, and sends mitogenic signals to induce proliferation and survival of endothelial cells (Furdui et al., 2006; Itoh and Ornitz, 2011; Lonic et al., 2008; Mohammadi et al., 1996; Oladipupo et al., 2014; Sarabipour and Hristova, 2016; Suhardja and Hoffman, 2003). During phase 2 of FGFR1 activation, two additional tyrosine residues (Tyr677 and Tyr766) are phosphorylated; this additional phosphorylation event is required for the activation of STAT3 and phospholipase Cγ

(PLCγ) pathways (Dudka et al., 2010; Lonic et al., 2008; Mohammadi et al., 1991, 1996; Ornitz and Itoh, 2015). FGF exerts its proangiogenic effects by regulating endothelial cell proliferation, migration, protease production and expression of integrins and cadherin (Javerzat et al., 2002).

#### 1.9.1.2 Anti-angiogenic factors

The three major anti-angiogenic factors are thrombospodin (TSP), angiostatin (AGS) and endostatin (Huang and Bao, 2004). The two major isotypes of TSP, TSP1 and TSP2, are potent endogenous inhibitors of angiogenesis that exert their action through CD36, CD47 and integrins. TSPs antagonize pro-angiogenic effects of VEGF and inhibit endothelial cell proliferation, survival, and migration (Bornstein, 2009; Lawler, 2002; Lawler and Lawler, 2012; Mirochnik et al., 2008). AGS, a cleavage protein of plasminogen, is another endogenous anti-angiogenic factor that causes tumor vasculature regression, leading to tumor growth inhibition; however, prolonged treatment is required for a successful outcome (Dell'Eva et al., 2002; Jendraschak and Sage, 1996). Endostatin, a fragment protein of collagen XVIII, also inhibits tumor growth by directly inhibiting tumor-associated angiogenesis (O'Reilly et al., 1997). Kim et al. (2002) suggest that endostatin induces anti-angiogenic activities by blocking VEGF-mediated MAPK and p125 activation. These endogenous anti-angiogenic agents have been considered for possible use in the treatment of breast cancer (Castañeda-Gill and Vishwanatha, 2016).

### 1.9.2 Molecular mechanisms involved in tumor-associated angiogenesis

Pro-angiogenic factors released by the tumor cells and tumor-associated fibroblasts induce the formation of new blood vessels that continue to supply fresh oxygen and nutrients to the growing tumor. Stabilization of HIF under hypoxic conditions induces the synthesis of VEGF (Liu et al., 2012), the most potent pro-angiogenic factor released by tumor cell or stromal cells in the tumor microenvironment (McMahon, 2000). Secreted VEGF exerts pro-angiogenic effects on endothelial cells of the tumor-associated vasculature mainly through VEGFR2 (Koch and Claesson-Welsh, 2012; Stacker and Achen, 2013). VEGFR2 is a tyrosine kinase receptor; therefore, its activation leads to many downstream signaling pathways, including Akt (Abid et al., 2004; Ahmed and Bicknell, 2009; D 'angelo et al., 1995; Gerber et al., 1998). Downstream effects of Akt

activation were detailed in Section 1.7.2.1 and its relevance to angiogenesis is detailed in Figure 1.5. In addition, VEGF suppresses the apoptotic death of endothelial cells through a mechanism mediated by PI3K (Gerber et al., 1998). Collectively, the activation of cell survival pathways and inhibition of apoptotic pathways leads to the proliferation and survival of endothelial cells. Therefore, VEGF signaling is an attractive target in the development of anti-angiogenic drugs such as bevacizumab. VEGF binds to other tyrosine kinase receptors such as TIE and also interacts with angiopoietin-1 / angiopoietin receptor-2 (TIE2) signaling pathway (Singh et al., 2009a). Endothelial cell proliferation and survival is mediated through Ang-1/TIE2 pathway when the VEGF signaling pathway is blocked (Huang et al., 2009).

bFGF is another potent pro-angiogenic factor that is released by tumor stromal cells. The angiogenic activity of bFGF is mediated through VEGF-independent mechanisms; tumor-associated fibroblasts serve as an important source of secreted bFGF (Shiga et al., 2015; Zhang et al., 2010). Tumor-associated fibroblasts in TNBC tumors express higher levels of bFGF in comparison to hormone receptor-positive breast cancer cells; therefore, the angiogenic signaling network in TNBC is more powerful (Fabris et al., 2010; Giulianelli et al., 2008). Phosphorylation of FGFR following binding of bFGF leads to the activation of downstream Akt and MAPK signaling pathways, leading to the proliferation and survival of endothelial cells (Figure 1.5) (Hadari et al., 2001; Holgado-Madruga et al., 1997; Ong et al., 2000). Tumor-associated fibroblasts also express IL-6, which triggers defective angiogenesis, increasing the formation of irregular blood vessels (Gopinathan et al., 2015).

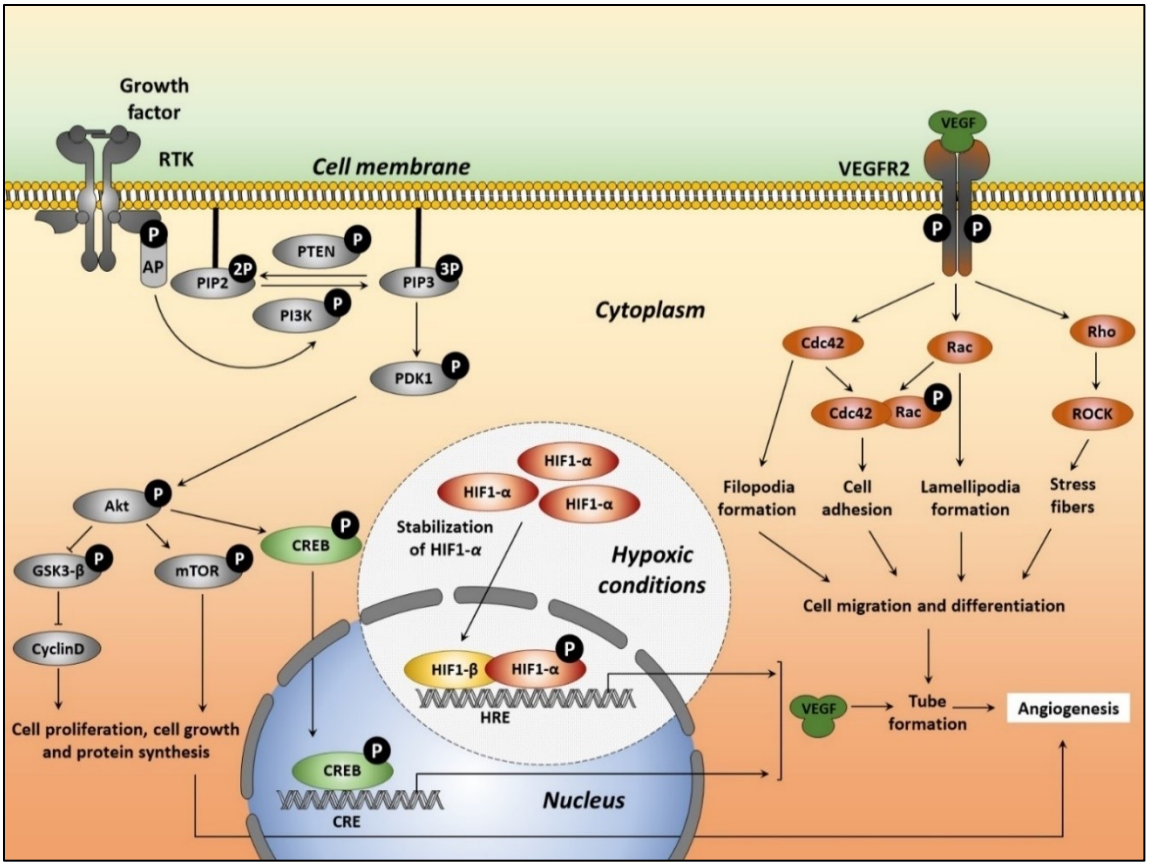


**Figure 1.5. Signal transduction pathways involved in tumor-associated angiogenesis.** **Akt**: protein kinase B; **AP**: activator protein; **Cdc42, Rac1/2/3** and **RhoA**: Rho family Small GTPases; **CRE**: cAMP (cyclic adenosine monophosphate) response element; **CREB**: cAMP (cyclic adenosine monophosphate) response element binding protein; **GSK3-β**: glycogen synthase kinase 3-β; **HIF**: hypoxia-inducible factor; **HRE**: hypoxia response element; **MEK**: mitogen-activated protein kinase kinase; **mTOR**: mammalian target of rapamycin; **p21**: cyclin-dependent kinase inhibitor 1; **PDK1**: phosphoinositide-dependent kinase-1; **PI3K**: phosphoinositide 3-kinase; **PIP2**: phosphatidylinositol-4,5-bisphosphate; **PIP3**: phosphatidylinositol-3,4,5-trisphosphate; **PTEN**: phosphatase and tensin homolog; **ROCK**: Rho-associated protein kinase; **RTK**: receptor tyrosine kinase; **VEGF**: vascular endothelial growth factor; **VEGFR2**: vascular endothelial growth factor receptor 2.

### 1.9.3 *In vitro* and *in vivo* anti-angiogenic activity of flavonoids and their derivatives

Before considering the *in vitro* and *in vivo* anti-angiogenic activity of flavonoids, it is important to note that in some cases, both pro-angiogenic and anti-angiogenic activities have been attributed to the same compound. These opposite effects are directly related to the concentrations of flavonoids used in the cell cultures or in animal models of angiogenesis; concentration-dependent effects on oxidative-stress may play a role in flavonoid-induced pro- and anti-angiogenic effects (Diniz et al., 2017).

Quercetin inhibits the proliferation and differentiation of pulmonary arterial endothelial cells by inhibiting the activation of Akt and ERK1/2 signaling pathways (Huang et al., 2017). *In vitro*, quercetin reduces VEGF-induced migration and tube formation by HUVECs and inhibits *in vivo* angiogenesis in Matrigel plug assay. Quercetin also attenuates PC3 human prostate tumor-associated angiogenesis in Balb/cA nude male mice by inhibiting the Akt/mTOR/p70S6K pathway (Pratheeshkumar et al., 2012). Quercetin-induced anti-angiogenic activity in MCF-7 xenograft-bearing Balb/c nude female mice causes a reduction in calcineurin activation, as well as reduced expression of VEGF, and VEGFR2 in the xenografts (Zhao et al., 2016). Green tea catechins inhibit *in vitro* angiogenesis by bovine aortic endothelial cells and human microvascular endothelial cells by inhibiting the expression of VEGFR2, suggesting that catechin-induced anti-angiogenic activity is VEGF-dependent (Lamy et al., 2002). Another study suggests that green tea catechins and apple procyanidins also block the VEGF-VEGFR2 signaling axis in HUVECs, thereby inhibiting *in vitro* angiogenesis (Moyle et al., 2015). Further experiments from the same research group suggest that the galloyl group in the C3 position of catechins is strongly related to its VEGFR2 inhibitory effects (Cerezo et al., 2015). Another well studied aspect of angiogenesis is the role of Rho GTPases in tumor-associated angiogenesis (Bryan and D'Amore, 2007; van der Meel et al., 2011; Van Nieuw Amerongen et al., 2003; Soga et al., 2001). Treatment of HUVECs with morelloflavone, an anti-oxidant biflavonoid, inhibits endothelial cell proliferation and arrests the cell cycle at $G_2$/M. Morellofavone does not affect VEGFR2 activity; rather, morellofavone largely inhibits VEGF-induced ERK activation. In addition, morelloflavone inhibits VEGF-stimulated Rho GTPase activation (RhoA-GTP and Rac1-GTP) and VEGF-induced angiogenesis in C57BL/6 mice. Intraperitoneal administration

of morelloflavone to PC3 prostate xenograft-bearing male SCID mice results in reduced tumor growth and the reduction blood vessel number in tumors, indicating the *in vivo* efficacy of morelloflavone (Pang et al., 2009). Flavokawain B, one of the three major chalcones present in *Piper excelsum* (kawakawa plant), inhibits *in vitro* angiogenesis by brain endothelial cells, as well as *in vivo* angiogenesis in zebrafish (Rossette et al., 2017). Albini et al. (2006) demonstrated that xanthohumol, a major flavonoid found in *Humulus lupulus*, inhibits the angiogenesis-related cellular activities of HUVECs by inhibiting NF-κB signaling and Akt activation (Albini et al., 2006). A series of xanthohumol derivatives synthesized by inserting additional functional groups into the B ring improves its antiangiogenic activity, as demonstrated by reduced HUVEC proliferation, migration, adhesion to fibronectin and tube formation *in vitro* (Nuti et al., 2017). A flavonoid precursor derivative known as 4-hydroxychalcone attenuates *in vitro* angiogenesis by HUVECs and human foreskin microvascular endothelial cells *via* inhibition of ERK signaling (Varinska et al., 2012).

### 1.10 Flavonoid fatty acid ester derivatives

The use of saturated and mono- or poly-unsaturated fatty acids as the acyl donors in the flavonoid esterification reactions in the presence of CA-LB is known to result in highly regioselective acylated-flavonoids. A molecular modeling study conducted by De Oliveira and colleagues proves the CA-LB-induced regioselectivity in flavonoid acylation occurs at an atomic level. (De Oliveira et al., 2009). This method has been widely used to synthesize flavonoid fatty acid esters; some of these novel derivatives show improved pharmacological activities, including anti-cancer activity. Mello et al. (2006) report that oleic-, linoleic-, and γ-linoleic acid-acylated rutin and naringin derivatives inhibit VEGF secretion by K562 lymphoblastoma cells more effectively than the parent compounds (Mellou et al., 2006). Acylation of the 4'-*O* position of rutin with oleic acid increases the compound's anti-oxidant activity (Katsoura et al., 2006). Fatty acid acylated-isoquercitrin shows increased anti-oxidant activity and xanthine oxidase inhibitory effect compared to parent compounds. Furthermore, the panel of novel derivatives show improved anti-proliferative effects against Caco-2 human colon cancer cells than that of isoquecitrin (Salem et al., 2010). Ardhaoui et al. (2004) suggest that CA-LB catalyses the acylation of flavonoid glycosides, rutin, esculin and hesperidin but

not flavonoid aglycone, quercetin (Ardhaoui et al., 2004). Ziaullah and co-workers suggest that acylation of PZ and isoquecitrin with long chain fatty acids increases their tyrosinase inhibitory activity, as well as anti-oxidant activity relative to parent flavonoids (Ziaullah et al., 2013). Another study from the same researchers suggest that acylation of quercetin-3-*O*-glucoside with long chain fatty acids improves anti-oxidant activity and, thereby, decreases the lipid oxidation (Warnakulasuriya et al., 2014).

### 1.11 Research hypothesis

I hypothesize that PZ-DHA, and/or its active phase I/phase II metabolites inhibit the metastasis of triple negative-mammary carcinoma cells by inhibiting their proliferation, invasion and EMT and/or tumor-associated angiogenesis.

### 1.12 General research objective and research approach

The general objective of this research is to evaluate the effect of PZ-DHA and its potential metabolites on three different aspects of metastasis; tumor cell proliferation, phenotypic transformation and metastasis of tumor cells, and tumor-associated angiogenesis, using *in vitro* cell cultures and *in vivo* mouse models of breast cancer.

Phloridzin docosahexaenoate (PZ-DHA) (Figure 1.6C), a fatty acid ester derivative of polyphenol combines PZ (Figure 1.6A), a flavonoid precursor abundantly found in apple peels, and DHA (Figure 1.6B), an ω-3-fatty acid, through an acylation reaction (Ziaullah et al., 2013). It was expected that the conjugation of PZ with DHA would improve the cellular uptake of PZ and suppress the auto-oxidation of DHA. Previous work has shown that PZ-DHA inhibits the *in vitro* growth of HepG2 human hepatocellular carcinoma cells and THP1 acute monocytic leukemia cells without any harmful effects to non-malignant HP-F human hepatocytes and RTCP10 rat hepatocytes (Nair et al., 2014). Another study suggests that PZ-DHA is cytotoxic to chronic myelogenous leukemia cells (K562) and acute T cell leukemia cells (Jurkat) *in vitro* and inhibits the growth of Jurkat cell xenografts in zebrafish (Arumuggam et al., 2017). PZ-DHA also inhibits lipopolysaccharide-induced pro-inflammatory responses by THP-1-derived macrophages *in vitro* (Sekhon-Loodu et al., 2015). PZ-DHA-induced cytotoxic effects on MDA-MB-231 TNBC cells were evaluated during my MSc thesis research, which found that PZ-DHA selectively kills breast cancer cells without affecting the viability of normal non-

malignant human mammary epithelial cells (Fernando, 2014; Fernando et al., 2016). In addition, I found that intra-tumoral administration of cytotoxic doses of PZ-DHA inhibits the growth of MDA-MB-231 xenografts in NOD-SCID female mice (Fernando, 2014; Fernando et al., 2016). Data from these previous studies was used to inform the design of the current project, which evaluated the pharmacokinetic parameters, anti-proliferative, anti-metastatic, and anti-angiogenic activity of PZ-DHA at sub-cytotoxic concentrations. Furthermore, the effect of PZ-DHA on various signaling pathways in non-malignant mammary epithelial cells, mammary carcinoma cells and endothelial cells was also tested using the same sub-cytotoxic concentrations.

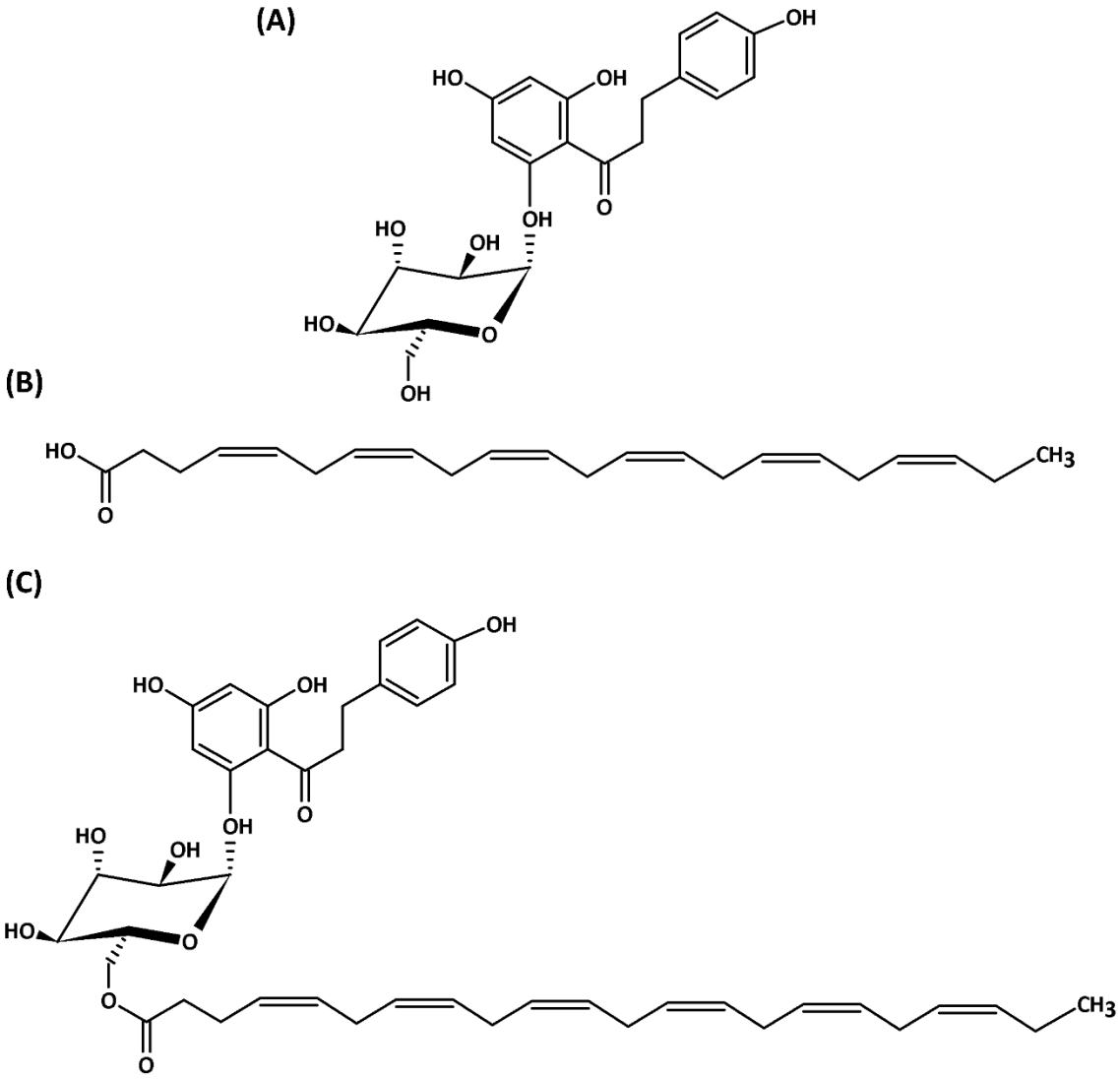


**Figure 1.6. Chemical structures of PZ, DHA and PZ-DHA.**
**(A)** Phloridzin, PZ: $C_{21}H_{24}O_{10}$, MW=436.413 g/mol, 1-[2,4-dihydroxy-6-[(2S,3R,4S,5S,6R)-3,4,5-trihydroxy-6-(hydroxymethyl)oxan-2-yl]oxyphenyl]-3-(4-hydroxyphenyl)propan-1-one **(B)** Docosahexaenoic acid, DHA: $C_{22}H_{32}O_2$, MW=328.496 g/mol, (4Z,7Z,10Z,13Z,16Z,19Z)-docosa-4,7,10,13,16,19-hexaenoic acid **(C)** Phloridzin docosahexaenoate, PZ-DHA: $C_{43}H_{54}O_{11}$, MW=746.88 g/mol, (6-{3,5-dihydroxy-2-[3-(4-hydroxyphenyl)propanoyl]phenoxy}-3,4,5-trihydroxytetra- hydro-2H-pyran-2-yl)methyl (4Z,7Z,10Z,13Z,16Z,19Z)- 4,7,10,13,16,19-docosahexaenoate.

## 1.13 Specific research objectives

Specific research objectives were as follows.

Chapter 3:

1. To identify the *in vitro* metabolites of PZ-DHA by combining PZ-DHA with freshly prepared mouse hepatic microsomes.
2. To establish the pharmacokinetic parameters, organ distribution and *in vivo* metabolites of PZ-DHA by intraperitoneal administration of PZ-DHA into Balb/c female mice.

Chapter 4:

1. To determine the cytotoxic activity of high dose PZ-DHA and the anti-proliferative effect of a sub-cytotoxic concentration of PZ-DHA using triple negative and ER+ mammary carcinoma cells.
2. To determine the tumor suppressor activity of PZ-DHA using Balb/c and NOD-SCID female mice orthotopically implanted/xenografted with mouse and human mammary carcinoma cells, respectively.

Chapter 5:

1. To evaluate the effect of PZ-DHA on the migration and invasion of mouse and human mammary carcinoma cells using cell culture systems.
2. To assess the *in vivo* effect of PZ-DHA on the metastasis of orthotopically implanted/xenografted mammary carcinoma cells to the lungs of Balb/c and NOD-SCID female mice.

Chapter 6:

1. To establish the inhibitory effects of PZ-DHA on proliferation, migration and tube formation by umbilical (large) vein and capillary (small) endothelial cells.
2. To determine the effect of PZ-DHA on *in vivo* angiogenesis using Balb/c female mice implanted with pro-angiogenic factor-containing Matrigel plugs.

# CHAPTER 2 : MATERIAL AND METHODS

## 2.1 Stock solutions of test compounds

Stock solutions of PZ, DHA and PZ-DHA used for all *in vitro* assays were made in DMSO at 40 mM (final DMSO concentration in cell cultures: ≤ 0.075% v/v) and stored at -20°C in 100 µL aliquots. Stock solutions for MTS assay, MTT assay, 7-AAD assay, cellular uptake assay and breast cancer spheroid assay were made in DMSO at 100 mM (final DMSO concentration in cell cultures: ≤ 0.05% v/v and final DMSO concentration in *in vitro* metabolite studies: 0.3% v/v) and stored in -20°C in 100 µL aliquots. PZ-DHA stock solutions used for *in vivo* experiments were made in DMSO at 150 mg/mL (final DMSO concentration in intraperitoneal injection, 6.8% v/v) and stored at -20°C in 75.25 µL aliquots.

## 2.2 Chemicals and reagents

The HRP/DAB detection system was purchased from Agilent Technologies (Mississauga, ON). Di-potassium hydrogen orthophosphate ($K_2HPO_4$), potassium dihydrogen orthophosphate ($KH_2PO_4$), and potassium chloride (KCl) were purchased from BDH chemicals (Mississauga, ON). MACH 4 MR AP polymer, mouse-on-mouse HRP polymer, Rodent block M, and Vulcan fast red chromogen kit 2 were purchased from Biocare Medical (Markham, ON). Bradford assay reagent and precision protein ladder were purchased from Bio-Rad Laboratories, Inc. (Mississauga, ON). Acrylamide/bis-acrylamide 30% solution 29:1, ammonium persulphate (APS), dimethyl sulfoxide (DMSO), ethylene glycol tetraacetic acid (EGTA), glycerol, glycine, paraformaldehyde (PFA), sodium dodecyl sulfate (SDS), sucrose, tetramethylethylenediamine (TEMED), Tris base, and Tween-20 were purchased from BioShop Canada Inc. (Burlington, ON). Alamethicin, Glucuronic acid, and phenol red-free Matrigel were obtained from Corning Life Sciences (Tewkbury, MA). Cell viability dye 7-aminoactinomycin (7-AAD) solution was purchased from eBioscience Inc. (San Diego, CA). Di-sodium hydrogen phosphate ($Na_2HPO_4$) and ethylene diamine tetraacetic acid (EDTA) were purchased from EM Industries Inc. (Hawthorne, NY). Calcium chloride ($CaCl_2$) and sodium orthovanadate ($Na_3VO_4$) were purchased from EMD Chemicals, Inc. (Gibbstown, NJ). Sodium acetate ($CH_3COO^-Na^+$), sodium hydroxide (NaOH), Triton-X-100 were purchased from Fisher

Scientific Canada (Ottawa, ON). Annexin-V-488, B27 serum-free supplement, Dulbecco's Modified Eagle's Medium (DMEM), F12, F12/DMEM, fetal bovine serum (FBS), L-glutamine, N-2-hydroxyethylpiperazine-N′-2-ethanesulfonic acid (HEPES), Oregon Green 488, penicillin-streptomycin (Pen-strep) solution, propidium iodide (PI), TryPLE Express, and trypsin [0.25% with EDTA (1×)] were obtained from Life Technologies Inc. (Burlington, ON, Canada). Endothelial basal medium (EBM)/supplements, fibroblast basal medium (FBM)/supplements and mycoplasma kit were purchased from Lonza Inc. (Walkersville, MD). Docosahexaenoic acid (DHA) was purchased from Nu-Chek Prep Inc (Elysian, MN). Human basic fibroblast growth factor (bFGF), human epidermal growth factor (EGF), human transforming growth factor-β (TGF-β), human tumor necrosis factor-α (TNF-α), and human vascular endothelial growth factor-165 ($VEGF_{165}$) were purchased from PeproTech (Rocky Hill, NJ). Cell viability assay dye 5-[3-(carboxymethoxy) phenyl]-3-(4,5-dimethyl-2-thiazolyl)-2-(4-sulfophenyl)-2H-tetrazolium inner salt (MTS) was purchased from Promega (Madison, WI). RNase was obtained from Qiagen Inc. (Mississauga, ON, Canada). Annexin-V-FLUOS and NADPH were obtained from Roche Diagnostics (Laval, QC). Diff-Quik staining kit was purchased from Siemens Healthcare Diagnostics (Los Angeles, CA). Trypan blue dye (0.4%), 3-(4,5-dimethylthiazol-2-yl)-2,5-diphenyltetrazolium bromide (MTT), 30% Brij 23 solution, 3'-phosphoadenosine-5'-phosphosulfate (PAPS), 6-thioguanine, acetone, acetonitrile, ammonium chloride ($NH_4Cl$), aprotinin, bovine insulin, bovine serum albumin (BSA), collagenase from *Clostridium histolyticum*, DNAse I from bovine pancreas, Drabkin's reagent, elastase from porcine pancreas, formic acid, Hank's balanced salt solution (HBSS), human hemoglobin, hydrocortisone, isopropanol, leupeptin, methanol, mitomycin C from *Streptomyces caespitosus*, Nonidet P-40 (NP-40), paclitaxel (TXL), pepstatin A, phenazine methosulfate (PMS),phenylmethylsulfonyl fluoride (PMSF), phloridzin (PZ), phosphatase substrate, phosphate-buffered saline (PBS), porcine gelatine, potassium biocarbonate ($KHCO_3$), puromycin, quercetin, S-adenosylmethionine (SAM), sodium azide ($NaN_3$), sodium deoxycholate and sodium fluoride (NaF) were purchased from Sigma-Aldrich (Oakville, ON).

## 2.3 Antibodies

### 2.3.1 Akt, MAPK, drug transporters, small molecular Rho GTPase signaling and secondary antibodies

Anti-total-PTEN rabbit monoclonal antibody (Ab) (#9188), anti-phospho-PTEN (Ser380) rabbit monoclonal Ab (#9188), anti-total-Akt rabbit monoclonal Ab (#9272), anti-phospho-AKt (Ser473) rabbit monoclonal Ab (#4060), anti-phospho-Akt (Thr308) rabbit monoclonal Ab (#13038), anti-total-PDK1 rabbit monoclonal Ab (#3062), anti-phospho-PDK1 (Ser241) rabbit monoclonal Ab (#3438), anti-total-GSK-3β rabbit monoclonal Ab (#12456), anti-phospho- GSK-3β (Ser9) rabbit monoclonal Ab (#5558), anti-total-mTOR rabbit monoclonal Ab (#2983), anti-phospho-mTOR (Ser2448) rabbit monoclonal Ab (#5536), anti-total-cRAF rabbit monoclonal Ab (#9422), anti-phospho-cRAF (Ser259) rabbit monoclonal Ab (#9421), anti-total-ERK1/2 rabbit monoclonal Ab (#4695), anti-phospho-ERK1 (Thr202)/ERK2(Thy204) rabbit monoclonal Ab (#4370), anti-total-CREB rabbit monoclonal Ab (#9197), phospho-CREB (Ser133) rabbit monoclonal Ab (#9198), anti-RhoA rabbit monoclonal Ab (#2117), anti-RhoB rabbit monoclonal Ab (#2098), anti-RhoC rabbit monoclonal Ab (#3430), anti-Rac1/2/3 rabbit monoclonal Ab (#2465), anti-Cdc42 rabbit monoclonal Ab (#2466), anti-Rac1/Cdc42 (Ser71) rabbit monoclonal Ab (#2461), anti-total-Smad3 rabbit monoclonal Ab (#9523), anti-phospho-Smad3 (Ser423/425) rabbit monoclonal Ab (#9520), HRP-conjugated rabbit anti-β-actin (#12620), anti-α tubulin rabbit monoclonal Ab (#5335), HRP-conjugated donkey anti-rabbit (#7074) and goat anti-mouse IgG Ab were purchased from Cell Signaling Technology Inc. (Danvers, MA). Anti-Ki67 rabbit monoclonal Ab (Ab15580) was purchased from Abcam Inc. (Toronto, ON). Anti-phospho-GSK3β (Tyr216) Ab (05-413) was purchased from Millipore Sigma (Oakville, ON). FITC-conjugated anti-Ki67 Ab (652410) was obtained from eBioscience Inc. (San Diego, CA).

### 2.3.2 Cell cycle

Anti-cyclin D3 mouse monoclonal Ab (#2936), anti-cyclin B1 mouse monoclonal Ab (#4135), anti-CDK4 rabbit monoclonal Ab (#12790), anti-CDK2 rabbit monoclonal Ab (#2546), and anti-ABCG2 rabbit monoclonal Ab (#4477) were purchased from Cell Signaling Technology (Danvers, MA). Anti-cyclin A2 mouse monoclonal Ab (05-374SP)

and anti-CDK1 rabbit monoclonal Ab (06-923SP) were obtained from Millipore Sigma (Oakville, ON). Anti-MRP1 mouse monoclonal Ab (SC-18835) was purchased from Santa Cruz Biotechnology (Santa Cruz, CA).

### 2.3.3 Epithelial-to-mesenchymal transition

Anti-slug rabbit monoclonal Ab (#9585), anti-β-catenin rabbit monoclonal Ab (#8480), anti-TCF8/ZEB1rabbit monoclonal Ab (#3396), anti-vimentin rabbit monoclonal Ab (#5741), anti-pan-cadherin rabbit monoclonal Ab (#4073) were purchased from Cell Signaling Technology (Danvers, MA). Anti-MMP2 mouse monoclonal Ab (ab86607) was purchased from Abcam Inc. (Toronto, ON).

## 2.4 Cells and cell culture conditions

Two human TNBC cell lines (MDA-MB-231 and MDA-MB-468), one mouse triple-negative mammary carcinoma cell line (4T1), two human ER+ breast cancer cell lines (MCF-7 and T-47D), one paclitaxel resistant-human TNBC cell line (MDA-MB-231-TXL), one green fluorescence protein (GFP)-transfected human TNBC cell line (GFP-MDA-MB-231), non-malignant mammary epithelial cells (MCF-10A), human dermal fibroblasts (HDF) and two primary human endothelial cell types, human umbilical vein endothelial cells (HUVEC) and human microvascular vein endothelial cells (HMVEC), were used in this project. For cryopreservation of all cells, DMEM basal medium supplemented with 5 mM HEPES (pH 7.4), 2 mM L-glutamine, 100 U/mL penicillin and 100 μg/mL streptomycin, 20% v/v heat inactivated FBS and 10% v/v DMSO were used and cells were stored in the vapour phase of liquid nitrogen. DMEM basal medium supplemented with 2 mM L-glutamine, 100 U/mL penicillin and 100 μg/mL streptomycin and 10% v/v heat inactivated FBS was used for thawing cryopreserved cells. All cell lines were routinely tested for mycoplasma contamination throughout the project.

### 2.4.1 Mammary carcinoma cells

MDA-MB-231 and GFP-MDA-MB-231 cells were obtained from Dr. S. Drover (Memorial University of Newfoundland, St. John's, NL) and Dr. Paola Marcato (Dalhousie University, Halifax, NS), respectively. MCF-7 and MDA-MB-231-TXL cells were provided by Dr. K. Goralski (Dalhousie University, Halifax, NS). 4T1 mouse

mammary carcinoma cells were obtained from Dr. D. Waisman (Dalhousie University, Halifax, NS). T-47D cells were provided by Dr. J. Blay (Dalhousie University, Halifax, NS). MDA-MB-468 cells were obtained from Dr. P. Lee (Dalhousie University, Halifax, NS). Mammary carcinoma cell lines were authenticated by short tandem repeat analysis conducted by American Type Culture Collection (ATCC; Manassas, VA) (MDA-MB-231, MDA-MB-468, and MCF-7) and DDC Medical DNA Diagnostic Center (Fairfield, OH) (4T1 and T-47D). DMEM basal medium supplemented with 10% v/v heat-inactivated FBS, 5 mM HEPES (pH 7.4), 2 mM L-glutamine, 100 U/mL penicillin and 100 µg/mL streptomycin was used as the growing medium (cDMEM) for all mammary carcinoma cell lines. To facilitate the selective growth of GFP-transfected MDA-MB-231 cells, cDMEM was supplemented with 0.25 µg/mL puromycin. MDA-MB-231-TXL cell cultures were maintained in cDMEM containing 0.4 µg/mL paclitaxel. All malignant cell cultures were maintained at 37ºC in a humidified incubator supplied with 10% $CO_2$ (NuAire, Plymouth, MN). Cells were sub-cultured every 3-4 days (~ 90% confluency) in 1:1, 1:2, 1:3, 1:4, 1:5 or 1:6 ratio except 4T1 and MDA-MB-231-TXL cells for which sub-culturing was performed every 2-3 and 4-5 days, respectively. Adherent cells were trypsinized using 0.25% (w/v) Trypsin - 0.53 mM EDTA solution as the dissociation solution. Trypsinization was ceased by adding the respective growth media. Detached cells were carefully aspirated and sub-cultured into T-75 culture flasks. Cells used for *in vitro* and *in vivo* experiments were consistently 95-100% viable by Trypan blue staining.

### 2.4.2 Non-malignant cells

HDFs were purchased from Lonza Inc. (Walkersville, MD) and grown in fibroblast basal medium supplemented with FBS, insulin, recombinant human bFGF, and gentamicin sulfate & amphotericin B, according to instructions given by Lonza Inc. MCF-10A cells were obtained from Dr. P. Marcato (Dalhousie University, Halifax, NS) and grown in F12/DMEM (1:1) medium supplemented with 10% horse serum, 0.02 µg/mL EGF, 0.5 µg/mL hydrocortisone, 10 µg/mL bovine insulin, 100 U/mL penicillin and 100 µg/mL streptomycin. HUVECs and HMVECs were purchased from Lonza Inc. and grown in 0.1% gelatin-coated 6-well plates, 10 mm Petri dishes or T-75 culture flasks. Cells were maintained in endothelial basal medium supplemented with FBS, recombinant human bFGF, ascorbic acid, recombinant long $R^3$-IGF1, recombinant human EGF, recombinant

human VEGF, heparin, hydrocortisone, and gentamicin sulfate & amphothericin B according to instructions provided by Lonza Inc (EGM). All non-malignant cells were maintained at 37ºC in a humidified incubator supplied with 5% $CO_2$. Cells were sub-cultured every 4-5 days (~ 90% confluency). Adherent cell monolayers were washed using 1×PBS and trypsinized using 0.25% (w/v) Trypsin - 0.53 mM EDTA solution as the dissociation solution. Trypsinization was ceased by adding respective growth media and traces of trypsin were eliminated before sub-culturing. Cells used for *in vitro* experiments were consistently 95-100% viable by Trypan blue staining.

### 2.5 Mice

Ethical approval for animal use was obtained from the Dalhousie University Committee on Laboratory Animals. Six to eight-weeks-old C57BL/6, Balb/c and NOD-SCID mice were purchased from Charles River Canada (Lasalle, QC) and housed in the Carlton Animal Care Facility, Tupper Medical Building of Dalhousie University. C57BL/6 and Balb/c mice were fed with regular rodent chow, and water was supplied *ad libitum*. NOD-SCID mice were housed under sterile conditions, fed with sterile rodent chow and sterile water was supplied *ad libitum*.

### 2.6 Software

All chemical structures reported in this thesis were generated using ChemSketch 2015 software (version 2: C10E41; Advanced Chemistry Development Labs, Toronto, ON). Collection and analysis of UPLC/MS data was performed using MassLynx control software (version 4.0, Waters Limited, Mississauga, ON). All statistical analyses, generation of bar charts and scattered plots presenting data were performed using GraphPad prism software (version 5; La Jolla, CA). Data obtained in the form of photographs (except *in vitro* angiogenesis assay) were quantified using ImageJ software (National Institute of Health, Ottawa, ON). Collection of flow cytometric data was performed using BD CellQuest™ software (version 3.3; BD Biosciences, Mississauga, ON) and data were analyzed using FCS Express software (version 3.0; De Novo Software, Thornhill, ON), with the exception of cell cycle analysis which was analyzed using ModFit LT software (Verity Software House, Topsham, ME). Quantification of protein concentrations was carried out using SoftMax software (version Pro 4.3 15;

Molecular Devices). Western blots developed using X-ray film exposure were quantified using Image Studio Digits™ software (version 4.0; Lincoln, NE) and blots developed using Bio-Rad Chemidoc system were analyzed using Bio-Rad Image Lab™ software (version 6.0; Bio-Rad Laboratories, Mississauga, ON).

### 2.7 Flow cytometry

Fluorescence of fluorochrome-labeled or GFP-tagged-cells was measured using a FACSCalibur flow cytometer (BD Biosciences, Mississauga, ON) equipped with BD CellQuest™ software. Appropriate unstained and/or single dye-stained control cells were used in assays involving cells co-stained with two different fluorochromes or dyes with overlapping emission spectra, and data acquisition was corrected using the compensation option. A minimum of $1 \times 10^4$ cells was collected for flow cytometric analysis. Cell counts were gated on the live cell population on FSC-H versus SSC-H plot and linked to relevant acquisition plots, except for Annexin-V-FLUOS/PI, Annexin-V-488/PI, 7-AAD staining and GFP-tagged-MDA-MB-231 cell analysis in NOD-SCID mouse lungs in which all cells were counted. The threshold was set to 52 on FSC-H for all assays, except for the cell cycle analysis coupled with or without Ki67 staining, in which a threshold of 20 on FL2-H was set.

### 2.8 Liquid chromatography/Mass spectrometry

PZ-DHA and/or PZ-DHA metabolites in malignant/non-malignant epithelial cell lysates, *in vitro* microsome enzyme reaction mixtures and mouse serum aliquots were determined using UPLC-ESI-MS/MS instrument (Waters Limited, Mississauga, ON). All mass spectroscopic analyses were performed using mass scan (MS; identification of unknowns) and single ion monitoring (SIM; quantification of PZ, DHA, PZ-DHA, and quercetin) modes of a Waters H-class UPLC separations module coupled with a Micromass Quattro micro API MS/MS system and MassLynx V4.0 control software. An Allure biphenyl (100 mm × 2.5 mm, 5.0 µm) column (Restek Pure Chromatography, Bellefonte, PA) and a flow rate of 0.3 mL/min was employed. ESI- mode with a capillary voltage of 3000 V and a nebulizer gas ($N_2$) temperature of 375°C were used. A volume of 2 µL sample was injected and the retention times were recorded using the solvent system detailed in Table 2.1.

**Table 2.1. Solvent system used for LC/MS analysis**

| Time (min) | Solvent gradient (% in mixture) | |
|---|---|---|
| | 0.1% v/v Formic acid in water | 0.1% v/v Formic acid in acetonitrile |
| 0 | 50 | 50 |
| 10 | 30 | 70 |
| 14 | 0 | 100 |
| 17 | 0 | 100 |
| 18 | 50 | 50 |
| 20 | 50 | 50 |

## 2.9 *In vitro* experiments

### 2.9.1 Preparation of mouse hepatic microsomal enzyme extractions

Mouse hepatic microsomes were freshly isolated from the livers of 2-6 month-old C57BL/6 female mice, and the entire extraction procedure was carried out at 4°C. Freshly harvested livers were snap frozen in liquid nitrogen and stored at -80°C. For microsome extraction, frozen livers were slowly thawed on ice and minced using sterile scalpel and forceps in 6-well plates. Minced livers were homogenized in KCl/Sucrose phosphate buffer (0.154 M KCl, 0.25 M sucrose in 50 mM potassium phosphate buffer ($K_2HPO_4/KH_2PO_4$) (PPB), pH 7.5), using a hand-held homogenizer. Cell/tissue debris were separated out by centrifuging homogenized livers at 12,000 ×g for 22 min at 4°C (Avanti J30I centrifuge, Beckman Coulter, Kraemer Blvd. Brea, CA). The supernatant was collected and centrifuged at 100,000 ×g for 70 min at 4°C (Avanti J30I centrifuge, Beckman Coulter, Kraemer Blvd. Brea, CA). The pellet was gently rinsed using 50 mM PPB and resuspended in glycerol/phosphate buffer (20% glycerol (v/v), 80% 0.1 M PPB pH 7.5). The protein concentration was determined using a Bradford assay ($R^2$=1.00) and SoftMax software (version Pro 4.3 15; Molecular Devices) and microsomes were stored in 900 µL aliquots at -80°C.

### 2.9.2 Cellular uptake assay

Cells (MDA-MB-231, MDA-MB-468, 4T1, MCF-7, and MCF-10A) were seeded at a density of $3 \times 10^5$ cells (MDA-MB-231, MDA-MB-468, MCF-7, and MCF-10A) or $1 \times 10^5$ cells (4T1) /T-75 flask. The cells were cultured overnight to promote cell adhesion. Adherent cells were treated with 20 µM of PZ, DHA or PZ-DHA and cultured for 72 h at 37°C. The supernatant was carefully removed, and cell monolayers were washed with cold 1×PBS. Cells were harvested using TrypLE Express and washed thoroughly with cold 1×PBS. Cell pellet was resuspended in 3 mL of cold acetone containing 0.05 mg/mL quercetin as the internal standard, and immediately transferred into glass scintillation vials, and incubated overnight at 4°C. Cell lysates were collected by centrifugation at 14,000 ×g for 15 min at 4°C and samples were concentrated by evaporating acetone under a stream of nitrogen gas. Dry pellets were reconstituted in 300 µL methanol and filtered through a 0.22 µm nylon filter, and 200 µL of the filtered lysate was transferred to HPLC inserts placed in an HPLC vial. Sample was analysed using a UPLC/ESI/MS system (see Supplementary Figure 1 for chromatograms). Cell uptake was quantified using standard curves of PZ ($R^2$=0.99), DHA ($R^2$=0.98) or PZ-DHA ($R^2$=0.99) made in methanol.

### 2.9.3 Determination of *in vitro* metabolites of PZ-DHA

Potential i*n vitro* phase I and phase II metabolites of PZ-DHA were detected by incubating PZ-DHA in the presence of freshly-prepared mouse hepatic microsome preparations. Phase I metabolites were determined by incubating 300 µM PZ-DHA with 100 mM NADPH in the presence of mouse hepatic microsome for 1 h at 37°C (Table 2.2). Phase II methylation (Table 2.3), glucuronidation (Table 2.4) and sulphation (Table 2.5) of PZ-DHA was determined by incubating 300 µM PZ-DHA with 1 mM SAM, 2 mM UDP-glucuronic acid (UDPGA) and 0.5 mM PAPS, respectively, in the presence of freshly prepared mouse hepatic microsome for 1 h at 37°C (see Supplementary Figure 2 for chromatograms of control experiments). To assess the efficiency of the metabolic process, controls were incubated in parallel to the test. Reactions were terminated by adding a mixture of 4 mL ice-cold acetonitrile:acetone (80:20) containing 0.05 mg/mL quercetin as the internal standard. Proteins were precipitated by incubating the reaction

mixture at 4°C overnight and separated by centrifuging at 14,000 ×g for 15 min at 4°C. Supernatants were concentrated under nitrogen flush, filtered and PZ-DHA and/or PZ-DHA metabolites were identified using UPLC/ESI/MS analysis.

**Table 2.2. Reaction mixture used for the determination of *in vitro* phase I metabolism of PZ-DHA.**

DMSO: Dimethyl sulfoxide; NADPH: Nicotinamide adenine dinucleotide phosphate; PPB: Potassium phosphate buffer; PZ-DHA: Phloridzin docosahexaenoate.

| Sample ID | Components of the reaction mixture (*Final concentration) | | | |
|---|---|---|---|---|
| | PZ-DHA in DMSO (*300 µM) (µL) | Mouse hepatic microsomes (*3 mg/mL) (µL) | NADPH in PPB (*100 mM) (µL) | PPB (µL) |
| Test | 6 | 334 | 100 | 1560 |
| Control 1 | - | 334 | 100 | 1566 |
| Control 2 | 6 | - | 100 | 1894 |
| Control 3 | 6 | 334 | - | 1660 |
| Control 4 | 6 | - | - | 1994 |

**Table 2.3. Reaction mixture used for the determination of *in vitro* phase II methylation of PZ-DHA.**

DMSO: Dimethyl sulfoxide; PZ-DHA: Phloridzin docosahexaenoate; SAM: S-(5′-Adenosyl)-L-methionine chloride.

| Sample ID | Components of the reaction mixture (*Final concentration) | | | |
|---|---|---|---|---|
| | PZ-DHA in DMSO (*300 µM) (µL) | Mouse hepatic microsomes (*3 mg/mL) (µL) | SAM in purified water (*1 mM) (µL) | Purified water (µL) |
| Test | 6 | 334 | 200 | 1460 |
| Control 1 | - | 334 | 200 | 1466 |
| Control 2 | 6 | - | 200 | 1894 |
| Control 3 | 6 | 334 | - | 1660 |

**Table 2.4. Reaction mixture used for the determination of *in vitro* phase II glucuronidation of PZ-DHA.**

DMSO: Dimethyl sulfoxide; PZ-DHA: Phloridzin docosahexaenoate; UDPGA: UDP-glucuronic acid.

| Sample ID | Components of the reaction mixture (*Final concentration) | | | | |
|---|---|---|---|---|---|
| | PZ-DHA in DMSO (*300 µM) (µL) | Mouse hepatic microsomes (*6 mg/mL) (µL) | UDPGA – Sol A (*2 mM) (µL) | Buffer with Alamethicin – Sol B (*25 µg/mL) (µL) | Purified water (µL) |
| Test | 6 | 334 | 160 | 400 | 1100 |
| Control 1 | - | 334 | 160 | 400 | 894 |
| Control 2 | 6 | - | 160 | 400 | 1434 |
| Control 3 | 6 | 334 | - | 400 | 1260 |

**Table 2.5. Reaction mixture used for the determination of *in vitro* phase II sulphation of PZ-DHA.**

DMSO: Dimethyl sulfoxide; PAPS: Adenosine 3′-phosphate 5′-phosphosulfate lithium salt hydrate; PZ-DHA: Phloridzin docosahexaenoate.

| Sample ID | Components of the reaction mixture (*Final concentration) | | | |
|---|---|---|---|---|
| | PZ-DHA in DMSO (*300 µM) (µL) | Mouse hepatic microsomes (*3 mg/mL) (µL) | PAPS in purified water (*0.5 mM) (µL) | Purified water (µL) |
| Test | 6 | 334 | 200 | 1460 |
| Control 1 | - | 334 | 200 | 1466 |
| Control 2 | 6 | - | 200 | 1894 |
| Control 3 | 6 | 334 | - | 1660 |

### 2.9.4 MTS assay

The metabolic activity of drug-treated human triple-negative, mouse triple-negative, human estrogen receptor-positive mammary carcinoma cells and non-malignant

mammary epithelial cells was measured using MTS assays (Fernando et al., 2016). Cells were seeded at the optimum density and cell attachment was supported by overnight culture. Adherent cells were treated with PZ, DHA, PZ-DHA (10, 50, 75, 100, 150 and 200 µM), vehicle control or medium control alone and cultured at 37°C for 3, 6, 12, 18 and 24 h. At the end of the incubation, 10 µL of combined MTS/PMS reagent (333 µg/mL MTS and 25 µM PMS) was added and incubated at 37°C for 3 h. The absorbance was measured at 490 nm using a microplate reader (BMG-LABTECH, Ortenberg, Germany) and the % metabolic activity was determined using the formula (2.1), where, $A_T$: absorbance of cells treated with drugs; $A_{TB}$: absorbance of treatment blank; $A_C$: absorbance of cells treated with vehicle control; $A_{CB}$: absorbance of vehicle blank.

$$\%\ \text{Relative metabolic activity} = \ (A_T - A_{TB}/A_C - A_{CB}) \times 100 \text{ ----------(2.1)}$$

### 2.9.5 MTT assay

The inhibitory effect of PZ-DHA and its parent compounds on the growth of MDA-MB-231-TXL cells (in comparison to parent MDA-MB-231) and endothelial cells (HUVECs and HMVECs) was tested using MTT assays (Greenshields et al., 2015). Cells were seeded in flat-bottom 96-well plates. MDA-MB-231 and MDA-MB-231-TXL cells were treated with PZ, DHA, PZ-DHA at 25, 50 and 100 µM and endothelial cells were treated with 10, 20, 30 and 40 µM drug concentrations for various times. At the end of the treatment, 10 µL of MTT reagent was added (454 µg/mL) and incubated at 37°C for 3 h. Formazan crystals were collected by centrifuging plates at 1400 ×g for 5 min. The supernatant was removed, and formazan crystals were dissolved in 100 µL of DMSO. The absorbance was measured at 570 nm using an Expert microplate reader (Admiral Place, Guelph, ON) and the % metabolic activity was determined using the formula, (2.2), where, $A_T$: absorbance of cells treated with drugs; $A_C$: absorbance of cells treated with vehicle control.

$$\%\ \text{Relative metabolic activity} = \ (A_T/A_C) \times 100 \text{ ----------(2.2)}$$

### 2.9.6 Annexin-V-FLUOS/PI and Annexin-V-488/PI staining

Induction of early apoptosis and late apoptosis/necrosis by PZ-DHA and its parent compounds was determined using Annexin-V-FLUOS/PI (MDA-MB-231, HDF, and

MCF-10A) or Annexin-V-488/PI (MDA-MB-231-TXL) staining (Greenshields et al., 2015). Cells grown in monolayers were seeded at a density of $5 \times 10^4$ (48 and 72 h) or $1 \times 10^5$ (24 h) cells per well in 6-well plates and cultured overnight at 37°C to induce cell adhesion. Adherent cells were treated with 50 μM of PZ, DHA, PZ-DHA, vehicle control or medium control alone at 37°C for 24-72 h. Cells grown in monolayers were harvested using TrypLE express and combined with their respective medium. Cells were centrifuged and rinsed with 1×PBS and incubated with Annexin-V-FLUOS or Annexin-V-488 (1 μg/mL) and PI (1 μg/mL) in staining buffer (10 mM HEPES, 10 mM NaCl, and 5 mM $CaCl_2$) at room temperature for 15 min. Flow cytometric analysis was performed using a FACSCalibur instrument (BD Bioscience, Mississauga, ON) on detectors, FL1 and FL2. Cells ($1 \times 10^4$) were counted per sample, and both live and dead cells were included in counts.

### 2.9.7 7-AAD assay

All *in vitro* cellular uptake, anti-proliferative, anti-metastatic and anti-angiogenic assays were performed using sub-cytotoxic concentrations of PZ, DHA, and PZ-DHA. The sub-cytotoxic concentration ranges of PZ-DHA and parent compounds toward MDA-MB-231 cells, HUVECs and HMVECs were determined using flow cytometric assay of 7-AAD-stained cells (Fernando et al., 2016). 7-AAD distinguishes dead cells from viable cells by intercalating between cytosine and guanine bases of DNA of dead cells (Philpott et al., 1996; Schmid et al., 1992). MDA-MB-231 cells, HUVECs or HMVECs were plated at a density of $5 \times 10^4$ cells per well in 6-well plates. The cells were cultured overnight to induce cell adhesion. Adherent cells were treated with 10, 20, 30, 40 and 50 μM of PZ, DHA, PZ-DHA, vehicle control or medium control alone and cultured for 72 h. Cells were harvested using TrypLE Express, washed and resuspended in 1×PBS. Cells in PBS were incubated with 5 μL of 7-AAD viability staining solution (eBioscience Inc. San Diego, CA) at room temperature for 5 min. Flow cytometric analysis was performed using a FACSCalibur instrument (BD Bioscience, Mississauga, ON) on the detector, FL3. Cells ($1 \times 10^4$ cells/sample) were counted; both live and dead cells were included in counts.

### 2.9.8 Oregon Green 488 staining

Sub-cytotoxic antiproliferative activity of PZ-DHA on MDA-MB-231 cells, HUVECs and HMVECs was measured using Oregon Green 488 dye and flow cytometry (Greenshields et al., 2015). Cells were synchronized to $G_0$ phase by incubating the cell monolayers in serum-free medium for 20 h. Synchronized cells were plated in 6-well plates at a density of $5 \times 10^4$ cells/well. Cells were cultured overnight to promote cell adhesion. Adherent cells were stained with 1.25 µM Oregon Green 488 (Life Technologies Inc., Burlington, ON) in serum-free DMEM for 45 min. Oregon Green 488-stained cells were incubated in respective complete growth medium for 2 h to induce cell recovery and cells in two wells were harvested using TrypLE Express and fixed in 1% paraformaldehyde for future use as a reference. The remainder of the cells were treated with sub-lethal concentrations (10, 20 and 30 µM) of PZ, DHA, PZ-DHA, vehicle or medium control alone and cultured in the dark for 72 h. Cells were harvested using TrypLE Express, washed using 1×PBS and the flow cytometric analysis was performed using a FACSCalibur instrument (BD Bioscience, Mississauga, ON) on the detector, FL1. Cells ($1 \times 10^4$) were counted and only the live cells were included in counts. The number of cell divisions (n) took place was calculated using the formula (2.3), where, MF is the mean fluorescence.

$$MF_{control} = 2^n \times MF_{treatment} \text{----------(2.3)}$$

### 2.9.9 Cell cycle analysis

Anti-proliferative activity of PZ-DHA on MDA-MB-231 and HUVEC cells were further studied by conducting cell cycle analysis (Greenshields et al., 2015; Smith et al., 2016). Synchronized cells were seeded and cultured overnight to promote cell attachment. Attached cells were treated with sub-cytotoxic concentrations (10, 20 and 30 µM) of PZ, DHA, PZ-DHA, vehicle or medium control and cultured for 72 h. At the end of culture, cells were harvested using TrypLE Express, centrifuged at 500 ×g, rinsed with ice-cold 1×PBS, and resuspended in ice-cold 1×PBS. While vortexing, ice-cold 70% ethanol was flowed slowly, drop-by-drop and incubated for at least 24 h at -20°C to support fixing. Fixed cells were washed with 1×PBS and resuspended in cell cycle solution (0.1% v/v Triton-X-100 and 2 µL/mL DNA-free Rnase A in 1×PBS) containing 20 µL/mL PI and

incubated for 30 min at room temperature. Flow cytometric analysis was performed using a FACSCalibur instrument (BD Bioscience, Mississauga, ON) on FL2A and FL2W. Cells ($1 \times 10^4$) were counted per sample and counts were gated on the FL2A vs FL2W plot to eliminate cell aggregates.

### 2.9.10 Cell cycle analysis/Ki67 staining

Synchronized-MDA-MB-231 cells were seeded and cultured overnight to allow for adherence. Adherent cells were treated with PZ, DHA, PZ-DHA (30 μM), vehicle control or medium control for 72 h. Cells were harvested, washed and resuspended in ice-cold PBS. While vortexing, ice-cold 70% ethanol was slowly flowed and incubated for at least 24 h at −20°C to promote cell fixation. Ethanol was removed by centrifugation, and the fixed cells were washed thoroughly with staining buffer (PBS with 1% FBS and 0.09% $NaN_3$). Cells were incubated for 30 min at room temperature with 2.5 μg/mL FITC-conjugated anti-Ki67 antibodies in staining buffer. Cells were again washed thoroughly to remove excess antibodies and resuspended in cell cycle solution (0.1% Triton X-100 in PBS containing, 0.02 mg/ml PI and 0.2 mg/ml of DNA-free Rnase A) and incubated for another 30 min at RT. Flow cytometric analysis was performed using a FACSCalibur instrument (BD Bioscience, Mississauga, ON) on FL1, FL2A, and FL2W. Cells ($1 \times 10^4$) were counted per sample and only single cells were included in counts by gating on the FL2A vs FL2W plot to eliminate cell aggregates.

### 2.9.11 Breast cancer spheroid formation assay

MCF-7 cells ($1 \times 10^4$ cells) were grown in ultra-low adherent cell culture plates in spheroid growth medium (F12 medium supplemented with 20 ng/mL bFGF, 20 ng/mL EGF, 100 U/mL penicillin, 100 μg/mL streptomycin and B27 serum-free supplement) for 48 h and treated with PZ, DHA, PZ-DHA (50 μM), vehicle control or medium control alone for 72 h. Following culture, spheroids were photographed using a phase contrast microscope (Nikon eclipse TS 100 phase contrast microscope, Melville, NY) and the viability of cells in spheroids was determined using an acid phosphatase assay (Greenshields et al., 2015, 2017).

### 2.9.12 Acid phosphatase assay of spheroids

The viability of drug-treated MCF-7 cells in breast cancer spheroids was measured using acid phosphatase assay. The acid phosphatase assay measures the phosphatase enzyme activity of live cells. This assay was chosen over an MTS assay because the acid phosphatase assay buffer lyses the cells prior to analysis, allowing determination of the total phosphatase activity of cells in the entire spheroid population. In contrast, the MTS assay reagent mixture would not reach the cells in the core of the spheroids. For acid phosphatase assays, spheroids were washed using 1×PBS and resuspended in 1 mL acid phosphatase assay solution (0.1 M sodium acetate at pH 5.5, 0.1% Triton-X-100, 4 mg/mL phosphatase substrate) and incubated for 2 h at 37°C in the dark. The reaction was stopped by adding 25 µL 1 N NaOH. Absorbance was measured at 405 nm and % acid phosphatase activity was determined as in formula (2.4), where, $A_T$: absorbance of cells treated with drugs; $A_C$: absorbance of cells treated with vehicle control; $A_B$: absorbance of the blank.

$$\%\ \text{Relative acid phosphatase activity} = (A_T - A_B / A_C - A_B) \times 100 \text{ ----------(2.4)}$$

### 2.9.13 Adhesion assay

The effect of PZ, DHA, and PZ-DHA on the interaction of breast cancer cells with endothelial cells was modeled by studying the *in vitro* adhesion of GFP-tagged MDA-MB-231 cells to HUVECs grown as a monolayer in 0.1% w/v gelatine-coated 12-well plates. GFP-tagged MDA-MB-231 cells were seeded in 6-well plates and cultured overnight at 37°C to promote cell attachment. Adherent GFP-MDA-MB-231 cells were treated with 20 µM of PZ, DHA, PZ-DHA, vehicle or medium control and cultured for 24 h. Confluent HUVEC monolayers were activated by 20 ng/mL TNF-α treatment for 4 h. Activated HUVECs were incubated with 1% w/v BSA prepared in 1×PBS for 15 min at 37°C to block any non-specific binding sites. PZ-, DHA-, PZ-DHA-, vehicle- or medium-treated GFP-MDA-MB-231 cells were detached and seeded onto HUVEC monolayers at a $5\times10^4$ cells/well density and incubated for 30 min at 37°C. At the end of the incubation, the supernatant was removed and the HUVEC monolayer was carefully rinsed with PBS. All cells were detached using TryPLE Express and GFP-expressing MDA-MB-231 cells were detected using a SSC-H vs FL1 plot of a FACSCalibur

instrument (BD Bioscience, Mississauga, ON). Only live cells ($1\times10^4$) were included in counts.

### 2.9.14 Gap closure assay

The ability of PZ-DHA and its parent compounds to inhibit the migration of mammary carcinoma cells and endothelial cells were first tested using the gap closure assay (Doucette et al., 2013; Greenshields et al., 2015). In the gap closure assay, MDA-MB-231 cells ($10^4$ cells/well), 4T1 cells ($8 \times 10^3$ cells/well) and HUVECs ($10^4$ cells/well) were seeded in cell culture inserts (ibidi GmbH, Martinsried, Germany) placed in 6-well plates. Cells were cultured overnight at 37°C to support cell adhesion, and monolayers were treated with mitomycin C for 2 h (MDA-MB-231: 10 μM, 4T1: 20 μM, HUVEC: 10 μM) to suppress the proliferation of cells. Cells were allowed to recover overnight and treated with 20 μM of PZ, DHA, PZ-DHA (MDA-MB-231 and 4T1) or 10 μM PZ, DHA, PZ-DHA (HUVEC), vehicle or respective medium control alone for 24 h. At the end of the treatment, inserts were carefully removed exposing a "gap" and monolayers were washed with 1×PBS. Treatments were continued, and the gap was photographed until the gap was completely closed by medium-treated control cells (Nikon Eclipse TS 100 phase contrast microscope, Melville, NY). Images were quantified using ImageJ software and % number of cells migrated toward the gap were determined and normalized to the medium control.

### 2.9.15 Trans-well chemo-migration and chemo-invasion assays

Chemotactic migration and invasion of MDA-MB-231 cells, TGF-β-induced MCF-10A/MDA-MB-231 migration, and HUVEC migration toward serum was studied using chemotaxis chamber assays (Zhou et al., 2014). Cells were seeded and cultured overnight to allow cell adhesion. Adherent cells were treated with 10 μM (HUVEC) or 20 μM (MDA-MB-231 and MCF-10A) of PZ, DHA, PZ-DHA, vehicle control or medium control alone for 24 h and treatments were continued in serum-free medium for another 6 h (MDA-MB-231 and HUVEC) or 12 h (MCF-10A). When studying TGF-β-induced MCF-10A/MDA-MB-231 migration, cells were pre-treated with 10 ng/mL TGF-β for 24 h and followed by 5 ng/mL TGF-β in the presence of test compounds. At the end of the treatment, cells were harvested using TryPLE Express, resuspended in warm serum-free

medium at $1 \times 10^6$ cells/mL density, and 50 µL of cell suspension was loaded to the wells of the of the top chamber. Cells were allowed to migrate through an 8 µm porous membrane for 22 h and migrated cells were stained using a Diff-Quik™ staining set (Siemens Healthcare Diagnostics, Los Angeles, CA). Stained cells were photographed (Nikon eclipse TS 100 phase contrast microscope, Melville, NY) and % migrated cells were quantified using ImageJ software and normalized to the medium control.

### 2.9.16 Preparation of protein-rich cell lysates

Whole cell lysates were prepared using MDA-MB-231 cells, MDA-MB-231-TXL cells, MCF-10A cells or HUVECs treated with 10 or 20 µM of PZ, DHA, PZ-DHA, vehicle control or medium control alone for 24 or 72 h. Harvested cells were incubated in ice-cold lysis buffer (50 mM Tris (pH 7.5), 150 mM NaCl, 50 mM $Na_2HPO_4$, 0.25% sodium deoxycholate (w/v), 0.1% Nonidet P-40 (v/v), 5 mM ethylenediaminetetraacetic acid and 5 mM ethylene glycol tetraacetic acid) containing freshly added protease inhibitors (100 µM $Na_3VO_4$, 10 mM NaF, 1 mM phenylmethylsulfonylfluoride (freshly added), 10 µg/mL aprotinin, 5 µg/mL leupeptin, 10 µM phenylarsine oxide, 1 mM dithiothreitol and 5 µg/mL pepstatin) for 15 min. Cell lysates were separated by centrifugation at 14,000 ×g for 10 min at 4°C, and the protein concentration was determined by Bradford protein assay ($R^2$=0.99-1.00). After adding SDS PAGE sample buffer, protein samples were stored at -80°C.

### 2.9.17 Western blot analysis

The effect of PZ-DHA on PI3K/Akt/mTOR, MAPK signaling pathways, small molecular Rho GTPase signaling, expression of cell cycle proteins, drug efflux transporters and transcription factors involved in EMT pathway was investigated using western blot analysis. Protein-rich cell lysates (10 -40 µg proteins) were loaded into 7.5, 10, 12 or 15% SDS polyacrylamide gels, as appropriate for the protein being studied. Proteins were transferred to nitrocellulose membranes, and blots were incubated in 5% non-fat milk or 5% BSA prepared in Tween-TBS [0.25 M Tris (pH 7.5), 150 mM NaCl and 0.2% Tween-20] for 1 h to block nonspecific binding. Blots were probed overnight at 4°C with primary Ab against phospho-PTEN (Ser380), phospho-PDK1 (Ser241), phospho-Akt (Ser473/Thr308), phospho-mTOR (Ser2448), phospho-GSK3-β (Ser9), phospho-GSK3-β

(Tyr216), phpspho-cRAF (Ser259), phospho-ERK1/2 p44 (Thr202)/p42 (Tyr204), phospho-CREB (Ser 133), total-PTEN, total-PDK1, total-Akt, total-mTOR, total-GSK3-β, total-RAS-GRF1, total-cRAF, total-ERK1/2 p44/p42, and CREB to test the effect of PZ-DHA and its parent compounds on Akt and MAPK signaling pathways. The effect of test compounds on cell cycle progression was tested by probing blots with Ab against CDK1, CDK2, CDK4, cyclinA2, cyclinB1 and cyclinD3. PZ-DHA-mediated expression of drug efflux transporters were tested by probing the blots with Ab against ABCG2 and MRP1. PZ-DHA-induced changes to the transcription factors involved in EMT of breast cancer cells was determined by probing blots with Ab against ZEB1, β-catenin, slug1, vimentin, pan-cadherin and MMP2. The effect of PZ-DHA on the expression of small molecular Rho GTPases was determined by probing blots with Ab against RhoA, Cdc42, and Rac1/2/3. Then the blots were washed thoroughly with 0.05% Tween-TBS and probed with HRP-conjugated donkey anti-rabbit or goat anti-mouse IgG Ab for 1 h at room temperature. Even protein loading was confirmed by probing the blots with HRP-conjugated rabbit anti-actin Ab or primary Ab against α-tubulin followed with HRP-conjugated donkey anti-rabbit IgG Ab. The proteins of interest were visualized by X-ray film exposure or ChemidocTouch™ imaging system (Bio-Rad Laboratories, Mississauga, ON).

### 2.9.18 *In vitro* angiogenesis assay

When grown on a Matrigel matrix, endothelial cells differentiate to form tubule-like structures that create a polygonal network. The *in vitro* angiogenesis assay was performed using commercially available *in vitro* angiogenesis ECMatrix™ assay kit (EMD Millipore, Temecula, CA), according to manufacturer's instructions. Briefly, 9 parts of the Matrigel matrix was mixed with one part of the diluent buffer and 10 µL of the mixture was added into the inner well of the µ-slide angiogenesis plate (ibidi GmbH, Martinsried, Germany). The plate was incubated at 37°C for 1 h. HUVECs or HMVECs (7500 cells) treated with 10 µM (HMVECs) or 20 µM (HMVECs) PZ, DHA, PZ-DHA, vehicle control or medium control alone for 72 h were resuspended in 50 µL of EGM and seeded onto polymerized ECMatrix. Tube formation by HUVECs and HMVECs was monitored and photographed after 6 h and 4 h, respectively. Images were analyzed as detailed in table 2.6.

**Table 2.6. Angiogenesis pattern and scoring**

| Pattern of endothelial cell arrangement | Angiogenesis score |
|---|---|
| Well separated individual cells. | 0 |
| Cells begin to migrate and align themselves. | 1 |
| Capillary tubes visible; no sprouting. | 2 |
| Sprouting of new capillary tubes visible. | 3 |
| Closed polygons begin to form. | 4 |
| Complex mesh-like structures develop. | 5 |

### 2.9.19 Mycoplasma test

Apart from routine mycoplasma assays, rodent pathogen-free MDA-MB-231 and 4T1 cells used for *in vivo* experiments were specifically tested for mycoplasma prior to inoculation into mice. The mycoplasma test was performed per the manufacturer's instructions (MycoAlert® Mycoplasma detection kit, Lonza, Rockland, ME) the day before subcutaneous injection of cells. Briefly, culture medium (50 µL) was incubated with 50 µL of reagent for 5 min at room temperature and luminescence was read on a luminator and recorded the reading as "A". The substrate (50 µL) was added to the reaction mixture and incubated for another 10 min at room temperature and recorded the second reading, "B" on luminator. The ratio of B⁄A>1.2 considered to indicate mycoplasma contamination.

## 2.10 *Ex vivo* experiments

### 2.10.1 *Ex vivo* angiogenesis assay

The *ex vivo* angiogenesis assay was conducted as previously described with minor modifications (Bauer et al., 2000; Béliveau et al., 2002). Thoracic aortas from adult male Wistar rats were harvested. The inside and outside of the aortas were cleaned using sterile saline and aortas were sectioned into 1×3 mm sections. Sectioned aortas were then placed in a 48-well plate coated with 100 µL growth factor-reduced phenol red-free Matrigel and incubated in a humidified incubator supplied with 5% $CO_2$ at 37°C for 1 h. Aorta sections were covered with another 100 µL Matrigel and incubation was continued for another 30 min. Matrigel was covered with 200 µL EGM and incubated overnight at 37°C (day 0).

On day 1, aorta sections embedded in Matrigel was treated with PZ, DHA, PZ-DHA (20 μM), vehicle alone or medium alone for 8 days. Medium/treatment was changed on day 4. Development of tubules from aortic endothelium was monitored and photographed on day 5 and 8.

## 2.11 *In vivo* experiments

### 2.11.1 Determination of *in vivo* metabolites and pharmacokinetic parameters of PZ-DHA

Pharmacokinetic parameters and *in vivo* generation of PZ-DHA metabolites were studied using Balb/c female mice. Mice were randomly divided in to six groups (n=4) and PZ-DHA (100 mg/kg) was administered by intraperitoneal injection. Blood (800 μL) collection was performed by cardiac puncture, at six different time points (t=15, 30, 60, 90, 120 and 240 min). At the end of blood collection, mice were euthanized by cervical dislocation and organs (liver, lungs, kidneys, spleen and brain) were harvested. Blood samples were allowed to clot by leaving undisturbed at room temperature for 1 h and serum was separated by centrifuging at 2,000 ×g for 10 min at 4°C. Serum was carefully removed and stored on ice until further processing. Serum proteins were precipitated by incubating an aliquot of serum (500 μL) with a mixture of acetonitrile:acetone (80:20) (1 mL) containing 0.1 mg/mL quercetin (internal standard) at 4°C overnight. The supernatant was separated by centrifuging at 14,000 ×g for 10 min at 4°C. Excess solvent was evaporated using nitrogen flush to obtain a 200 μL volume, which was mixed with 200 μL methanol and filtered. The filtrate (200 μL) was transferred into HPLC inserts, and PZ-DHA and/or PZ-DHA-metabolites were identified using a UPLC-ESI-MS/MS instrument (Waters Limited, Mississauga, ON). A calibration curve ($R^2$=0.99) generated using a standard series of PZ-DHA concentrations prepared in mouse serum (spiked with 0.1 mg/mL quercetin) was used for quantification of PZ-DHA. Organs were stored in individual Eppendorf tubes and flash frozen by immersing in liquid nitrogen for 10-15 sec before storing at -80°C until further processing. Organs were thawed on ice, weighed and homogenized in PBS (1:5 w/v). Supernatants were collected by centrifugation at 14,000×g for 15 min at 4°C. Proteins were precipitated by incubating 1 volume of homogenate with 2 volumes of acetonitrile:acetone (80:20) containing 0.1 mg/mL

quercetin (internal standard) at 4°C overnight. Supernatants were treated as explained above, and PZ-DHA and/or PZ-DHA-metabolites were identified.

### 2.11.2 PZ-DHA treatment and blood collection

Saline or PZ-DHA (100 mg/kg, a dose typically used to investigate the pharmacological activities of phytochemicals (Gallo et al., 2008; Hashemzaei et al., 2017; Rahman et al., 2017)) was administered by intraperitoneal injection to 8-week old Balb/c female mice every second day for 9 days (5 doses). Body weights were recorded, and on day 10, blood (500 µL) was collected by cardiac puncture. Blood was allowed to clot by incubating at room temperature for 1 h and clot was removed by centrifuging at 2,000 ×g for 10 min at 4°C. Serum was carefully separated and alanine transaminase (ALT) and creatinine assays were performed.

### 2.11.3 Alanine transaminase (ALT) assay of Balb/c female mouse serum

The effect of PZ-DHA on the liver function of Balb/c female mice was tested using ALT activity assay of mouse serum (Cayman Chemical, Ann Arbor, MI). ALT is an enzyme abundantly found in liver; however, under certain disease conditions that cause liver damage, ALT is released into blood resulting in elevated serum ALT (Kim et al., 2008; Limdi and Hyde, 2003; Pratt and Kaplan, 2000). Crystalline L-alanine and porcine heart ALT were used as the ALT substrate and ALT positive control, respectively. Both substances were dissolved in ALT assay buffer (100 mM Tris-HCl, 10 mM sodium bicarbonate, 0.1 mM pyridoxal-5-phosphate and 0.01% sodium azide). NADH and LDH dissolved in ALT assay buffer were used as co-factors for the reaction. The assay was performed in a 96-well plate. L-alanine (150 µL), co-factor mixture (20 µL), porcine heart ALT or serum samples (20 µL) were added to wells and incubated at 37°C for 15 min. The reaction was initiated by adding 20 µL of 150 mM α-ketoglutarate, and absorbance was measured at 340 nm once every minute for a period of 5 min. The rate of change in absorbance at 340 nm ($\Delta A_{340}$) was determined using a calibration curve ($R^2$=0.99), and ALT enzyme activity was determined using the formula (2.5), where, ε is the extinction coefficient of NADH.

$$\text{ALT activity } \left(\frac{\text{U}}{\text{mL}}\right) = \frac{\Delta A_{340}/\text{min} \times 0.21\ mL}{\varepsilon\ mM^{-1}cm^{-1} \times 0.02\ mL} \text{ ----------(2.5)}$$

### 2.11.4 Creatinine assay of Balb/c female mouse serum

Creatinine is the breakdown product of creatine metabolism in muscles and creatinine clearance is often used for clinical measurement of renal function (Brater, 2002; Chu et al., 2016; Waikar and Bonventre, 2009; Zhang et al., 2015b). Therefore, a creatinine assay was used to determine the effect of PZ-DHA on the renal function of Balb/c female mice (Cayman Chemical, Ann Arbor, MI). A standard curve of creatinine was generated using a 20 mg/dL creatinine stock made in water. Creatinine standard or serum samples (15 µL) was diluted in 100 µL of assay reaction buffer (sodium borate, creatinine surfactant, and 1M sodium hydroxide solution) in a 96-well plate. Timing was begun immediately after adding 1.2% picric acid (100 µL), and absorbance was measured at 492 nm after 1 min and 7 min. Adjusted ΔOD was determined according to formula (2.6), and a creatinine calibration curve was generated. Creatinine concentration in samples was determined using the calibration curve ($R^2$=0.98).

$$\Delta OD = A_{492\,(7\,min)} - A_{492\,(1\,min)} \text{ ----------(2.6)}$$

### 2.11.5 4T1 mouse mammary carcinoma syngeneic metastatic model

4T1-implanted Balb/c mice are a well-established syngeneic model of mammary carcinoma cell metastasis. Inoculation of 4T1 cells was carried out as detailed in Figure 2.1A, with minor modifications (Abu et al., 2015; Lai et al., 2012). Rodent pathogen and mycoplasma-free highly aggressive 4T1 mouse mammary carcinoma cells were thawed from liquid-nitrogen five days before implantation and cultures were maintained in cDMEM. Cells were maintained on ice to achieve the maximum viability, and $10^5$ cells in 50 µL of sterile PBS were injected into the left inguinal mammary fat pad of Balb/c female mice (Day 0). On day 8, mice were randomly assigned into two groups (n=9) and intraperitoneal administration of saline or PZ-DHA (100 mg/kg) was started. Altogether, 5 doses of saline or PZ-DHA was administered every other day (Day 8, 10, 12, 14 and 16) for 9 days. Body weights and tumor volumes were recorded at the time of treatment. Tumor volume was calculated per the formula (2.7), where L is the longest tumor diameter and P is the diameter perpendicular to the longest diameter measured using a digital caliper. Mice were monitored for another day and euthanized on day 17. Mice and their primary 4T1 tumors were excised and photographed. The primary tumors were

weighed and fixed in 10% v/v acetate-buffered formalin. Lungs were harvested and finely minced in 1 mL Hank's balanced salt solution (HBSS). Minced lungs were dissociated in digestion buffer (0.75 mg/mL collagenase from *Clostridium histolyticum*, 0.25 mg/mL DNAse I from bovine pancreas and 0.05 mg/mL elastase from porcine pancreas) at 37°C for 1 h. Cell homogenate was passed through a 40 µm cell strainer and rinsed with HBSS. The cell suspension was centrifuged at 500 ×g for 5 min. The cell pellet was resuspended in cDMEM supplemented with 6-thioguanine (60 µM) cultured in petri dishes at 1/10, 1/50, 1/250 and 1/500 dilutions. Petri dishes were incubated at 37°C for 14 days, and 4T1 colonies were visualized using 0.4% w/v crystal violet stain prepared in 25% methanol.

$$Tumor\ volume = L \times P^2 \text{ ----------(2.7)}$$

### 2.11.6 MDA-MB-231 human breast xenograft metastatic model

The anti-metastatic activity of PZ-DHA was further tested using NOD-SCID mice xenografted with GFP-MDA-MB-231 cells, as detailed in Figure 2.1B. Mouse pathogen-free GFP-tagged MDA-MB-231 cells were tested for mycoplasma contamination on the day before xenografting into NOD-SCID mice. MDA-MB-231 cells were placed on ice before xenografting, and $2 \times 10^6$ cells in 50 µL PBS mixed with 50 µL Matrigel were injected into the left inguinal mammary fat pad of NOD-SCID mice (Day 0). On day 21, mice were randomly divided into two groups (n=10) and intraperitoneal administration of saline or PZ-DHA (100 mg/kg) was started. Altogether, mice received 20 doses of saline or PZ-DHA every other day for 39 days (Day 21, 23, 25, …, 55, 57 and 59). Body weights and tumor volumes were measured at the time of treatment as described above and mice were euthanized on day 60. Primary tumors were processed as described above and lungs were harvested to quantify metastasis. Lungs were mechanically dissociated using a sterile scalpel and passed through a 40 µm cell strainer to obtain a single-cell suspension and incubated in red blood cell lysis buffer (8.4 mg/mL $NH_4Cl$ and 1 mg/mL $KHCO_3$ in $dH_2O$) for 5 min. Lung cells were washed and resuspended in 0.5 % w/v BSA in PBS. GFP-positive MDA-MB-231 cells were detected at FL1 using a FACSCalibur (BD Bioscience, Mississauga, ON). All cells were included in cell counts and $2 \times 10^4$ cells were counted.

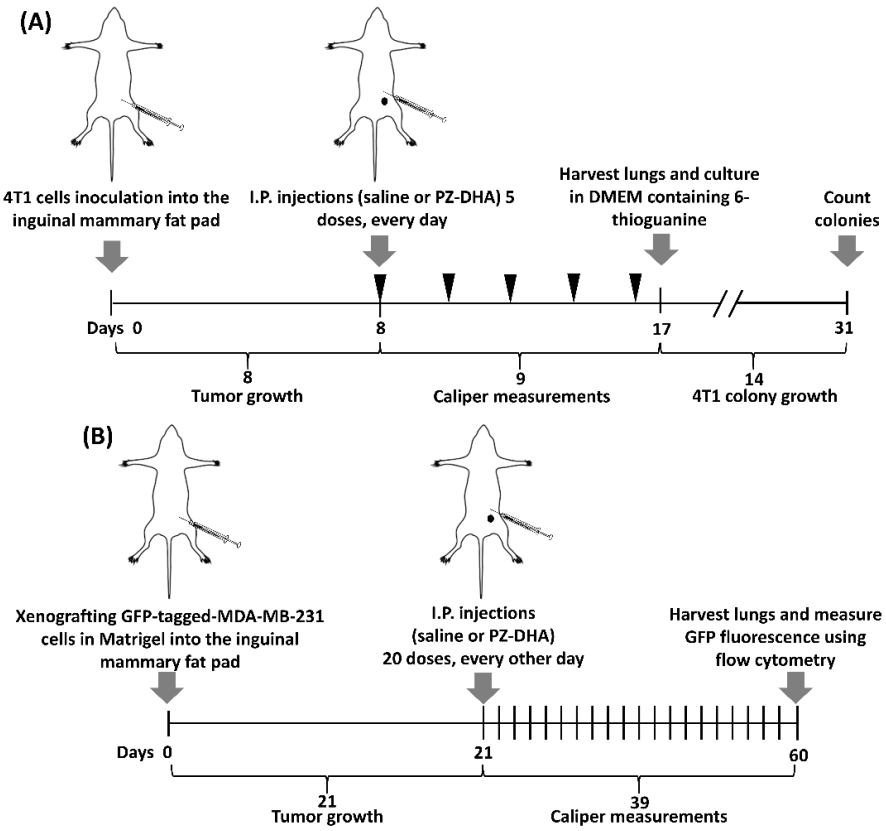


**Figure 2.1. Syngeneic and xenograft mouse models of mammary carcinoma cell growth and metastasis.**

Tumor suppressor activity and anti-metastatic activity of PZ-DHA was investigated using two mouse models of metastatic breast cancer. **(A)** 4T1 mouse mammary carcinoma cells ($1 \times 10^5$ cells) were injected into the left inguinal mammary fat pad of Balb/c female mice. Intraperitoneal injections of saline or PZ-DHA were started on day 8 and continued every second day until day 16. Caliper measurements of tumors were recorded and tumor volumes were determined as mean ($mm^3$)±SEM. On day 17, mice were euthanized and photographed. The primary tumors were harvested, weighed and photographed. Lungs were harvested to study the metastasis. Primary tumors were fixed in 10% buffered formalin and histological analysis was performed on sectioned tumors. Homogenized lungs were cultured on cDMEM containing 6-thioguanine (to promote selective growth of 4T1 cells) and incubated for 14 days at 37°C in a humidified incubator with 5% $CO_2$ and 95% filtered air. The number of cells metastasized into lungs were determined by colony-forming assay. **(B)** GFP-transfected MDA-MB 231 breast cancer cells ($2 \times 10^6$ cells) were injected into the left inguinal mammary fat pad of NOD-SCID female mice. Intraperitoneal administration of saline or PZ-DHA were started in day 21 and injections were continued every second day until day 59. Caliper measurements of tumors were recorded and tumor volumes were determined as mean ($mm^3$)±SEM. On day 60, mice were euthanized and photographed. The primary tumors were harvested, weighed and photographed. Lungs were harvested to study the metastasis. Primary tumors were fixed in 10% buffered formalin and sectioned. Sectioned tumors were subjected to histological analysis. The number of cells metastasized into lungs were determined by the FL1 detector of flow cytometry.

### 2.11.7 *In vivo* Matrigel plug assay

*In vivo* anti-angiogenic activity of PZ-DHA was assessed using the Matrigel plug assay, as previously described (Mader et al., 2006) with minor modifications. Phenol red-free Matrigel (300 µL) containing human $VEGF_{165}$ (2 µg/mL) and bFGF (2 µg/mL) was implanted by subcutaneous injection on both left and right sides along the mid-dorsal line of the lower posterior area of Balb/c female mice (Day 0). On day 1, mice were randomly assigned into two groups (n=12), and saline or PZ-DHA (100 mg/kg) was administered by intraperitoneal injection. Altogether, 5 doses of saline or PZ-DHA was administered every second day (Day 1, 3, 5, 7 and 9) for 9 days. Mice were euthanized by cervical dislocation and Matrigel plugs were harvested and photographed. One Matrigel plug from each mouse was weighed and hemoglobin concentration was determined.

### 2.11.8 Cyanmethemoglobin assay

The hemoglobin concentration in Matrigel plugs was determined using the cyanmethemoglobin method (Malinda, 2009; Pratheeshkumar et al., 2012). A human hemoglobin (0.717 mg/mL) solution made in Drabkin's reagent (containing 0.0005% v/v 30% Brij 23 solution) (cyanmethemoglobin solution) was used to generate the standard curve of cyanmethemoglobin ($R^2$=1.00). Matrigel plugs were homogenized in 500 µL of Drabkin's reagent and homogenates were centrifuged at 9600 ×g at 4°C for 6 min. The supernatant was collected and transferred into 96-well plates in triplicate. Absorbance was measured at 540 nm and cyanmethemoglobin concentration in Matrigel plugs was calculated using SoftMax software.

### 2.11.9 Histology

4T1 and MDA-MB-231 primary tumors harvested from Balb/c and NOD-SCID mice, respectively were subjected to histological analysis to detect tumor necrosis and test the effect of PZ-DHA on the expression of the proliferation marker Ki67, the invasion marker MMP2, and endothelial marker CD31. Tumors were fixed in 10% buffered-formalin and embedded in paraffin. Tumors were sectioned into 5 µm thick sections, mounted on glass slides and oven dried overnight. Dried sections were used for hematoxylin and eosin staining and immunohistochemistry.

#### 2.11.9.1 Hematoxylin and eosin staining

Tumor sections were deparaffinized using xylene and rehydrated using graded ethanol to water. The sections were rinsed under running tap water and incubated in Harris hematoxylin for 2 min at room temperature. Excess stain was rinsed under running tap water and incubated in Scott's water for 2 min at room temperature. Excess reagents were rinsed under running tap water and quickly dipped in 2% nitric acid to remove any possible calcification of the tumors. After a thorough rinse in water, sections were retuned into Scott's water and incubated until tumor sections turned into blue. After rinsing excess reagent, the sections were stained with eosin Y and dehydrated using graded ethanol to water. Dehydration was completed by immersing in xylene and sectioned were covered and observed under a bright-field microscope at ×200 and ×400 magnification. A number of tumor-associated blood vessels were counted and Pearson correlation statistics were performed.

#### 2.11.9.2 Immunohistochemistry

Deparaffinized tumor sections were pre-treated with sodium acetate (pH 6.0) (Ki67 and MMP2) or TAE buffer (pH 9.0) (CD31) for heat-mediated antigen retrieval. Sections designated for Ki67 and MMP2 were incubated in 3% v/v $H_2O_2$ for 10 min. Then tumor sections were blocked for non-specific binding using Rodent M block and incubated with mouse monoclonal anti-Ki67, mouse monoclonal anti-MMP2 or rabbit monoclonal anti-CD31 Ab overnight at room temperature. Slides incubated with rabbit monoclonal anti-CD31 Ab were then incubated in 3% v/v $H_2O_2$ for 10 min. Ki67-stained tumor sections were incubated with MACH 4 MR AP polymer and detected using Vulcan fast red chromogen kit 2. MMP2-stained sections were incubated with mouse-on-mouse HRP-polymer for 30 min at room temperature and detected using HRP/DAB detection system. CD31-stained sections were incubated with anti-rabbit HRP-polymer and detected using HRP/DAB detection system. Tumor sections were thoroughly washed using Tween20-tris-buffered saline (pH=8.4) between each step and counter stained using Mayer's hematoxylin and aqueous mounting was carried out. Dried sections were examined under a bright-field microscope at ×200 and ×400 magnification and expression of Ki67,

MMP2 or CD31 in the tumor interior and tumor periphery was examined (AxioPlan 11 MOT AxioCam HRc, Carl Zeiss Canada Ltd, Toronto, ON).

### 2.12 Statistical analysis

All experiments were conducted in triplicate or quadruplicate except for flow cytometric assays and cellular uptake assays in which one sample per treatment was included. Results of all experiments are expressed as mean±SEM of three or more independent experiments. A growth medium-treated control was used in all *in vitro* and *ex vivo* experiments, and data generated by DMSO vehicle or test compound-treated cells/tissues were normalized against the medium control. Statistical analyses were performed using GraphPad Prism software (version 5; La Jolla, CA) at 0.05, 0.01 or 0.001 significance level (α). Student's t-test or analysis of variance (ANOVA) was performed, and differences among means were analyzed using Tukey's multiple means post-comparison method. Differences among means were considered statistically significant when $p< 0.05$ ($\alpha=0.05$), $p< 0.01$ ($\alpha=0.01$) or $p< 0.001$ ($\alpha=0.001$).

# CHAPTER 3 : PHARMACOKINETICS OF PZ-DHA

## 3.1 Introduction

Establishment of pharmacokinetic parameters is a necessary prelude in the early stages of drug development (Hassan et al., 2011). Pharmacokinetics explains the absorption, distribution, metabolism and excretion of drugs/xenobiotics introduced into the body. Pharmacological activity of a drug depends on the ability of the drug of interest to reach the target site of action, as well being available in adequate concentrations. Even though the dose largely determines the availability of a drug in the systemic circulation and at the target site of action, dose is not the sole determinant of these parameters (MacGowan, 2001; Rizk et al., 2017). Absorption, tissue distribution, phase I and II metabolism, and clearance also play a major role as critical contributing factors toward the pharmacological activity of a drug. In addition, drug-induced toxicity and adverse side effects may also be explained by impaired distribution, metabolism and/or excretion of a particular drug (Archer, 2013; Benet, 1993; Eason et al., 1990; Hassan et al., 2011).

Flavonoids, a sub-group of plant polyphenols, possess a wide-range of disease-fighting properties, including anti-cancer activities (Hui et al., 2013; Kozłowska and Szostak-Wegierek, 2014; Obakan-Yerlikaya et al., 2017; Xiao et al., 2011) and some of them have been studied broadly for their anti-metastatic activity (Ni et al., 2012; Weng et al., 2012; Yan et al., 2016). Flavonoids known to undergo phase II metabolism and the metabolites also show similar or stronger biological effects compared to parent flavonoids (Manach et al., 1998; Petri et al., 2003; Sesink et al., 2001; Walle, 2004). However, their clinical applications are restricted by poor cellular uptake and bioavailability; therefore, attempts have been made to synthesize flavonoid derivatives, aiming to overcome these limitations. With such an objective, PZ-DHA was synthesized by acylation of PZ with DHA through an enzyme-catalyzed esterification reaction. In this chapter, the ability of PZ-DHA to penetrate the cell membrane of mammary carcinoma/non-malignant mammary epithelial cells and the stability of PZ-DHA in the cellular environment over a prolonged period was studied. For comparison purposes, the parent compounds of PZ-DHA were also included in the experiments. In addition, the

biological fate and toxicity of PZ-DHA was investigated following its intraperitoneal administration to Balb/c female mice.

## 3.2 Results

### 3.2.1 Determination of sub-cytotoxic concentrations of PZ, DHA and PZ-DHA to MDA-MB-231 cells

The Sub-cytotoxic concentrations of PZ-DHA were identified by 7AAD staining of MDA-MB-231 TNBC cells. A right-ward shift of fluorescence on the FL3 detector of flow cytometer indicates dead cells. PZ, DHA and PZ-DHA concentrations up to 30 μM did not decrease the % live cell population significantly in comparison to DMSO vehicle treated cells, suggesting that below 30 μM the drugs did not affect the viability of MDA-MB-231 cells (Figure 3.1). However, at concentrations higher than 30 μM (40 and 50 μM), DHA and PZ-DHA induced the death of MDA-MB-231 cells. Therefore, all *in vitro* cellular uptake (Chapter 3), anti-proliferative (Chapter 4) and anti-metastatic (Chapter 5) assays were conducted using 10, 20 or 30 μM concentrations of PZ, DHA and PZ-DHA within 72 h post-treatment.

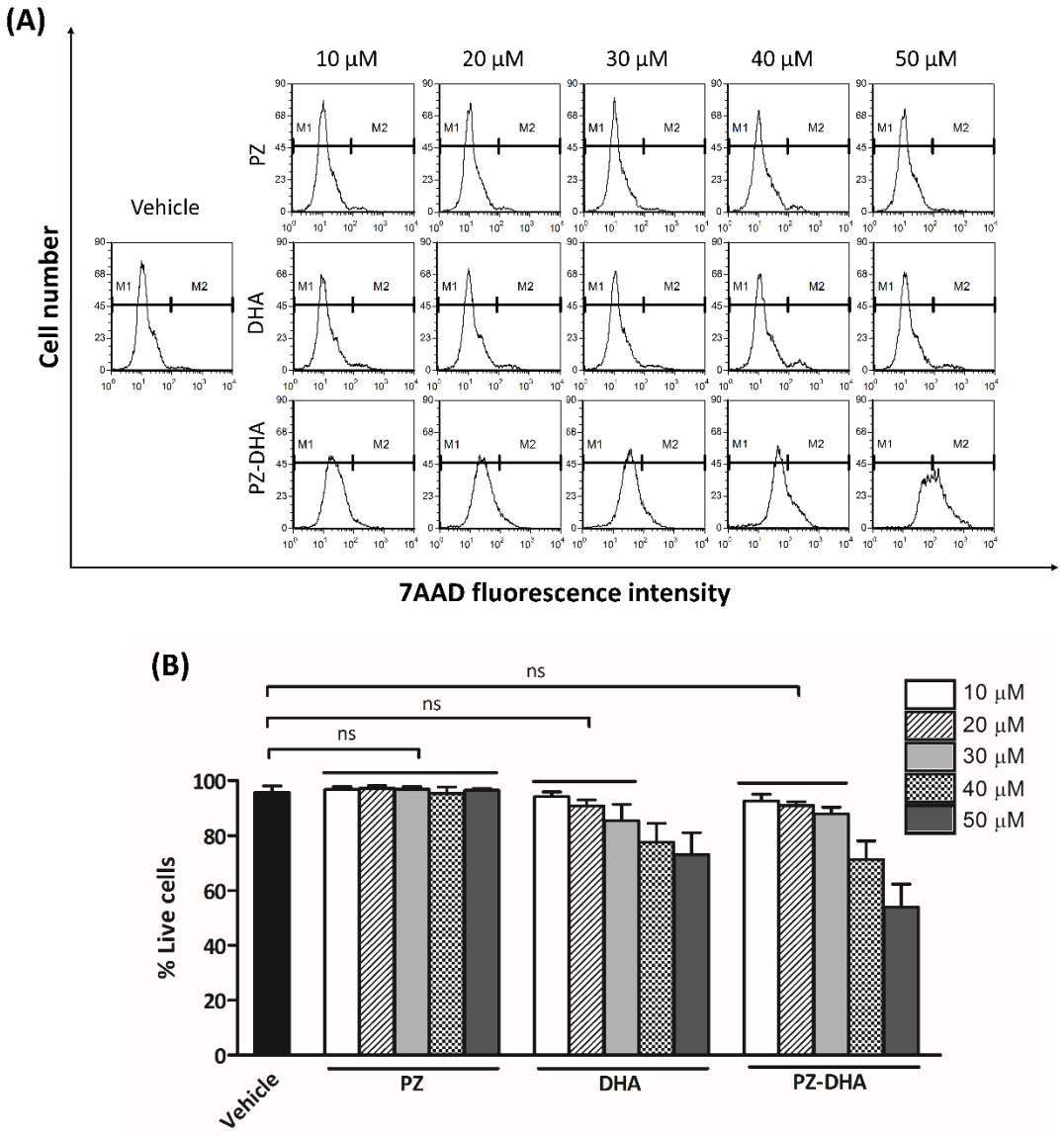


**Figure 3.1. Determination of sub-cytotoxic concentrations of PZ-DHA for MDA-MB-231 breast cancer cells.**

MDA-MB-231 cells were seeded and treated with PZ, DHA, PZ-DHA (10 to 50 µM), vehicle or medium control alone, cultured for 72 h and stained with 7AAD for analysis by flow cytometry. Percent live cells were determined. Data shown are **(A)** representative histograms of drug-treated cells (M1; Marker 1: Live cells and M2; Marker 2: Dead cells) and **(B) %** mean live cell counts±SEM of three independent experiments. ANOVA multiple means comparison statistical method was performed and differences among means were compared using Tukey's test; ns: not significant.

### 3.2.2 PZ-DHA cellular uptake by breast cancer cells

An analysis of PZ, DHA and PZ-DHA uptake by mammary carcinoma cells and mammary epithelial cells was carried out using LC/MS analysis of cell lysates made in acetone followed by reconstitution in methanol. Cell uptake was quantified using standard curves of PZ ($R^2$=0.99), DHA ($R^2$=0.98) or PZ-DHA ($R^2$=0.99) made in methanol. A 0.25 mg/mL standard PZ-DHA stock made in methanol was used to determine the retention time (RT) (8.96 min) (Figure 3.2A) of PZ-DHA on a Resteck column. Four malignant (MDA-MB-231, MDA-MB-468, 4T1, and MCF-7) and one non-malignant mammary epithelial cell type (MCF-10A) were used in the assay with the aim of investigating whether PZ-DHA cellular uptake is cell type-dependent. Cells were grown as monolayers in T-75 cell culture flasks and when treated with a sub-cytotoxic concentration (20 μM), PZ-DHA crossed the cell membrane and accumulated in the cells (Figure 3.2A). Acylation of PZ with DHA increased the intra-cellular availability of PZ and DHA by 319.6±205.9 and 149.5±89.6 fold, respectively, in MDA-MB-231 cells. This was reflected by a significant increase in cellular uptake of PZ-DHA (percentage mean cellular uptake±SEM) versus PZ and DHA; (PZ, 0.6±0.3%; DHA, 1.1±0.8%; PZ-DHA, 51.5±15.2%) ($p$<0.05). Of all malignant cells, the highest PZ-DHA internalization was shown by MDA-MB-468 cells (PZ, 0.6±0.3%; DHA, 5.81±5.1%; PZ-DHA, 84.7±33.7%) ($p$<0.05); however, the fold increase of intra-cellular PZ and DHA availability was not as high as in MDA-MB-231 cells (PZ, 248.9±106.1; DHA, 56.6±32.2). PZ-DHA was also readily taken-up by 4T1 mouse mammary carcinoma cells (PZ, 0.8±0.4%; DHA, 3.8±2.5%; PZ-DHA, 43.8±20.2%) ($p$<0.05). The availability of PZ and DHA was increased by 181.4±138.4 and 24.8±10.8, respectively, in 4T1 cells. Interestingly, the lowest % PZ-DHA cellular uptake of 21.4±6.6% (in comparison to PZ, 0.7±0.3%; DHA, 2.9±2.2%) ($p$<0.05) was observed in MCF-7, ER+ breast cancer cells. However, a significant increase of stability and availability of PZ by 150.3±119.1 fold and DHA by 40.9±21.7 fold resulted when introduced as a conjugated single compound (PZ-DHA) to MCF-7 cells. PZ-DHA was taken up by MCF-10A non-malignant mammary epithelial cells (PZ, 1.1±0.9%; DHA, 0.6±0.5%; PZ-DHA, 105.2±17.7%) ($p$<0.001) and resulted in a 543.8±400.4 and 299.1±223.1 increase of intracellular PZ and DHA concentrations, respectively (Figure 3.2B and C).

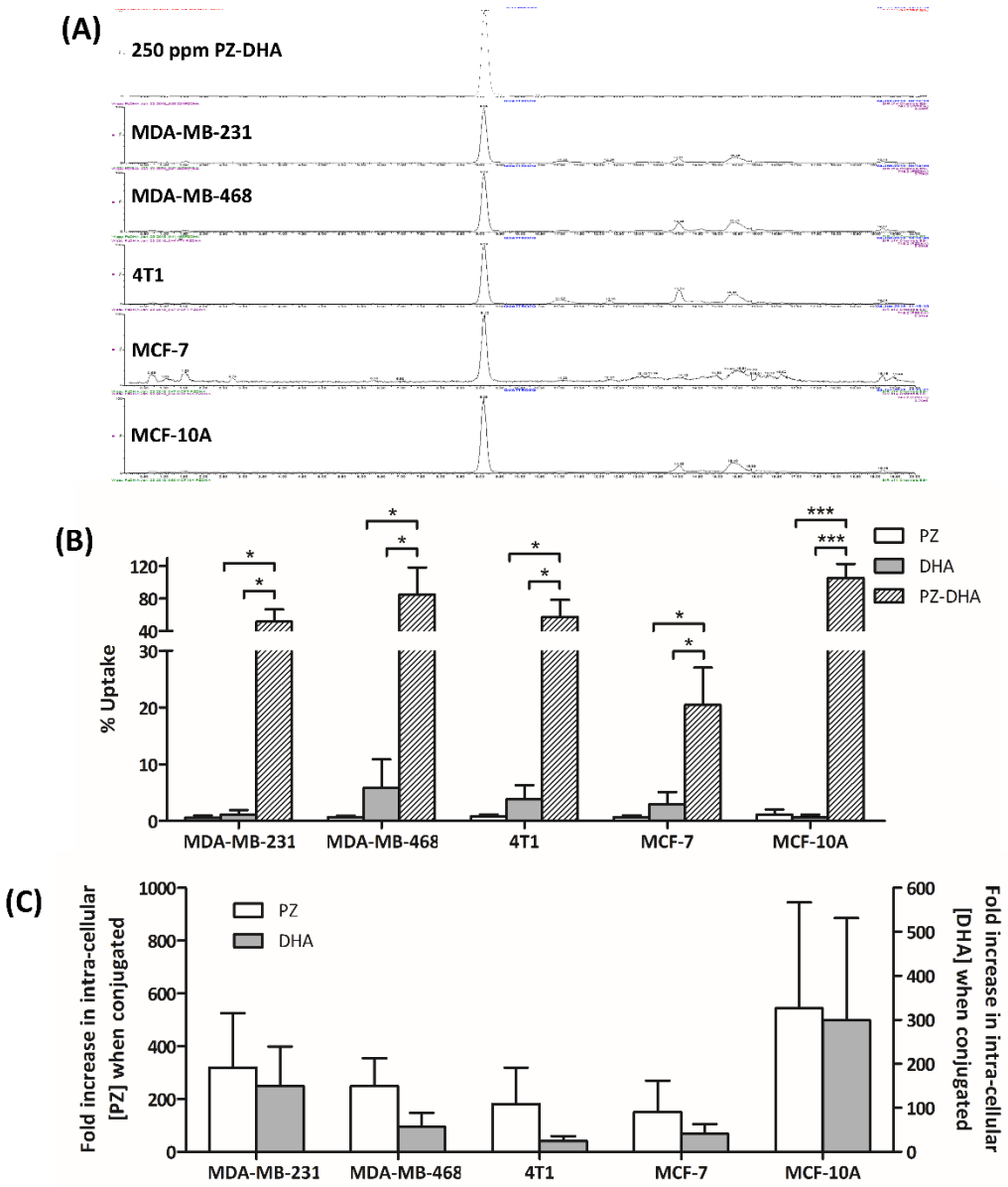


**Figure 3.2. PZ-DHA is absorbed by mammary carcinoma cells and non-malignant mammary epithelial cells.**

MDA-MB-231, MDA-MB-468, 4T1, MCF-7, and MCF-10A cells were treated with 20 µM of PZ, DHA or PZ-DHA and cultured for 72 h at 37°C. Cells were harvested and washed thoroughly using cold PBS. Cells were lysed in cold acetone containing 0.05 mg/mL quercetin and cell lysates were collected by centrifugation. Acetone was evaporated, and the lysate was reconstituted in methanol to analyze using a UPLC/ESI/MS system. **(A)** Representative chromatograms **(B)** mean % cellular uptake±SEM and **(C)** mean fold increase of PZ and DHA concentrations±SEM of three independent experiments are shown. ANOVA multiple means comparison statistical method was performed and differences among means were compared using Tukey's test; *$p$<0.05.

### 3.2.3 PZ-DHA undergoes phase I metabolism i*n vitro*

*In vitro* formation of PZ-DHA metabolites was determined following the incubation of PZ-DHA (300 μM) at 37°C for 1 h, in the presence of freshly prepared microsomes from C57BL/6 female mouse livers. Protein concentration of microsome preparations was determined using a BSA standard curve ($R^2$=1.00) followed by Bradford protein assay (Figure 3.3).

Four potential phase I reactions, namely, hydrolysis of PZ-DHA, hydroxylation of PZ, hydroxylation of PZ-DHA, epoxidation of DHA and epoxidation of PZ-DHA were predicted and tested. Metabolites matching the molecular weights of PZ (MW=436.4 g/mol) and DHA (MW=328.47 g/mol) were identified as the products of hydrolysis of PZ-DHA (Figure 3.4A). Two hydroxylated metabolites of PZ (3-hydroxy-phloridzin, MW=451.41 g/mol; 3,5'-dihydroxy-phloridzin, MW=467.41 g/mol) (Figure 3.4B) and one mono-hydroxylated metabolite of PZ-DHA (3-hydroxy-phloridzin docosahexaenoate, MW=761.88 g/mol) (Figure 3.4C) were identified. Three epoxy metabolites of PZ-DHA were also identified; however, collected data was not adequate to predict the precise sites of epoxidation on the long carbon chain (mono-epoxy-phloridzin docosahexaenoate, MW=761.88 g/mol; tri-epoxy-phloridzin docosahexaenoate, MW=793.2 g/mol; tetra-epoxy-phloridzin docosahexaenoate, MW=809.2 g/mol;) (Figure 3.4D). No epoxy-DHA metabolites were detected during the study.

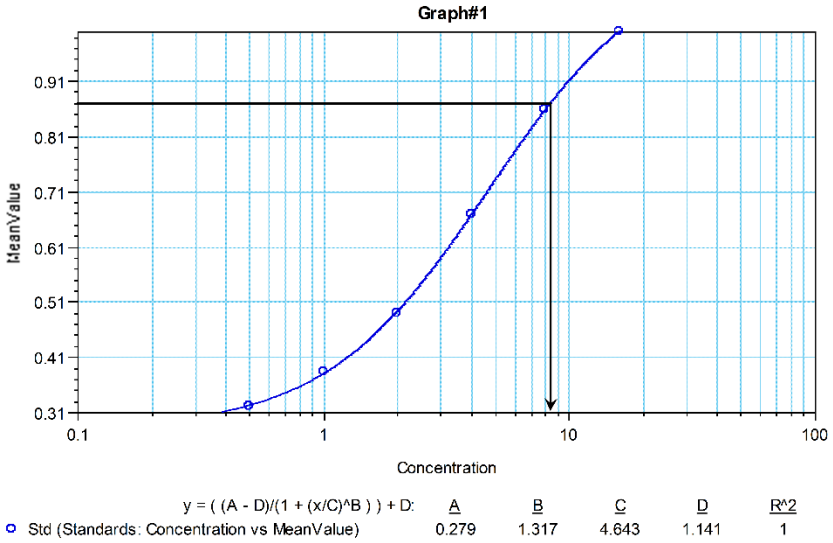


**Figure 3.3. Protein assay of mouse liver microsome preparation.**
Mouse hepatic microsomes were freshly isolated from the livers of C57BL/6 female mice. Livers were minced using sterile scalpel and forceps. Minced livers were homogenized in homogenizing buffer (0.154 M KCl, 0.25 M sucrose in 50 mM potassium phosphate buffer ($K_2HPO_4/KH_2PO_4$) pH 7.5) using a hand-held homogenizer. Cell/tissue debris were removed by centrifuging homogenized livers at 12,000 ×g for 22 min at 4°C. Supernatant was collected and centrifuged at 100,000 ×g for 70 min at 4°C. The pellet was gently rinsed using 50 mM potassium phosphate buffer and resuspended in glycerol/phosphate buffer (20% glycerol (v/v), 80% 0.1 M potassium phosphate buffer pH 7.5). The protein concentration was assayed using the Bradford assay and SoftMax software and microsomes were stored at -80°C.

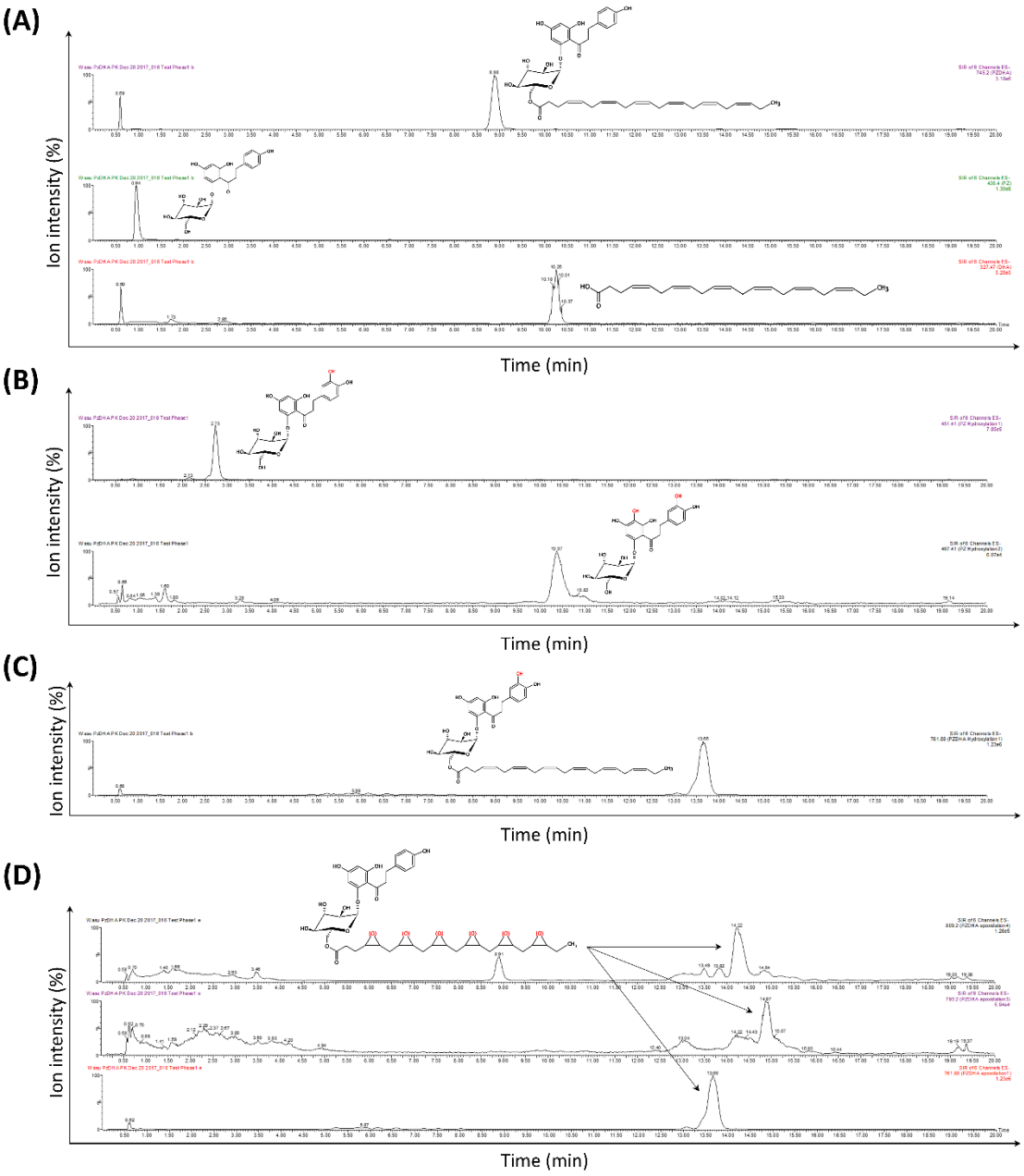


**Figure 3.4. PZ-DHA undergoes phase I metabolism in the presence of freshly prepared mouse liver microsomes.**
PZ-DHA (300 µM) was incubated with 100 mM NADPH in the presence of mouse liver microsome for 1 h at 37°C. The reaction was halted by adding an ice-cold mixture of acetone:acetonitrile (20:80) containing quercetin (0.05 mg/mL) as the internal standard. Reaction mixture was incubated at 4°C overnight to precipitate proteins. Supernatant was collected at centrifuging at 14,000 ×g for 15 min and concentrated under nitrogen gas. Metabolites from PZ-DHA **(A)** Hydrolysis, **(B)** and **(C)** hydroxylation and **(D)** epoxidation were identified using single ion monitoring of UPLC/ESI/MS analysis.

### 3.2.4 PZ-DHA undergoes phase II metabolism *in vitro*

Phase II metabolites of PZ-DHA were identified by incubating PZ-DHA with SAM, UDPGA or PAPS in the presence of freshly prepared mouse hepatic microsomal preparations. One methylated-metabolite (4,4',6'-tri-*O*-methyl-phloridzin docosahexaenoate, MW=788.88 g/mol, RT =14.10 min) (Figure 3.5), two glucuronides (phloridzin docosahexaenoate-4-*O*-glucuronide, MW=923.02 g/mol, RT=3.78 min and phloridzin docosahexaenoate-4'-*O*-glucuronide, MW=923.02 g/mol, RT=4.68 min) (Figure 3.6) and one sulphated-metabolite (phloridzin docosahexaenoate-4,4'-di-*O*-sulphide MW=906.20 g/mol, RT=11.40 min) (Figure 3.7) were identified. Control experiments were performed to investigate the stability of PZ-DHA and co-factors in the reaction mixtures, as well as the role of microsome and co-factors in conjugation reactions (Supplementary Figure 2).

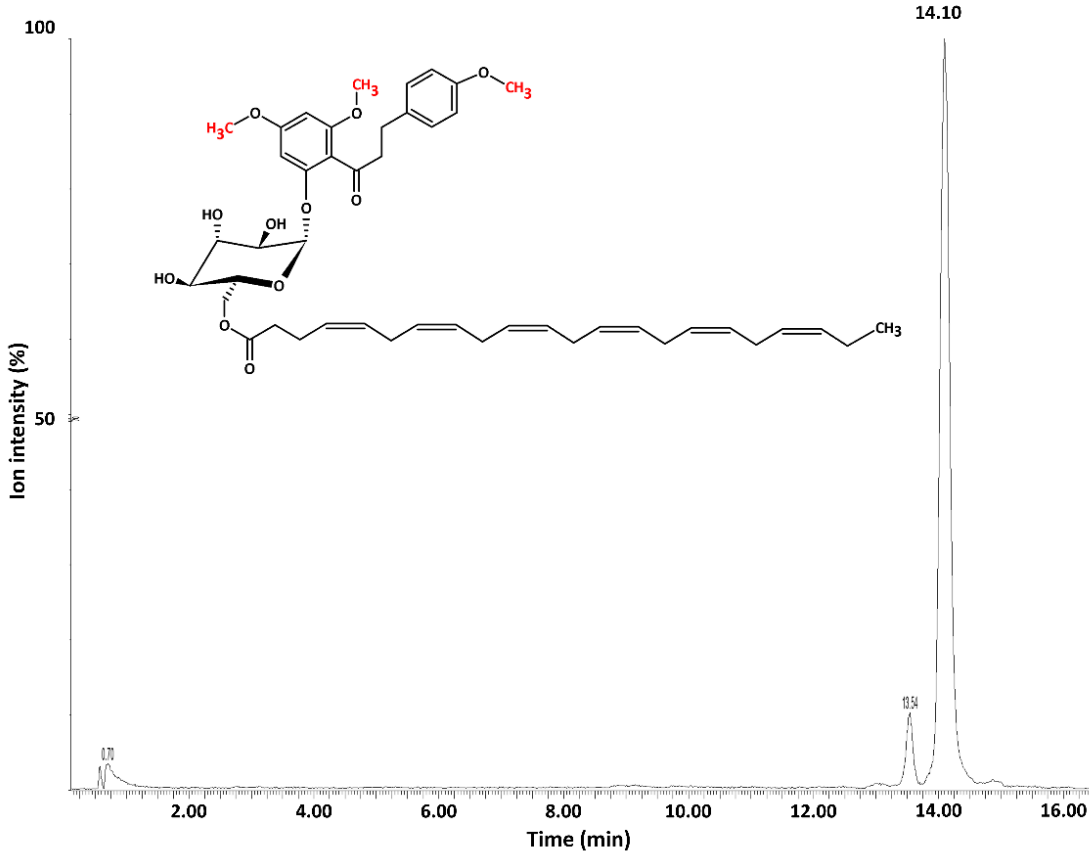


**Figure 3.5. PZ-DHA undergoes phase II methylation in the presence of freshly prepared mouse liver microsomes.**
PZ-DHA (300 µM) was incubated with *S*-(5′-Adenosyl)-*L*-methionine chloride dihydrochloride (1 mM) in the presence of mouse liver microsomal enzymes (3 mg/mL) at 37°C for 1 h. The reaction was halted by adding an ice-cold mixture of acetone:acetonitrile (20:80) containing quercetin (0.05 mg/mL) as the internal standard. Reaction mixture was incubated at 4°C overnight to precipitate proteins. Supernatant was collected at centrifuging at 14,000 ×g for 15 min and concentrated under nitrogen gas. Tri-methylated-PZ-DHA (4,4',6'-tri-*O*-methyl-phloridzin docosahexaenoate) metabolite (MW=788.88 g/mol) was identified using single ion monitoring of UPLC/ESI/MS analysis.

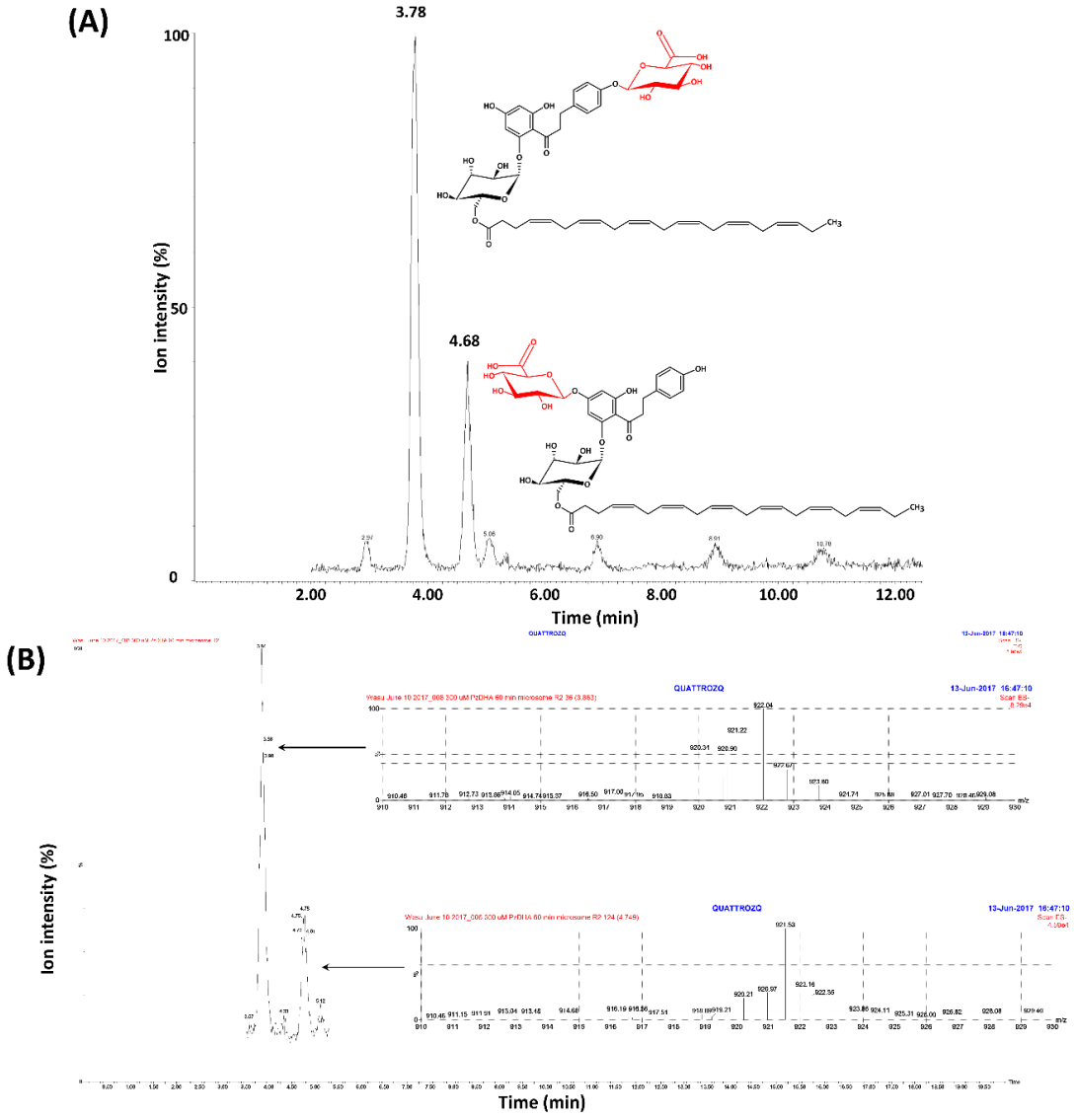


**Figure 3.6. PZ-DHA undergoes phase II glucuronidation in the presence of freshly prepared mouse liver microsomes.**
PZ-DHA (300 µM) was incubated with glucuronic acid (2 mM) and alamethicin (25 µg/mL) in the presence of mouse liver microsomal enzymes (3 mg/mL) at 37°C for 1 h. The reaction was halted by adding an ice-cold mixture of acetone:acetonitrile (20:80) containing quercetin (0.05 mg/mL) as the internal standard. Reaction mixture was incubated at 4°C overnight to precipitate proteins. Supernatant was collected at centrifuging at 14,000 ×g for 15 min and concentrated under nitrogen gas. **(A)** Phloridzin docosahexaenoate-4-*O*-glucuronide (MW=923.02 g/mol) and phloridzin docosahexaenoate-4'-*O*-glucuronide (MW=923.02 g/mol) were identified using single ion monitoring and m/e ratios were confirmed by **(B)** mass scan of UPLC/ESI/MS analysis.

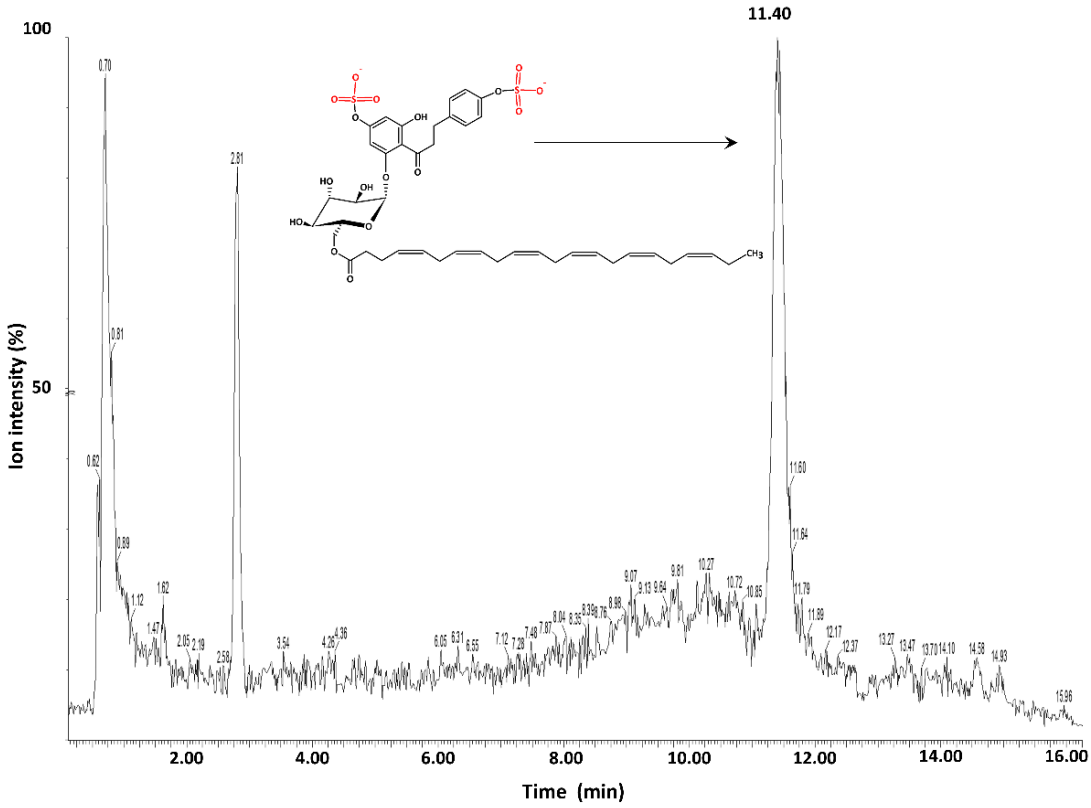


**Figure 3.7. PZ-DHA undergoes phase II sulphation in the presence of freshly prepared mouse liver microsomes.**

PZ-DHA (300 µM) was incubated with adenosine 3′-phosphate 5′-phosphosulfate lithium salt, hydrate (0.5 mM) in the presence of mouse liver microsomal enzymes (3 mg/mL) at 37°C for 1 h. The reaction was halted by adding an ice-cold mixture of acetone:acetonitrile (20:80) containing quercetin (0.05 mg/mL) as the internal standard. Reaction mixture was incubated at 4°C overnight to precipitate proteins. Supernatant was collected at centrifuging at 14,000 ×g for 15 min and concentrated under nitrogen gas. Disulphated-PZ-DHA (phloridzin docosahexaenoate-4,4'-di-*O*-sulphide) metabolite (MW=906.20 g/mol) was identified using single ion monitoring of UPLC/ESI/MS analysis.

### 3.2.5 PZ-DHA is absorbed through intraperitoneal route and undergoes phase I and phase II metabolism in Balb/c female mice

Pharmacokinetic parameters and *in vivo* metabolism of PZ-DHA was tested by intraperitoneal administration of PZ-DHA (100 mg/kg) to Balb/c female mice. Blood collection was performed periodically and PZ-DHA and its metabolites in serum was detected by LC/MS analysis. To understand the organ distribution of PZ-DHA and its metabolites, liver, lungs, kidneys, spleen and brain were also harvested and subjected to LC/MS analysis.

PZ-DHA was available in systemic circulation in a detectable amount following intraperitoneal administration as early as 15 min post administration (0.9±0.4 μM). Systemic availability of PZ-DHA rapidly increased; however, PZ-DHA was continuously detected up to 240 min post administration (Figure 3.8A). Phase I metabolism of PZ-DHA in mice was evident by the availability of PZ and DHA in serum. In addition, PZ-DHA was detected in all organs tested; its distribution was highest in the liver (6.2±1.3 μM). Concentration vs time curve showed that PZ-DHA continued to accumulate in all organs; the highest detected concentrations in kidneys, lungs, spleen, and brain were 1.2±0.3 μM, 0.2±0.1 μM, 1.6±0.3 μM, and 1.0±0.2 μM, respectively (Figure 3.9A). Further, tri-methylated PZ-DHA phase II metabolite (4,4',6'-tri-*O*-methyl-phloridzin docosahexaenoate) was also quantified in comparison to PZ-DHA concentrations in each tissue. This metabolite was detected in the liver, lungs, and kidneys; however, it was not found in the spleen or brain. 4,4',6'-tri-*O*-methyl-phloridzin docosahexaenoate reached the maximum concentration before 1 h of post injections in all organs except for serum in which the concentration remained constant (Figure 3.9B) throughout the experimental period. The di-sulphide metabolite of PZ-DHA, phloridzin docosahexaenoate-4,4'-di-*O*-sulphide, was also studied; it was detected in the liver for a short period of time but was not found in any other organ or in serum at a detectable concentration (Figure 3.9C).

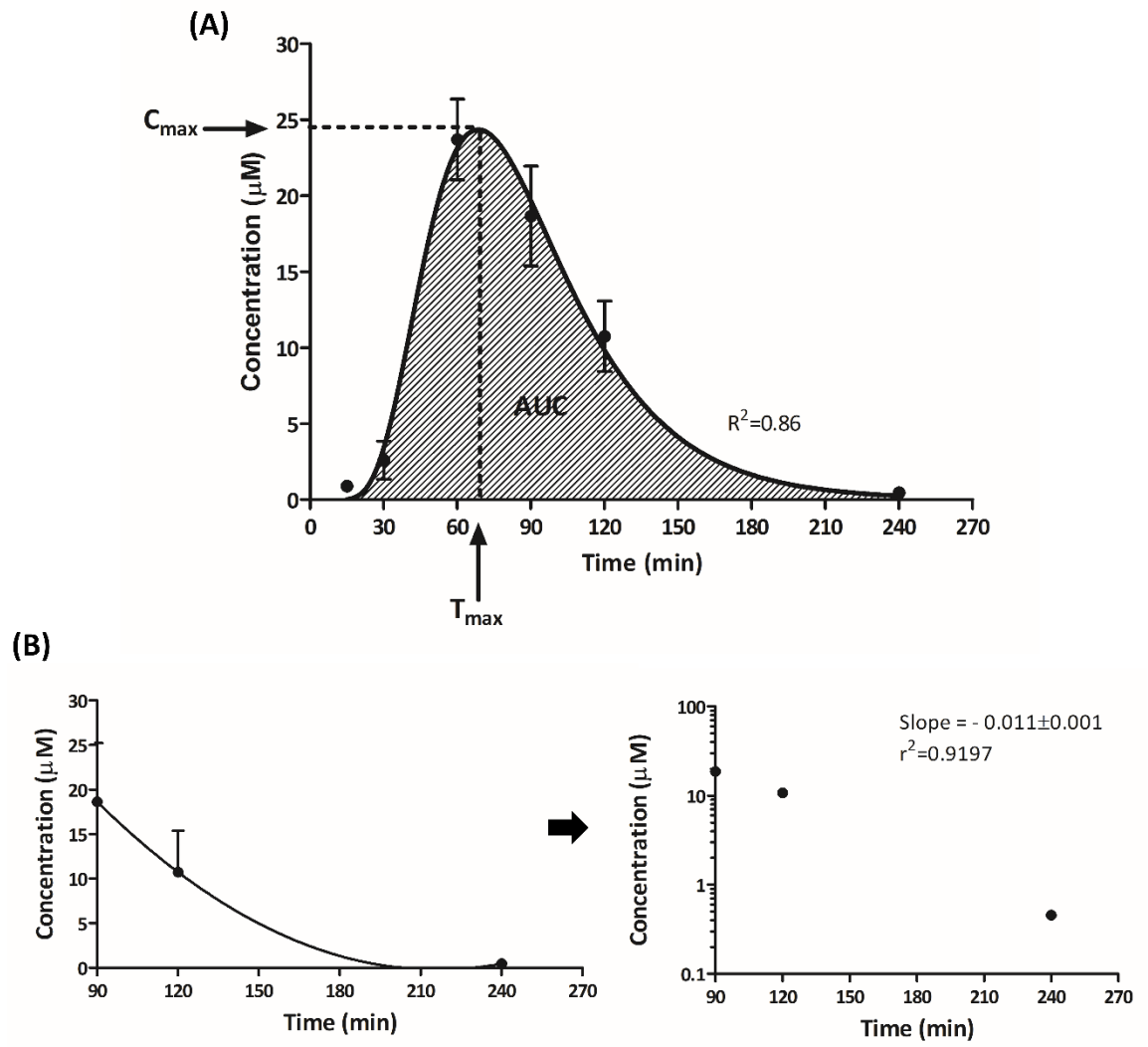


**Figure 3.8. Intraperitoneal administration of PZ-DHA results in absorption into the systemic circulation of Balb/c female mice.**

Mice were randomly divided in to six groups (n=4) and PZ-DHA (100 mg/kg) was administered intraperitoneally. Blood (800 µL) collection was performed by cardiac puncture, from each group at six different time points (t=15, 30, 60, 90, 120 and 240 min). Serum was separated and serum proteins were precipitated by incubating an aliquot of serum (500 µL) with a mixture of acetonitrile:acetone (80:20) (1 mL) containing 0.1 mg/mL quercetin (internal standard) at 4°C overnight. Supernatant was separated by centrifuging at 14,000 ×g for 10 min at 4°C. Solvent was evaporated to 200 µL using nitrogen flush and mixed with 200 µL methanol and filtered. Filtrate (200 µL) was transferred into HPLC inserts and PZ-DHA was identified and quantified using a calibration curve ($R^2$=0.99) generated using a standard series of PZ-DHA concentrations made in mouse serum (spiked with 0.1 mg/mL quercetin). **(A)** PZ-DHA concentration was plotted against time. **(B)** Elimination rate of PZ-DHA was determined using a semi-log curve of PZ-DHA concentration vs time curve.

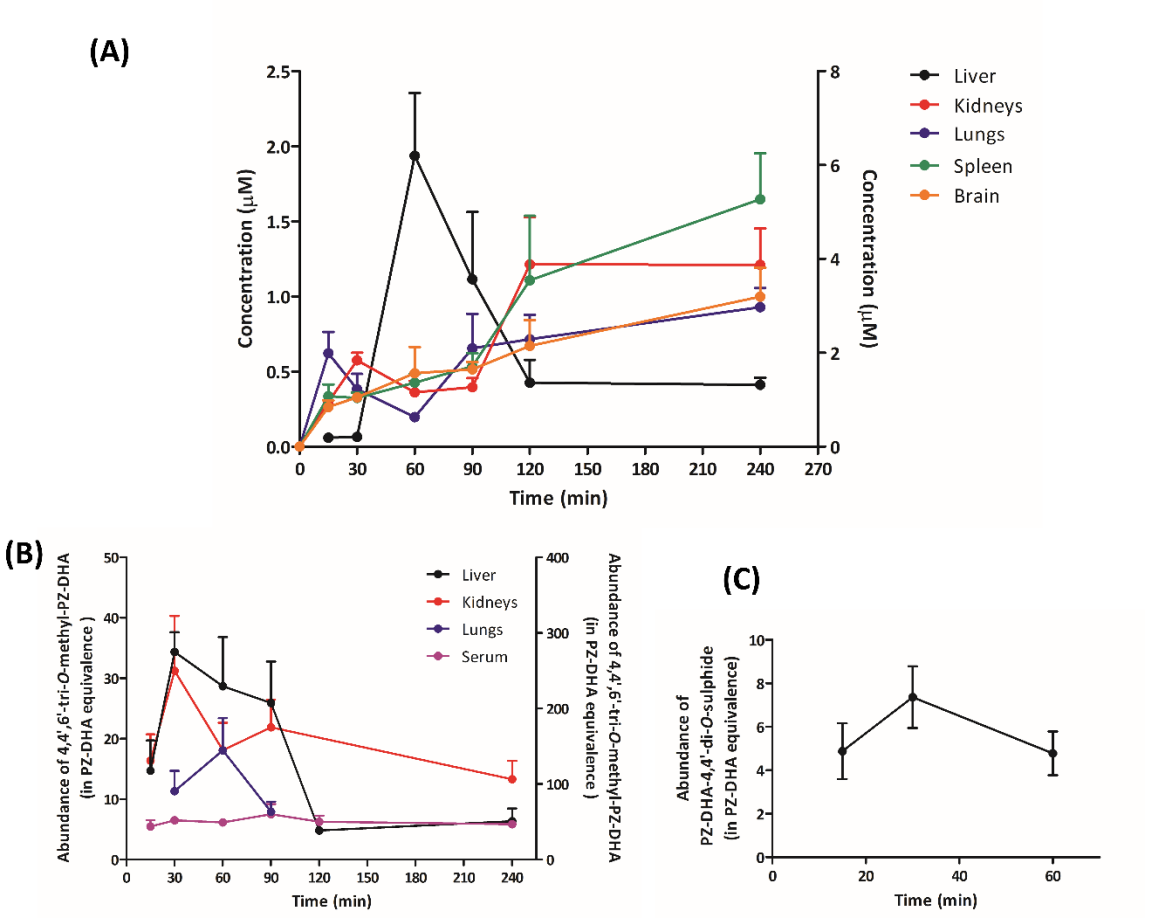


**Figure 3.9. Organ distribution of PZ-DHA and its metabolites in Balb/c female mice.** PZ-DHA (100 mg/kg) was administered by intraperitoneal injection and liver, lungs, kidneys, spleen and brain were harvested from Balb/c female mice at six different time points (t=15, 30, 60, 90, 120 and 240 min). Organs were homogenized in PBS (1:5 w/v) and supernatants were collected by centrifugation at 14,000×g for 15 min at 4°C. Proteins were precipitated by incubating 1 volume of homogenates with 2 volumes of acetonitrile:acetone (80:20) containing 0.1 mg/mL quercetin (internal standard) at 4°C overnight. Supernatant was separated by centrifuging at 14,000 ×g for 10 min at 4°C. Solvent was evaporated to 200 µL using nitrogen flush and the former solute was mixed with 200 µL methanol and filtered. Filtrate (200 µL) was transferred into HPLC inserts and PZ-DHA in **(A)** liver (right y-axis), kidneys, lungs, spleen, and brain (left y-axis) was identified and quantified using a calibration curve ($R^2$=0.99) generated using a standard series of PZ-DHA concentrations made in mouse serum (spiked with 0.1 mg/mL quercetin). Abundance of **(B)** 4,4',6'-tri-*O*-methyl-phloridzin docosahexaenoate in liver (right y-axis), kidneys, lungs, and serum) (left y-axis) and **(C)** phloridzin docosahexaenoate-4,4'-di-*O*-sulphide in liver was determined in PZ-DHA equivalence.

### 3.2.6 Pharmacokinetic parameters of PZ-DHA in Balb/c female mice

PZ-DHA was absorbed into systemic circulation upon intraperitoneal administration and accumulated in blood, reaching a highest serum concentration ($C_{max}$) of 24.4 µM at 68.6 min ($T_{max}$) post administration (Figure 3.8A). The distribution of PZ-DHA in blood followed a log Gaussian curve and the elimination of PZ-DHA from serum followed a first order curve. The elimination rate ($K_e$) was 0.011 µM/min$^{-1}$ (Figure 3.8B) and $T_{1/2}$ was estimated as 27.3 min (Table 3.1).

**Table 3.1. Pharmacokinetic parameters of PZ-DHA in Balb/c female mice**

| Pharmacokinetic parameter | Symbol | Estimated value |
|---|---|---|
| Maximum serum concentration | $C_{max}$ | 24.4 µM |
| Time to reach maximum serum concentration | $T_{max}$ | 68.6 min |
| Biological half life | $T_{1/2}$ | 27.3 min |
| Area under the curve | AUC | 2168.4 µM.min |
| Elimination rate | $K_e$ | 0.011 µM/min$^{-1}$ |

### 3.2.7 PZ-DHA does not induce liver or kidney toxicity in Balb/c female mice

Since PZ-DHA is absorbed and available in the systemic circulation, the potential to cause liver and kidney toxicity was tested by measuring serum ALT and creatinine, respectively. PZ-DHA did not increase ALT activity when compared to saline-treated mice (mean ALT activity±SEM: saline, 0.013±0.002 U/mL; PZ-DHA, 0.012±0.002 U/mL) ($p$=0.7942) (Figure 3.10A and B). Similarly, creatinine concentration in the serum of saline- and PZ-DHA-treated mice was also determined, and no significant difference was noted (mean creatinine concentration±SEM: saline, 61.7±3.3 µM; PZ-DHA, 62.3±3.8 µM) ($p$=0.904) (Figure 3.10C and D). However, intraperitoneal administration of PZ-DHA significantly affected the body weight of mice ($p$<0.05) (Figure 3.11A); therefore, correlation statistics were carried out to understand whether kidney and/or liver function was influenced by the reduction in body weight. No positive or negative correlation between the body weights and liver (saline, Pearson r=0.2242; $p$=0.5075; PZ-

DHA, Pearson r=-0.1883) ($p$=0.5792) or kidney (saline, Pearson r=-0.1744; $p$=0.6080; PZ-DHA, Pearson r=-0.2599) ($p$=0.4402) function was revealed (Figure 3.11B and C).

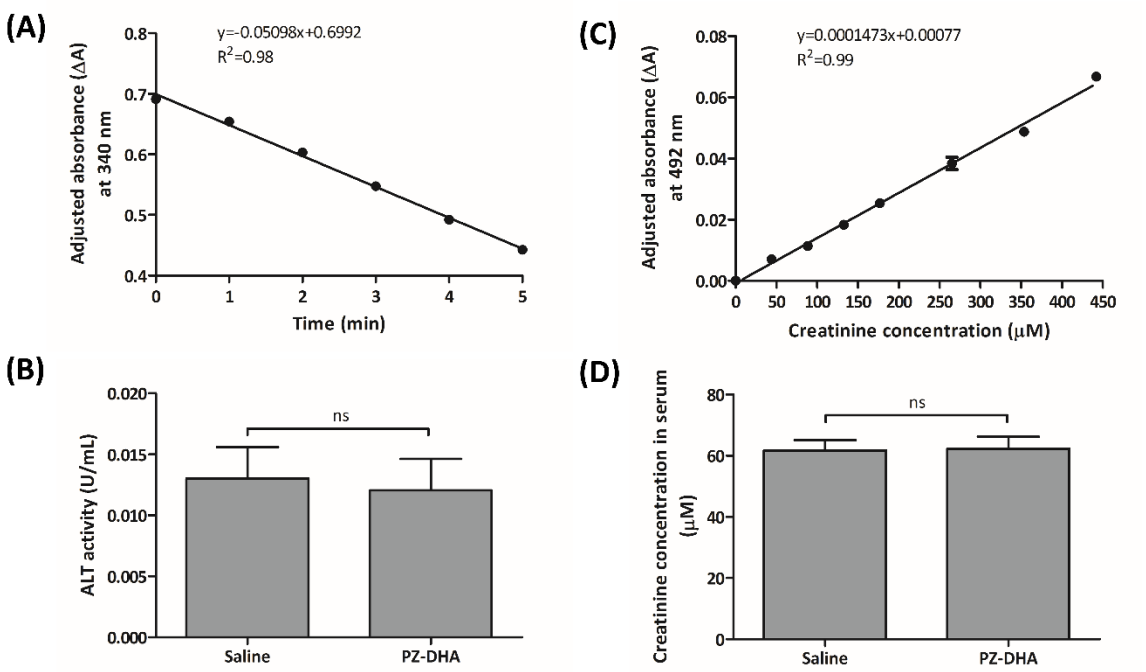


**Figure 3.10. PZ-DHA does not induce liver or kidney toxicity in Balb/c female mice.** Saline or PZ-DHA (100 mg/kg) was administered to 8-week old Balb/c female mice every second day for 9 days (5 doses). On day 10, blood (500 μL) was collected by cardiac puncture and serum was separated. Using **(A)** standard calibration of NADH decay, **(B)** mean ALT activity±SEM was determined. **(C)** A standard calibration curve of creatinine was generated and **(D)** mean concentration of creatinine in serum±SEM was determined. ANOVA multiple means comparison statistical method was performed and differences among means were compared using Tukey's test; ns: not significant.

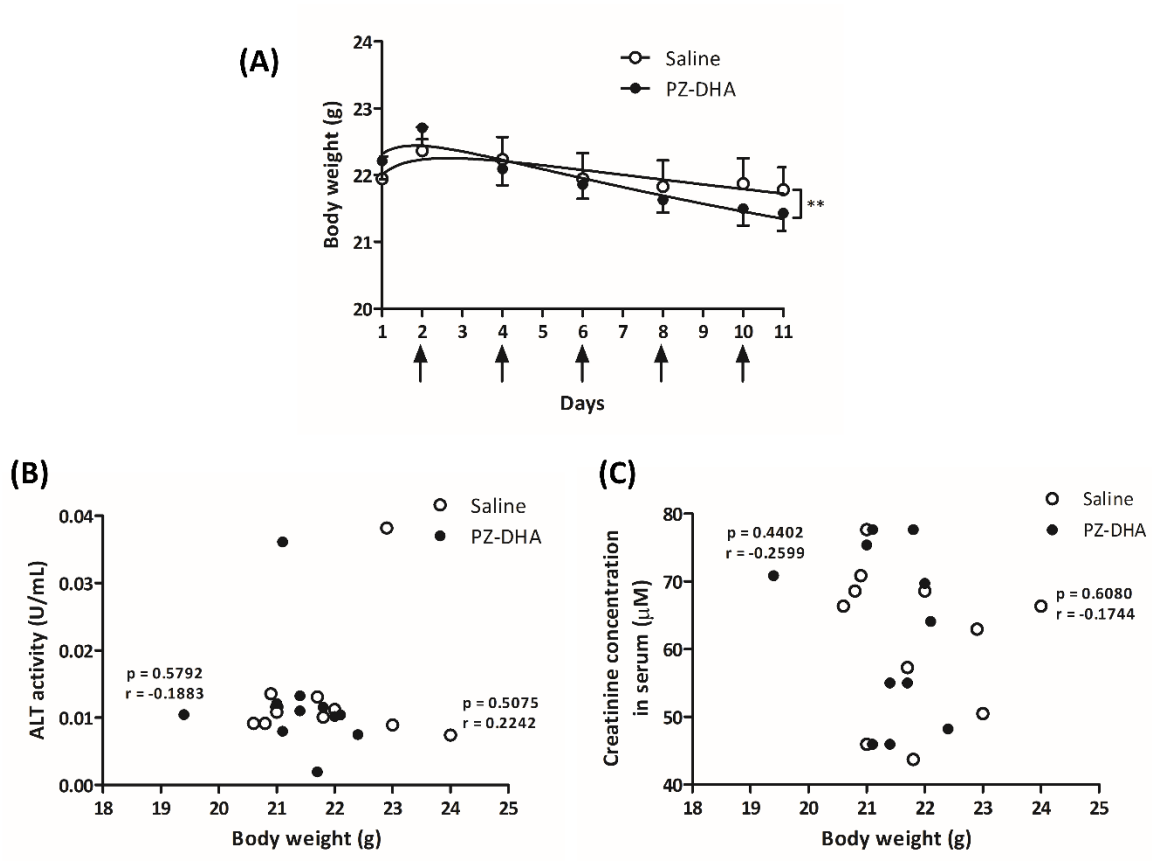


**Figure 3.11. Correlation of body weight to liver and kidney function of PZ-DHA-treated Balb/c female mice.**

Saline or PZ-DHA (100 mg/kg) was intraperitoneally administered by intraperitoneal injection to 8-week old Balb/c female mice every second day for 9 days (5 doses). **(A)** Body weights were recorded as mean±SEM. Best fit line was determined using non-linear regression method and the difference between regression curves was statistically tested using Student's t-test; ** $p<0.01$. On day 10, blood (500 μL) was collected by cardiac puncture and serum was separated for ALT activity and creatinine level determination. Correlation between body weights and **(B)** ALT activity and **(C)** creatinine concentration was determined using Pearson correlation test.

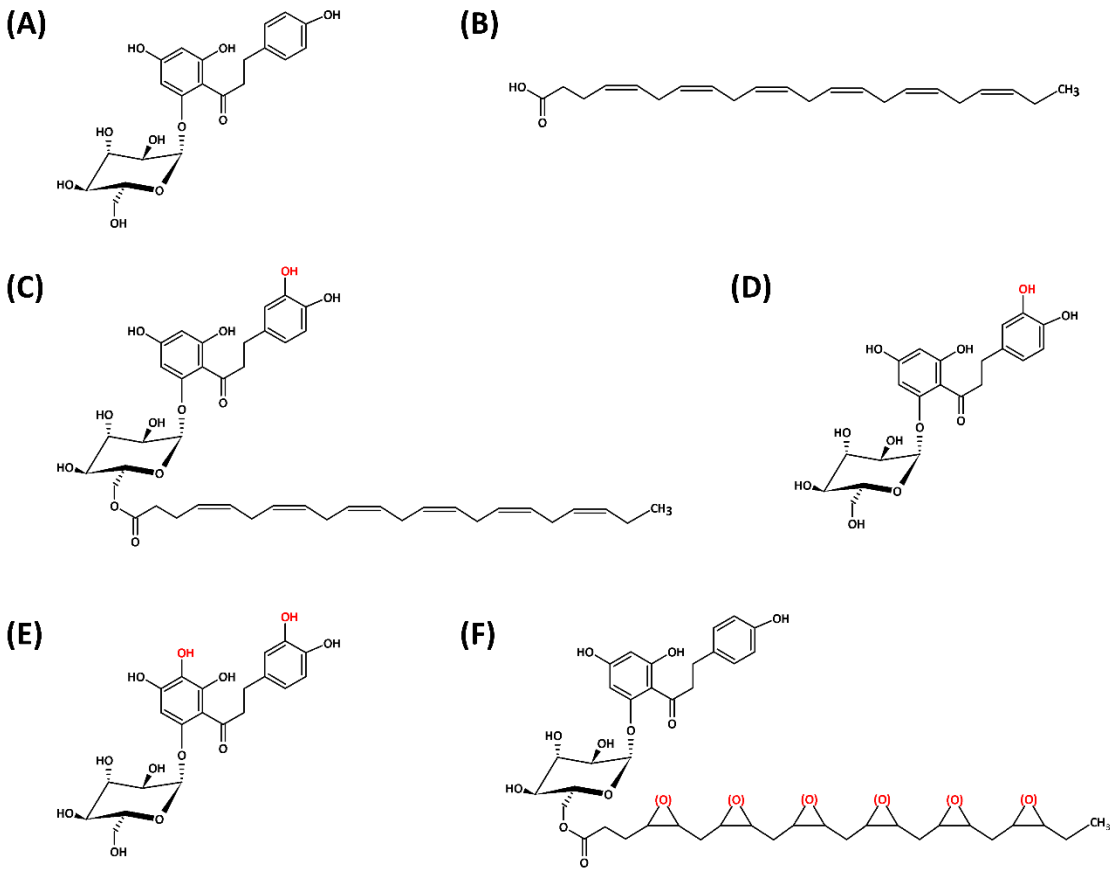


**Figure 3.12. Chemical structures of potential phase I metabolites of PZ-DHA.** **(A)** PZ (MW=436.4 g/mol) **(B)** DHA (MW=328.47 g/mol) **(C)** 3-hydroxy-phloridzin docosahexaenoate (MW=761.88 g/mol) **(D)** 3-hydroxy-phloridzin (MW=451.41 g/mol) **(E)** 3,5'-dihydroxy-phloridzin (MW=467.41 g/mol) **(F)** mono-epoxy-phloridzin docosahexaenoate (MW=761.88 g/mol) tri-epoxy-phloridzin docosahexaenoate (MW=793.2 g/mol) tetra-epoxy-phloridzin docosahexaenoate (MW=809.2 g/mol)

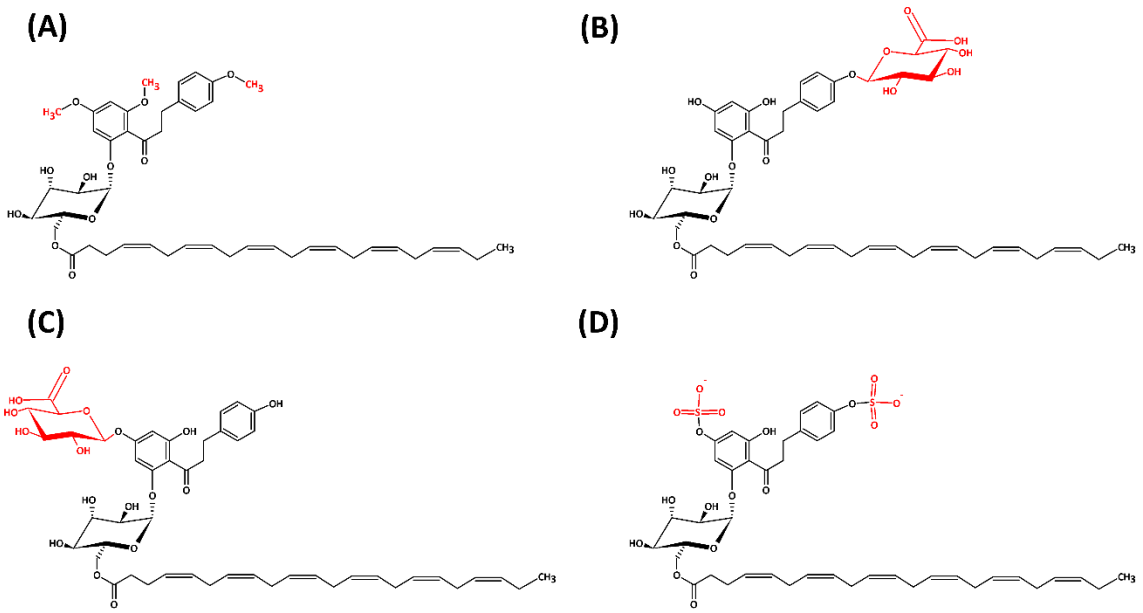


**Figure 3.13. Chemical structures of potential phase II metabolites of PZ-DHA.** **(A)** 4,4',6'-tri-*O*-methyl-phloridzin docosahexaenoate (MW=788.88 g/mol) **(B)** phloridzin docosahexaenoate-4-*O*-glucuronide (MW=923.02 g/mol) **(C)** phloridzin docosahexaenoate-4'-*O*-glucuronide (MW=923.02 g/mol) **(D)** phloridzin docosahexaenoate-4,4'-di-*O*-sulphide (MW=906.20 g/mol)

## 3.3 Discussion

The rationale of combining PZ with DHA through an acylation reaction was to improve the cellular uptake and stability of PZ and DHA, respectively. This hypothesis was tested by conducting cellular uptake experiments of PZ, DHA and PZ-DHA using mammary carcinoma cells and non-malignant mammary epithelial cells. The metabolism, pharmacokinetics and toxicity of PZ-DHA was also investigated using *in vitro* and *in vivo* pharmacokinetic models with the aim of establishing the most appropriate *in vitro* and *in vivo* doses of PZ-DHA and time points to be used to study the pharmacological activities of PZ-DHA reported in subsequent chapters (Chapter 4, 5 and 6).

PZ-DHA was taken-up by all tested mammary carcinoma (MDA-MB-231, MDA-MB-468, 4T1 and MCF-7) and non-malignant mammary epithelial cells (MCF-10A), when treated with a sub-cytotoxic concentration (20 μM). Notably, MCF-7, ER+ breast cancer cells showed the lowest PZ-DHA internalization. Quercetin, a commonly used internal standard in LC/MS analysis of flavonoids, was used to determine the % recovery of test compounds. As anticipated, PZ was absorbed into cells in trace amounts; however, intra-cellular DHA concentrations were also low (Figure 3.2B). The metabolism of DHA is highly cell type-dependent. Park et al. (2016) shows that, following initial metabolism, DHA is esterified into cell lipids and retroconversion of DHA (22: 6n-3) to EPA (20: 5n-3) is 5-6 fold greater in non-neural cells compared to neural cells (Park et al., 2016). Further, Parks et al. (2017) reveals red blood cells as long-term stable intakes of DHA (Parks et al., 2017). Another study conducted using bovine aortic endothelial cell cultures shows that DHA is taken up by endothelial cells; however, the majority of DHA is incorporated into phospholipids (Hadjiagapiou and Spector, 1987). Incubation with 20 μM $^{13}$C-(22: 6n-3) shows a cellular uptake by MCF-7 and HepG2 epithelial cells up to 24 h, as well as retroconverted products, $^{13}$C-(20: 5n-3), $^{13}$C-(22: 6n-3), and tetracosahexaenoic acid ($^{13}$C-(24: 6n-3)) (Park et al., 2016). However, little is known about the stability and intra-cellular availability of DHA with prolonged incubation. On the other hand, DHA undergoes extensive auto-oxidation, oxidative degradation and lipid peroxidation, resulting in a number of oxidative products such as mono/poly hydroxylated-DHA and epoxides (Brand et al., 2010; Ismail et al., 2016; Lee et al., 2003; Mason and Sherratt, 2017; Pogash et al., 2015; Shin et al., 2017; Suphioglu et al., 2010).

Therefore, it is possible that DHA was also readily taken up by all mammary carcinoma/mammary epithelial cells used in the current study, but the detection was low as a result of its incorporation into phospholipids and other compartments of the cells and/or extensive degradation. However, PZ-DHA showed a stable abundance throughout the experimental period (72 h), suggesting that conjugation of PZ with DHA increases the stability and availability of both PZ and DHA, which may lead to an increased biological activity. Collectively, PZ-DHA increased the intra-cellular availability of PZ by at least 200-300-fold and DHA by 20-200-fold in mammary carcinoma cells.

*In vitro* phase I and phase II metabolism of PZ-DHA was studied using freshly prepared liver microsomal enzymes from the livers of C57BL/6 female mice. Liver microsome preparations were stored at -80°C in 20% glycerol PPB and repeated freeze-thaw cycles were avoided to prevent degradation of microsomal enzymes. Three major NADPH-dependent phase I bio-transformations (hydrolysis, hydroxylation and epoxidation) of PZ-DHA were identified and potential structures were suggested (Figure 3.12). PZ and DHA were recorded along with intact PZ-DHA as the two major products of PZ-DHA hydrolysis (Figure 3.4B) and further metabolism of PZ was indicated by the formation of 3-hydroxy-phloridzin and 3,5'-dihydroxy-phloridzin (Figure 3.4B). Further, the unsaturated long carbon chain of PZ-DHA was subjected to epoxidation (Figure 3.4D); however, no further metabolism of DHA was recorded, suggesting a rapid degradation and/or accumulation of DHA into cellular compartments such as phospholipid bilayer when hydrolyzed from PZ-DHA.

PZ-DHA undergoes at least three phase II conjugation reactions (methylation, glucuronidation and sulphation) resulting in four major metabolites (Figure 3.13). Phase II conjugation reactions typically serve as detoxifying reactions; however, certain phase II metabolites could be more potent or toxic than the parent compounds (Jancova et al., 2010). On the other hand, certain phase II conjugated metabolites are less or as equally potent as parent compounds; yet, results in an improved pharmacological activity by significantly increasing the retention time/duration of action of parent drugs in the systemic circulation. Manach et al. (1998) shows that 3'-*O*-methylquercetin, quercetin-3-*O*-sulfate, quercetin glucuronides retain their antioxidant activities by prolonging the lag phase of the antioxidant activity (Manach et al., 1998). Another study shows that

glucuronide conjugates of quercetin (quercetin-4′-glucuronide, quercetin-3′-glucuronide, quercetin-7-glucuronide and quercetin-3-glucuronide) act as potent xanthine oxidase and lipoxygenase inhibitors *in vitro* (Day et al., 2000b). Access of drugs/xenobiotics to the brain is strictly controlled by the BBB. Multiple *in vitro* studies have shown that methylated and glucuronide conjugates of flavonoids cross the BBB and enter the brain (Faria et al., 2012, 2014; Youdim et al., 2003). In addition, some of the studies have discussed the clinical application of flavonoid conjugates (Ho et al., 2013; Ishisaka et al., 2014).

Intact PZ-DHA was found in all the organs tested; the highest concentration was seen in the liver, suggesting that PZ-DHA is rapidly localized to the liver. Furthermore, two phase II conjugated metabolites, 4,4',6'-tri-*O*-methyl-phloridzin docosahexaenoate and phloridzin docosahexaenoate-4,4'-di-*O*-sulphide, were abundant in the liver, reaching peak concentrations within 1 h suggesting that PZ-DHA was readily metabolized by liver microsomal enzymes *in vivo* (Figure 3.9). PZ-DHA and tri-methylated-metabolite accumulated in the kidneys during the serum elimination phase of PZ-DHA, signifying renal excretion of PZ-DHA both in intact and methylated forms. Interestingly, PZ-DHA was detected in the spleen and in the brain, suggesting potential clinical applications of PZ-DHA in the disorders related to the immune system and central nervous system. Toxicological studies confirmed that PZ-DHA did not induce liver or kidney toxicity in Balb/c female mice. However, a reduction in body weights was observed with PZ-DHA treatment. In general, body weights of both saline- and PZ-DHA-treated groups showed a trend towards weight loss with the start of intraperitoneal injections. The significant body weight reduction in PZ-DHA-treated mice may partially be attributed to the distress caused by experimental conditions such as handling, as well PZ-induced glucose uptake inhibition through inhibition of sodium/glucose co-transporter-1 (SGLT1) activity (Ho et al., 2013; Ishisaka et al., 2014). Other studies have shown that prolonged DHA intake results body weight reduction through increased-lipid metabolism (Buckley and Howe, 2010; Howe et al., 2014; Innis, 2014; Vasickova et al., 2011).

Taken together, *in vivo* pharmacokinetic experiments and related LC/MS analysis shows that following intraperitoneal administration, PZ-DHA is readily absorbed into the systemic circulation and distributed widely throughout the body. PZ-DHA undergoes

both phase I (hydrolysis) and phase II metabolism in the liver, and is then eliminated, possibly by conjugation followed by renal excretion. The findings presented in this chapter provides the basis and justification for most appropriate *in vitro* and *in vivo* experimental conditions to be employed in experiments detailed in the following chapters of the thesis.

# CHAPTER 4 : PZ-DHA IS SELECTIVELY CYTOTOXIC TO BREAST CANCER CELLS

## 4.1 Introduction

Many significant improvements such as advanced non-invasive early detection methods (Campuzano et al., 2017; Trecate et al., 2016), and novel treatment strategies (Germa et al., 2017; Kingston and Johnston, 2016; Lux et al., 2017), have been introduced over the past few decades, resulting in a significant reduction in breast cancer mortality (Gunsoy et al., 2014; Narod et al., 2015; van Schoor et al., 2011; Sighoko et al., 2018; Weedon-Fekjær et al., 2014); yet, breast cancer continues to be a major health burden world-wide. Patients bearing ER+ and HER2+ breast cancers are largely benefited by these improvements in targeted treatments (Tolcher, 2001). Chemotherapy remains the major therapeutic option in the management of TNBC; however, these patients have not benefited from recent advances in targeted therapy directed against hormone receptors and HER2. Due to the lack of targeted therapies for TNBC, this disease is associated with development of drug-resistance and, thereby, recurrence of metastatic disease. Furthermore, the selectivity of most chemotherapeutic drugs is poor and causes a considerable amount of toxicity to non-malignant normal cells. Therefore, it is essential that these issues are carefully addressed when developing novel therapies to treat TNBC.

*In vitro* and *in vivo* cytotoxic and anti-proliferative effects, as well as potential clinical applications of flavonoids and ω-3 fatty acids have been studied extensively. Studies have shown that regular intake of flavonoids is inversely proportional to breast cancer risk in humans (Fink et al., 2006, 2007; Peterson et al., 2003). A case-control study conducted by Peterson et al. (2003) found a strong statistically significant inverse correlation of flavone intake with breast cancer risk; however, flavanones, flavan-3-ols, flavonols, anthocyanidins or isoflavones intake had no such correlation with breast cancer risk (Peterson et al., 2003). Interestingly, Wang and colleagues reported that the negative correlation of flavan-3-ol intake was evident with ER- but not ER+ breast cancer risk, suggesting a protective effect of plant-based diets against ER- breast cancer development (Wang et al., 2014b). Furthermore, many studies suggest that anti-oxidant activity of dietary flavonoids play a significant role in alleviating adverse side effects of

chemotherapy, as well as in cancer chemo-prevention (Amawi et al., 2017; Kuo et al., 2016; Sak, 2012). Flavonoid-induced cytotoxic and chemo-preventive activities are linked to the ability of flavonoids to influence multiple cellular events in biological systems such as inhibition of protein kinases, cell cycle progression, metastasis, angiogenesis, multi-drug resistance, metabolism of carcinogens and pro-oxidant enzymes (Batra and Sharma, 2013). However, Matsuo et al. (2005) showed that high concentrations of flavonoids exhibit cytotoxic activity in cultured normal human cells *via* increased intracellular ROS production (Matsuo et al., 2005). ω-3 fatty acid intake also shows an inverse association with breast cancer risk (Fabian et al., 2015a, 2015b; Hidaka et al., 2015; Iyengar et al., 2013; Rahman et al., 2013; Zheng et al., 2013). Hidaka et al. (2015) suggest associations between tissue levels of ω -3 (including docosahexaenoic acid, DHA) with ω -6 fatty acids and a reversible tissue biomarker of breast cancer risk (Hidaka et al., 2015). Long-term (6 months) daily intake of large doses of EPA (1,860 mg) and DHA (1500 mg) ethyl esters demonstrate favorable effects in a proteomics array for proteins involved in mitogen signaling and cell-cycle arrest; however, the downstream effector of Akt, mTOR, is not affected (Fabian et al., 2015a).

In the current chapter, the selective cytotoxic activity of PZ-DHA toward malignant mammary epithelial cells was shown by culturing MDA-MB-231, MCF-10A and HDF cells in the presence or absence of PZ-DHA. Furthermore, the antiproliferative effect and impact of PZ-DHA on the expression of Ki67/cell cycle regulatory proteins and MDA-MB-231 cell cycle progression was shown using sub-cytotoxic concentrations of PZ-DHA. The effect of PZ-DHA on Akt- and MAPK-mediated cell survival and mitogenic signaling was also investigated. Because chemotherapy often fails due to the development of chemoresistance, the effectiveness of PZ-DHA on the suppression of paclitaxel-resistant MDA-MB-231 cell growth and inhibition of MCF-7 spheroid formation was also tested. PZ and DHA were included in all *in vitro* experiments for comparison purposes. My previous work shows that intra-tumoral administration of PZ-DHA significantly inhibits the growth of MDA-MB-231 cells xenografted into the flasks of NOD-SCID female mice (Fernando, 2014; Fernando et al., 2016). In the present study, the systemic activity of PZ-DHA (intraperitoneal administration) was studied using Balb/c and NOD-SCID female mice orthotopically implanted/xenografted with 4T1

mouse mammary carcinoma cells and GFP-transfected MDA-MB-231 human mammary carcinoma cells, respectively.

## 4.2 Results

Chapter 3 showed that culture of malignant and non-malignant cells with 10-30 μM concentration of PZ-DHA for 72 h confirms drug internalization without induction of a cytotoxic effect in breast cancer cells and non-malignant mammary epithelial cells. Therefore, these concentrations and incubations were chosen to investigate the anti-proliferative activities of PZ-DHA in *in vitro* cell culture systems in Chapter 4. *In vivo* tumor suppression experiments were conducted using 100 mg/kg PZ-DHA dose.

### 4.2.1 PZ-DHA causes morphological changes in mammary carcinoma cells

Cells undergoing apoptosis are characterized by a series of energy-dependent biochemical and morphological changes taking place in the cells (Elmore, 2007). These changes are observed during naturally occurring and experimentally-induced cell death (Elmore, 2007; Häcker, 2000; Ziegler and Groscurth, 2004). One of the key changes in the cell morphology during apoptosis is the condensation of chromatin and nuclear material. Toward the end of the apoptotic process, the cytoplasmic contents are condensed and form apoptotic bodies (Elmore, 2007; Häcker, 2000). Both DHA and PZ-DHA induce morphological changes in MDA-MB-231 cells (Supplementary figure 3A). In the current study, 4 different mammary carcinoma cell types were cultured in the presence of 50 μM (low) and 100 μM (high) concentrations of PZ, DHA and PZ-DHA for 24 h and morphological changes were recorded using a Nikon eclipse TS 100 phase-contrast microscope at 200× magnification. PZ did not cause any distinguishable changes to the cellular morphology of mammary carcinoma cells. DHA-induced morphological changes at the low concentration were evident by the condensation of nuclear material in all cells; most clearly in MDA-MB-468 cells and MCF-7 cells (indicated by solid-line arrows in Figure 4.1A). When treated with a high concentration of DHA, the entire morphology of the cells was notably changed; however, cytoplasmic condensation (except for a few MDA-MB-468 cells) and formation of apoptotic bodies were not observed in any type of cells. Nuclear (solid-line arrows) and cytoplasmic condensation (dashed-line arrows) of PZ-DHA-treated cells were noted at both low and high

concentrations (Figure 4.1A and B). In addition, apoptotic bodies (dotted-line arrows) were also seen in PZ-DHA-treated cell cultures, and all three morphological changes were dramatically increased with the incubation of cells in the presence of a high concentration of PZ-DHA (Figure 4.1B).

### 4.2.2 PZ-DHA inhibits the metabolic activity of mammary carcinoma cells

The effect of PZ-DHA and its parent compounds on the metabolic activity of mammary carcinoma cells was measured using an MTS assay. With the aim of understanding whether drugs-induced growth inhibitory effects are cell line specific, a panel of mammary carcinoma cell lines with different molecular sub-type profiles (ER, PR, HER2 receptor expression; p53 status) was tested. MDA-MB-468 (ER-, PR-, HER2-, p53 mutant), 4T1 (murine ER-, PR-, ERB-, p53 null), MCF-7 (ER+, PR+, HER2-, p53 wild-type) and T-47D (ER+, PR+, HER2-, p53 mutant) cells were treated using a series of drug concentrations and cultured for different periods of time. All cell lines were consistently resistant to all tested concentrations of PZ; although, at 24 h, metabolic activity of MCF-7 cells was slightly affected (Figure 4.2A, D, G, and J). DHA had no significant effect at concentrations up to 75 μM; however, a concentration- and time-dependent cell growth inhibition was noted with higher (100-200 μM) concentrations in all cell lines (Figure 4.2B, E, H, and K). My previous work highlights the inhibitory effects of PZ-DHA against MDA-MB-231 cells (Supplementary Figure 3B). In the present study, PZ-DHA attenuated the growth of all mammary carcinoma cells tested at 50-200 μM in a concentration- and time-dependent manner, suggesting a broad spectrum of growth inhibitory activity of PZ-DHA (Figure 4.2C, F, I, and L). Interestingly, ER+ mammary carcinoma cells seemed to be more vulnerable to PZ-DHA treatment in comparison to ER- mammary carcinoma cells.

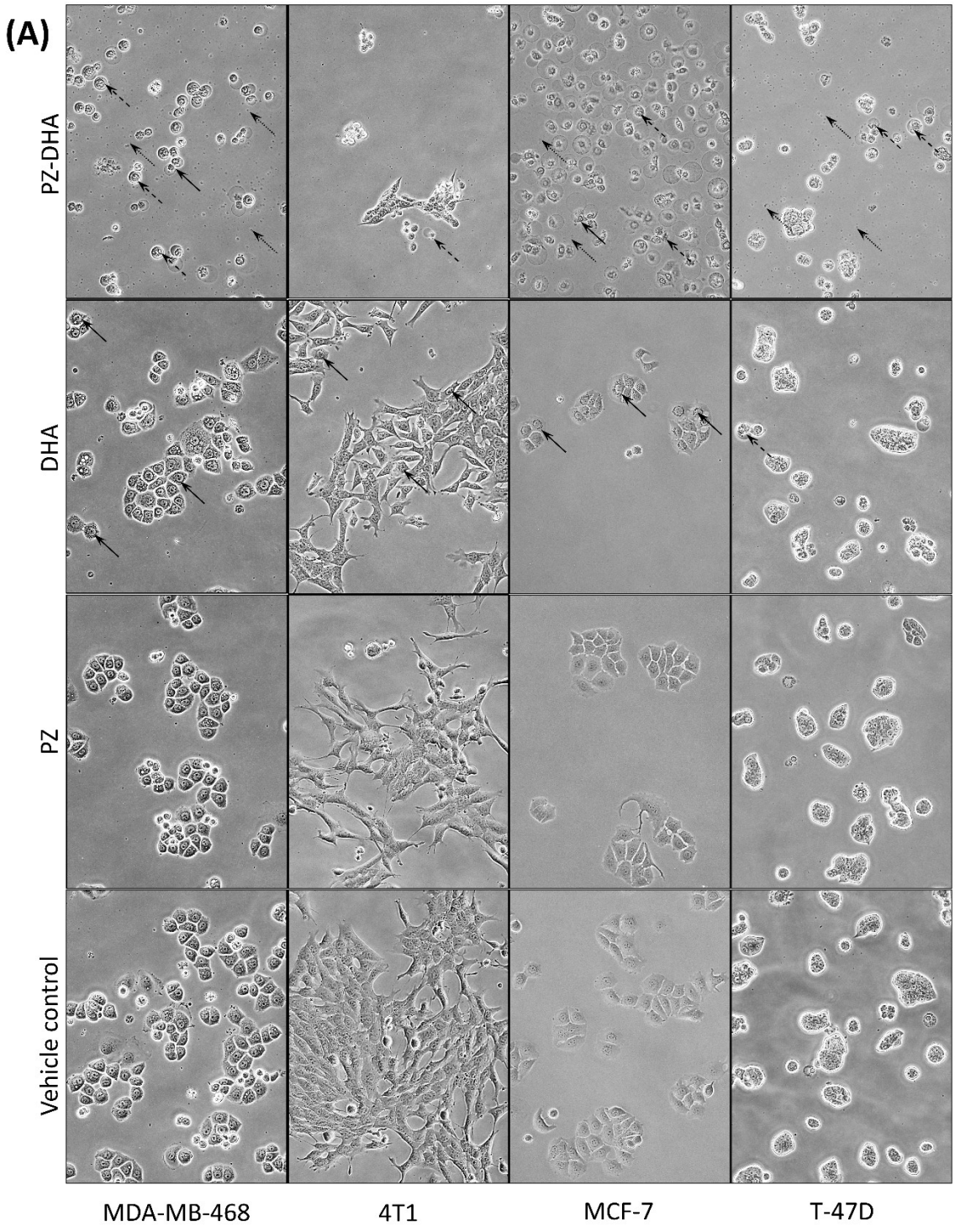


**Figure 4.1. PZ-DHA induces morphological changes in mammary carcinoma cells *in vitro*. (Figure 4.1 is continued on the next page.)**

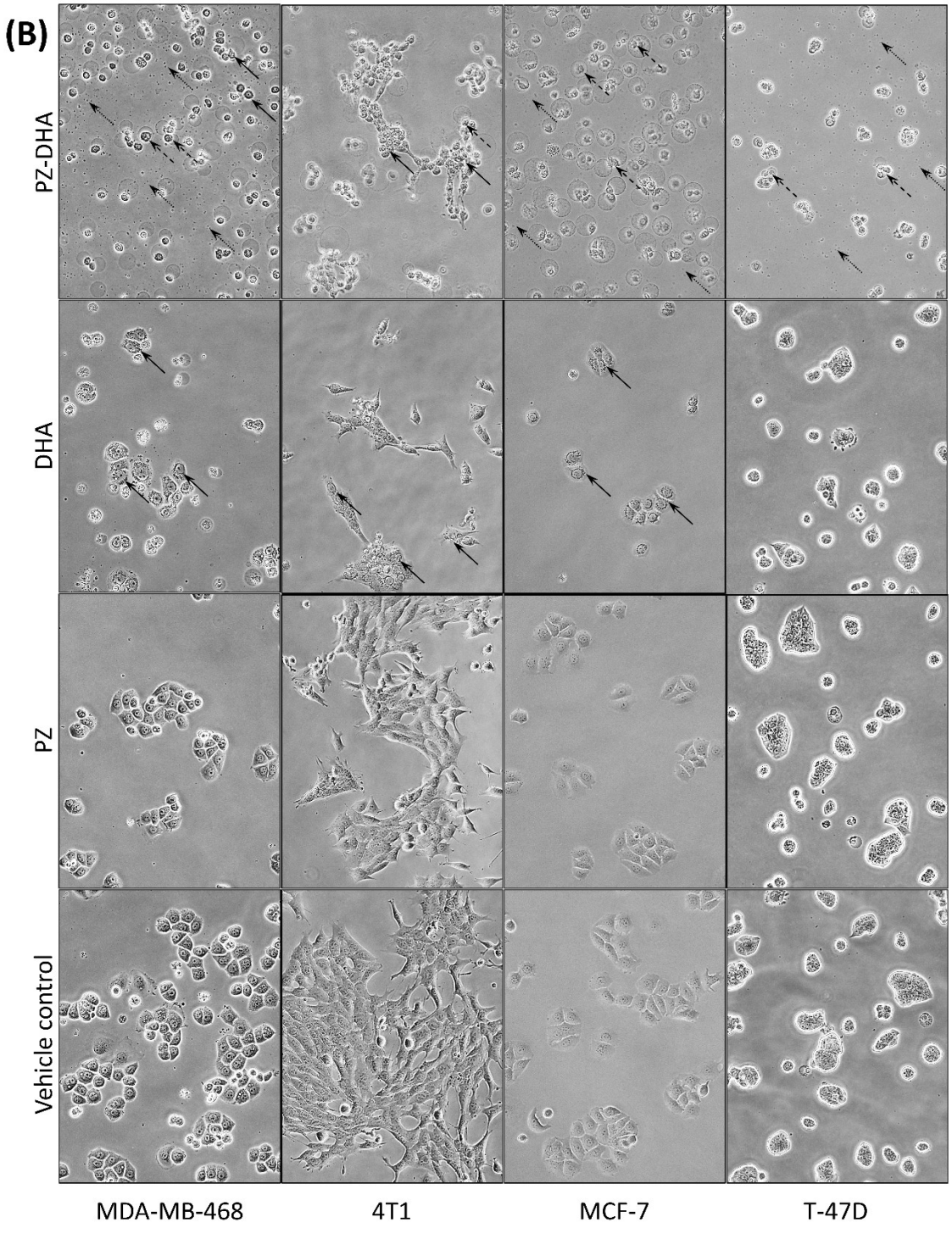
(B)
PZ-DHA
DHA
PZ
Vehicle control
MDA-MB-468
4T1
MCF-7
T-47D

**Figure 4.1. PZ-DHA induces morphological changes in mammary carcinoma cells *in vitro*.**
MDA-MB-468, 4T1, MCF-7 and T-47D mammary carcinoma cells were seeded into 12-well plates, and adherent cells were treated vehicle, **(A)** 50 μM or **(B)** 100 μM of PZ, DHA, or PZ-DHA and cultured for 24 h. Following culture, cells were photographed using a Nikon eclipse TS 100 phase contrast microscope equipped with Infinity 1 camera at ×200 magnification.

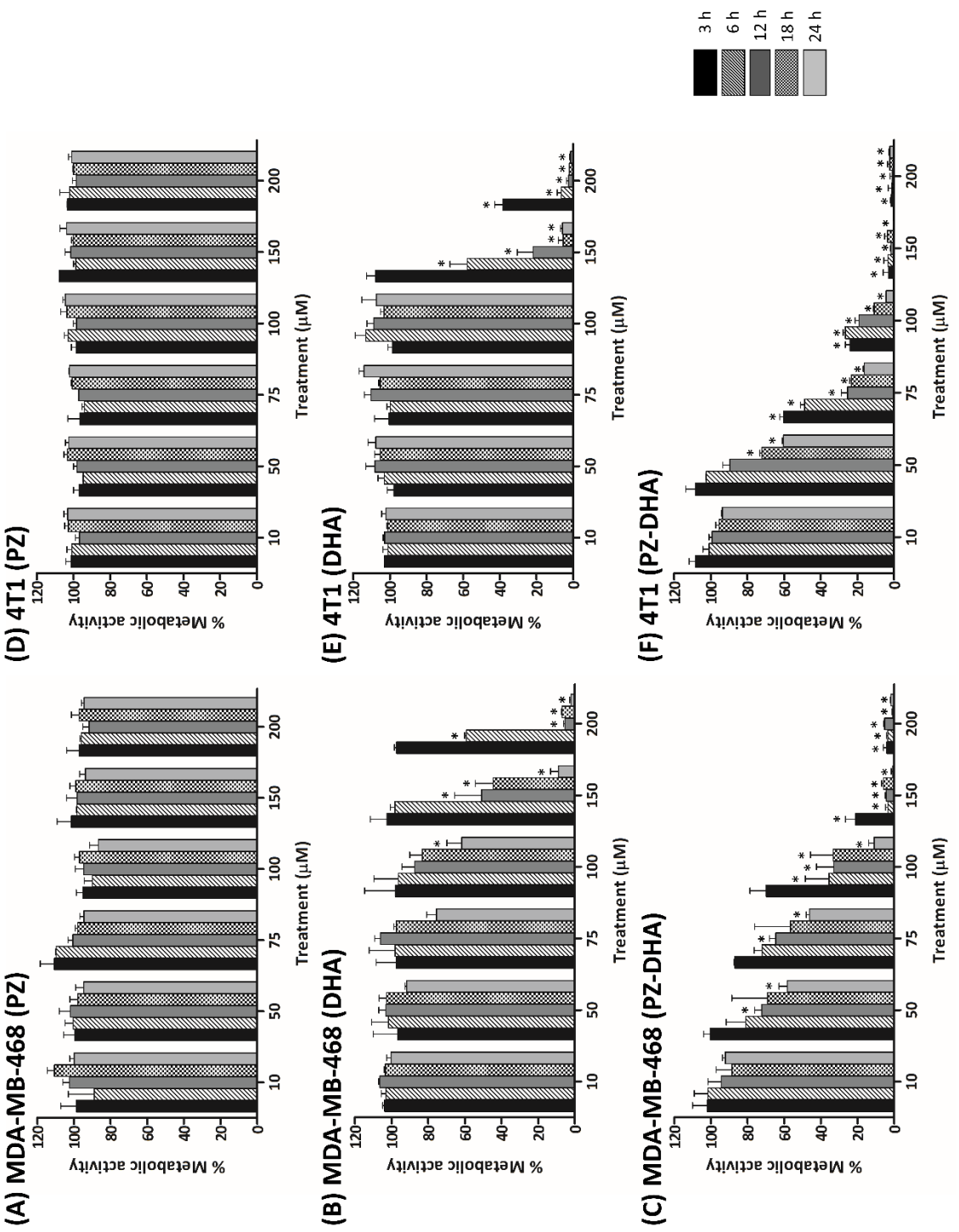


**Figure 4.2. PZ-DHA inhibits the metabolic activity of mammary carcinoma cells in a concentration- and time-dependent manner.**

**(Figure 4.2 is continued on the next page.)**

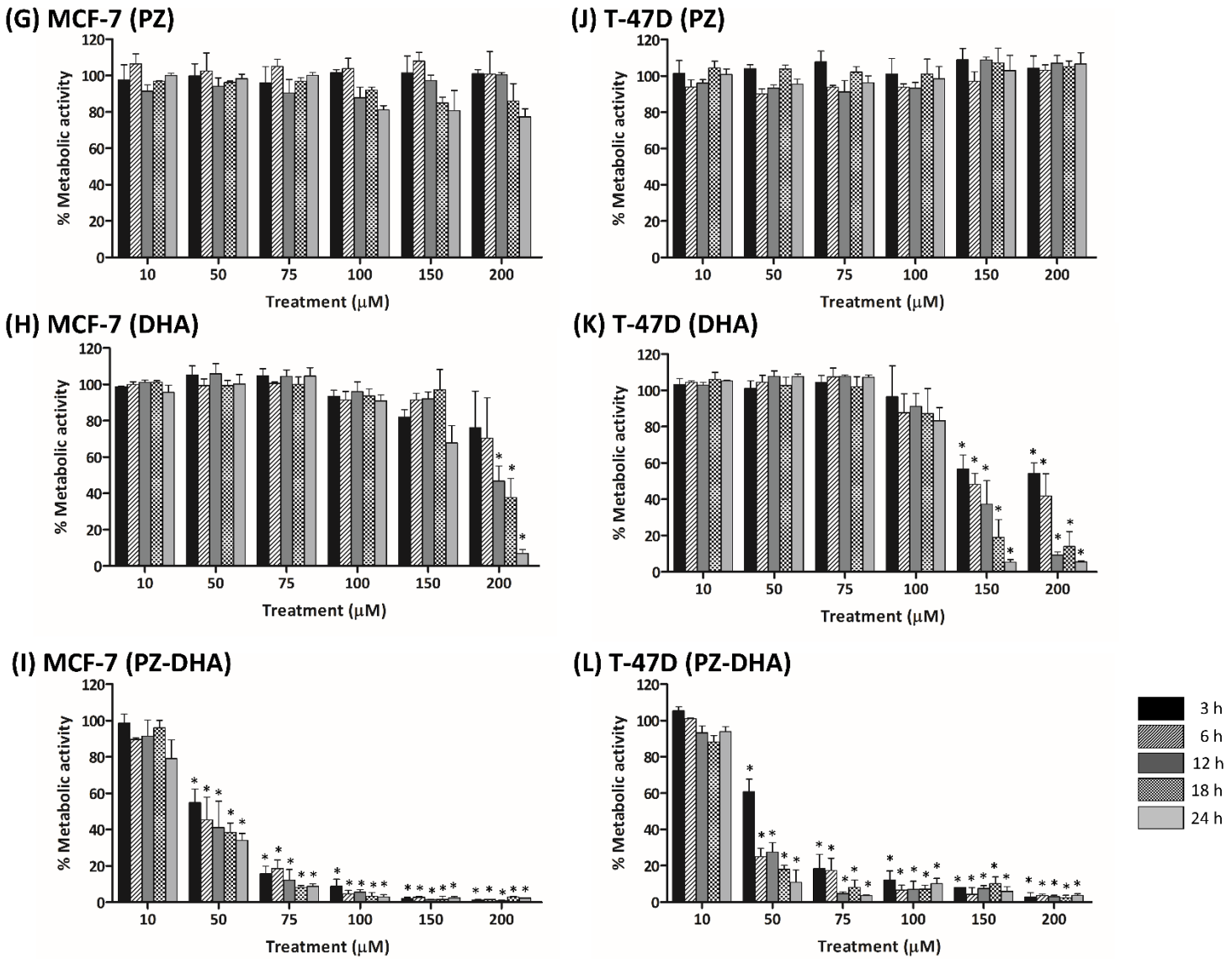
(G) MCF-7 (PZ)
(J) T-47D (PZ)
(H) MCF-7 (DHA)
(K) T-47D (DHA)
(I) MCF-7 (PZ-DHA)
(L) T-47D (PZ-DHA)
% Metabolic activity
Treatment (μM)
10
50
75
100
150
200
3 h
6 h
12 h
18 h
24 h

**Figure 4.2. PZ-DHA inhibits the metabolic activity of mammary carcinoma cells in a concentration- and time-dependent manner.**
MDA-MB-468 cells (**(A)** PZ, **(B)** DHA, **(C)** PZ-DHA), 4T1 cells (**(D)** PZ, **(E)** DHA, **(F)** PZ-DHA), MCF-7 cells (**(G)** PZ, **(H)** DHA, **(I)** PZ-DHA), and T-47D cells (**(J)** PZ, **(K)** DHA, **(L)** PZ-DHA) were treated and cultured for 24 h. At the end of culture, cells were incubated in the presence of MTS/PMS for 3 h and development of the formazan product was determined by measuring the absorbance at 490 nm. Metabolic activity of the cells was calculated using the equation, % relative metabolic activity= $((A_T-A_{TB})/(A_C-A_{CB}))\times100$, where, $A_T$: absorbance of cells treated with drugs; $A_{TB}$: absorbance of treatment blank; $A_C$: absorbance of cells treated with vehicle control; $A_{CB}$: absorbance of vehicle blank at 24 and 48 h post-treatment compared using one-way ANOVA multiple means comparison method and differences among means were compared using Tukey's multiple means comparison method. Data presented as mean ± SEM are averaged results of three independent experiments performed in quadruplicates. *$p<0.05$.

### 4.2.3 PZ-DHA-induced cytotoxic activity is greater than PZ and DHA combined effect

Sections 4.2.1 and 4.2.2 outlined that, when conjugated into a single chemical entity, PZ-DHA showed greater cytotoxic activity than its two parent compounds, PZ and DHA. MDA-MB-231 cells were treated with a mixture of PZ and DHA with the aim of comparing the effects of combined PZ and DHA to PZ-DHA. When used at a high concentration (100 μM) for 18 h, PZ-DHA caused a significant reduction in the metabolic activity of MDA-MB-231 cells (% mean metabolic activity±SEM: PZ and DHA, 66.7±5.4%; PZ-DHA, 27.8±4.8%) ($p$<0.001) when compared to the PZ and DHA mixture. At concentrations lower than 100 μM, the mixture was as equally potent as PZ-DHA (Figure 4.3A). However, following prolonged exposure (24 h), PZ-DHA-induced inhibition of metabolic activity of MDA-MB-231 cells was significantly greater from than that of combined PZ and DHA, even at concentrations as low as 50 μM (% mean metabolic activity±SEM : PZ and DHA, 82.7±4.9%; PZ-DHA, 49.4±2.2) ($p$<0.001) and 75 μM (% mean metabolic activity ± SEM: PZ and DHA, 53.2±4.2%; PZ-DHA, 10.6±1.1) ($p$<0.001) and at 100 μM (% mean metabolic activity±SEM: PZ and DHA, 26.7±3.5%; PZ-DHA, 12.1±1.8) ($p$<0.01) (Figure 4.3B).

### 4.2.4 PZ-DHA induces early and late apoptosis of breast cancer cells

The effect of PZ-DHA on the induction of early/late apoptosis of MDA-MB-231 cells was tested using a 50 μM concentration that caused 53.9±8.3% cell death by 7AAD staining at 72 h post-treatment (Chapter 3, Figure 3.1). DHA significantly increased the % number of MDA-MB-231 cells undergoing early apoptosis (Annexin-V-FLUOS(+)/PI(-)-stained cells) (% mean number of cells ± SEM by the vehicle, 3.9±1.3; PZ, 4.3±0.7; DHA, 9.4±1.5; and PZ-DHA, 6.6±0.7) ($p$<0.05), as well as late apoptosis along with PZ-DHA (Annexin-V-FLUOS(+)/PI(+)-stained cells) (% mean number of cells±SEM by the vehicle, 6.6±1.9; PZ, 6.4±2.1; DHA, 25.5±4.2; and PZ-DHA, 44.4±4.9) ($p$<0.001) (Figure 4.4A). Furthermore, PZ-DHA caused an increase in MDA-MB-231 cell death that was statistically different from its parent compounds ($p$<0.001) (Figure 4.4B).

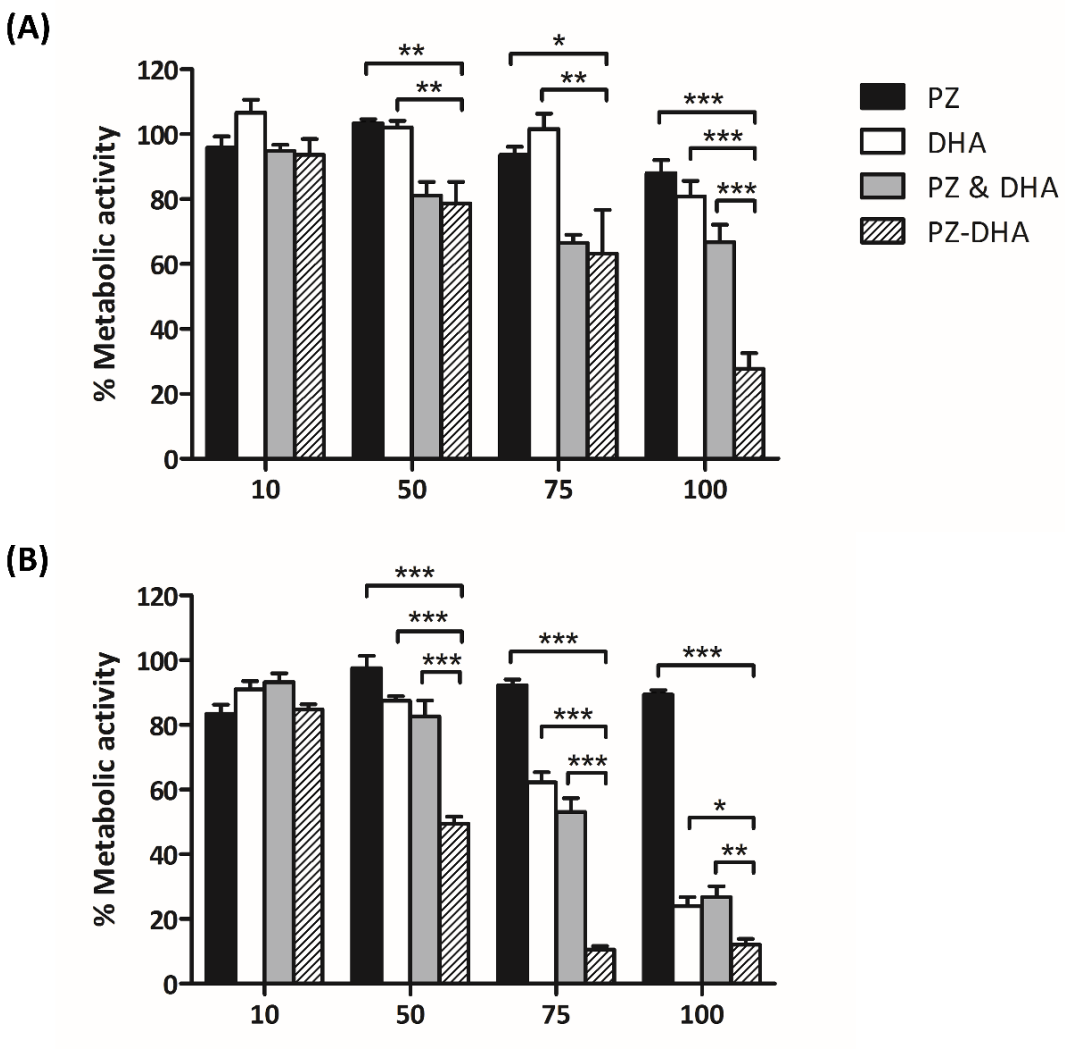


**Figure 4.3. PZ-DHA-induced *In vitro* cytotoxic activity in MDA-MB-231 cells is greater than the effect of combined PZ and DHA.**
PZ-DHA-induced cytotoxic activity against MDA-MB-231 cells was compared to PZ-, DHA- and PZ+DHA-induced cytotoxic activities using MTS assays. Cells were treated with PZ, DHA, PZ+DHA, PZ-DHA or vehicle and cultured for **(A)** 18 h or **(B)** 24 h. Cells were incubated in the presence of MTS for 3 h, and the absorbance was measured at 490 nm. Metabolic activity of the cells was compared using one-way ANOVA multiple means comparison method and differences among means were compared using Tukey's post means comparison method. Data presented as mean±SEM are averaged results of three independent experiments performed in quadruplicates. *$p$<0.05, **$p$<0.01, ***$p$<0.001.

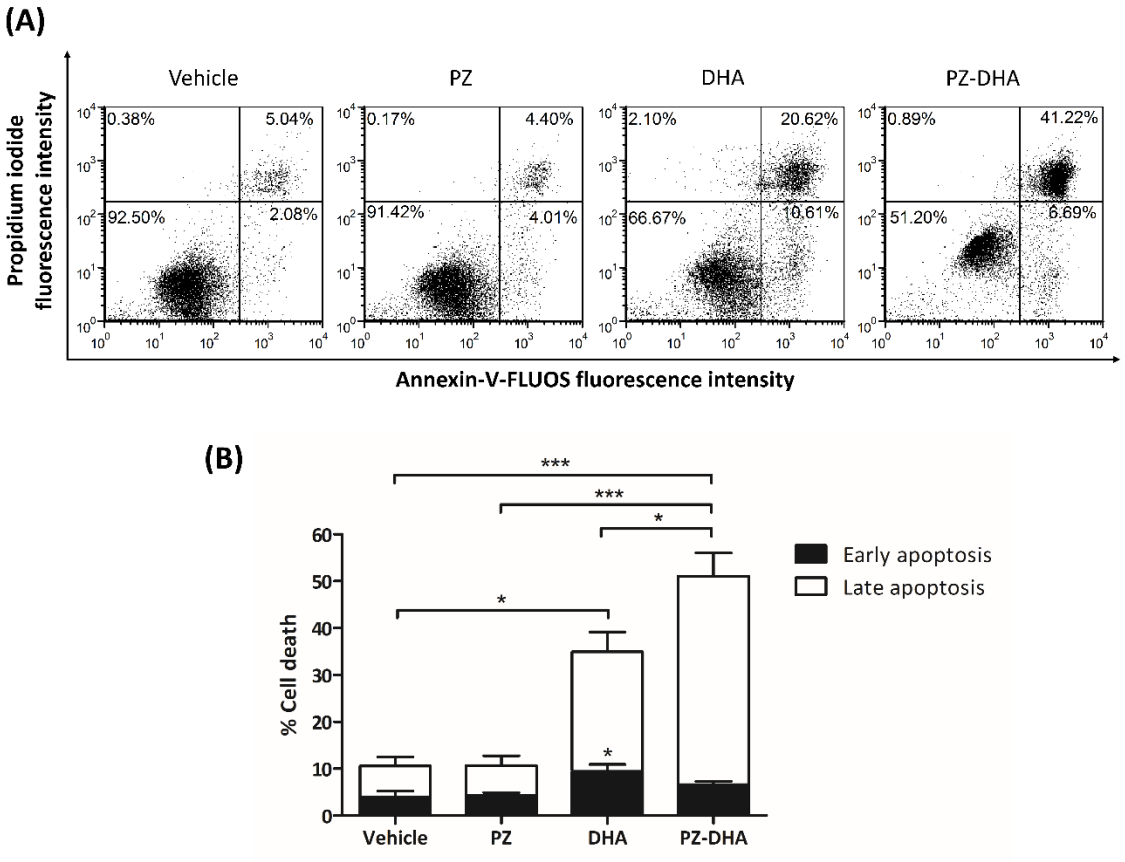


**Figure 4.4. PZ-DHA induces early and late apoptosis/necrosis of MDA-MB-231 cells.**

MDA-MB-231 cells were in 6-well plates treated with PZ, DHA, PZ-DHA (50 μM), vehicle or medium and cultured for 24 h. Cells were stained with Annexin-V-FLUOS/PI and analyzed by flow cytometry on FL1 and FL2. Data shown are **(A)** representative dot plots and **(B)** mean percentages of cells undergoing early apoptosis and late apoptosis/necrosis of three independent experiments±SEM. Data were analyzed using one-way ANOVA multiple means comparison method. Differences among means were compared using Tukey's post mean comparison test. **p*<0.05, ***p*<0.01, ****p*<0.001.

### 4.2.5 PZ-DHA is less cytotoxic toward non-malignant cells

Although treatment of MCF-10A cells with 50 μM or 100 μM PZ-DHA or its parent compounds did not inhibit metabolic activity (50 μM % mean metabolic activity±SEM: vehicle, 101.3±8.1; PZ, 86.43±4.12; DHA, 91.1±10.6; PZ-DHA, 83.7±14.9) ($p$=0.6420) (100 μM % mean metabolic activity ± SEM: vehicle, 101.3±8.1; PZ, 102.8±4.3; DHA, 105.1±5.2; PZ-DHA, 83.8±6.5) (p=0.1359), 200 μM PZ-DHA significantly suppressed MCF-10A metabolic acitivty (% mean metabolic activity±SEM: vehicle, 101.3±8.1; PZ, 105.6±9.3; DHA, 111.3±5.1; PZ-DHA, 48.2±0.6) ($p$<0.05) (Figure 4.5A). The selectivity of PZ-, DHA- and PZ-DHA-induced cytotoxic activity was further confirmed by treating MCF-10A cells and HDFs with a 50 μM concentration that was toxic to mammary carcinoma cells. Drug-treated non-malignant cells were stained with Annexin-V-FLUOS/PI and subjected to flow cytometric analysis to identify early and late apoptotic/necrotic cells. PZ-DHA-induced MDA-MB-231 % cell death (51.1±4.3%) was 7.7 and 8.6 times greater than that of in HDFs (6.6±1.6%) and MCF-10A cells (5.9±0.9%) (Figure 4.4B and Figure 4.5D), respectively.

### 4.2.6 Sub-cytotoxic concentrations of PZ-DHA suppress MDA-MB-231 cell proliferation

Oregon Green 488 is a cell-permeable fluorescent dye that binds to intra-cellular proteins, the fluorescence of which gets halved when the cell divides. Therefore, a left-ward shift of fluorescence by Oregon Green 488-stained cells indicates an increase in cell division and cell number due to proliferation. MDA-MB-231 cell proliferation was not affected by 20 μM PZ, DHA, or PZ-DHA (mean number of cell divisions±SEM by the vehicle, 3.0±0.1; PZ, 3.1±0.3; DHA, 3.1±0.3; PZ-DHA, 2.5±0.3) ($p$=0.3537); however, PZ-DHA at 30 μM reduced the proliferation of MDA-MB-231 cells by 2.3 fold in comparison to the DMSO vehicle control (mean number of cell division±SEM by the PZ, 2.5±0.4; DHA: 2.3±0.3; PZ-DHA, 1.3±0.3) ($p$<0.01) (Figure 4.6). This suggests that PZ-DHA has anti-proliferative activity at a sub-cytotoxic concentration.

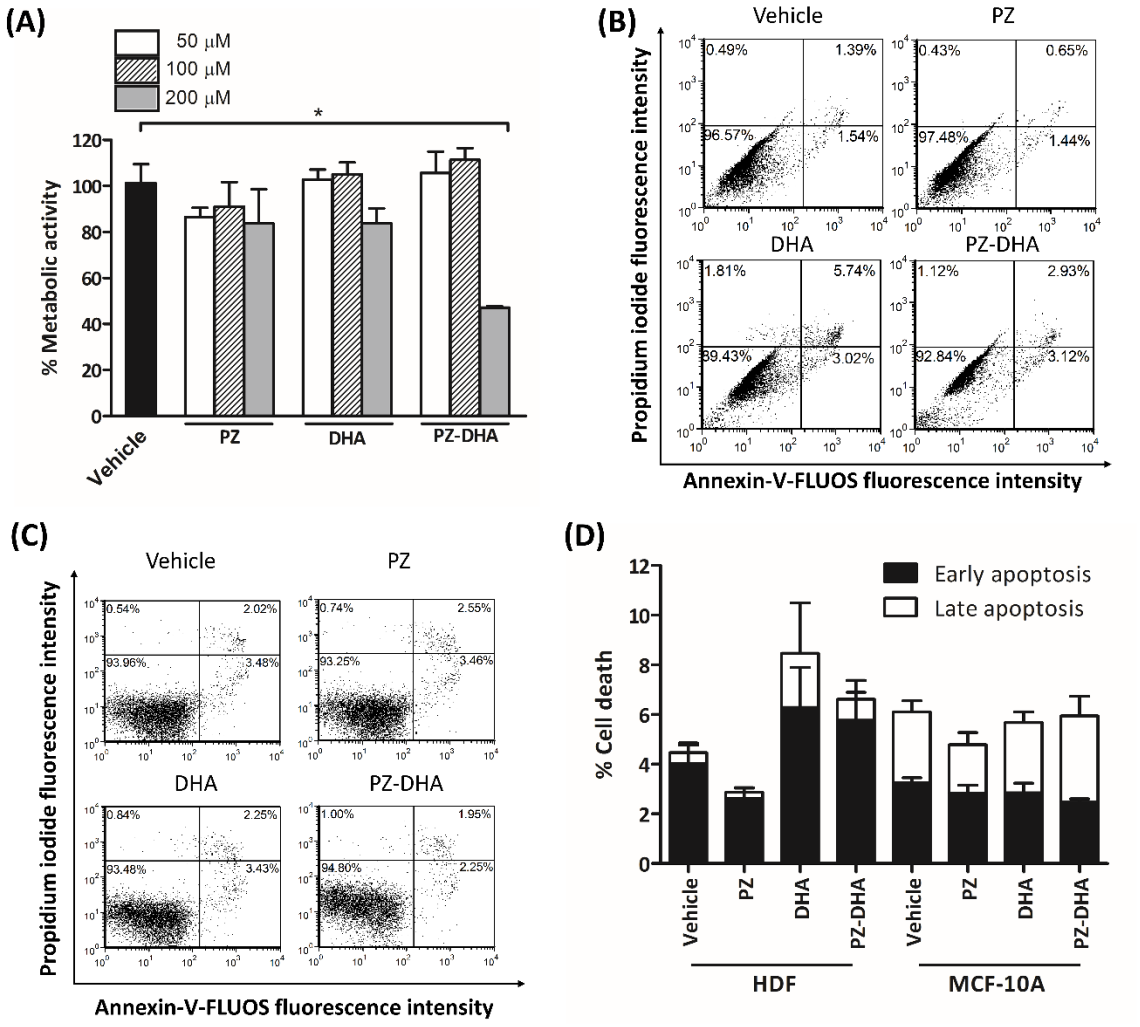


**Figure 4.5. PZ-DHA does not kill non-malignant cells.**
**(A)** Metabolic activity of PZ, DHA, and PZ-DHA-treated non-malignant mammary epithelial cells (MCF-10A) was measured using MTS assays. Cells were treated with 50 µM, 100 µM, and 200 µM of PZ, DHA, PZ-DHA, vehicle or medium alone and cultured for 24 h. At the end of culture cells were incubated with MTS/PMS mixture for 3 h, and the absorbance was measured at 492 nm. Data expressed as mean ± SEM are averaged results of three independent experiments conducted in quadruplicate. Cells undergoing early and/or late apoptosis/necrosis were detected using Annexin-V-FLUOS/PI staining. Non-malignant MCF-10A cells and HDFs were treated with PZ, DHA, PZ-DHA (all at 50 µM), vehicle or medium and cultured for 24 h. Cells were stained with Annexin-V-FLUOS/PI and analyzed by flow cytometry on FL1 and FL2. Data shown are representative dot plots of **(B)** HDFs and **(C)** MCF-10A cells and **(D)** mean percentages of cells in early apoptosis and late apoptosis/necrosis of three independent experiments±SEM. Data were analyzed using one-way ANOVA multiple means comparison method. Differences among means were compared using Tukey's post mean comparison test. *$p$<0.05.

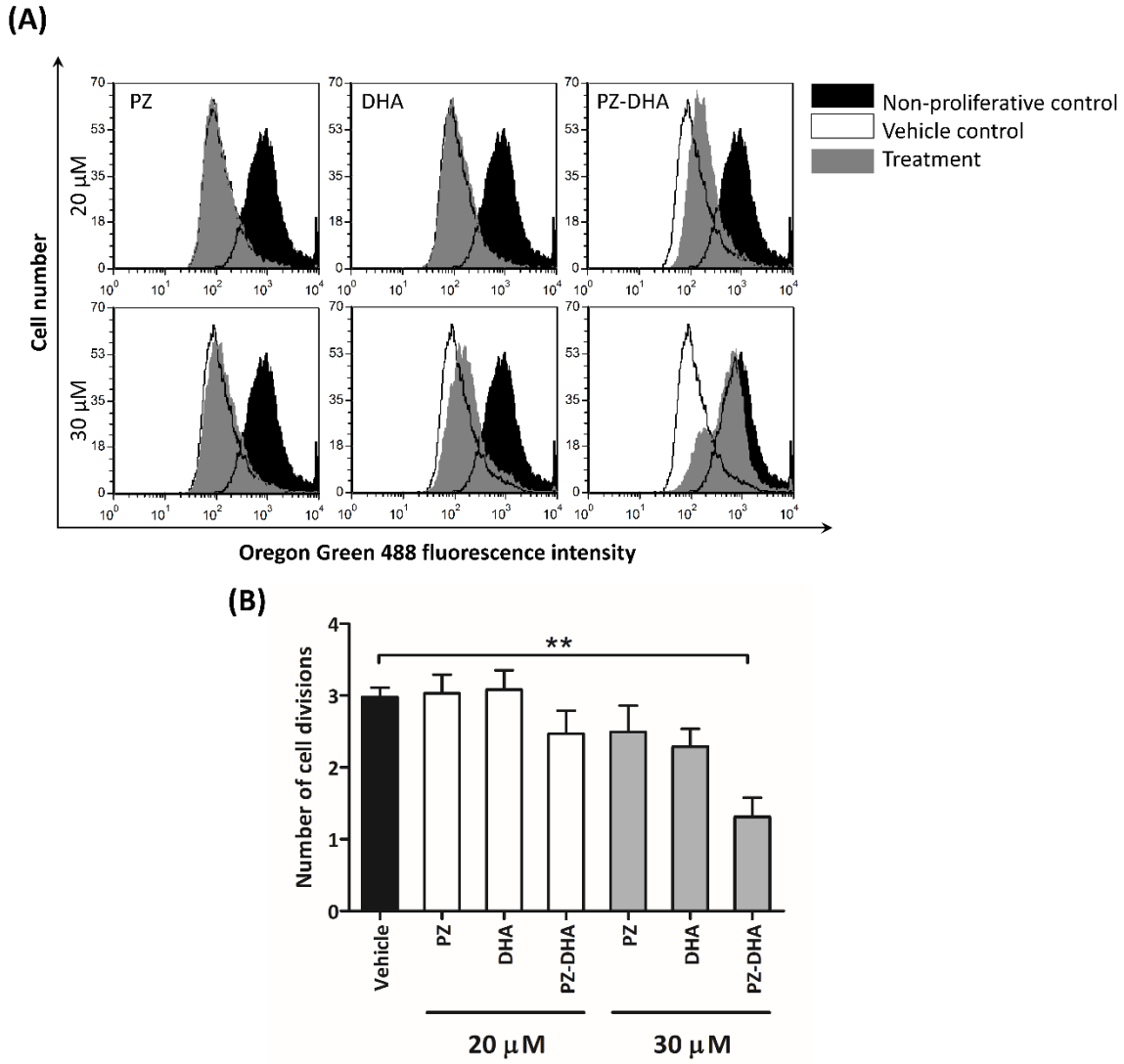


**Figure 4.6. Sub-cytotoxic concentrations of PZ-DHA inhibit the proliferation of MDA-MB-231 cells *in vitro*.**

MDA-MB-231 cells were synchronized to $G_0$ phase by culturing cells in serum-free DMEM overnight. Synchronized cells were seeded and stained with Oregon Green 488 dye, then treated with PZ, DHA, PZ-DHA (20 or 30 µM) or vehicle and cultured for 72 h at 37°C. At the end of culture, cells were harvested and analyzed by flow cytometry on FL1. Data shown are **(A)** representative histograms of cells treated with PZ, DHA or PZ-DHA with respect to the vehicle and non-proliferative control and **(B)** mean number of cell divisions±SEM from three independent experiments. Differences among means were compared using Tukey's post mean comparison test. $^{**}p<0.01$.

### 4.2.7 Sub-cytotoxic concentrations of PZ-DHA inhibits the expression of Ki67 in MDA-MB-231 cells

The antiproliferative activity of PZ-DHA at a cellular level was shown by the reduction in the number of cell divisions of Oregon Green 488–stained MDA-MB-231 cells. The anti-proliferative activity of PZ-DHA at a molecular level was confirmed by quantifying the expression of the proliferation marker, Ki67, in each phase of the cell cycle separately, as well as collectively (Figure 4.7). PZ-DHA consistently decreased Ki67 expression in all phases of the cell cycle; although the trend in reduction did not reach statistical significance when each phase was considered separately (mean % relative Ki67 expression in $G_1$ phase±SEM: vehicle, 94.5±11.1; PZ, 103.2±5.7; DHA, 90.3±7.9; PZ-DHA, 75.2±5.7), (mean % relative Ki67 expression in S phase±SEM: vehicle, 95.1±12.4; PZ, 106.4±5.3; DHA, 95.2±9.8; PZ-DHA, 79.5±8.1) and (mean % relative Ki67 expression in $G_2$/M phase±SEM: vehicle, 92.7±10.7; PZ, 102.3±4.1; DHA, 90.7±9.9; PZ-DHA, 70.3±7.1) (Figure 4.7B). However, when all phases were considered together, the PZ-DHA-induced reduction in Ki67 expression was statistically significant, suggesting a reduction in MDA-MB-231 cell proliferation (mean % relative Ki67 expression±SEM: vehicle, 93.9±2.9; PZ, 100.4±7.3; DHA, 81.5±5.9; PZ-DHA, 70.7±2.7) ($p<0.05$) (Figure 4.7C).

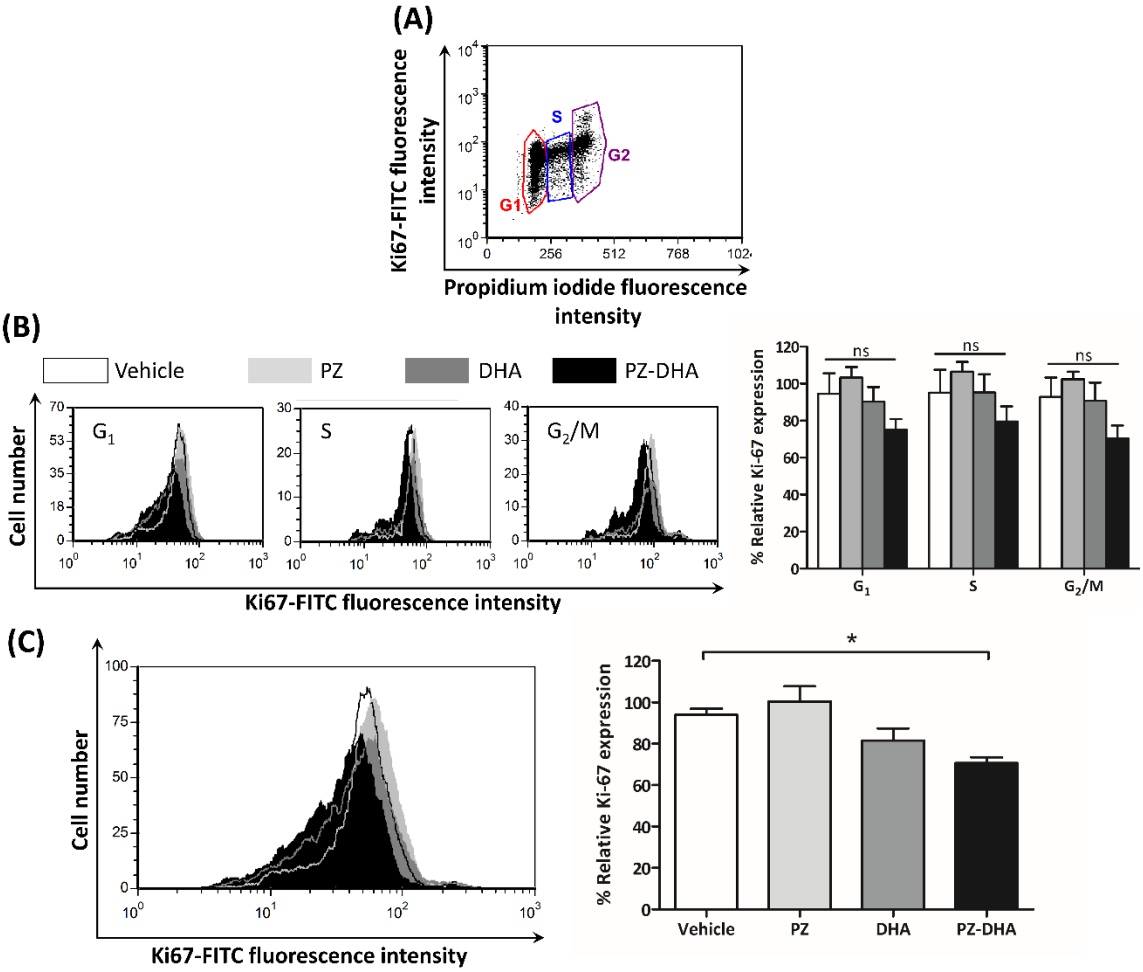


**Figure 4.7. A sub-cytotoxic concentration of PZ-DHA suppress the expression of Ki67 proliferation marker in MDA-MB-231 cells *in vitro*.**
MDA-MB-231 cells were synchronized, treated with PZ, DHA, PZ-DHA (30 µM) or vehicle l and cultured for 72 h. Cells were harvested and fixed in 70% cold ethanol. Fixed cells were stained with FITC-conjugated Ki67 Ab and/or PI in the presence of RNase and analyzed by flow cytometry on FL1 and FL2. Data shown are **(A)** representative dot plots showing gating for cell cycle phases, Ki67 expression of MDA-MB-231 cells gated at **(B)** $G_1$, S and $G_2$/M phases and **(C)** overall Ki67 expression. Mean % relative Ki67 expression±SEM were determined after four independent experiments. Statistical analysis was performed using one-way ANOVA multiple means comparison method and differences among means were compared using Tukey's post mean comparison method. *$p$<0.05.

### 4.2.8 Sub-cytotoxic concentrations of PZ-DHA arrest MDA-MB-231 cell cycle at $G_2$/M phase

Cell cycle analysis was performed to understand whether PZ-DHA arrested the growth of MDA-MB-231 cells at any particular phase(s) of the cell cycle. Treatment of MDA-MB-231 cells with 30 μM PZ-DHA arrested cell proliferation at $G_2$/M phase (Figure 4.8); however, at 20 μM, none of the drugs influenced cell cycle progression (Figure 4.8A and B). At 30 μM, neither PZ nor DHA arrested MDA-MB-231 cell cycle progression at $G_2$/M (mean % cell number in $G_2$/M phase±SEM, vehicle, 15.9±1.6; PZ, 16.9±1.6; DHA, 16.5±0.2; PZ-DHA, 25.5±0.6) ($p$<0.05). Furthermore, % mean cell number in the $G_0/G_1$ phase was significantly reduced by PZ-DHA treatment (mean % cell number in $G_0/G_1$ phase±SEM, vehicle, 51.9±0.9; PZ, 51.1±0.1; DHA, 51.4±2.2; PZ-DHA, 41.5±1.6); however, S phase (mean % cell number in S phase±SEM, vehicle, 32.2±1.5; PZ, 32.0±1.6; DHA, 31.9±2.3; and PZ-DHA, 33.0±2.1) was not affected, suggesting that PZ-DHA-induced cell cycle arrest is confined to the $G_2$/M phase of the cell cycle (Figure 4.8A and C). The effects of PZ-DHA, PZ and DHA on key cell cycle regulatory kinases and cyclins were also tested using western blot analysis. PZ-DHA and DHA significantly reduced the expression of cyclinB1 by 58.6% and 63.9% respectively (Figure 4.9A) (% mean relative expression of cyclin B1±SEM: vehicle, 93.9±5.6%; DHA, 35.3±9.4%; PZ-DHA, 29.9±7.6%); however, only PZ-DHA (vehicle, 99.5±6.7%; PZ-DHA, 37.2±11.1%) inhibited the kinase activity of CDK1 (Figure 4.9B), causing a 62.3% reduction compared to the vehicle control. Consistent with the cell cycle analysis data, neither cyclin D3/CDK4 nor cyclin A/CDK2 were affected by any of the drugs (Figure 4.9C and D).

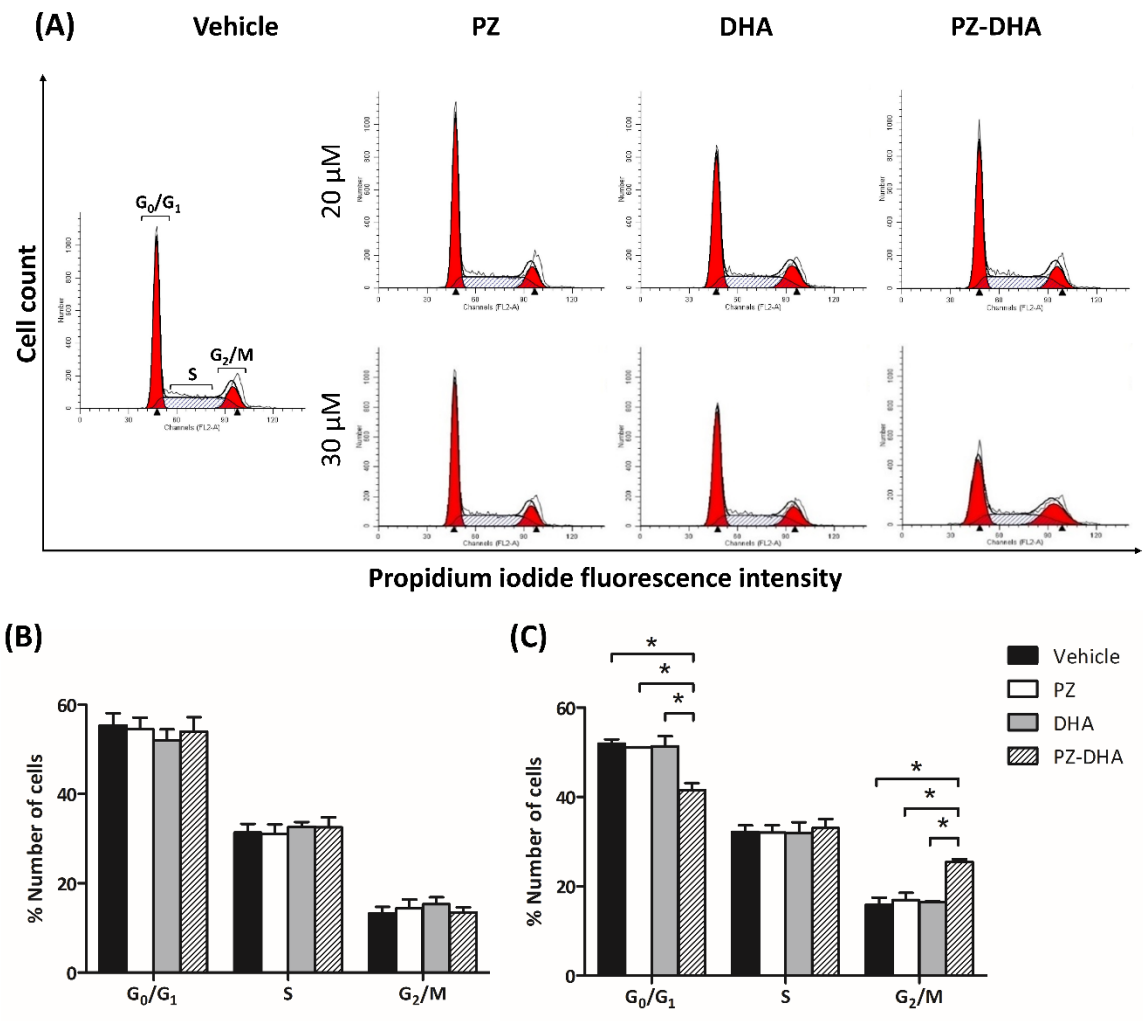


**Figure 4.8. A sub-cytotoxic concentration of PZ-DHA arrests MDA-MB-231 cell replication at $G_2$/M phase.**

MDA-MB-231 cells were synchronized and treated with PZ, DHA, PZ-DHA (20 or 30 µM) or vehicle and cultured for 72 h, then cells were harvested and fixed in 70% cold ethanol. Fixed cells were stained with PI in the presence of RNase and analyzed by flow cytometry on FL2. **(A)** Representative histograms of cells treated with PZ, DHA, PZ-DHA or vehicle and analyzed using ModFit software are shown. Mean % number±SEM of cells treated with **(B)** 20 µM and **(C)** 30 µM of test compounds in each phase of cell cycle was calculated after three independent experiments. Statistical analysis was performed using one-way ANOVA multiple means comparison method and differences among means were compared using Tukey's post mean comparison method. *$p$<0.05.

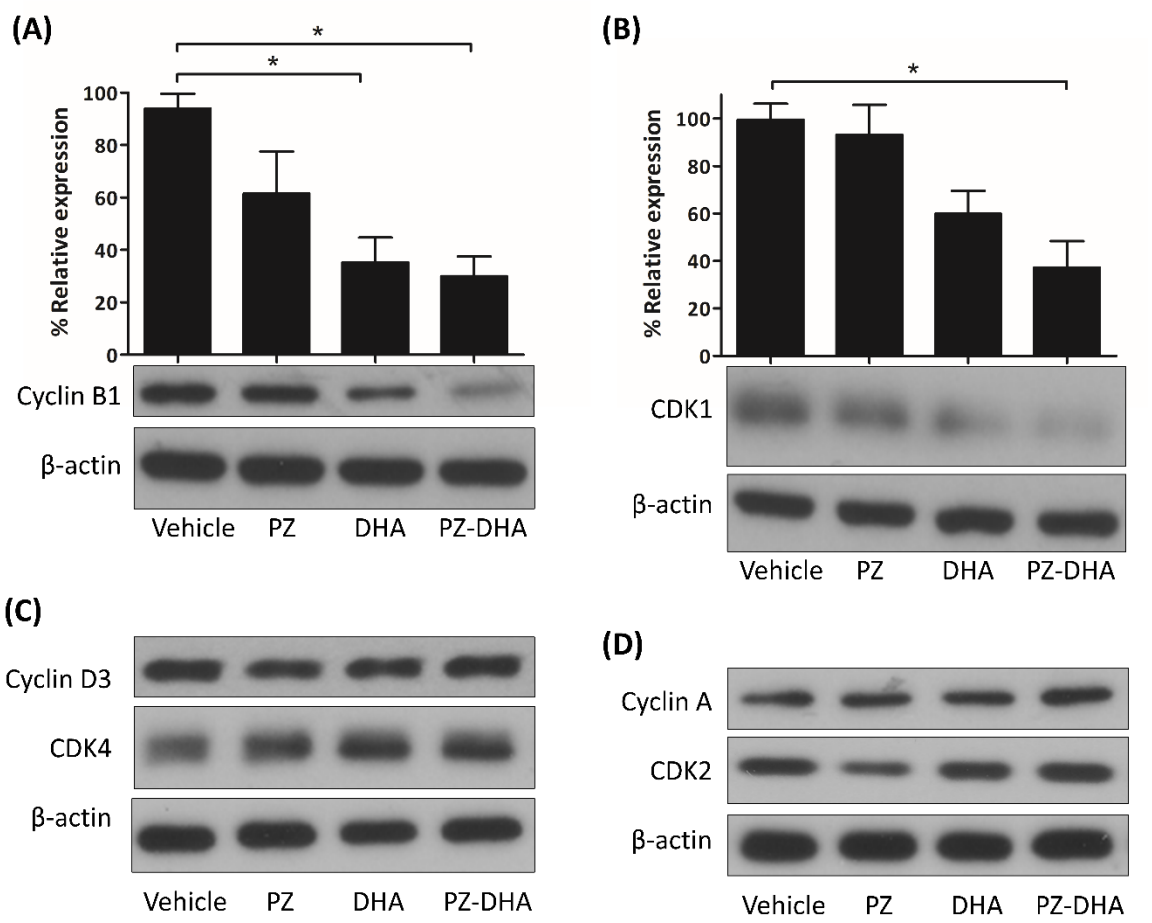


**Figure 4.9. A sub-cytotoxic concentration of PZ-DHA down-regulates the expression by MDA-MB-231 cells of cell cycle proteins involved in $G_2$/M progression.**
MDA-MB-231 cells were treated with 20 μM of PZ, DHA, PZ-DHA, vehicle or medium alone and cultured for 24 h. Cell lysates were prepared, and relative expression of cell cycle regulatory proteins were determined using western blot analysis. Representative blots showing **(A)** cyclin B1 **(B)** CDK1 **(C)** cyclin D3 and CDK4 **(D)** cyclin A and CDK2 expression from a representative experiment (n=3) are shown. Relative expression of cyclin B1 and CDK1 was calculated and normalized to the medium control. One-way ANOVA multiple mean comparison statistical analysis was performed, and differences among means were compared using Tukey's post means comparison method. *$p$<0.05.

### 4.2.9 PZ-DHA inhibits Akt signaling in MDA-MB-231 cells

The molecular mechanism(s) involved in the anti-proliferative activity of PZ-DHA were studied using western blot analysis of cell lysates prepared from medium-, vehicle-, PZ-, DHA-, or PZ-DHA-treated MDA-MB-231 and MCF-10A cells. PZ-DHA inhibited Akt signaling in MDA-MB-231 cells (Figure 4.10). Phosphorylation of PTEN (at Ser380), the upstream inhibitor of Akt signaling, was significantly upregulated by PZ-DHA (mean % relative expression±SEM: vehicle, 81.2±5.4; PZ, 85.5±5.4; DHA, 108.4±5.8; PZ-DHA, 138.5±8.1) ($p$<0.001) (Figure 4.10A) and the phosphorylation of PDK1 (at Ser241), the upstream Akt inducer, was downregulated (mean % relative expression±SEM: vehicle, 103.7±8.4; PZ, 57.2±4.8; DHA, 56.7±2.9; PZ-DHA, 34.1±5.2) ($p$<0.001) (Figure 4.10B). Furthermore, reduced Akt activity in PZ-DHA-treated MDA-MB-231 cells was also evident by the decreased phosphorylation of the downstream Akt-effector molecule, mTOR (mean % relative expression±SEM: vehicle, 101.6±8.4; PZ, 87.8±3.6; DHA, 83.3±5.8; PZ-DHA, 64.1±6.6) ($p$<0.05) (Figure 4.10C), at Ser2448. PZ-DHA treatment had the opposite effect on the phosphorylation of GSK3β at serine and tyrosine sites; phosphorylation at Ser9 (mean % relative expression±SEM: vehicle, 94.0±5.8; PZ, 91.6±8.3; DHA, 148.6±4.3; PZ-DHA, 179.6±10.1) ($p$<0.001) (Figure 4.10D) was increased while Tyr216 phosphorylation was not affected (mean % relative expression±SEM: vehicle, 80.6±0.6; PZ, 88.6±4.2; DHA, 74.1±7.2; PZ-DHA, 66.9±8.1) ($p$=0.3054) (Figure 4.10E). In contrast, PZ-DHA had either no effect or the opposite effect on MCF-10A cells, with the exception of mTOR phosphorylation (Figure 4.11B).

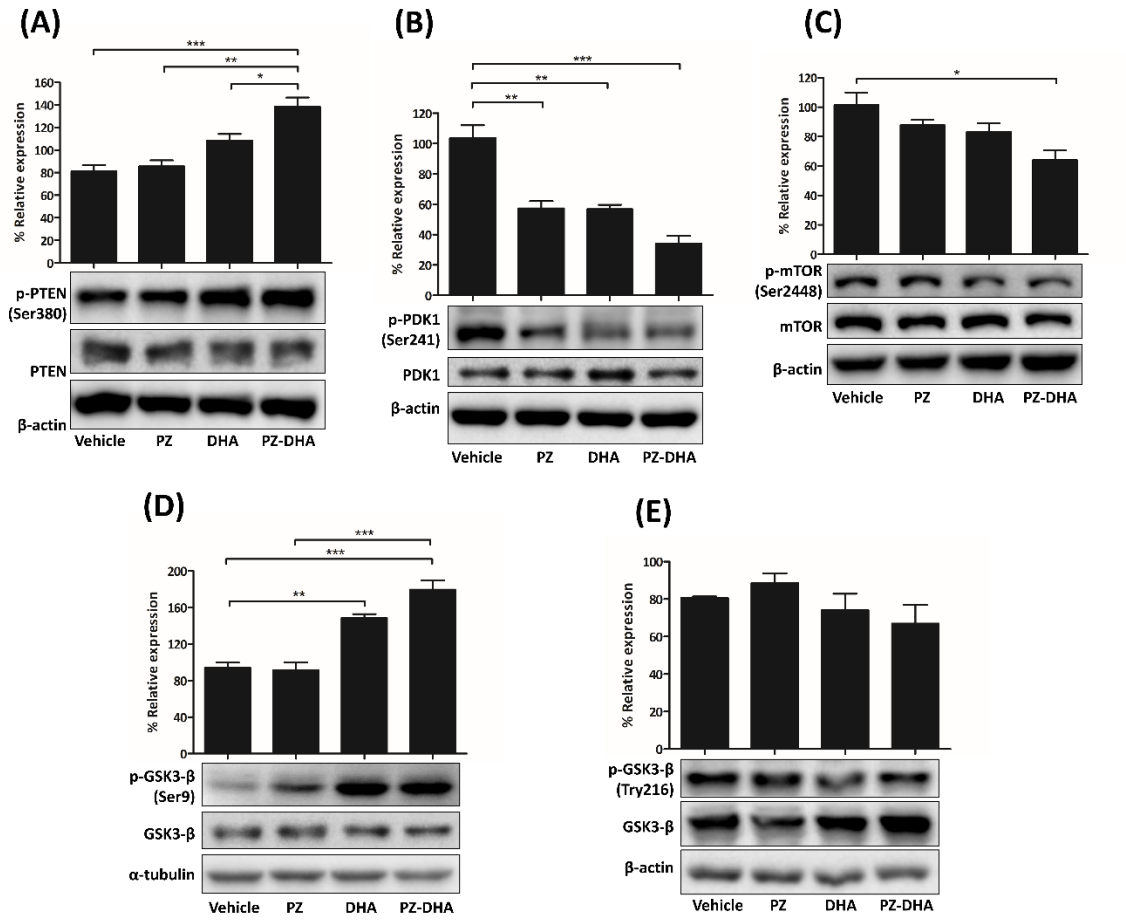


**Figure 4.10. A sub-cytotoxic concentration of PZ-DHA inhibits PI3K/Akt/mTOR pathway *in vitro*.**

MDA-MB-231 cells were treated with PZ, DHA, PZ-DHA (20 μM) or vehicle alone and cultured for 72 h. Cells were harvested, and protein-rich cell lysates were prepared. Equal amounts of protein (20 μg) were loaded on to 10%, 12% or 15% SDS-polyacrylamide gels and electrophoresed. Proteins were transferred to nitrocellulose membranes and blots probed with Ab against **(A)** phospho-PTEN (Ser380)/total-PTEN, **(B)** phospho-PDK1 (Ser241)/total-PDK1, **(C)** phospho-mTOR (Ser2448)/total-mTOR, **(D)** phospho-GSK3β (Ser9)/total-GSK3β and **(E)** phospho-GSK3β (Tyr216)/total-GSK3β. Blots were incubated with the respective secondary Ab and equal protein loading was confirmed by β-actin or α-tubulin expression. Data shown are mean % relative expression±SEM of three independent experiments. ANOVA multiple means comparison statistical method was performed and differences among means were compared using Tukey's test; *$p$<0.05, **$p$<0.01 and ***$p$<0.001.

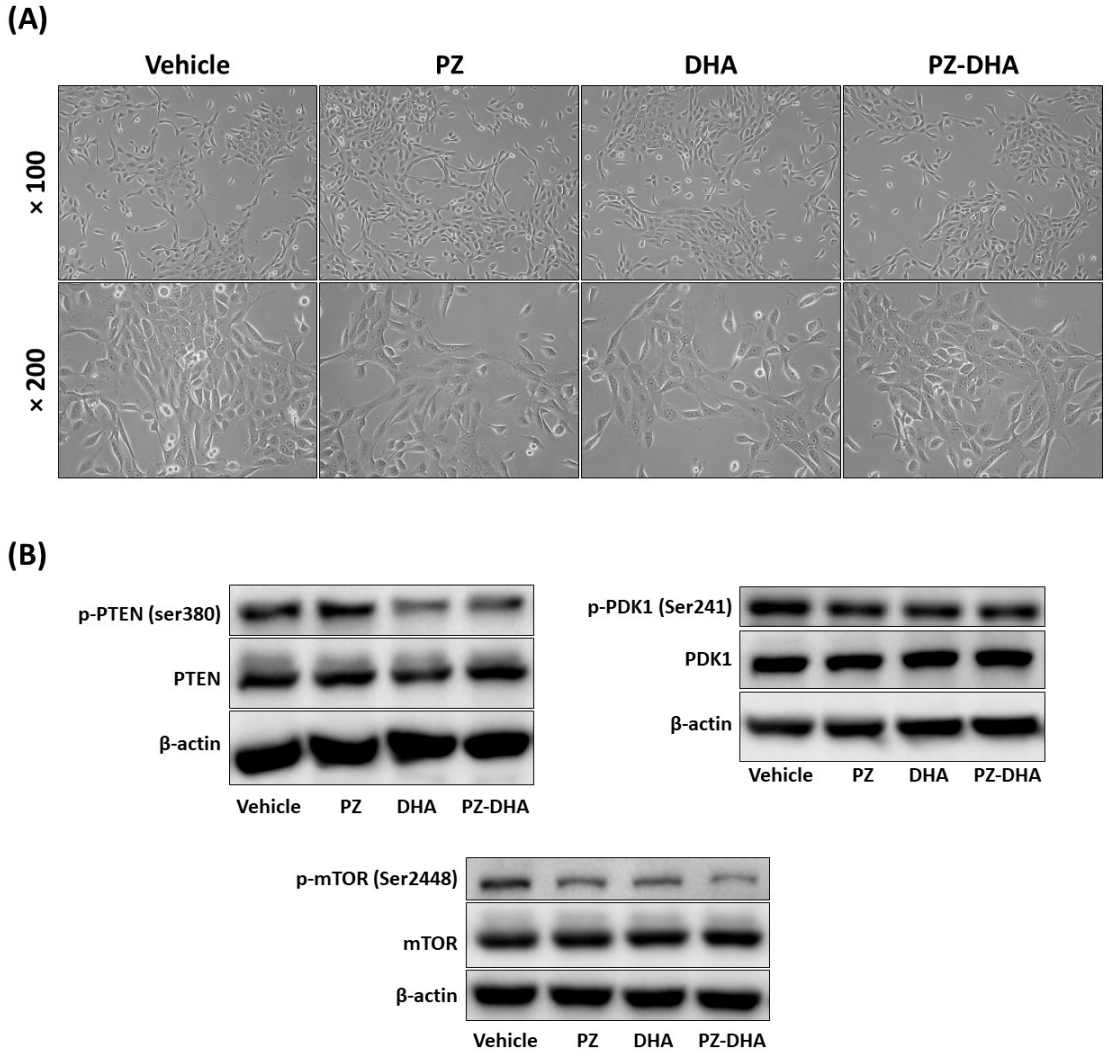


**Figure 4.11. A concentration of PZ-DHA that is cytotoxic to MDA-MB-231 cells does not affect the morphology of MCF-10A cells; a sub-cytotoxic concentration of PZ-DHA does not inhibit the PI3K/Akt/mTOR pathway in MCF-10A cells *in vitro*.** **(A)** MCF-10A mammary epithelial cells were seeded into 12-well plates, and adherent cells were treated with vehicle, 50 μM of PZ, DHA, or PZ-DHA and cultured for 24 h. Following culture, cells were photographed using a Nikon eclipse TS 100 phase contrast microscope equipped with Infinity 1 camera at ×100 and ×200 magnification. **(B)** MCF-10A cells were treated with PZ, DHA, PZ-DHA (20 μM) or vehicle alone and cultured for 72 h. Cells were harvested, and protein-rich cell lysates were prepared. Equal amounts of protein (20 μg) were loaded on to SDS-polyacrylamide gels and electrophoresed. Proteins were transferred to nitrocellulose membranes and blots probed with Ab against phospho-PTEN (Ser380)/total-PTEN, phospho-PDK1 (Ser241)/total-PDK1, and phospho-mTOR (Ser2448)/total-mTOR. Blots were incubated with the respective secondary Ab and equal protein loading was confirmed by β-actin.

### 4.2.10 PZ-DHA inhibits MAPK signaling in MDA-MB-231 cells

Next, the effect of PZ-DHA on MAPK signaling was studied since cell proliferation and differentiation are largely regulated by MAPK signaling pathways (Seger and Krebs, 1995). Phosphorylation of RAF and ERK1/2 was detected by western blot analysis. Activation of RAF, the upstream inducer of ERK1/2, was markedly reduced by PZ-DHA, which inhibited phosphorylation at Ser259 (mean % relative expression±SEM: vehicle, 104.2±7.2; PZ, 85.4±6.3; DHA, 39.2±6.4; PZ-DHA, 19.6±5.9) ($p$<0.001) (Figure 4.12A). PZ-DHA significantly decreased the phosphorylation of ERK1 and ERK2 at Thr202 and Tyr204, respectively. PZ and DHA also significantly reduced ERK1/2 phosphorylation; however, the PZ-DHA-induced inhibitory effect was significantly lower than that of both parent compounds (mean % relative ERK1 expression±SEM: vehicle, 89.4±3.5; PZ, 54.5±7.8; DHA, 41.9±2.5; PZ-DHA, 24.5±4.7) and (mean % relative ERK2 expression±SEM: vehicle, 94.7±1.4; PZ, 47.8±6.5; DHA, 36.3±3.4; PZ-DHA, 12.3±4.6) ($p$<0.001) (Figure 4.12B).

### 4.2.11 PZ-DHA inhibits stem cell-like activity of breast cancer cells

Cancer stem cells are a dormant rare cancer cell sub-population with a distinct genetic signature which allows them to possess characteristics associated with normal stem cells such as self-renewal and differentiation (Batlle and Clevers, 2017). Therefore, cancer stem cells are more tumorigenic and drug-resistance compared to other cancer cells from the same tumor. Cancer stem cell targeted therapy is therefore important for killing chemotherapy-resistant cancer stem cells and overcoming cancer relapse. PZ-DHA attenuated spheroid formation by MCF-7 cells and decreased the acid phosphatase activity of MCF-7 cells in spheroids (mean % acid phosphatase activity±SEM: vehicle, 96.9±7.5; PZ, 100.1±9.2; DHA, 70.1±14.4; PZ-DHA, 23.5±2.6) at a concentration that was non-toxic to non-malignant MCF-10A mammary epithelial cells (50 μM) ($p$<0.001) (Figure 4.13A and B). Furthermore, PZ-DHA also inhibited the formation of secondary spheroids by MCF-7 cells isolated from primary spheroids (Figure 4.13C).

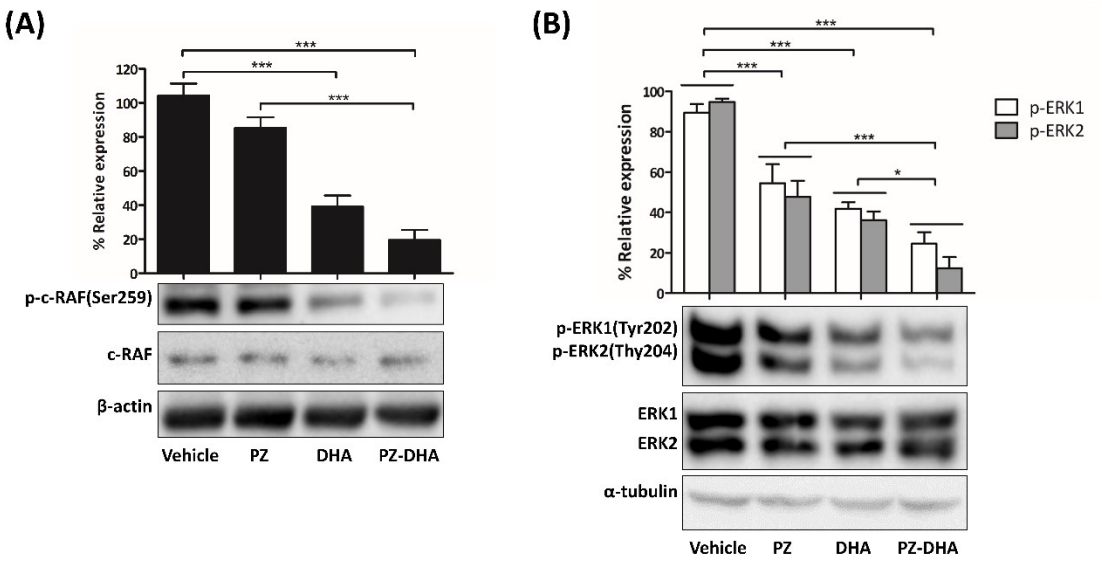


**Figure 4.12. A sub-cytotoxic concentration of PZ-DHA inhibits MAPK signaling *in vitro*.**
MDA-MB-231 cells were treated with PZ, DHA, PZ-DHA (20 μM) or vehicle alone and cultured for 72 h. Cells were harvested, and protein-rich cell lysates were prepared. Equal amounts of protein (20 μg) were loaded on to 10%, 12% or 15% SDS-polyacrylamide gels and electrophoresed. Proteins were transferred on to nitrocellulose membranes, and blots were probed with primary Ab against **(A)** phospho-c-RAF (Ser259)/total-c-RAF, **(B)** phospho-ERK1/2 p44 (Thr202)/p42 (Tyr204)/total-ERK1/2 p44/p42. Equal protein loading was confirmed by β-actin or α-tubulin expression. Data shown are mean % relative expression±SEM of three independent experiments. ANOVA multiple means comparison statistical method was performed and differences among means were compared using Tukey's test; *$p$<0.05, and ***$p$<0.001.

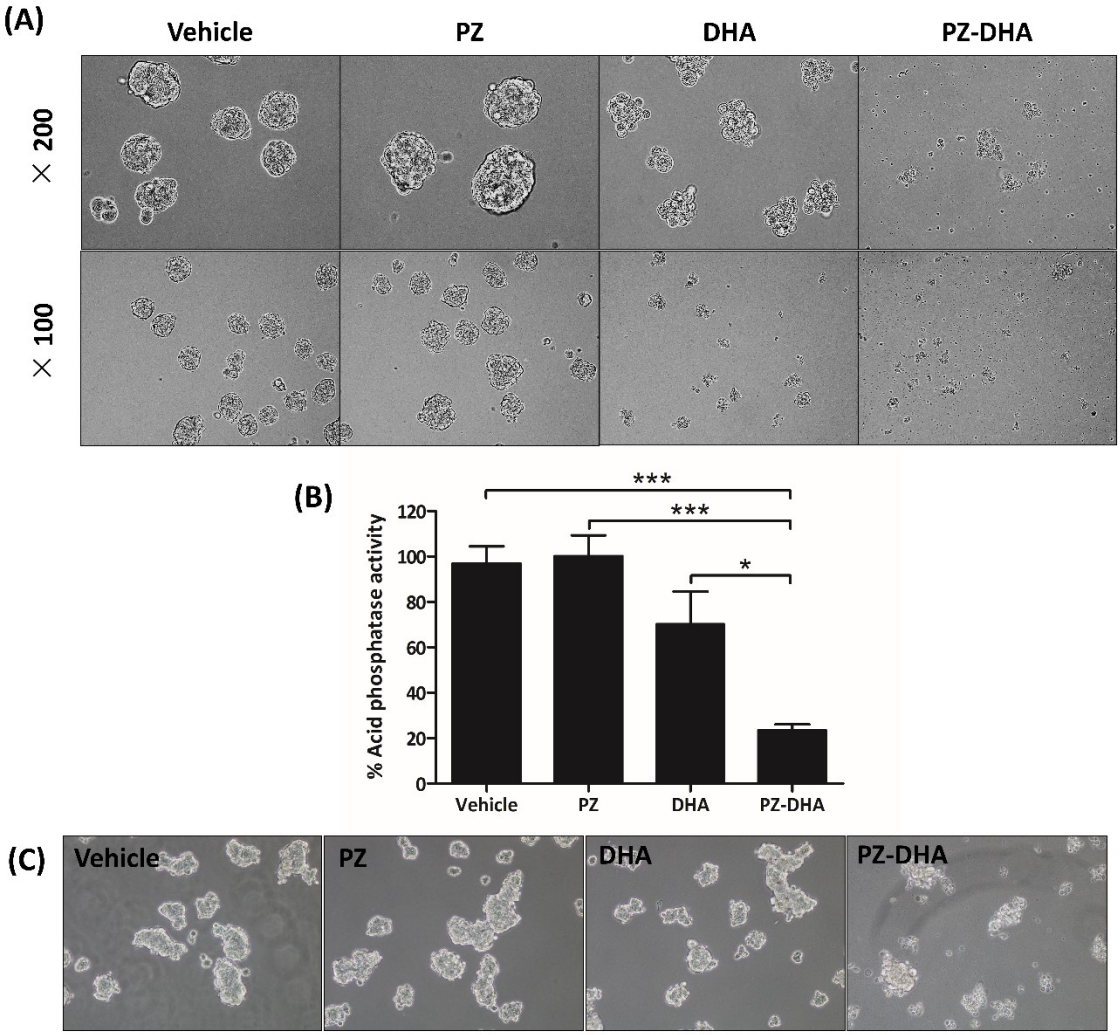


**Figure 4.13. PZ-DHA inhibits spheroid formation by breast cancer cells *in vitro*.** MCF-7, which are ER+ breast cancer cells, were grown in ultra-low adherent cell culture plates in spheroid growth medium for 48 h, treated with PZ, DHA, PZ-DHA (50 µM) or vehicle alone, and cultured for 72 h. **(A)** Spheroids were photographed and **(B)** the metabolic activity of spheroid cells was measured by acid phosphatase assay. Data shown are mean acid phosphatase activity±SEM of three independent experiments. ANOVA multiple means comparison statistical method was performed and differences among means were compared using Tukey's test; ns: not significant, *$p$<0.05 and ***$p$<0.001. **(C)** MCF-7 spheroids were dispersed into single cell suspensions and the growth of secondary spheroids was monitored in the presence or absence of PZ, DHA, and PZ-DHA.

### 4.2.12 PZ-DHA is cytotoxic to paclitaxel-resistant MDA-MB-231 (MDA-MB-231-TXL) cells

TNBC cells lack ER, PR and HER2; therefore, TNBC cells develop resistance to current conventional chemotherapy. Paclitaxel is one of the leading drugs used in the treatment of TNBC. The efficacy of PZ-DHA against paclitaxel-resistant MDA-MB-231 (MDA-MB-231-TXL) cells was tested using MTT assays, 7AAD and Annexin-V-488/PI staining, and western blot analysis. PZ-DHA caused morphological changes to MDA-MB-231-TXL cells and reduced the number of cells in the culture, suggesting anti-proliferative and/or cytotoxic activity (Figure 4.14A). The metabolic activity of drug-treated MDA-MB-231-TXL cells was tested using MTT assays and inhibition induced by PZ-DHA was compared to its parent compounds. PZ-DHA treatment at low concentrations (10 and 25 μM) for 24 h did not affect the metabolic activity of MDA-MB-231-TXL cells; however, a dose-dependent significant reduction of the metabolic activity was noted with longer treatment. High concentrations of PZ-DHA induced a significant inhibitory effect within 24 h (50 μM, 88.6±0.8%; 100 μM, 41.1±3.9%) and continued to be active for at least 48 h (50 μM,70.4±2.5%; 100 μM,24.2±3.3%) ($p$<0.001) (Figure 4.14B and C). MDA-MB-231-TXL cells were 15% more resistant to PZ-DHA treatment compared to MDA-MB-231 cells when cultured for 24 h ($p$<0.05); however, the resistance of MDA-MB-231-TXL cells diminished with further culture in the presence of PZ-DHA (Figure 4.14D).

Flow cytometric analysis of PZ-DHA-treated MDA-MB-231-TXL cells showed a significant increase in cell death (Figure 4.15A) due to early and late apoptosis/necrosis (Figure 4.15B). A reduction of the pro-caspase3 level in MDA-MB-231-TXL cells was evident following treatment with PZ-DHA; however; cleaved-caspase3 was not detected. Treatment with DHA resulted in an increase in cleaved-caspase3 (fraction 2, MW=17kDa), suggesting the involvement of caspase3 activation in DHA-induced death of MDA-MB-231-TXL cells (Figure 4.15C). The effect of PZ-DHA and its parent compounds on two drug transporters (ABCG2 and MRP1) was also investigated using western blot analysis; however, no effect was noted (Figure 4.15D).

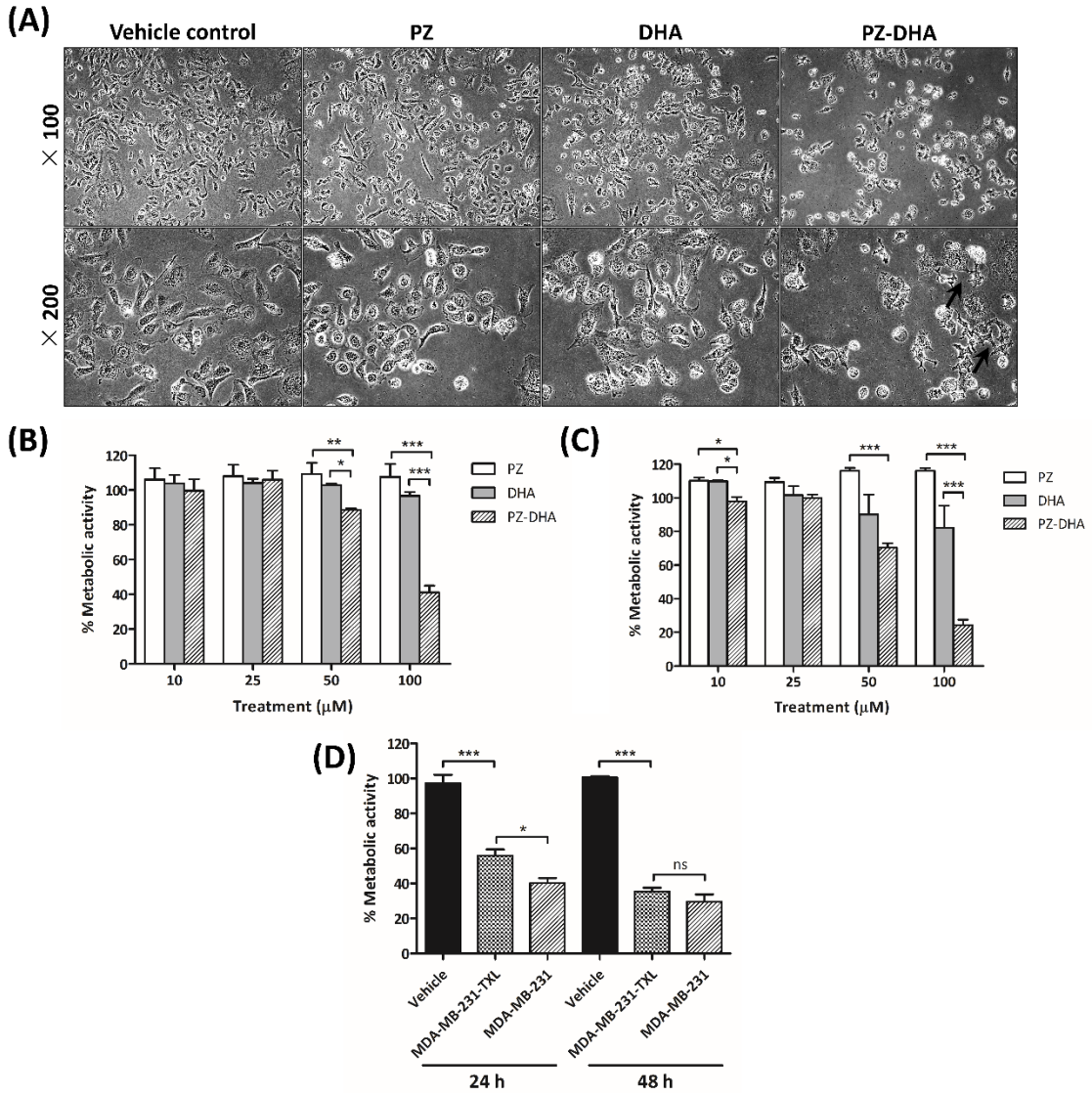


**Figure 4.14. PZ-DHA inhibits the metabolic activity of paclitaxel-resistant MDA-MB-231 (MDA-MB-231-TXL) breast cancer cells in a concentration- and time-dependent manner.**

Paclitaxel-resistant MDA-MB-231 (MDA-MB-231-TXL) cells and parental MDA-MB-231 cells were treated with PZ, DHA, PZ-DHA (10 - 100 μM), vehicle, or medium alone and cultured for 24 or 48h, and then an MTT assay was performed. **(A)** Morphological changes of MDA-MB-231-TXL cells were observed after 48 h, and the metabolic activity of MDA-MB-231-TXL cells was determined at **(B)** 24 and **(C)** 48 h post-treatment. **(D)** The effect of PZ-DHA on the resistance of MDA-MB-231-TXL cells was compared to the parental cell line. Data shown are mean metabolic activity±SEM from three independent experiments. ANOVA multiple means comparison statistical method was performed and differences among means were compared using Tukey's test; ns: not significant, *$p$<0.05, **$p$<0.01, and ***$p$<0.001.

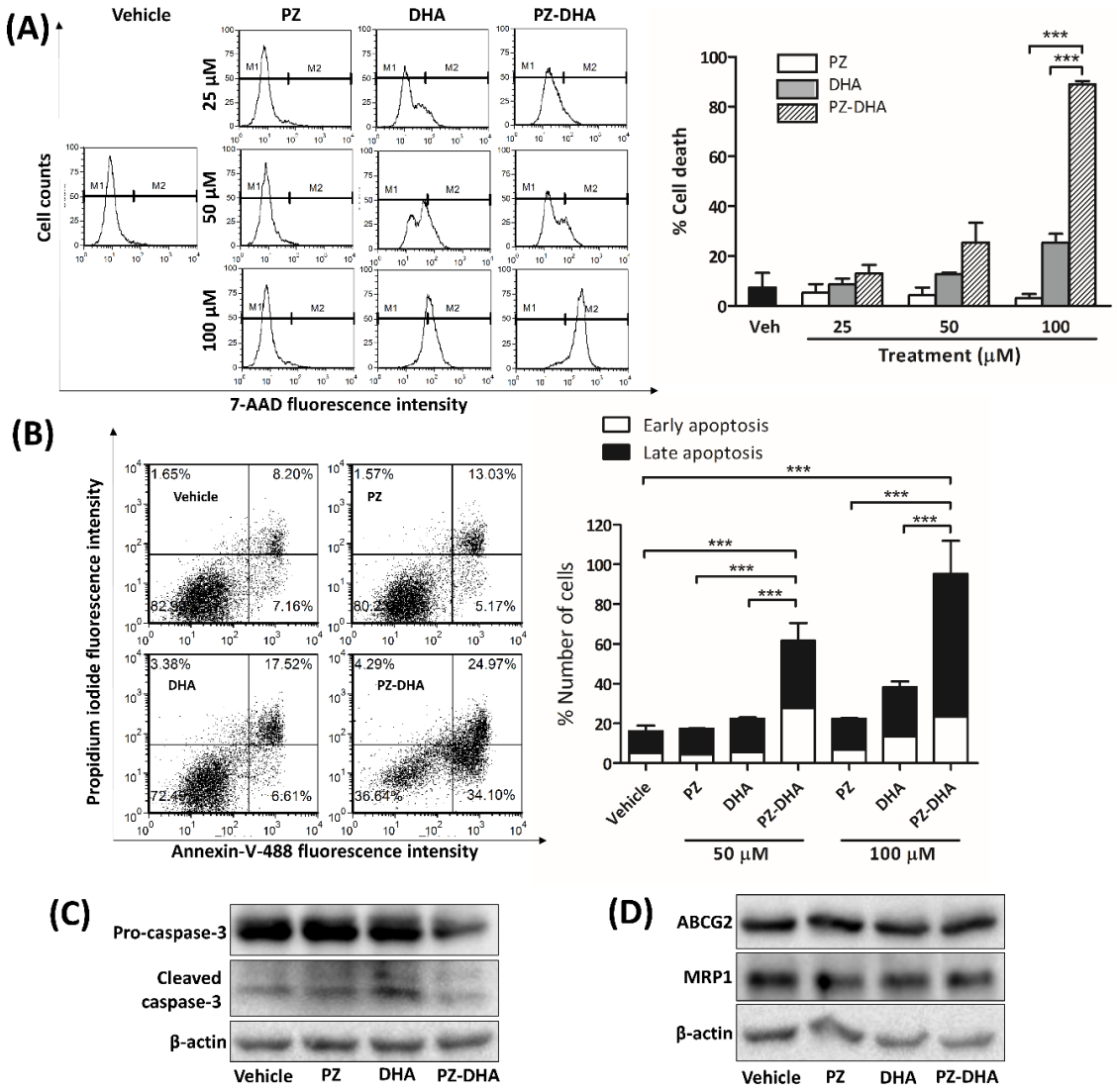


**Figure 4.15. PZ-DHA kills paclitaxel-resistant MDA-MB-231 (MDA-MB-231-TXL) breast cancer cells.**

**(A)** MDA-MB-231-TXL cells were treated with PZ, DHA, PZ-DHA (25, 50 or 100 µM) or the vehicle alone, cultured for 48 h, and stained with 7-AAD for analysis by flow cytometry. Representative histograms; M1: live cells and M2: dead cells are shown, and data are expressed as mean % cell death ± SEM of three independent experiments. **(B)** MDA-MB-231-TXL cells were treated with PZ, DHA, PZ-DHA (50 or 100 µM) or vehicle alone for 24 h and then stained with Annexin-V-488/PI and analyzed by flow cytometry. Data shown are representative dot plots of cells treated with 50 µM of the drugs and the mean % of cells in early apoptosis and late apoptosis/necrosis of three independent experiments±SEM. ANOVA multiple means comparison statistical method was performed and differences among means were compared using Tukey's test; ***$p$<0.001. Effect of PZ-DHA (20 µM) on **(C)** caspase 3 activation and the expression of **(D)** drug efflux transporters was determined using western blot analysis. Equal protein loading was confirmed by probing blots for β-actin.

### 4.2.13 PZ-DHA suppresses the growth of orthotopically implanted/xenografted mammary carcinoma cell growth in mice

A syngeneic model (4T1 mouse mammary carcinoma cells implanted into Balb/c female mice) and a xenograft model (GFP-transfected-MDA-MB-231 cells xenografted into NOD-SCID female mice) of breast cancer were used to test the *in vivo* tumor suppressor activity of PZ-DHA. In both models, mammary carcinoma cells were implanted orthotopically into the inguinal mammary fat pad by subcutaneous injection and PZ-DHA (100 mg/kg body weight) or saline was administered by intraperitoneal injection. PZ-DHA significantly reduced the volume of the primary tumor in both models (mean 4T1 tumor volume±SEM: saline, 283.4±30.1 $mm^3$; PZ-DHA, 165.9±27.4 $mm^3$) ($p<0.001$) (Figure 4.16A); mean MDA-MB-231 xenograft volume ± SEM: saline, 691.4±77.3 $mm^3$; PZ-DHA, 456.1±52.6 $mm^3$) ($p<0.001$) (Figure 4.17A); however, the tumor weight was significantly reduced only in the xenograft model (mean 4T1 tumor weight±SEM: saline, 269.4±29.9 mg; PZ-DHA, 184.4±32.1 mg) ($p=0.0705$) (Figure 4.16D); (mean MDA-MB-231 xenograft weight±SEM: saline, 700.8±49.1 mg; PZ-DHA, 530.9±36.7 mg) ($p<0.05$) (Figure 4.17D). Major internal organs (except lungs, in which metastasis was anticipated and evident) of all mice from both models appeared normal and healthy. Furthermore, there was no evidence of any significant body weight loss, reduced food/water intake, motility or morbidity in any treatment group, suggesting that the systemic administration of PZ-DHA did not induce adverse side effects or physical distress. Tumors excised from mice (Figure 4.16C and Figure 4.17C) were fixed in 10% buffered-formalin and necrotic tumor regions were identified by hematoxylin and eosin staining; interestingly, tumor necrosis was more distinct in the xenograft model. Sections from primary tumors were also subjected to immunohistochemical staining to visualize Ki67 expression. A slight reduction of Ki67 was observed in PZ-DHA-treated tumors from the syngeneic model (Figure 4.18A). The number of cells expressing Ki67 in the PZ-DHA-treated tumors from the xenograft model was markedly lower than the saline-treated mice (Figure 4.18B).

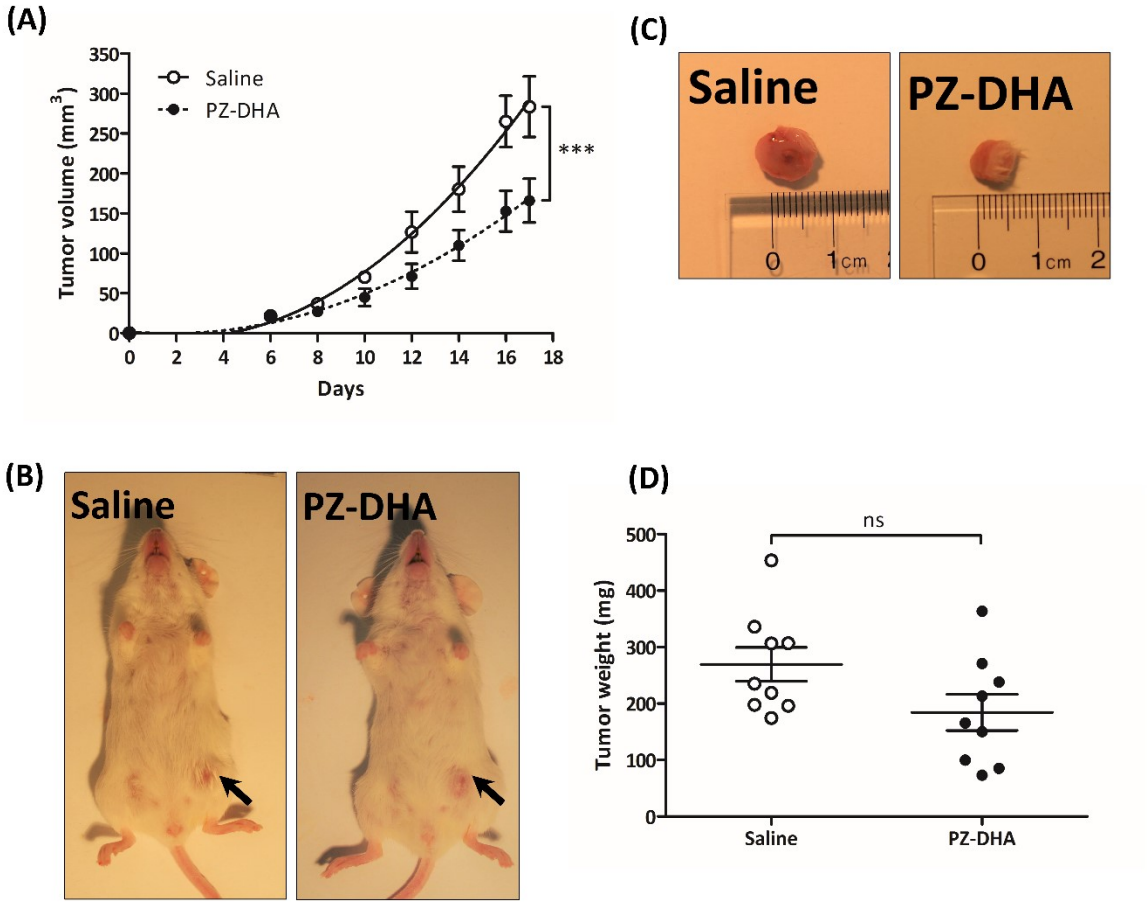


**Figure 4.16. Intraperitoneal administration of PZ-DHA inhibits 4T1 tumor growth in Balb/c mice.**

4T1 mouse mammary carcinoma cells ($1 \times 10^5$ cells) were injected into the left abdominal mammary fat pad of Balb/c female mice. Intraperitoneal injections of saline or PZ-DHA (100 mg/kg) were started on day 8 and continued every second day (days 8, 10, 12, 14 and 16) until day 16. Caliper measurements of tumors were recorded on days 6, 8, 10, 12, 14, 16, and 17 using a digital caliper. **(A)** Tumor volume was calculated according to the equation, $(L \times P^2)/2$ where L is longest tumor diameter and P is diameter perpendicular to the longest diameter and shown as mean±SEM. On day 17, the mice were euthanized. **(B)** Mice and their **(C)** tumors were photographed and tumors were **(D)** weighed and tumor weights are shown as mean±SEM. Statistical differences between means were compared using Student's t-test; ***$p$<0.001.

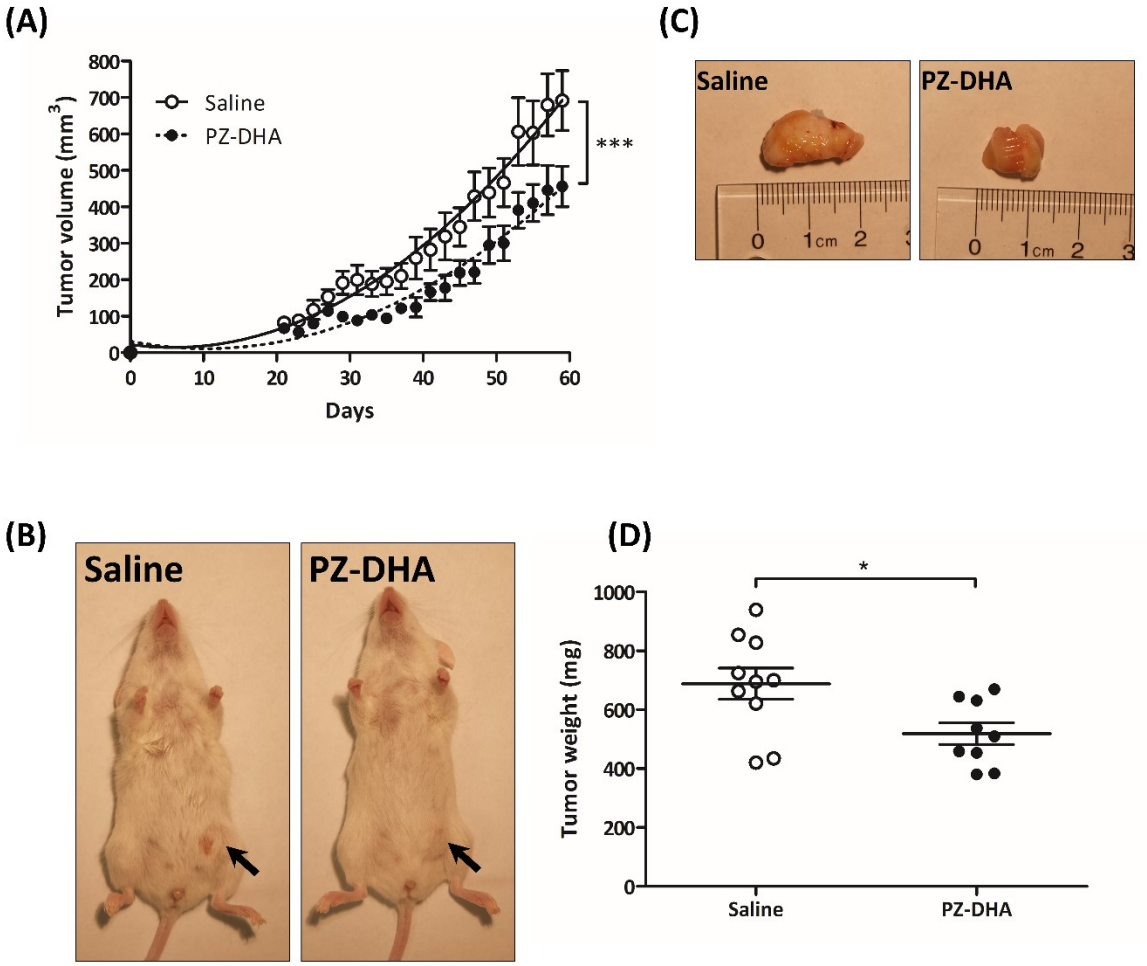


**Figure 4.17. Intraperitoneal administration of PZ-DHA inhibits GFP-tagged MDA-MB-231 tumor growth in NOD-SCID mice.**
MDA-MB-231 human breast cancer cells ($2 \times 10^6$ cells) were injected into the left abdominal mammary fat pad of NOS/SCID female mice. Intraperitoneal injections of saline or PZ-DHA (100 mg/kg) were started on day 21 and continued every second day from day 21 until day 59. Caliper measurements of tumors were recorded on every injection day using a digital caliper. **(A)** Tumor volume was calculated according to the equation, $(L \times P^2)/2$ where L is longest tumor diameter and P is diameter perpendicular to the longest diameter and shown as mean ± SEM. On day 60, the mice were euthanized. **(B)** Mice and their **(C)** tumors were photographed and tumors were **(D)** weighed and tumor weights are shown as mean±SEM. Statistical differences between means were compared using Student's t-test; *$p$<0.05, ***$p$<0.001.

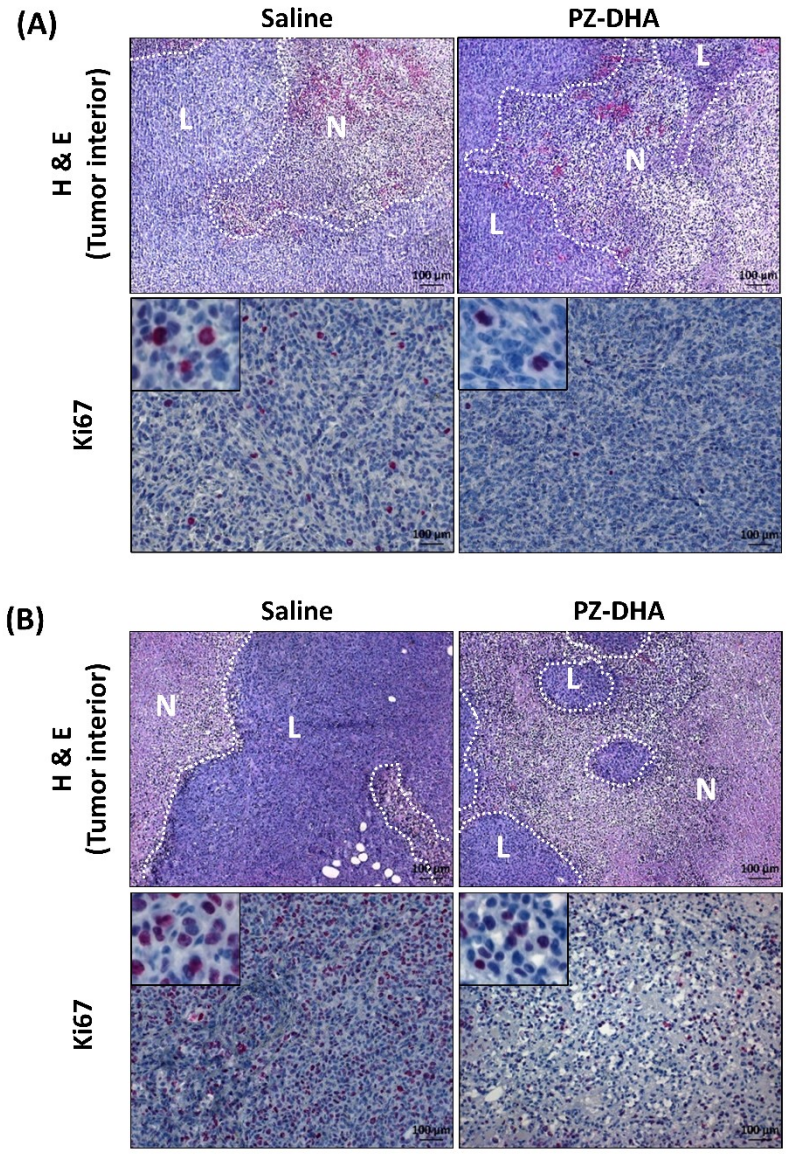


**Figure 4.18. PZ-DHA induces necrosis and decreases Ki67 expression of 4T1 and MDA-MB-231 tumors.**
Formalin-fixed **(A)** 4T1 tumor sections and **(B)** GFP-MDA-MB-231 xenograft sections were stained with haematoxylin and eosin to visualize tumor necrosis. IHC was carried out using anti-rabbit Ki67 Ab to test the effect of PZ-DHA on the proliferation of tumor cells. Necrotic tumor regions are shown by eosin-stained (pink-colored) cells (N) and live tumor regions are denoted by (L).

## 4.3 Discussion

In the current chapter, the selectivity of PZ-DHA and its impact on breast cancer cell proliferation, cell survival signaling pathways, as well as the *in vivo* efficacy of PZ-DHA were studied in detail. My previous work shows that PZ-DHA is less cytotoxic for primary human mammary epithelial cells when compared to MDA-MB-231 cells in an MTS assay (Fernando et al., 2016). Here, four additional mammary carcinoma cell lines (MDA-MB-468, 4T1, MCF-7 and T-47D), one drug-resistant mammary carcinoma cell line (MDA-MB-231-TXL) and two more non-malignant cell types (MCF-10A and HDF) were studied to further understand the selectivity of PZ-DHA-induced cytotoxicity.

Both DHA and PZ-DHA killed TNBC cells, and ER+ breast cancer cells; however, PZ-DHA-induced cytotoxic activity was greater than that of DHA. PZ did not significantly influence the viability of any malignant cells. Wang et al. (2010) reported that PZ exhibits estrogenic activity in MCF-7 cells in the absence of 17β-estradiol and shows an opposite (anti-estrogenic) activity in the presence of 17β-estradiol (Wang et al., 2010a). My findings are not in line with those of Wang et al. (2010), most likely because of differences between the two experimental models. Ester linkages are readily hydrolyzed by hydrolytic enzymes such as lipases, esterases and proteases (Antonopoulou et al., 2016; De Araújo et al., 2017; Stauffer and Zeffren, 1970; Viskupicova et al., 2012). Hydrolysis takes place at the hydrophilic-hydrophobic interphase and results in the release of free fatty acid and the flavonoid/flavonoid glycoside. Therefore, the potential of PZ and DHA to initiate an antagonistic, additive or synergistic reaction following hydrolysis was modeled and tested using MTS assay. Screening of PZ-DHA for sub-cytotoxic concentrations, which was explained and discussed in chapter 3, showed that none of the drugs at 10-30 μM showed cytotoxic activity to MDA-MB-231 cells. Similarly, the combination of PZ and DHA at 10 μM was not cytotoxic to MDA-MB-231 cells. The PZ and DHA-combined effect was not significantly different from that of PZ-DHA-induced cytotoxic activity at low concentrations; however, with prolonged incubation, PZ-DHA significantly decreased the metabolic activity of breast cancer cells, even at low concentrations (Figure 4.3). When employed at high concentrations, PZ-DHA was more potent than the combined effect of PZ and DHA suggesting that MDA-MB-231 cells were more sensitive to PZ-DHA-induced cytotoxic activity than

cytotoxicity by the combination of PZ and DHA. When conjugated, PZ and DHA uptake is enhanced; this is likely responsible for the increased potency of the conjugate. Therefore, it is important to look further into the pharmacological effects of PZ-DHA.

Chemotherapy-associated adverse side effects and complications are directly or indirectly related to drug-induced toxicities to non-malignant cells (Chen et al., 2000; Liu et al., 2015a; Robinson, 1993; Sak, 2012). Therefore, it is necessary that the selectivity of a drug candidate is tested during early stages of the drug development. The selectivity of PZ-DHA in killing malignant cells was studied against non-malignant human mammary epithelial cells and HDFs. PZ-DHA caused morphological changes and reduced the metabolic activity of all malignant cell types (Figure 4.1 and 4.2); however, the morphology (Figure 4.11A) and viability of the non-malignant cells was not affected. Furthermore, PZ-DHA induced early and late apoptosis/necrosis of cancer cells without harming normal cells (Figure 4.5). At sub-cytotoxic concentrations, PZ-DHA inhibited Akt and MAPK signaling in MDA-MB-231 cells, while the phosphorylation of Akt pathway components (PTEN and PDK1) in MCF-10A cells were not affected, suggesting that the selective activity of PZ-DHA is extended to the molecular level. However, PZ-DHA inhibited the phosphorylation of mTOR in MCF-10A cells, which may indicate the activation of stress response pathways.

Flavonoids kill various types of cancer cells, including breast cancer cells, while having little or no effect on normal cells (Hrvatsko prirodoslovno društvo. Biološka sekcija. et al., 2009; Matsuo et al., 2005; Romanouskaya and Grinev, 2009; Sak, 2014; Srivastava et al., 2016; Yadegarynia et al., 2012). The cytotoxic/anti-proliferative activities of flavonoids result in cell cycle arrest, caspase activation and dysregulation of oxidative stress (Nair et al., 2014; Rupasinghe et al., 2012; Sak, 2014; Smith et al., 2016; Yadegarynia et al., 2012). Similarly, flavonoid derivatives inhibit the proliferation of breast cancer cells while, in certain cases, showing improved biological activities (Martínez-Pérez et al., 2016; Rhodes et al., 2012). At a sub-cytotoxic concentration, PZ-DHA inhibited the proliferation of MDA-MB-231 cells, decreasing cell division by 2.3-fold (Figure 4.6). The antiproliferative activity of PZ-DHA was confirmed by a reduction in the expression of the cell proliferation marker, Ki67 (Figure 4.7), which is expressed in all active phases ($G_1$, S, and $G_2$/M) of the cell cycle (Yuan et al., 2015). Therefore, it

allows the quantification of Ki67 expression in each individual phase. PZ-DHA treatment caused an overall significant reduction in Ki67 expression. Flavonoids are known to cause $G_2$/M cell cycle arrest of various cancer cell types, including breast cancer cells (Choi et al., 1999; Vidya Priyadarsini et al., 2010; Zhao et al., 2009). PZ-DHA had a similar effect since PZ-DHA arrested MDA-MB-231 cells at $G_2$/M (Figure 4.8), which was associated with reduced expression of cyclin B1 and CDK1 (Figure 4.9). In contrast, Nair et al. (2014) showed that PZ-DHA arrests HepG2 liver cancer cells at $G_0/G_1$ (Nair et al., 2014); however, unlike HepG2 cells that have wild-type p53 (Vollmer et al., 1999), MDA-MB-231 cells express abundant mutated p53 (Hui et al., 2006). It is therefore possible that p53 status may partly explain the absence of $G_0/G_1$ arrest in PZ-DHA-treated MDA-MB-231 cells since p53 mutant cells are more likely to be arrested at $G_2$/M instead of $G_0/G_1$ (Abu et al., 2014). Consistent with cell cycle analysis, the expression of proteins that regulate the transition of a cell through $G_0/G_1$ (cyclin D3 and CDK4) or S (cyclin A and CDK2) phase was not affected by PZ-DHA or its parent compounds (Figure 4.9).

Dietary biomolecules have received distinct attention as anti-cancer and chemo-preventive agents and, as such, they have been extensively studied to understand their mode(s) of action. Flavonoids, the largest naturally-occurring phytochemical group, is known to have anti-cancer activity through targeting multiple cell signaling pathways at different levels. These mechanisms mainly involve transcriptional and post-transcriptional regulation, protein activation/inactivation and modulation of intracellular cell signaling associated with cell proliferation and survival (Chen and Liu, 2018; Surh, 2003; Upadhyay and Dixit, 2015). Among many cell signaling pathways impacted by flavonoids, PI3K/Akt/mTOR and MAPK pathways play central roles in the anti-cancer activities of flavonoids (Adhami et al., 2012; Borah et al., 2017; Fang et al., 2005; Granado-Serrano et al., 2006; Kim et al., 2007; Lee et al., 2011b; Mirzoeva et al., 2008; Pratheeshkumar et al., 2012; Ruiz and Haller, 2006; Zhang et al., 2014). Furthermore, ω-3 fatty acids also inhibit PI3K/Akt/mTOR and MAPK pathways of human cells (Akbar et al., 2005; Kim et al., 2015; Shin et al., 2013; Yin et al., 2017). Therefore, in the current project, the effects of PZ-DHA on PI3K/Akt/mTOR and MAPK pathways in MDA-MB-231 cells were tested in detail and compared with the parent compounds. The inhibitory

effect of PZ-DHA on Akt signaling was evident both upstream and downstream of Akt (Figure 4.10). PTEN antagonizes the activation of PI3K by converting PIP3 into PIP2 (Chalhoub and Baker, 2009). The negative regulatory effects of PZ-DHA on Akt signaling were associated with activation of PTEN by phosphorylation at Ser380. The effect of PZ-DHA on PTEN was significantly greater than that of its parent compounds. Akt is activated by its upstream kinase PDK1 and studies have shown that PDK1 phosphorylation at Ser241 is essential for its kinase activity (Casamayor et al., 1999; Ding et al., 2010). PZ-DHA, as well as its both parent compounds, inhibited the phosphorylation of PDK1 at Ser241. PZ-DHA also significantly inhibited the phosphorylation of mTOR, which is needed for activation of anabolic pathways that include protein, ribosome and nucleotide synthesis that are collectively important for cell and tissue growth (Kennedy and Lamming, 2016; Xie et al., 2016). Significant inhibition of mTOR phosphorylation at Ser2448 by PZ-DHA suggests a clear mechanism for the anti-proliferative effect of PZ-DHA on MDA-MB-231 cells. In addition, an overall reduction in GSK3β kinase activity was evident by increased phosphorylation of GSK3β at Ser9 (inactive form) and unchanged phosphorylation of GSK3β at Tyr216 (active form). Furthermore, Ding et al. (2000) suggested that at least two distinct pools of GSK3β are present in a cell, one being resistant to phosphorylation by Akt while the other is regulated by Akt-induced kinase activity (Ding et al., 2000). Although, PZ-DHA-induced inhibitory effects on PI3K/Akt/mTOR signaling pathway is promising, detection of phosphorylated Akt was not successful during the current project. Therefore, this limitation demands further clarification during future studies. PZ-DHA inhibited the phosphorylation of c-RAF and ERK1/2 at Ser259 and Thr202/Thy204, respectively, suggesting that decreased MAPK signaling contributes to PZ-DHA-induced cytotoxic and anti-proliferative activities (Figure 4.12). In agreement with Shin et al. (2013) and Yin et al. (2017), DHA also inhibited Akt activation and ERK1/2 phosphorylation, albeit to a lesser extent than PZ-DHA (Shin et al., 2013; Yin et al., 2017). PZ did not affect the phosphorylation of any Akt or MAPK pathway component except for PDK1 and ERK1/2; however, the inhibitory activity of PZ did not extend to downstream signaling molecules such as mTOR and/or GSK3β. Little is known about the effect of PZ on signaling pathways in malignant cells. However, the potent SGLT1/2 inhibitory activity

of PZ increases Akt activation in human umbilical vein endothelial cells, providing a protective effect against palmitic acid-induced endothelial dysfunction (Li et al., 2018), as well as preventing epithelial barrier damage and bacterial translocation in intestinal ischemia (Huang et al., 2011). PZ-DHA did not affect the morphology, metabolic activity or viability of non-malignant cells, suggesting selectivity of PZ-DHA-mediated inhibitory effects at the cellular level. To further understand the effects of PZ-DHA on non-malignant cells at a molecular level, the impact of PZ-DHA on Akt signaling pathways was investigated in MCF-10A mammary epithelial cells. As expected, PZ-DHA had either an opposite or no effect on Akt signaling in MCF-10A cells, although the phosphorylation of mTOR was inhibited by PZ-DHA. The inability of PZ-DHA to affect Akt signaling may partially explain the resistance of MCF-10A cells to PZ-DHA treatment.

Many cancers acquire resistance to conventional chemotherapy, which is considered as one of the major limitations of chemotherapeutic drugs (Dennis et al., 1998; Nooter and Stoter, 1996; Ozben, 2006). Nonetheless, chemotherapy remains the first-line treatment option for TNBC due to the lack of targeted therapeutic agents for TNBC. TNBC cells develop resistance to chemotherapy quite frequently, leading to more complicated clinical situations such as treatment failure, disease recurrence, and metastasis (Bao et al., 2017; Kennecke et al., 2010). Cancer stem cells, a sub population of cells in tumors, demonstrate distinct phenotypic and genotypic signatures (Chen et al., 2013; Lobo et al., 2007), which allows them to escape chemotherapy that targets rapidly-proliferating cancer cells (Chang, 2016; Liu et al., 2015b; Peitzsch et al., 2017). Suppression of stem cell-like activity in breast cancer cells by PZ-DHA was evident by the PZ-DHA-mediated inhibition of MCF-7 spheroid growth (Figure 4.13). Little is known about the inhibitory activity of phytochemicals on drug-resistant TNBC cells. A study conducted using methoxy and hydroxy flavones, and their 4-thio analogs, showed that these novel flavonoid derivatives reduce the viability of anthracycline-resistant MCF-7 cells and inhibit their proliferation by ER-dependent PARP cleavage and downregulation of GSK3β (Ravishankar et al., 2016). Furthermore, flavonoids (3',4',7-trimethoxyflavone and acacetin) also inhibit breast cancer resistance protein-mediated drug resistance of K562 cells, but do not inhibit MRP1. PZ-DHA inhibited the metabolic activity of MDA-

MB-231-TXL in a time- and concentration-dependent manner. PZ-DHA-induced MDA-MB-231-TXL cell death was also dose-dependent. PZ-DHA treatment decreased pro-caspase 3 levels, but, did not have any effect on cleaved-caspase 3. A previous study has shown DHA-induced caspase 3/7 activation in parental MDA-MB-231 cells (Fernando, 2014). DHA also increased levels of cleaved-caspase 3 while decreasing pro-caspase 3 in MDA-MB-231-TXL cells. None of the drugs affected the basal expression of drug transporters (ABCG2 or MRP1) in MDA-MB-231-TXL cells (Figure 4.14 and 4.15). However, the affinity of flavonoids to ABC family drug efflux transporters has been discussed widely (Di Pietro et al., 2002; Vázquez et al., 2014). Therefore, the interaction of PZ-DHA with other drug transporters need to be further evaluated during future studies.

Lastly, *in vivo* tumor suppressor activity of PZ-DHA was tested using two mouse models of breast cancer (4T1-implanted Balb/c mice and MDA-MB-231-xenografted NOD-SCID mice). Intraperitoneal administration of PZ-DHA caused a reduction in tumor volume in both models, suggesting an *in vivo* activity of PZ-DHA as a potent tumor suppressor. PZ-DHA-induced tumor cell necrosis was evident by hematoxylin and eosin staining, whilst immunohistochemistry of Ki67 of tumors confirmed the reduction of PZ-DHA-mediated cancer cell proliferation *in vivo*. Importantly, in chapter 3, I showed that chronic systemic exposure to PZ-DHA did not induce liver or kidney toxicity in Balb/c female mice. When taken together, these findings demonstrate that PZ-DHA systemic administration suppressed the growth of orthotopically implanted mouse and human mammary carcinoma cells without having any adverse organ toxicity.

In summary, this chapter discusses the selective cytotoxic activity of PZ-DHA toward malignant mammary epithelial cells and reveals PZ-DHA-mediated regulation of two major cell survival pathways in MDA-MB-231 cells. The mechanism(s) by which PZ-DHA exerts antiproliferative activity was also studied in-detail, exposing the effect of PZ-DHA on Ki67 expression, cell cycle progression and the expression of cell cycle-associated regulatory proteins. The efficacy of PZ-DHA against paclitaxel-resistant MDA-MB-231 cells and its inhibitory effect on MCF-7 spheroid growth suggested a potential use of PZ-DHA in the treatment of drug-resistant breast cancer and cancer stem cell targeted therapy. Most notably, PZ-DHA suppressed the growth of two aggressive

mammary carcinoma cell types in mice without being toxic for critical drug/xenobiotic metabolizing organs such as liver and kidneys. Further studies to investigate the anti-metastatic activity of PZ-DHA were designed based on the findings of this chapter and will be discussed in detail in chapter 5.

# CHAPTER 5 : PZ-DHA INHIBITS THE METASTASIS OF TRIPLE-NEGATIVE MAMMARY CARCINOMA CELLS

## 5.1 Introduction

TNBC, which lacks hormone receptors (ER, PR) and HER2, is one of the most aggressive types of breast cancers with poor prognosis (Dent et al., 2009; Königsberg et al., 2012; Ovcaricek et al., 2011) . Even though TNBC responds to chemotherapy initially, these cancer cells develop chemo-resistance following cancer recurrence. Therefore, TNBC metastasize into adjacent and/or distant organs *via* lymph and blood. Cancer cells disseminated from a primary tumor form secondary metastatic lesions, mostly in the lungs, bones, liver and brain (Anders and Carey, 2009; Choi et al., 2013; Gao et al., 2008; Ma et al., 2015; Ogata et al., 2015; Tseng et al., 2013). The vascular flow patterns, to a certain extent, explain the most potential sites of metastasis of a given cancer (Chambers et al., 2002; Ring and Ross, 2005; Sleeman et al., 2011); however, the exact mechanisms are not yet fully understood. Among many hypotheses of cancer metastasis mechanisms (Hunter et al., 2008), the concept of "seed and soil", which was first introduced in 1889 by Paget, is still widely accepted (Paget, 1889). For example, excessive expression of chemokine receptor 4 by breast cancer cells and its ligand 12 by cells in lymph nodes, lungs, liver, and bones may explain the secondary relapse of breast cancer at these sites. Aberrant activation of signaling pathways, including Akt, MAPK and small molecular Rho GTPase, trigger survival and migration of breast cancer cells (Burbelo et al., 2004; Ebi et al., 2013; Zhu et al., 2011). Rho GTPase signaling-induced cytoskeletal changes, together with the activation of EMT, cause phenotypic transformations of cancer cells resulting in a mesenchymal-like phenotype (Fedele et al., 2017). During this process, epithelial characteristics of the cancer cells are diminished, resulting in a decrease in expression of epithelial-like markers such as E-cadherin. These cellular events may initiate dissemination of cancer cells from a primary tumor, during which TGF-β functions as one of the potent stimulants of cell migration (Clark and Vignjevic, 2015; Moustakas and Heldin, 2014; Parri and Chiarugi, 2010; van Zijl et al., 2011). However, recent studies challenge this well-accepted concept suggesting that EMT is not always required for metastasis (Fischer et al., 2015; Zheng et al., 2015).

Degradation of extra-cellular matrix proteins by MMPs is also essential for several key steps of the metastasis including, intravasation, extravasation, and angiogenesis (Jin and Mu, 2015; Rundhaug, 2005; Stetler-Stevenson, 1999).

Anti-metastatic activities of many plant polyphenols (Abdal Dayem et al., 2016; Doo and Maskarinec, 2014; Sun et al., 2012), as well as flavonoids (Ni et al., 2012; Weng et al., 2012; Yan et al., 2016), have been tested using breast cancer cell lines. For example, a panel of myricetin-based novel flavonoids shows *in vitro* and pre-clinical anti-cancer activity through mitochondrial targeted-redox active mechanisms (Martínez-Pérez et al., 2016). VI-14, a novel flavonoid derivative, shows anti-metastatic activity against MDA-MB-231 and MDA-MB-435 breast cancer cells by inhibiting ECM degradation-associated proteins (Li et al., 2012). Yao et al. (2011) report imidazole ring-independent anti-proliferative activity of a series of flavone analogs that selectively bind to eukaryotic elongation factor 2A of breast cancer cells (Yao et al., 2011b). In addition, Rose et al. (1996) suggest that dietary intake of ω-3 fatty acids inhibits metastatic progression after surgical removal of human breast cancer xenografts grown in nude mice (Rose et al., 1996).

Since PZ, DHA or PZ-DHA at concentrations below 30 μM did not have anti-proliferative or cytotoxic effects, 10-20 μM concentrations were used to study the *in vitro* anti-metastatic activity of these compounds, as discussed in the current chapter. In this chapter, the anti-metastatic activity of PZ-DHA was tested using *in vitro* and *in vivo* models of breast cancer. The effects of PZ-DHA on breast cancer cell migration, invasion, TGF-β signaling and EMT was tested *in vitro* using 4T1 mouse mammary carcinoma cells and MDA-MB-231 human breast cancer cells. Anti-metastatic activity was tested using two mouse models of aggressive metastatic breast cancer in which 4T1 cells were implanted in immune-competent BABL/c female mice and GFP transfected-MDA-MB-231 cells were xenografted in to NOD-SCID female mice. Immunohistochemical analysis of primary tumors suggested potential explanations for *in vivo* anti-metastatic activity of PZ-DHA.

## 5.2 Results

According to chapter 3, culture of TNBC cells with 10-30 μM concentration of PZ-DHA for 72 h confirms drug internalization without induction of a cytotoxic effect. Therefore, these concentrations and incubations were chosen to investigate the anti-metastatic activities of PZ-DHA in *in vitro* cell culture systems in this chapter. *In vivo* anti-metastatic experiments were conducted using 100 mg/kg PZ-DHA dose.

### 5.2.1 A sub-cytotoxic concentration of PZ-DHA inhibits the migration of MDA-MB-231 and 4T1 cells *in vitro*

The effect of a sub-cytotoxic concentration of PZ-DHA (20 μM) and its parent compounds PZ and DHA on the migration of two aggressive mammary carcinoma cell lines was first tested using a gap closure assay. A "gap" was created by growing cells in culture inserts and the proliferation of cells was inhibited by mitomycin C treatment. PZ or DHA alone did not have a significant inhibitory effect on the motility of mammary carcinoma cells; in contrast, PZ-DHA significantly inhibited the migration of 4T1 (Figure 5.1A, B) and MDA-MB-231 (Figure 5.1C, D) cells by 46.2% (% mean migration±SEM: vehicle, 103.1±10.8%; PZ, 93.6±12.1%; DHA, 75.7±5.4%; PZ-DHA, 56.9±9.6%) ($p$<0.05) and 60.0% (% mean migration±SEM: vehicle, 108.3±21.7%; PZ, 63.3±6.2%; DHA, 70.4±7.0; PZ-DHA, 48.3±4.3%) ($p$<0.05), respectively. The migration of MDA-MB-231 cells was further tested using a trans-well cell migration assay. MDA-MB-231 cells ($1 \times 10^6$ cells/mL) were seeded into trans-well inserts in serum-free medium and migration toward serum was measured. Both DHA and PZ-DHA, but not PZ, suppressed the migration of MDA-MB-231 cells by 31.5% and 68.0%, respectively (Figure 5.2). Notably, the PZ-DHA-induced inhibitory effect on the directed migration of MDA-MB-231 cells (17.1±1.2%) was significantly greater than that of the vehicle control (85.1±2.9%) and both of PZ-DHA's parent compounds (PZ, 80.4±3.6% and DHA, 53.6±4.8%) ($p$<0.001).

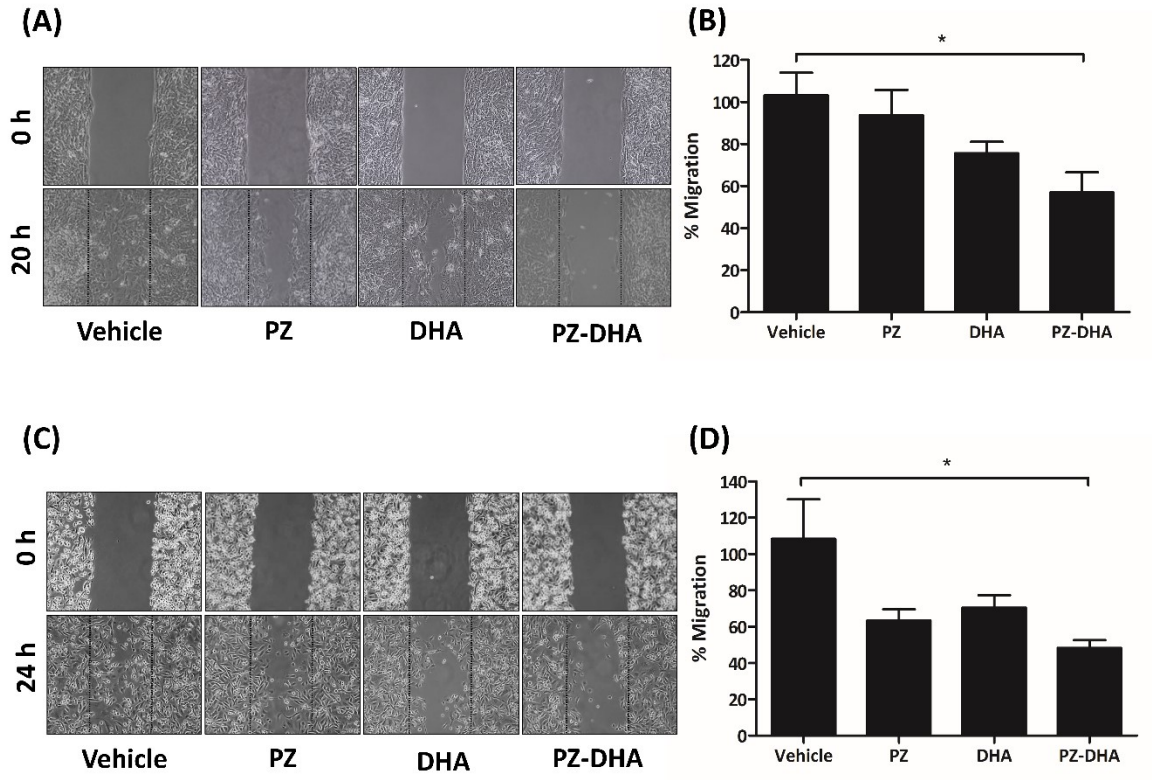


**Figure 5.1. A sub-cytotoxic concentration of PZ-DHA inhibits the migration of 4T1 and MDA-MB-231 cells *in vitro* in gap-closure assays.**
MDA-MB-231 ($1 \times 10^4$ cells) and 4T1 ($8 \times 10^3$ cells) cells were seeded into cell culture inserts and cultured overnight. Cell monolayers were then incubated with 10 µg/mL (MDA-MB-231) or 20 µg/mL (4T1) mitomycin C for 2h and were then allowed to recover overnight. Cells were then treated with PZ, DHA, PZ-DHA (20 µM), vehicle or medium and cultured for 24 h. Inserts were removed after 24 h, cells were rinsed with 1 × PBS and treatments were continued. The gap was photographed periodically until the gap was closed in medium controls. The number of cells migrated into the gap was quantified using ImageJ software and normalized to the medium control. Data shown are **(A)** representative pictures of 4T1 cells in the gap, **(B)** mean % migrated 4T1 cells±SEM **(C)** representative pictures of MDA-MB-231 cells in the gap **(D)** mean % migrated MDA-MB-231 cells±SEM from three independent experiments. One-way ANOVA multiple means comparison statistical analysis was performed and differences among means were compared using Tukey's multiple means comparison method; *$p$<0.05.

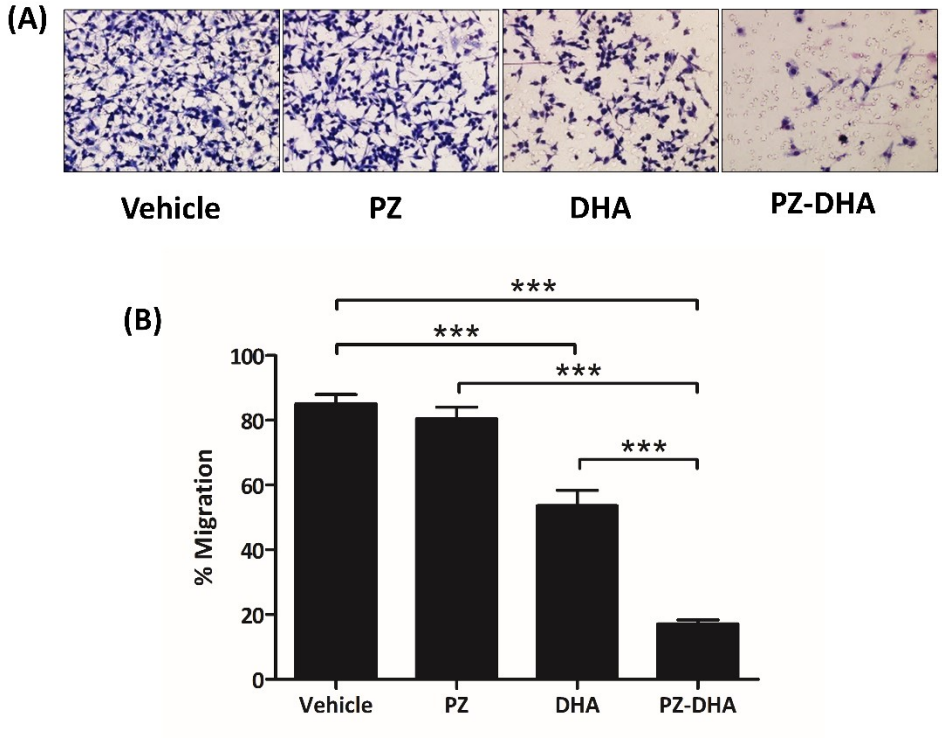


**Figure 5.2. A sub-cytotoxic concentration of PZ-DHA inhibits serum-induced chemotactic migration of MDA-MB-231 cells *in vitro* in trans-well cell migration assays.**

MDA-MB-231 cells were treated with PZ, DHA, PZ-DHA (20 µM) or vehicle alone and cultured for 24 h. Cells were then serum starved, resuspended in serum-free DMEM and migration toward serum through a 8 µm pore-sized membrane was determined. Images were analyzed using ImageJ software and % migration was calculated. Data shown are **(A)** representative pictures of MDA-MB-231 cells migrated through the porous membrane and **(B)** mean % migration±SEM of three independent experiments. ANOVA multiple means comparison statistical method was performed and differences among means were compared using Tukey's test; ***$p$<0.001.

### 5.2.2 A sub-cytotoxic concentration of PZ-DHA inhibits TGF-β-induced migration by MCF-10A and MDA-MB-231 cells *in vitro*

TGF-β is a potent regulator of cell migration and TGF-β-induced cell migration is mediated through Rho family small GTPases (Edlund et al., 2002). Therefore, the effects of PZ-DHA and its parent compounds on the expression of three Rho family GTPases (RhoA, Cdc42 and Rac1/2/3) in MCF-10A and MDA-MB-231 cells were measured in the presence and absence of TGF-β. Section 5.2.1 showed that PZ-DHA significantly inhibited the migration of MDA-MB-231 cells in both gap closure and trans-well cell migration assays. PZ-DHA and DHA, but not PZ, down-regulated the baseline RhoA and Cdc42 expression in MDA-MB-231 cells but not in MCF-10A cells. None of the drugs affected baseline Rac1/2/3 expression in MDA-MB-231 cells and MCF-10A cells (Figure 5.3). TGF-β increased MCF-10A cell migration (Figure 5.4A), as well as the expression of RhoA, Cdc42 and Rac1/2/3 expression by 71.3%, 37.1% and 60.5%, respectively. PZ-DHA and both parent compounds significantly decreased TGF-β-induced RhoA overexpression by MCF-10A cells (% mean relative expression±SEM: vehicle, 98.3±12.6%; PZ, 25.0±3.9%; DHA, 33.7±6.2%; PZ-DHA, 40.4±5.9%) ($p$<0.001) (Figure 5.4B). PZ-DHA, but not DHA and PZ, reversed TGF-β-induced Cdc42 overexpression (% mean relative expression±SEM: vehicle, 96.8±2.3%; PZ, 86.0±0.5%; DHA, 85.2±4.8%; PZ-DHA, 55.0±2.5%) ($p$<0.05) (Figure 5.4C); however, none of the drugs decreased TGF-β-induced Rac1/2/3 expression (% mean relative expression±SEM: vehicle, 83.3±1.1%; PZ, 81.4±1.0%; DHA, 87.3±1.8%; PZ-DHA, 81.4±0.9%) ($p$=0.136) (Figure 5.4D). TGF-β also increased the migration of MDA-MB-231 cells (Figure 5.4A). Since background Rho GTPase expression is greater in MDA-MB-231 cells than in MCF-10A cells, the % increase resulted by TGF-β treatment was not as high as that seen in MCF-10A cells. An increase of 32.3% (RhoA), 28.3% (Cdc42) and 32.4% (Rac1/2/3) was seen in MDA-MB-231 cells following TGF-β treatment. In contrast to the effect in MCF-10A cells, PZ-DHA significantly down-regulated expression of all three TGF-β-induced -proteins in MDA-MB-231 cells (% mean relative RhoA expression±SEM: vehicle, 111.1±3.2%; PZ, 81.3±2.1%; DHA, 75.1±11.1%; PZ-DHA, 55.0±9.0%) ($p$<0.01) (Figure 5.4B), (% mean relative Cdc42 expression±SEM: vehicle, 98.1±5.1%; PZ, 43.8±10.1%; DHA, 34.1±10.7%; PZ-DHA, 26.2±4.5%) ($p$<0.001) (Figure 5.4C) and

(% mean relative Rac1/2/3 expression±SEM: vehicle, 97.9±1.7%; PZ, 106.2±11.2%; DHA, 77.5±1.0%; PZ-DHA, 28.1±11.2%) ($p$<0.001) (Figure 5.4D).

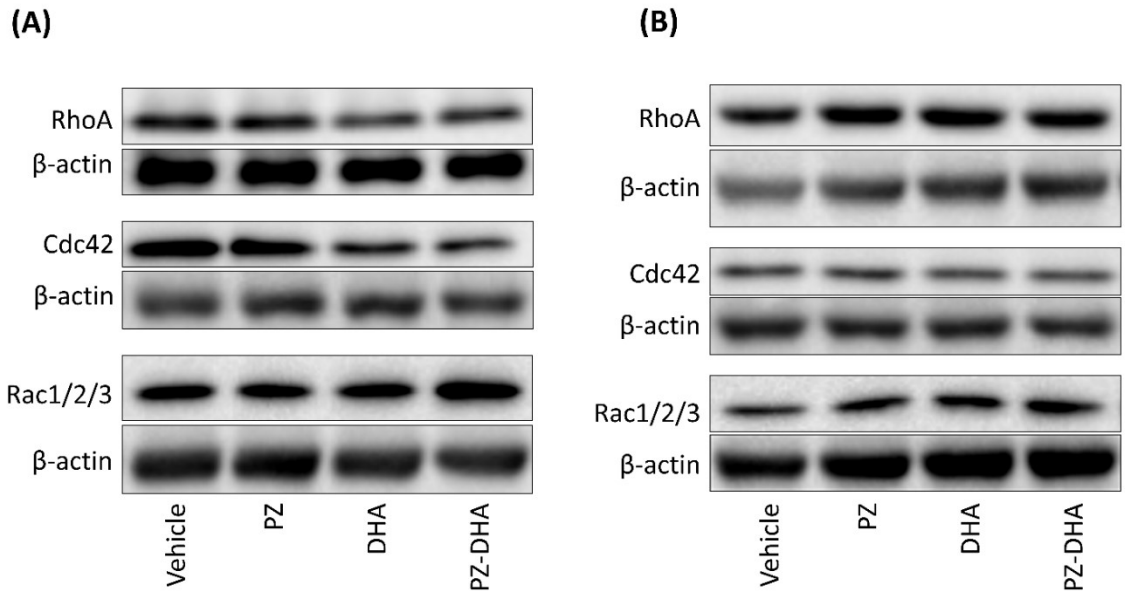


**Figure 5.3. A sub-cytotoxic concentration of PZ-DHA inhibits baseline expression of small Rho GTPase in MDA-MB-231 cells but not in MCF-10A cells i*n vitro*.**
The effect of PZ-DHA on background expression of small molecular Rho GTPases was determined using western blot analysis. **(A)** MDA-MB-231 and **(B)** MCF-10A cells were treated with PZ, DHA, PZ-DHA (20 μM), vehicle or medium alone and cultured in the absence of TGF-β for 72 h. Cells were harvested, lysed and protein concentration in lysates were determined using a Bradford assay and 20 μg of proteins were loaded in to 15% SDS-polyacrylamide gels. Blots were probed with Ab against RhoA, Cdc42 and Rac1/2/3. Equal protein loading was confirmed by β-actin expression.

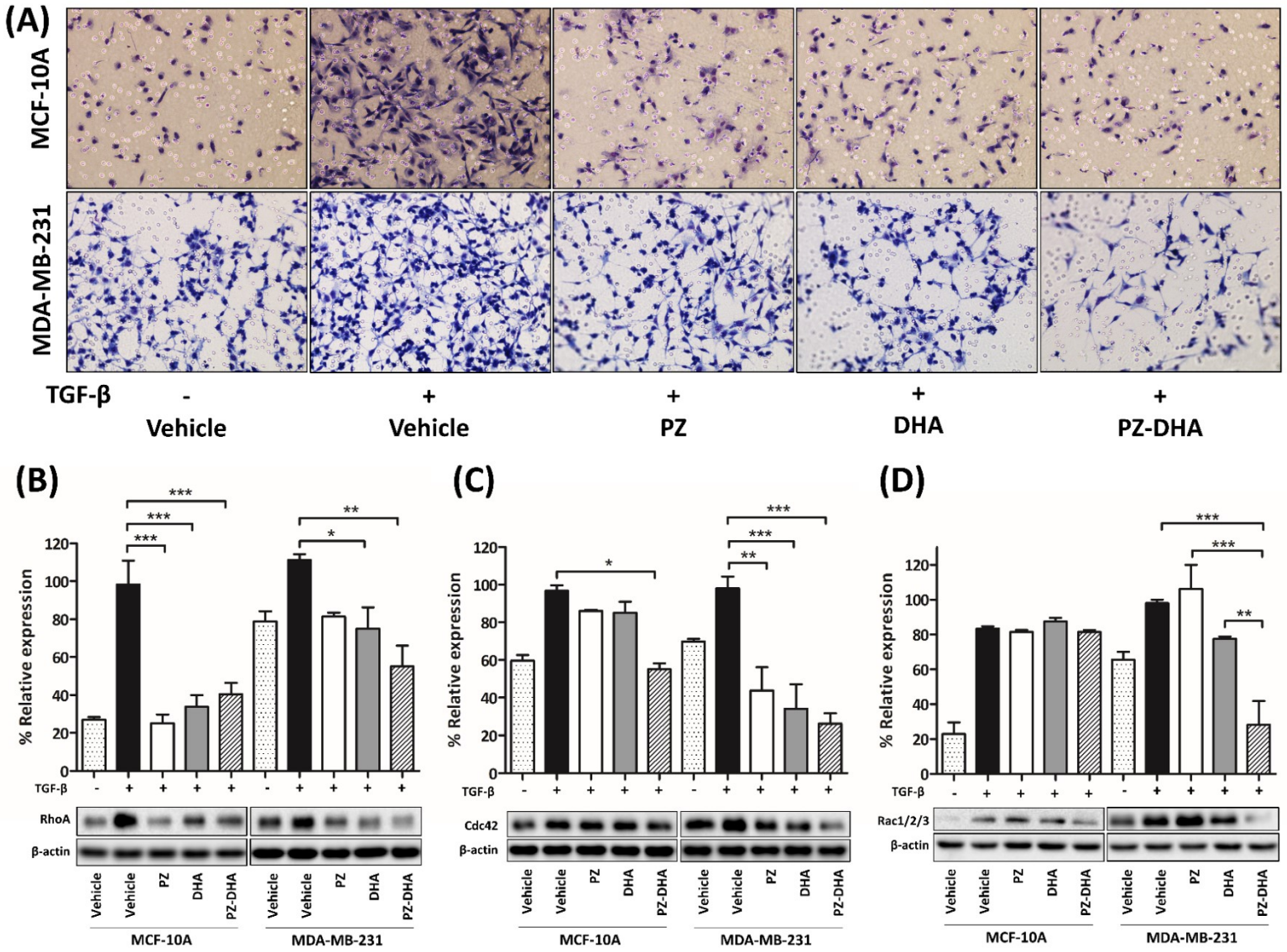
(A)
MCF-10A
MDA-MB-231
TGF-β - + + + +
Vehicle Vehicle PZ DHA PZ-DHA
(B)
% Relative expression
TGF-β
RhoA
β-actin
Vehicle Vehicle PZ DHA PZ-DHA Vehicle Vehicle PZ DHA PZ-DHA
MCF-10A MDA-MB-231
(C)
% Relative expression
TGF-β
Cdc42
β-actin
Vehicle Vehicle PZ DHA PZ-DHA Vehicle Vehicle PZ DHA PZ-DHA
MCF-10A MDA-MB-231
(D)
% Relative expression
TGF-β
Rac1/2/3
β-actin
Vehicle Vehicle PZ DHA PZ-DHA Vehicle Vehicle PZ DHA PZ-DHA
MCF-10A MDA-MB-231

**Figure 5.4. A sub-cytotoxic concentration of PZ-DHA inhibits TGF-β-induced migration by MDA-MB-231 and MCF-10A cells *in vitro*.**
**(A)** MCF-10A and MDA-MB-231 cells were pre-treated with 10 ng/mL TGF-β or medium and then treated with PZ, DHA, PZ-DHA (20 μM) or vehicle alone and cultured for 24 h in the presence or absence of 5 ng/mL TGF-β. Treated cells were serum starved and resuspended in serum-free F12/DMEM or DMEM and migration toward serum through a membrane with 8 μm pores was determined. MCF-10A and MDA-MB-231 cells that were pre-incubated with/without 10 ng/mL TGF-β were then treated with PZ, DHA, PZ-DHA (20 μM) or vehicle alone in the presence or absence of 5 ng/mL TGF- β and cultured for 72 h. Relative expression of TGF-β-induced **(B)** RhoA, **(C)** Cdc42 and **(D)** Rac1/2/3 was determined using western blot analysis. Equal protein loading was confirmed by β-actin expression. Data shown are mean % relative expression±SEM of three independent experiments. ANOVA multiple means comparison statistical method was performed and differences among means were compared using Tukey's test; *$p<0.05$, **$p<0.01$ and ***$p<0.001$.

### 5.2.3 A sub-cytotoxic concentration of PZ-DHA inhibits the expression of transcription factors involved in EMT of MDA-MB-231 cells

The effect of PZ-DHA and its parent compounds on EMT was tested using western blot analysis of whole cell lysates. Transcription factors involved in EMT such as Slug, Snail, Twist, and ZEB1 play a central role in phenotypic transformation of epithelial cells into more mesenchymal-like cells (Jin and Mu, 2015; Yang and Weinberg, 2008). PZ-DHA significantly inhibited the stabilization of β-catenin in MDA-MB-231 cells by 47.2% (% mean relative expression±SEM: vehicle, 104.0±5.3%; PZ, 87.3±6.6%; DHA, 85.3±13.6%; PZ-DHA, 56.8±12.2%) ($p$<0.05) (Figure 5.5A). The effect of PZ-DHA on two EMT-transcription factors, Slug (Snail family) and ZEB1 (ZEB family) were tested. PZ-DHA inhibited the expression of Slug by 58.9% (% mean relative expression±SEM: vehicle, 101.7±13.6%; PZ, 97.7±11.0%; DHA, 61.0±8.0%; PZ-DHA, 42.8±8.6%) ($p$<0.05) (Figure 5.5B) and ZEB1 by 52.0% (% mean relative expression±SEM: vehicle, 107.4±6.7%; PZ, 103.8±8.1%; DHA, 77.1±8.5%; PZ-DHA, 55.4±3.9%) ($p$<0.05) (Figure 5.5C). However, the expression of the EMT marker vimentin was not significantly affected by PZ-DHA or its parent compounds (% mean relative expression±SEM: Vehicle, 108.5±8.5%; PZ, 87.0±14.1%; DHA, 97.8±15.4%; PZ-DHA, 57.6±6.3%) ($p$=0.1197) (Figure 5.5D).

E-cadherin, which is the most important cell adhesion molecule of epithelial cells, is down-regulated during EMT and another adhesion molecule, N-cadherin, which is expressed by invasive cancer cells, is up-regulated during EMT(Hazan et al., 2004; Pećina-Slaus, 2003). This is known as EMT-induced cadherin switch. The effect of PZ-DHA on this process was investigated using western blot analysis of MDA-MB-231 cells. Treatment with a sub-cytotoxic concentration of PZ-DHA, but not PZ or DHA, resulted in a 48.9% significant increase of E-cadherin in MDA-MB-231 cells; (% mean relative expression±SEM: vehicle, 99.6±0.4%; PZ, 97.3±11.4%; DHA, 109.3±14.6%; PZ-DHA, 148.5±8.8%) ($p$<0.05) (Figure 5.6). Although PZ, DHA and PZ-DHA treatment resulted in a decreasing trend in N-cadherin expression compared to the vehicle control, the effect of these drugs failed to reach statistical significance (% mean relative expression±SEM: vehicle, 104.7±3.8%; PZ, 78.3±8.5%; DHA, 63.6±13.4%; PZ-DHA, 77.4±6.7%) ($p$=0.1153) (Figure 5.6).

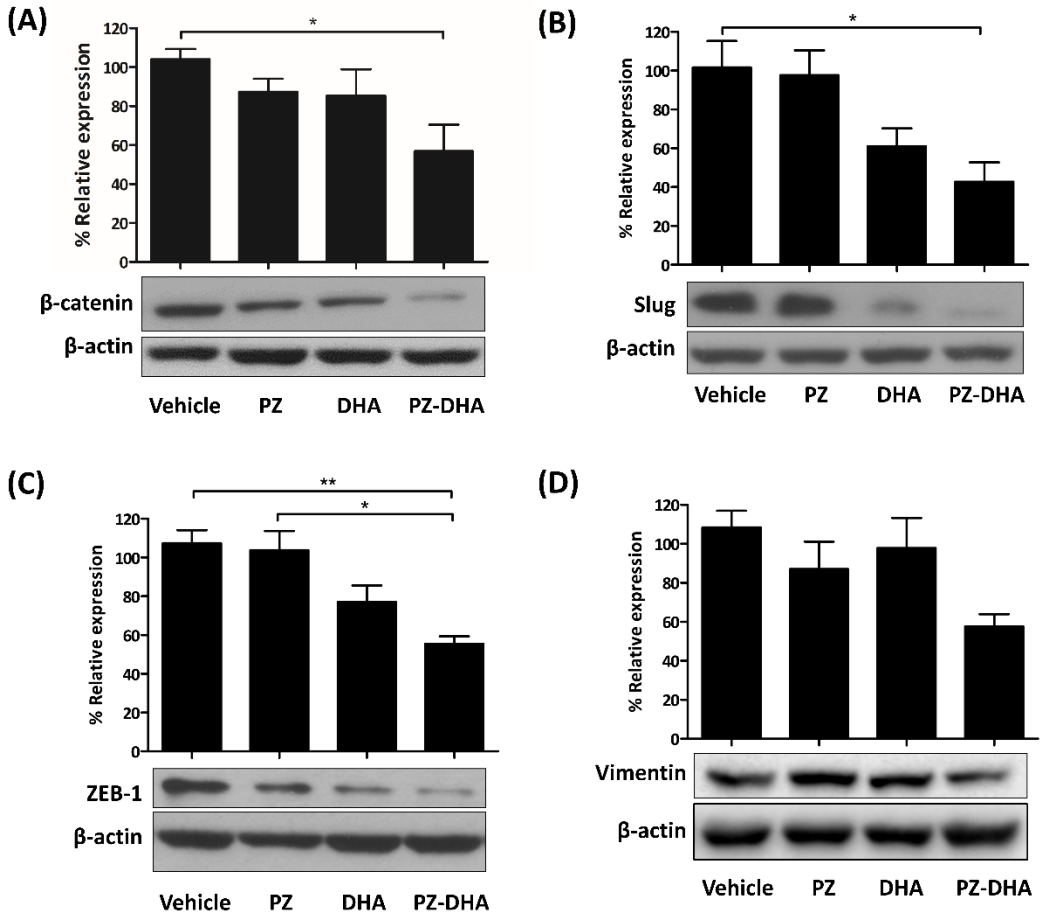


**Figure 5.5. A sub-cytotoxic concentration of PZ-DHA inhibits the expression of transcription factors involved in EMT of MDA-MB-231 cells *in vitro.***
MDA-MB-231 cells were treated with PZ, DHA, PZ-DHA (20 μM) or vehicle alone and cultured for 72 h. Cells were harvested, lysed and relative expression of proteins involved in EMT was determined using western blot analysis. Blots were probed with Ab against **(A)** β-catenin **(B)** Slug, **(C)** TCF8/ ZEB1 or **(D)** vimentin. Equal protein loading was confirmed by β-actin expression. Data shown are mean % migration±SEM of three or more independent experiments. ANOVA multiple means comparison statistical method was performed and differences among means were compared using Tukey's test; *$p$<0.05, **$p$<0.01.

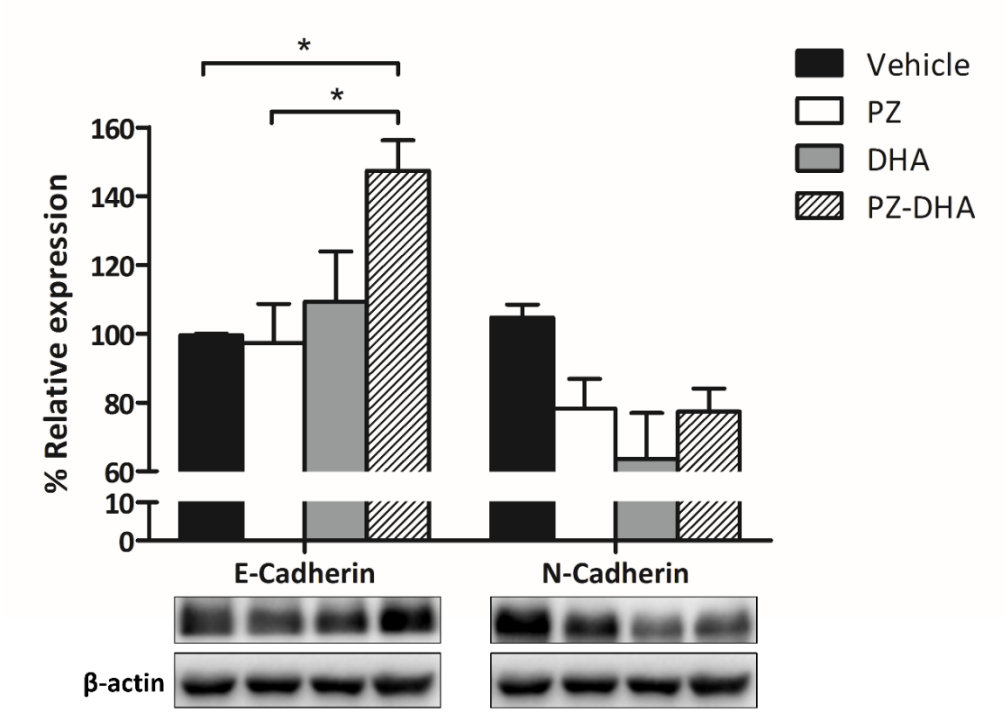


**Figure 5.6. A sub-cytotoxic concentration of PZ-DHA reverses the EMT-induced cadherin switch in MDA-MB-231 cells *in vitro*.**
MDA-MB-231 cells were treated with PZ, DHA, PZ-DHA (20 µM) vehicle or medium alone and cultured for 72 h. Cells were harvested, lysed and protein concentration in lysates was determined using a Bradford assay. Protein (40 µg) was then loaded on to 6% SDS-polyacrylamide gels. Blots were probed with Ab against pan-cadherin, and E-cadherin and N-cadherin bands were visualized based on their molecular weights (E-cadherin, 135 kDa, N-cadherin, 140 kDa). Equal protein loading was confirmed by β-actin expression. Data shown are mean % relative expression±SEM of three independent experiments. ANOVA multiple means comparison statistical method was performed and differences among means were compared using Tukey's test; *$p$<0.05.

### 5.2.4 A sub-cytotoxic concentration of PZ-DHA inhibits serum-induced invasive activity of MDA-MB-231 cells

During intravasation and extravasation, cancer cells that become dispersed from a primary tumor invade through the ECM and basement membrane of the epithelium, as well as the vascular endothelium (Chiang et al., 2016; Jeon et al., 2013; van Zijl et al., 2011). This process involves degradation of the ECM, which is often triggered by the MMPs secreted by the tumor cells in the primary tumor site. To model intravasation and extravasation i*n vitro*, porous polycarbonate membranes were coated with ECM proteins (fibronectin and gelatin) and invasion of MDA-MB-231 cells through the ECM protein-coated membranes was observed. PZ-DHA decreased the invasion of MDA-MB-231 cells through fibronectin-coated membranes by 79.3% (% mean relative migration±SEM: vehicle, 107.7±8.7%; PZ, 95.5±12.8%; DHA, 68.7±7.3%; PZ-DHA, 28.4±6.7%) ($p$<0.001) (Figure 5.7A and B), which was a significantly greater effect compared to vehicle, PZ and DHA. Furthermore, PZ-DHA decreased the invasion of MDA-MB-231 breast cancer cells through a gelatin-coated membrane by 90%, which was also significantly greater than vehicle-, PZ- and DHA-induced anti-invasive activities (% mean relative migration±SEM: vehicle, 96.0±9.3%; PZ, 99.7±3.8%; DHA, 51.4±4.7%; PZ-DHA, 6.0±0.6%) ($p$<0.001) (Figure 5.7C and D).

### 5.2.5 A sub-cytotoxic concentration of PZ-DHA inhibits the expression of matrix metalloproteinases in MDA-MB-231 cells

The effect of PZ-DHA on the expression of matrix metalloproteinases, which are ECM degradation proteins was assessed using western blot analysis. Both PZ-DHA and DHA significantly inhibited the expression of MMP2 in MDA-MB-231 cells (% mean relative expression±SEM: vehicle, 114.5±4.2%; PZ, 120.8±6.7%; DHA, 60.7±16.9%; PZ-DHA, 42.1±12.8%) ($p$<0.01) (Figure 5.8).

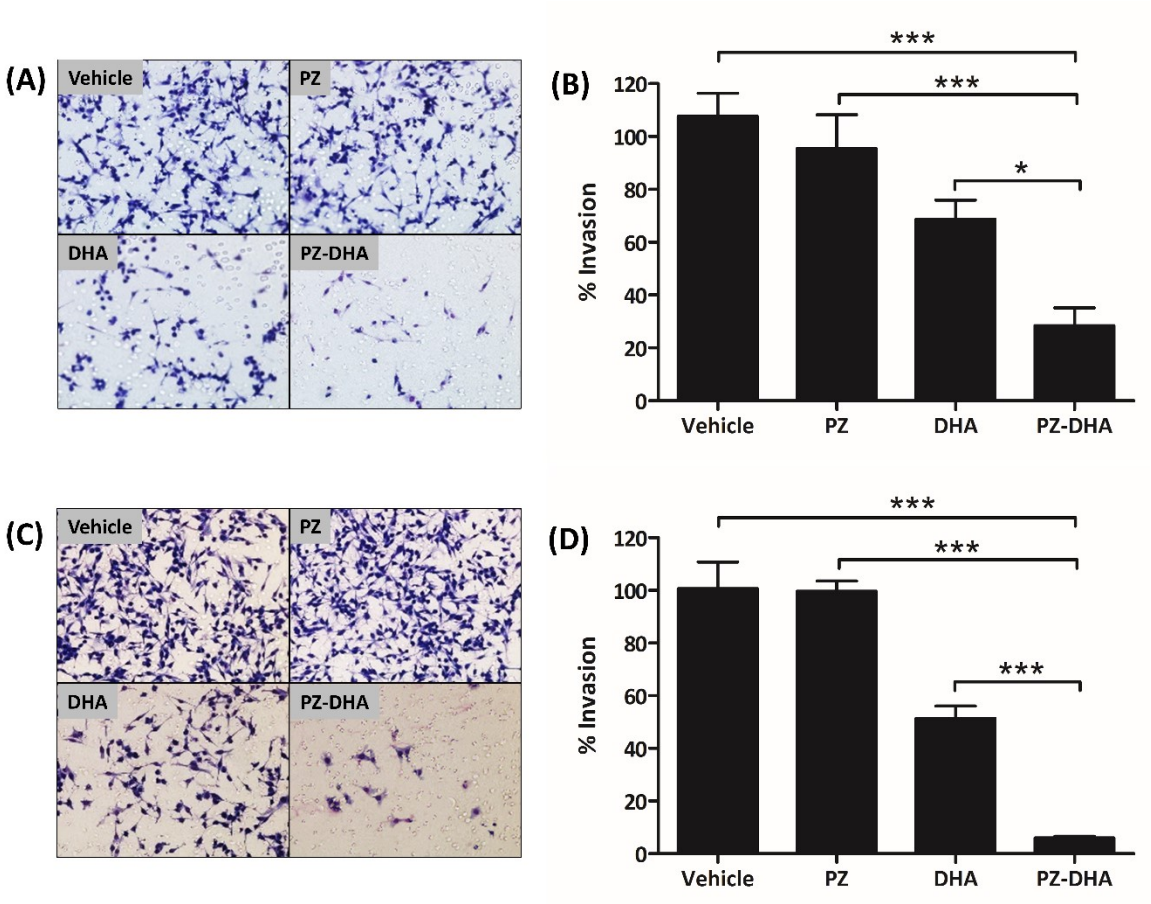


**Figure 5.7. A sub-cytotoxic concentration of PZ-DHA inhibits serum-induced invasion of MDA-MB-231 cells *in vitro*.**

MDA-MB-231 cells were treated with PZ, DHA, PZ-DHA (20 µM) or vehicle alone and cultured for 24 h. Treated cells were serum starved and resuspended in serum-free DMEM and migration toward serum through a 8 µm pore-sized membrane coated with **(A)** and **(B)** 10 µg/mL fibronectin or **(C)** and **(D)** 10 µg/mL gelatin was determined. Images were analyzed using ImageJ software and % invasion was calculated. Data shown are representative images and mean % invasion±SEM of three independent experiments. ANOVA multiple means comparison statistical method was performed and differences among means were compared using Tukey's test; *$p$<0.05 and ***$p$<0.001.

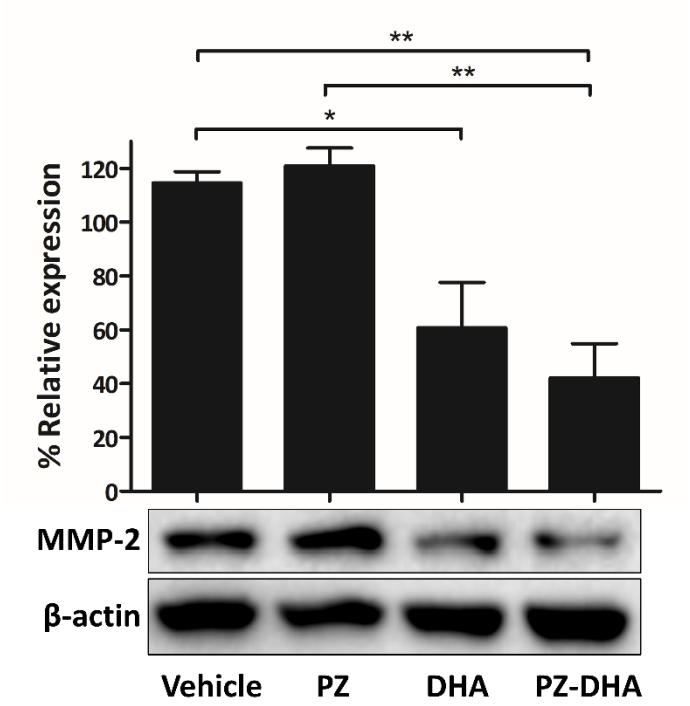


**Figure 5.8. A sub-cytotoxic concentration of PZ-DHA inhibits the expression MMP2 in MDA-MB-231 cells *in vitro*.**
MDA-MB-231 cells were treated with PZ, DHA, PZ-DHA (20 μM) or vehicle alone and cultured for 72 h. Cells were harvested and protein-rich cell lysates were prepared. Equal amounts of protein (40 μg) were loaded on to 12% SDS-polyacrylamide gels and electrophoresed. Proteins were transferred to nitrocellulose membranes and blots probed overnight at 4°C with primary Ab against MMP2. Equal protein loading was confirmed by β-actin expression. Data shown are mean % relative expression±SEM of three independent experiments. ANOVA multiple means comparison statistical method was performed and differences among means were compared using Tukey's test; *$p<0.05$, **$p<0.01$.

### 5.2.6 PZ-DHA does not affect the adhesion of MDA-MB-231 and 4T1 cells

Intravasation and extravasation were modeled *in vitro* using GFP transfected-MDA-MB-231 cells and HUVEC monolayers, which were activated using TNF-α. MDA-MB-231-GFP cells were treated with PZ, DHA, PZ-DHA, vehicle or medium and seeded on to activated HUVEC monolayer. In comparison to untreated HUVECs, TNF-α treatment increased carcinoma cell adhesion by 44%; however, none of the drugs significantly affected the adhesion of MDA-MB-231-GFP cells to endothelial cells (% mean relative adhesion±SEM: vehicle, 99.9±3.6%; PZ, 85.2±13.7%; DHA, 71.1±11.5%; PZ-DHA, 70.0±11.0%) ($p$=0.2368) (Figure 5.9).

### 5.2.7 PZ-DHA suppresses the metastasis of 4T1 cells to the lungs of Balb/c female mice

The effect of PZ-DHA on the metastasis of orthotopically implanted mouse mammary carcinoma cells was first investigated using a syngeneic mouse model of breast cancer. PZ-DHA was administered by intraperitoneal injection to 4T1-tumor bearing Balb/c female mice and metastasis of 4T1 cells into the lungs was measured using a colony-forming assay (Figure 5.10A). PZ-DHA reduced the metastasis of 4T1 cells by 71.2% in comparison to a saline-treated control group (mean number of cells metastasized into the lungs±SEM: saline, 94.4±22.1; PZ-DHA, 27.2±8.1) ($p$<0.05) (Figure 5.10B). Pearson correlation statistics showed that the anti-metastatic activity of PZ-DHA was independent from inhibition of primary tumor growth (Pearson r, 0.2891; p=0.4505), while metastasis was correlated to the tumor growth in the saline-treated mice (Pearson r, 0.7596; $p$<0.05) (Figure 5.10C). Tumors were fixed, sectioned and stained with hematoxylin and eosin. The number of tumor-associated blood vessels in the tumor periphery was determined (Figure 5.10D). PZ-DHA significantly reduced the development of blood vessels around the tumor (mean number of blood vessels±SEM: saline, 176.2±27.4; PZ-DHA, 80.6±21.0) ($p$<0.05) (Figure 5.10E) and Pearson correlation statistics indicated that the reduction of blood vessel development was independent from the tumor volume (saline: Pearson r, 0.5509; p=0.1242 and PZ-DHA, Pearson r, 0.5732; $p$=0.1067) (Figure 5.10F).

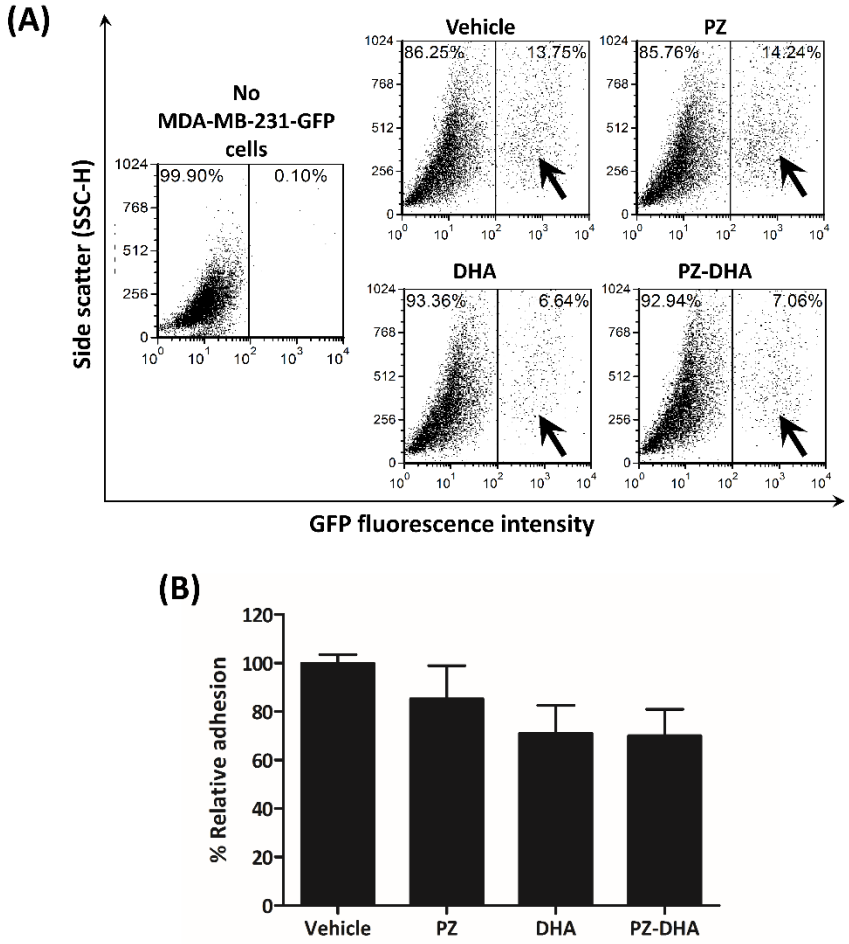


**Figure 5.9. A sub-cytotoxic concentration of PZ-DHA does not inhibit the adhesion of MDA-MB-231 cells to HUVECs.**

HUVECs were grown as a monolayer in 12-well plates. GFP-transfected MDA-MB-231 cells were treated with 20 μM of PZ, DHA, PZ-DHA, or vehicle or medium alone and cultured for 24 h. Confluent HUVEC monolayers were activated by treatment with 20 ng/mL TNF-α for 4 h. PZ-, DHA-, PZ-DHA-, vehicle- or medium-treated GFP-MDA-MB-231 cells were seeded on to HUVEC monolayers at a $5\times10^4$ cells/well density and incubated for 30 min at 37°C. At the end of the incubation, supernatant was removed and HUVEC monolayers with attached MDA-MB-231 cells were carefully rinsed with PBS. All cells were detached and GFP-expressing MDA-MB-231 cells were detected by flow cytometry. Data shown are **(A)** representative SSCH vs FL1 dot plots (arrows indicate GFP-MDA-MB-231 cells) and **(B)** mean % relative number of GFP-MDA-MB-231 cells±SEM attached to the HUVEC monolayers.

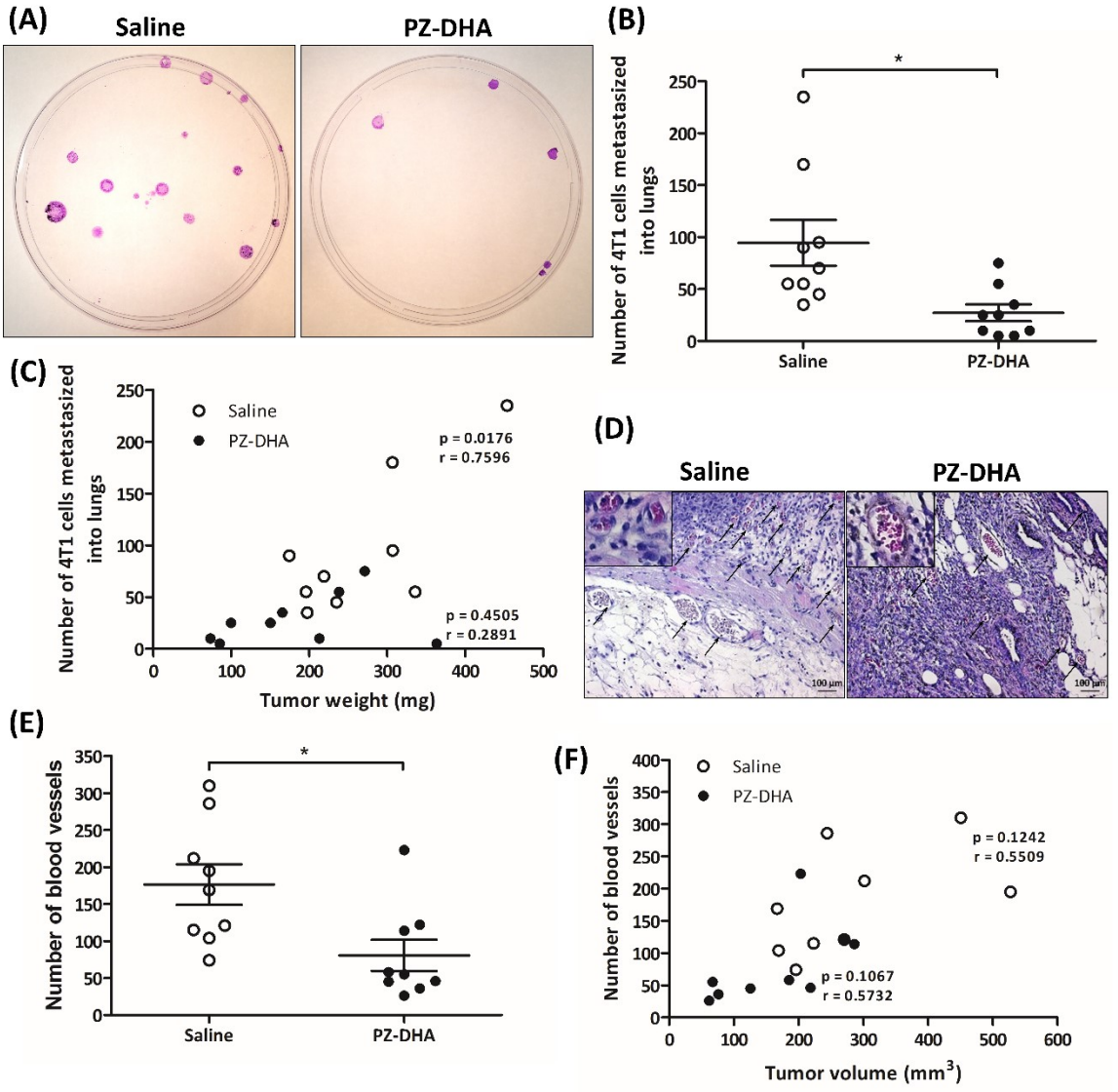


**Figure 5.10. Intraperitoneal administration of PZ-DHA suppresses the metastasis of orthotopically implanted-4T1 cells to the lungs of Balb/c mice.**
4T1 mouse mammary carcinoma cells were injected into the left inguinal mammary fat pad of syngeneic female Balb/c mice and saline or PZ-DHA (100 mg/kg) were administered every second day beginning at day 8 by intraperitoneal injection. The number of cells that metastasized into lungs was determined by colony-forming assay. **(A)** 4T1 cell colonies were visualized by staining with 0.4% crystal violet solution after 14 days. **(B)** Tumor cell colonies were counted and data shown as mean±SEM. **(C)** Correlation of primary tumor weight to number of 4T1 cells metastasized into lungs was determined using Pearson correlation statistical method. **(D)** The number of tumor-associated blood vessels in hematoxylin and eosin stained tumor sections was determined and **(E)** data are shown as mean±SEM. **(F)** Correlation of primary tumor volume to number of tumor associated-blood vessels was determined using Pearson correlation statistical method. Statistical differences between means were compared using Student's t-test; *$p$<0.05.

### 5.2.8 PZ-DHA suppresses the metastasis of GFP-transfected MDA-MB-231 cells to the lungs of NOD-SCID female mice

*In vivo* anti-metastatic activity of PZ-DHA was then tested using a xenograft mouse model, in which GFP transfected-MDA-MB-231 (Supplementary Figure 4) human breast cancer cells were orthotopically xenografted into the left inguinal mammary fat pad of NOD-SCID female mice. Intraperitoneal administration of PZ-DHA inhibited the metastasis of MDA-MB-231 breast cancer cells into the lungs of NOD-SCID mice by 45.7% compared to the saline-treated control group (% mean number of cells metastasized into the lungs±SEM: saline, 7.4±1.3%; PZ-DHA, 3.4±1.0%) ($p$<0.05) (Figure 5.11A and B). PZ-DHA-induced reduction in tumor metastasis was independent from primary tumor growth (Pearson r, 0.4568; $p$=0.2164), and a significant correlation between tumor growth and metastasis was indicated by the Pearson statistical correlation test in saline-treated control group (Pearson r, 0.6416; $p$<0.05) (Figure 5.11C). Furthermore, PZ-DHA treatment significantly reduced the formation of tumor-associated blood vessels (mean number of blood vessels±SEM: saline, 114.8±15.0%; PZ-DHA, 73.3±10.3%) ($p$<0.05) (Figure 5.11D and E). PZ-DHA-induced inhibitory activity toward tumor-associated blood vessel growth was also independent from tumor growth (saline: Pearson r, -0.3914; p=0.2634 and PZ-DHA, Pearson r, -0.2869; $p$=0.4541) (Figure 5.11F).

### 5.2.9 Immunohistochemical determination of MMP2 and CD31 expression in 4T1 and MDA-MB-231 tumor sections

Saline- and PZ-DHA-treated 4T1 and MDA-MB-231 tumor were subjected to immunohistochemical analysis to quantify the expression of MMP2 and CD31. MMP2 was down regulated by PZ-DHA in both tumors, with the reduction being most notable in the tumor periphery. PZ-DHA also down regulated the expression of the endothelial cell marker CD31. Fewer blood vessels were observed in the periphery of PZ-DHA-treated tumors in comparison to saline-treated tumors (Figure 5.12).

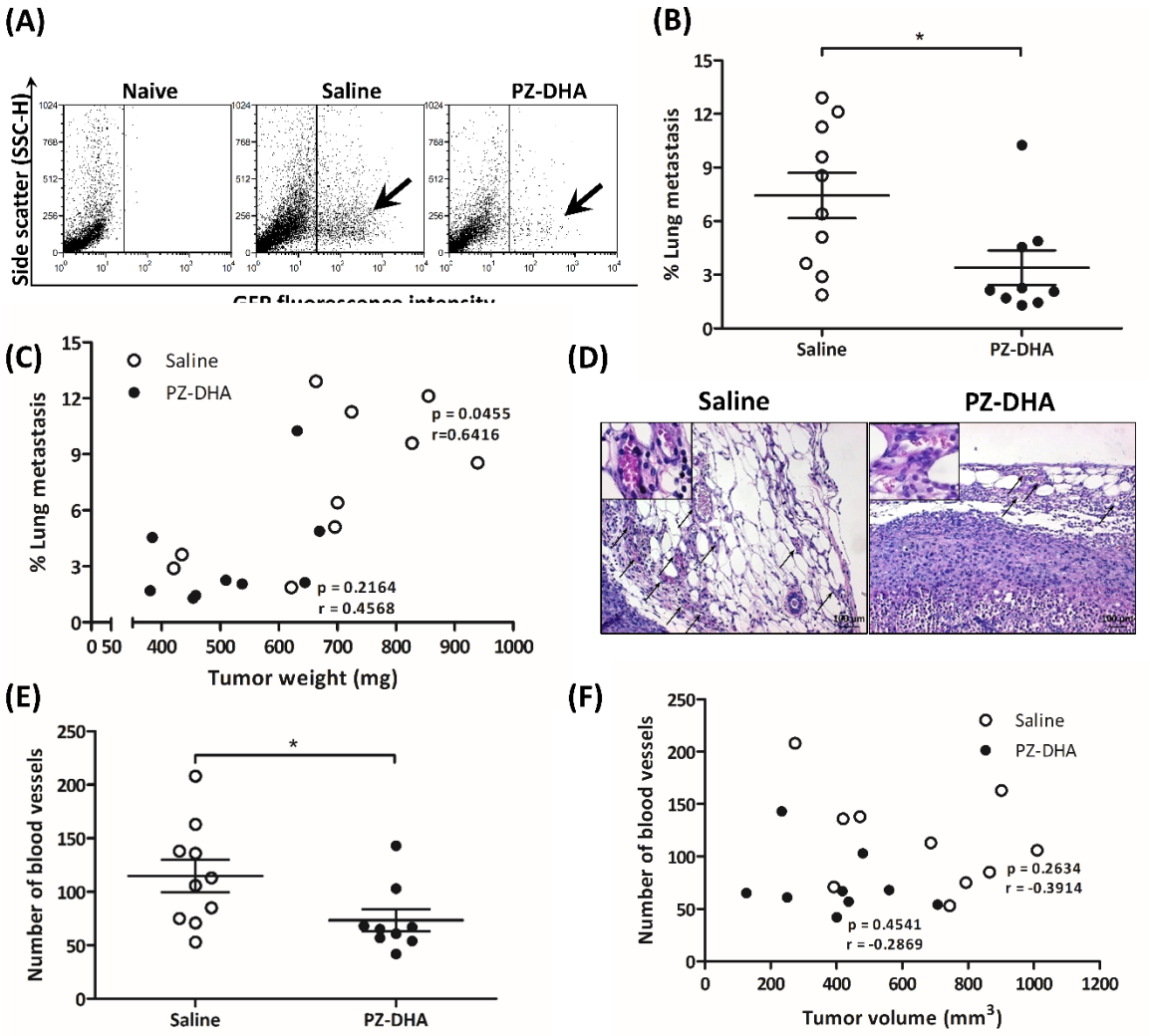


**Figure 5.11. Intraperitoneal administration of PZ-DHA suppresses the metastasis of orthotopically xenografted-MDA-MB-231 cells to the lungs of NOD-SCID mice.** GFP-tagged MDA-MB 231 breast cancer cells were mixed with Matrigel and injected into the left inguinal mammary fat pad of female NOD-SCID mice and saline or PZ-DHA (100 mg/kg) were administered every second day beginning at day 21 by intraperitoneal injection. On day 59, mice were euthanized, and lungs were harvested. Lungs were minced, and single cellular suspensions were analyzed by **(A)** flow cytometry and **(B)** % lung metastasis was determined as mean±SEM. **(C)** Correlation of primary tumor weight to number of 4T1 cells metastasized into lungs was determined using Pearson correlation statistical method. Statistical differences between means were compared using Student's t-test; *$p$<0.05. **(D)** Tumor-associated blood vessels were counted in a hematoxylin and eosin-stained tumor sections and **(E)** data are shown as mean±SEM. **(F)** Correlation of primary tumor volume to number of tumor associated-blood vessels was determined using Pearson correlation statistical method. Statistical differences between means were compared using Student's t-test; *$p$<0.05.

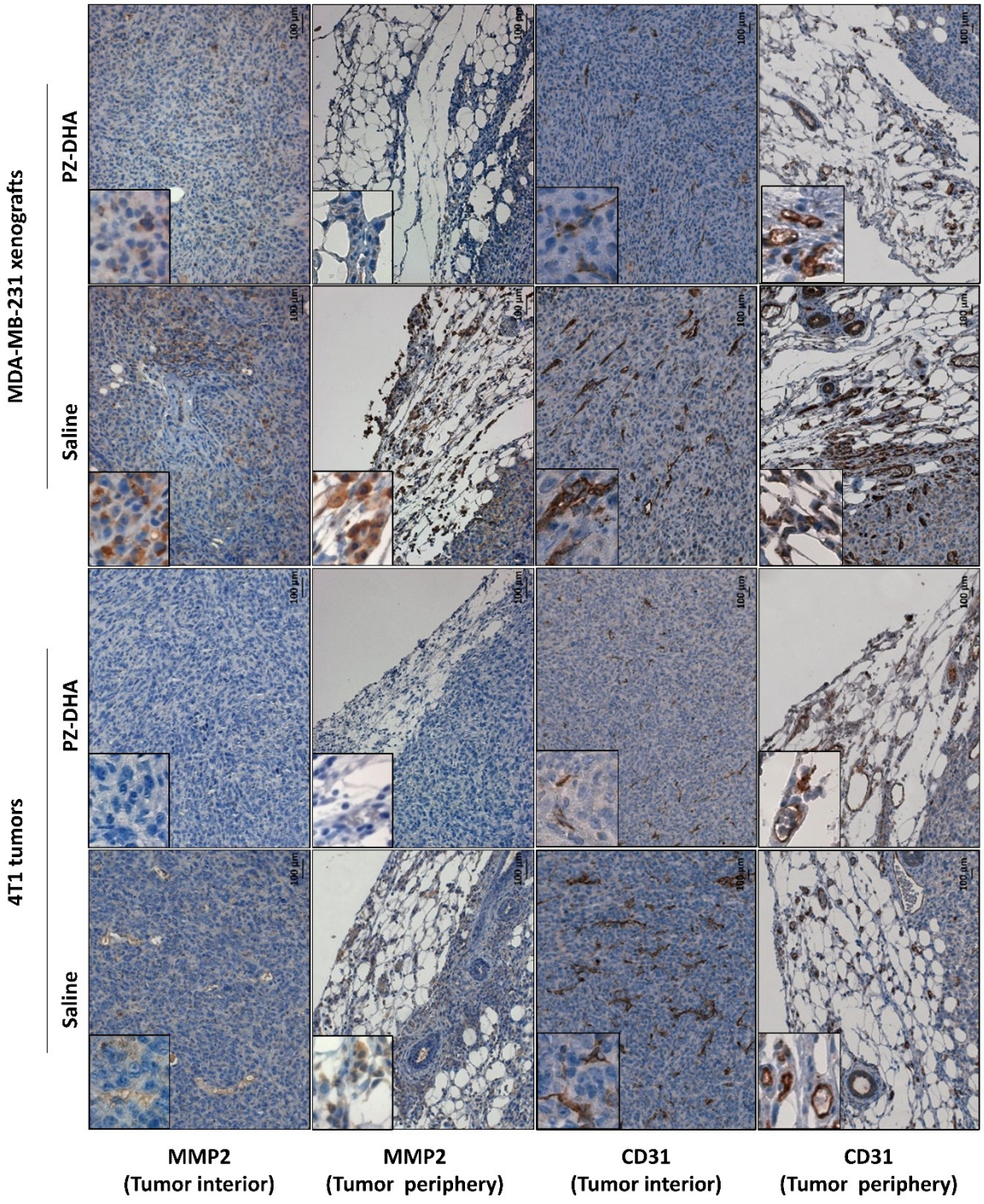
MDA-MB-231 xenografts
PZ-DHA
Saline
4T1 tumors
PZ-DHA
Saline
MMP2
(Tumor interior)
MMP2
(Tumor periphery)
CD31
(Tumor interior)
CD31
(Tumor periphery)

**Figure 5.12. PZ-DHA decreases the expression of MMP2 and CD31 in 4T1 and MDA-MB-231 tumors.**
Fixed tumors were embedded in paraffin and cut into 5 μm thick sections. Sections were mounted on glass slides and deparaffinized using xylene and rehydrated using graded ethanol to water. Deparaffinized tumor sections were pre-treated using heat-mediated antigen retrieval with sodium acetate (pH 6.0) (for MMP2) or TAE buffer (pH 9.0) (for CD31) and incubated in $H_2O_2$. Then tumor sections were blocked for non-specific binding using Rodent M block and incubated with mouse monoclonal anti-MMP2 Ab or rabbit monoclonal anti-CD31 Ab overnight at room temperature. MMP2-stained sections were incubated with mouse-on-mouse HRP-polymer and detected using HRP/DAB detection system. CD31-stained tumor sections were incubated with anti-rabbit HRP-polymer and detected using HRP/DAB detection system. Data shown are stained tumor sections photographed at ×200 and ×400 magnification using a bright-field microscope.

## 5.3 Discussion

Advanced cancer is characterized by metastasis, which is an enormously complex process. Completion of the entire process of metastasis by a cancer cell is a rare event (Hynes, 2003); yet, metastasis is a life-threatening disease which is responsible for nearly 90% of cancer-related deaths. According to Canadian Cancer Society, 10% of breast cancers are already metastatic when they are diagnosed and 30% of women who are diagnosed with early stages breast cancer will go on to develop metastatic disease (Canadian Cancer Statistics, 2017b). The main objective of this chapter is to study the anti-metastatic activity of PZ-DHA using *in vitro* and *in vivo* models of metastatic breast cancer. The effect of PZ-DHA on major steps of the metastatic cascade such as migration, invasion, EMT, intravasation/extravasation and formation of secondary metastatic lesions were modeled and tested during this chapter. Two aggressive mammary carcinoma cell lines were used in *in vitro* and *in vivo* experiments. 4T1 mouse mammary carcinoma cells were used to study metastasis in a syngeneic mouse model and GFP-transfected MDA-MB-231 cells were used to study metastasis in a xenograft model.

The number of cells that disseminate from a tumor is directly related to the rate of tumor cell proliferation (von Fournier et al., 1989). Furthermore, studies have shown that the pathological grade of a primary tumor is closely related to the growth rate of the metastatic lesions (Oda et al., 2001). Anti-proliferative effects of PZ-DHA, which were discussed in-detail in chapter 4, suggested that this primary determinant of cancer metastasis was blocked by sub-cytotoxic concentrations of PZ-DHA, leading to a potential decrease in the number of cancer cells shed into the circulation. However, this does not necessarily suggest that the metastatic ability of tumor cells circulating in the blood is inhibited. Therefore, experiments were carried out to investigate PZ-DHA-induced anti-metastatic effects using concentrations of drug (10 and 20 μM) that spare mammary carcinoma cell proliferation, but effectively inhibit metastasis. The effect of PZ-DHA on the migration of mammary carcinoma cells was tested using gap-closure (4T1 and MDA-MB-231) and trans-well cell migration (MDA-MB-231) assays. It was necessary to inhibit the proliferation of 4T1 and MDA-MB-231 cells with mitomycin C prior to drug treatment in gap-closure assays to ensure that cell migration is the sole determinant of the assay outcome. Mitomycin C-induced antiproliferative effects were

confirmed by flow cytometric analysis of Oregon Green-488-stained cells (Supplementary Figure 5 and 6). PZ-DHA inhibited the migration of both 4T1 and MDA-MB-231 cells in the gap-closure assay, suggesting an inhibitory effect on the migration of TNBC cells (Figure 5.1). This inhibitory effect was confirmed in a trans-well cell migration assay, in which PZ-DHA significantly suppressed the directed migration of serum-starved MDA-MB-231 cells toward serum (Figure 5.2). Migration of MDA-MB-231 cells through a 8 μm pore-sized membrane coated with fibronectin and gelatin was also inhibited by PZ-DHA, suggesting an inhibitory effect on the invasive capacity of MDA-MB-231 cells (Figure 5.7). MMPs secreted from tumor cells and surrounding stromal cells degrade ECM proteins and pave the path for invading cancer cells (Bhowmick et al., 2004; Finger and Giaccia, 2010; Kessenbrock et al., 2010; Westermarck and Kahari, 1999). MMP2 is a type IV collagenase- and gelatinase-degrading enzyme that plays a significant proteolytic role in tumor cell invasion (Gialeli et al., 2011; Kumar et al., 2000; Stankovic et al., 2010). PZ-DHA significantly inhibited the expression of MMP2 by MDA-MB-231 cells, indicating a likely mechanism for PZ-DHA-mediated *in vitro* anti-invasive effects in the trans-well migration assay (Figure 5.8).

TGF-β regulates cellular events such as growth, differentiation, and EMT that play a major role in the embryogenesis (Hogan et al., 1994; Johnson et al., 1993; Millan et al., 1991; Wu and Hill, 2009). However, TGF-β is also important for cancer progression by acting as a potent stimulator of tumorigenesis, migration, cancer-associated type III EMT and metastasis (de Caestecker et al., 2000; Derynck et al., 2001; Kalluri and Weinberg, 2009; Lebrun, 2012; Padua and Massagué, 2009; Pickup et al., 2013). Small molecular Rho GTPase family proteins and their up-stream and down-stream signaling molecules play a significant role in cancer metastasis by promoting actin polymerization-mediated cell motility (Guilluy et al., 2011; Hanna and El-Sibai, 2013; Jansen et al., 2018; Ridley, 2015). Furthermore, TGF-β-mediated EMT and cancer cell migration occur through a RhoA-dependent mechanism (Bhowmick et al., 2001). Over-expression of RhoA, Cdc42 and Rac1/2/3 is associated with cell migration through formation of lamellipodia and filopodia (Hanna and El-Sibai, 2013). Rho GTPase signaling also plays a central role in actin dynamics and highly deregulated in many cancers (Porter et al., 2016; Raftopoulou

and Hall, 2004; Tojkander et al., 2012). The effect of flavonoids on Rho GTPase signaling has been shown in relation to the development of the nervous system and the progression of multiple sclerosis (Hendriks et al., 2004; Palazzolo et al., 2012); however, little is known about the role of flavonoids on Rho GTPase signaling in cancers. The effect of PZ-DHA on the expression of Rho GTPase proteins was tested in the presence and absence of TGF-β using non-malignant MCF-10A cells and malignant MDA-MB-231 cells. In the absence of TGF-β, PZ-DHA inhibited cell migration and decreased baseline levels of RhoA and Cdc42, but not Rac1/2/3, expression in MDA-MB-231 cells. This suggests that PZ-DHA might inhibit the formation of filopodia but not lamellipodia during the migration of MDA-MB-231 cells. In contrast, PZ-DHA or its parent compounds did not affect baseline expression of Rho GTPase levels in MCF-10A cells, indicating a selective activity towards malignant cells (Figure 5.3). TGF-β signaling (confirmed by Smad3 phosphorylation at Ser423/425) (Supplementary Figure 7) stimulated MCF-10A and MDA-MB-231 cell migration and expression of Rho GTPases. PZ-DHA inhibited TGF-β-induced RhoA and Cdc42 expression in both MCF-10A and MDA-MB-231 cells; however, TGF-β-induced Rac1/2/3 expression was decreased only in MDA-MB-231 cells following PZ-DHA treatment (Figure 5.4). Taken together, these findings imply that PZ-DHA-induced suppression of Rho GTPases signaling is restricted to malignant cells.

It was initially believed that GSK3β is a constitutively activated kinase (Zhang et al., 2003); however, more recent research suggests that the kinase activity of GSK3β is regulated by a variety of means such as phosphorylation, protein complex association, priming/substrate specificity, subcellular localization, and proteolytic cleavage (Medina and Wandosell, 2011). Phosphorylation at Ser9 inhibits the kinase activity of GSK3β (Fang et al., 2000) whereas GSK3β is activated by phosphorylation at Tyr216 (Hartigan et al., 2001). However, Simón et al. (2008) report that the pharmacological inhibition of GSK3β is not strictly correlated with decreased phosphorylation at Tyr216 (Simón et al., 2008). Section 4.2.9 of chapter 4 showed that PZ-DHA increased the phosphorylation of GSK3β at ser9 but did not significantly affect Tyr216 phosphorylation. Regardless, PZ-DHA significantly decreased β-catenin stabilization, implying a potential for upstream activation of GSK3β. However, this was not evident by any increased phosphorylation of

GSK3β at Tyr216 or decreased phosphorylation at Ser9. Kern et al. (2006) showed that a mixture of apple polyphenols containing PZ and PT decrease GSK3β activity in HT29 colorectal adenocarcinoma cells in a dose-dependent manner, even though the decrease was not associated with the stabilization of β-catenin (Kern et al., 2006). On the other hand, Antika and co-workers suggest a GSK3β/β-catenin-dependent beneficial effect of PT and PZ on non-malignant MC3T3 murine osteoblast cells and femoral bone tissue of senescence-accelerated resistant mouse strain prone-6 mice employed in a senile osteoporosis study (Antika et al., 2017). Therefore, it is possible that apple polyphenols such as PT and PZ have effects on β-catenin that are associated with GSK3β activation in non-malignant cells but not in malignant cells. This may explain PZ-DHA-induced downregulation of β-catenin stabilization in the cytoplasm and/or nuclear translocation, even when GSK3β activation was not observed in MDA-MB-231 cells. Furthermore, decreased-β-catenin activity was consistent with increased expression of E-cadherin in PZ-DHA-treated MDA-MB-231cells (Figure 5.6). TGF-β acts as a key regulator of the EMT process (Katsuno et al., 2013; Pang et al., 2016; Papageorgis, 2015). Increased activity of EMT transcription factors in epithelial cells causes loss of epithelial markers, thereby stabilizing the mesenchymal phenotype (Liu et al., 2016; Wu et al., 2016b). PZ-DHA treatment decreased the expression of EMT transcription factors Slug and ZEB-1; however, PZ-DHA had no significant effect on the expression of vimentin, which regulates the formation of lamellipodia during cell migration (Hunter et al., 2008). This re-confirms that PZ-DHA does not inhibit the formation of lamellipodia or baseline levels of signaling molecules associated with lamellipodia formation such as Rac1/2/3 and vimentin in MDA-MB-231 cells. Rac1 and its endogenous inhibitor Rac1b control TGF-β responses in cancer cells in an antagonistic manner (Melzer et al., 2017; Ungefroren et al., 2014). When TGF-β signaling was activated, a further increase of Rac1/2/3 was observed that PZ-DHA was not expected to reverse. As expected, TGF-β-induced Rac1/2/3 overexpression remained unchanged in PZ-DHA-treated MCF-10A cells (Figure 5.4). Surprisingly, PZ-DHA significantly decreased TGF-β-induced expression of Rac1/2/3 in MDA-MB-231 cells. Therefore, it is possible that PZ-DHA may have an additional stimulating effect on Rac1b when TGF-β signaling is activated in malignant

cells. However, further experiments are needed to confirm the effects of PZ-DHA on TGF-β-dependent and -independent activation of Rac and Rac1b signaling.

Intravasation and extravasation requires the adhesion of cancer cells to the endothelium lining of blood vessel walls. Several growth factors and adhesion molecules are involved in the regulation of breast cancer cell adhesion to the endothelium (Dippel et al., 2013; Mine et al., 2003; Narita et al., 1996). However, PZ-DHA did not affect the adhesion of MDA-MB-231 cells to HUVEC monolayers, suggesting that PZ-DHA likely did not affect the expression of cell adhesion molecules on MDA-MB-231 cells (Figure 5.9). However, it is important to note that PZ-DHA increased the expression of E-cadherin in MDA-MB-231 cells. Studies have shown that epithelial cells that survive in a suspension extensively undergo cellular aggregation with increased E-cadherin expression (Day et al., 1999; Hsu et al., 2011). Therefore, PZ-DHA-induced upregulation of E-cadherin may have affected, to some extent, the adhesion of MDA-MB-231 cells to HUVECs.

The site of the metastatic lesion development is specific to the molecular subtype of the primary breast tumor (Smid et al., 2008). Lung and brain metastases are common among TNBC patients (Kelly et al., 2017; Kimbung et al., 2015; Smid et al., 2008; Soni et al., 2015). Therefore, in the current study, the metastasis of mammary carcinoma cells to the lungs was studied. The *in vivo* anti-metastatic activity of PZ-DHA was studied using two different mouse models. In both models, PZ-DHA inhibited the metastasis of orthotopically implanted mammary carcinoma cells to the lungs. Section 4.2.13 of chapter 4 shows that systemic administration of PZ-DHA inhibited the growth of mammary carcinoma cells in immune-competent and immune-deficient mice. Pearson correlation statistics were conducted to determine whether there is a correlation between inhibition of tumor growth and the anti-metastatic potential of PZ-DHA. In saline-treated Balb/c and NOD-SCID mice, the metastatic burden was significantly correlated with primary tumor burden (as measured by tumor weight), implying that the number of 4T1 or MDA-MB-231 cells disseminated into the systemic circulation was proportional to the primary tumor growth rate. However, no such correlation was found between the primary tumor weight and metastasis in PZ-DHA-treated mice (Figure 5.10 and 5.11). This strongly suggests that *in vivo* anti-metastatic activities of PZ-DHA are independent of its tumour suppressor potential and are not merely an artefact of reduced tumor burden.

Furthermore, PZ-DHA caused a strong reduction in MMP2 expression in 4T1 and MDA-MB-231 primary tumors, suggesting a reduction in proteolytic activity and, as a result, a diminished tumor cell mobilization (Figure 5.12). Tumor-associated blood vessels capture cancer cells from the primary tumor site and deliver these cells to secondary organs; therefore, this process serves as one of the main routes of metastatic cancer cell spread (Jahroudi and Greenberger, 1995). In contrast, inhibition of neo-angiogenesis minimizes the hematogenic spread of cancer cells (Bielenberg and Zetter, 2015). The effect of PZ-DHA on neo-angiogenesis was investigated by studying the tumor-associated vasculature in 4T1 and MDA-MB-231 tumors excised from mice. Exposure to PZ-DHA significantly reduced the number of tumor-surrounding blood vessels in a tumor volume-independent manner (Figure 5.10 and 5.11). A reduction in the endothelial marker, CD31 was also noted following immunohistochemical staining of primary tumors (Figure 5.12).

In summary, PZ-DHA suppressed the migration of aggressive 4T1 and MDA-MB-231 mammary carcinoma cell types *in vitro* and reduced the invasive capacity of MDA-MB-231 cells. Inhibition of EMT, TGF-β-induced Rho GTPase signaling and re-establishment of E-cadherin cell-cell adhesion molecules suggested molecular mechanisms for the observed *in vitro* inhibition of MDA-MB-231 cell motility by PZ-DHA. *In vivo* experiments revealed that PZ-DHA inhibited the metastasis of 4T1 and MDA-MB-231 cells in mice without necessarily reducing primary tumor burden. PZ-DHA also reduced MMP2 expression in primary tumors, as well as tumor-associated angiogenesis. Further experiments to investigate the effects of PZ-DHA on angiogenesis will be detailed in chapter 6.

# CHAPTER 6 : PZ-DHA INHIBITS ANGIOGENESIS

## 6.1 Introduction

PZ-DHA-induced anti-proliferative and anti-metastatic activities toward mammary carcinoma cells were shown in chapter 4 and 5 respectively. In this chapter, another important aspect of metastasis, angiogenesis, is the focus. Anti-angiogenic activity of PZ-DHA was studied using *in vitro*, *ex vivo* and *in vivo* models.

An oxygen and nutrient supply is essential for the continuous growth of solid tumors, as well as promoting their metastatic potential. In fact, early studies have shown that the size of an avascularised solid tumor is restricted to 1-2 $mm^3$ (Folkman, 1990; Folkman et al., 1966; Lien and Ackerman, 1970). In a growing solid tumor, vasculature is mostly located around the tumor, creating a hypoxic environment in the tumor interior. Development of a hypoxic environment in the tumor interior contributes to stabilization of the transcription factor, HIF-1α, leading to the activation of target genes such as VEGF (Chua et al., 2010; Liu et al., 2012; Wang et al., 1995). Studies have shown that the partial pressure of oxygen does not correlate with the increased tumor interstitial pressure, suggesting that tumor hypoxia does not contribute to unusual elevation of interstitial pressure in the tumor microenvironment (Boucher et al., 1995). However, hypoxia-induced VEGF activation stimulates the growth of new blood vessels to the tumor interior (Chua et al., 2010; Liu et al., 2012; Wang et al., 1995). Mechanisms that determine the increased interstitial pressure in the tumor interior are not clearly understood; however, it is believed that VEGF-induced formation of large numbers of leaky, irregular-shaped blood vessels, as well as fibroblast-mediated tumor contractility play a significant role (Heldin et al., 2004; McDonald and Baluk, 2002; Nagy et al., 2009). In addition, many studies suggest that increased interstitial pressure within solid tumors restricts the delivery of chemotherapy into the tumor core (Heldin et al., 2004; Lunt et al., 2008; Salnikov et al., 2003). Tumor-associated blood vessels also serve as the main route by which cancer cells enter the systemic circulation and become disseminated. Therefore, inhibition of angiogenesis suppresses cancer progression by reducing the metastatic spread of cancer cells, as well as by increasing the penetration of

chemotherapy into the tumor interior (Bielenberg and Zetter, 2015; Folkman, 2002; Zetter, 1998).

Because of the above-mentioned roles of angiogenesis in tumor progression and metastasis, strategies for suppression of angiogenesis have been extensively studied. The majority of approaches are aimed at blocking receptors such as VEGFR2, which functions as the principal endogenous target of pro-angiogenic signaling molecules (Falcon et al., 2016). In addition, endothelial cell survival pathways such as Akt and MAPK signaling have also received distinct attention as therapeutic targets in the development of anti-angiogenic drugs (Dormond-Meuwly et al., 2011; Liu et al., 2006). Flavonoids have also been studied widely for their anti-angiogenic activity and chalcones, in particular, are known to inhibit Akt and MAPK signaling, as well as VEGFR2-mediated angiogenic signals in endothelial cells (Fernando et al., 2015; Kim, 2003; Mirossay et al., 2018; Mojzis et al., 2008). Furthermore, anti-angiogenic activity of dietary ω-3 fatty acids, including DHA and its metabolites, have been shown by many research groups (Matesanz et al., 2009; Zhang et al., 2013); however, one study shows that DHA stimulates angiogenesis in the first trimester placental cells *via* increased synthesis of VEGF (Duttaroy and Basak, 2012). Nevertheless, Sun et al., demonstrate that flavonoid fatty acid conjugates show at least comparable, if not higher, anti-angiogenic activity when compared to parent flavonoids (Sun et al., 2017).

In this study, the impact of PZ-DHA on proliferation, migration and tube formation by HUVECs and HMVECs was tested *in vitro*. PZ-DHA-induced inhibitory effects on Akt and small molecular Rho GTPase signaling in HUVECs was tested in the presence or absence of VEGF using western blot analysis. *Ex vivo* anti-angiogenic activity was tested using thoracic aortic sections harvested from male Wistar rats. Finally, the *in vivo* anti-angiogenic activity of systemically administered PZ-DHA was investigated using Balb/c female mice implanted with VEGF- and bFGF-containing Matrigel plugs.

## 6.2 Results

### 6.2.1 PZ-DHA inhibits the metabolic activity of HUVECs and HMVECs

First, the effect of 10 μM – 40 μM PZ-DHA on the metabolic activity of HUVECs and HMVECs was tested using an MTT assay and compared to its parent compounds. Neither PZ nor DHA inhibited the metabolic activity of HUVECs; however, PZ-DHA suppressed the growth of HUVECs at 40 μM, but not at 10 μM- 30 μM (mean % metabolic activity±SEM: 29.0±8.3) ($p$<0.05) (Figure 6.1A). In contrast, PZ-DHA inhibited the metabolic activity of HMVECs in a concentration-dependent manner (10 μM – 40 μM), suggesting that HMVECs are more sensitive to PZ-DHA than HUVECs (mean % metabolic activity±SEM: 10 μM, 83.4±4.4; 20 μM, 69.3±4.4; 30 μM, 47.0±4.1; 40 μM, 33.2±8.2) ($p$<0.05) (Figure 6.1B). PZ did not affect the growth of HMVECs; however, DHA significantly inhibited HMVEC growth at the highest (40 μM) concentration (mean % metabolic activity±SEM: 68.7±8.1) ($p$<0.05) (Figure 6.1A).

### 6.2.2 Sub-cytotoxic concentrations of PZ-DHA inhibit the proliferation of HUVECs and HMVECs

Sub-cytotoxic concentrations of PZ-DHA and its parent compounds for HUVECs and HMVECs were identified using a 7AAD assay. Since 40 μM PZ-DHA inhibited the metabolic activity of both HUVECs and HMVECs by 59.0% and 61.4%, respectively, the viability of endothelial cells was tested using only 10 μM - 30 μM concentrations of the drugs. Drug-induced morphological changes were also observed. Endothelial cells are polygonal in shape. None of the tested concentrations of PZ altered the shape/morphology or number of HUVECs or HMVECs in the cultures. DHA, when used at a high concentration (30 μM), changed the polygonal morphology of HUVECs and prevented the formation of an endothelial cell monolayer (indicated by arrows in Figure 6.2A). At 30 μM concentration, the morphology of HMVECs was not affected by DHA; however, number of HMVECs was reduced. PZ-DHA, at up to 20μM concentration, did not change the morphology of HUVECs; however, HUVEC morphology as well as the cell number was drastically affected by treatment with 30 μM PZ-DHA (indicated by arrows in Figure 6.2A).

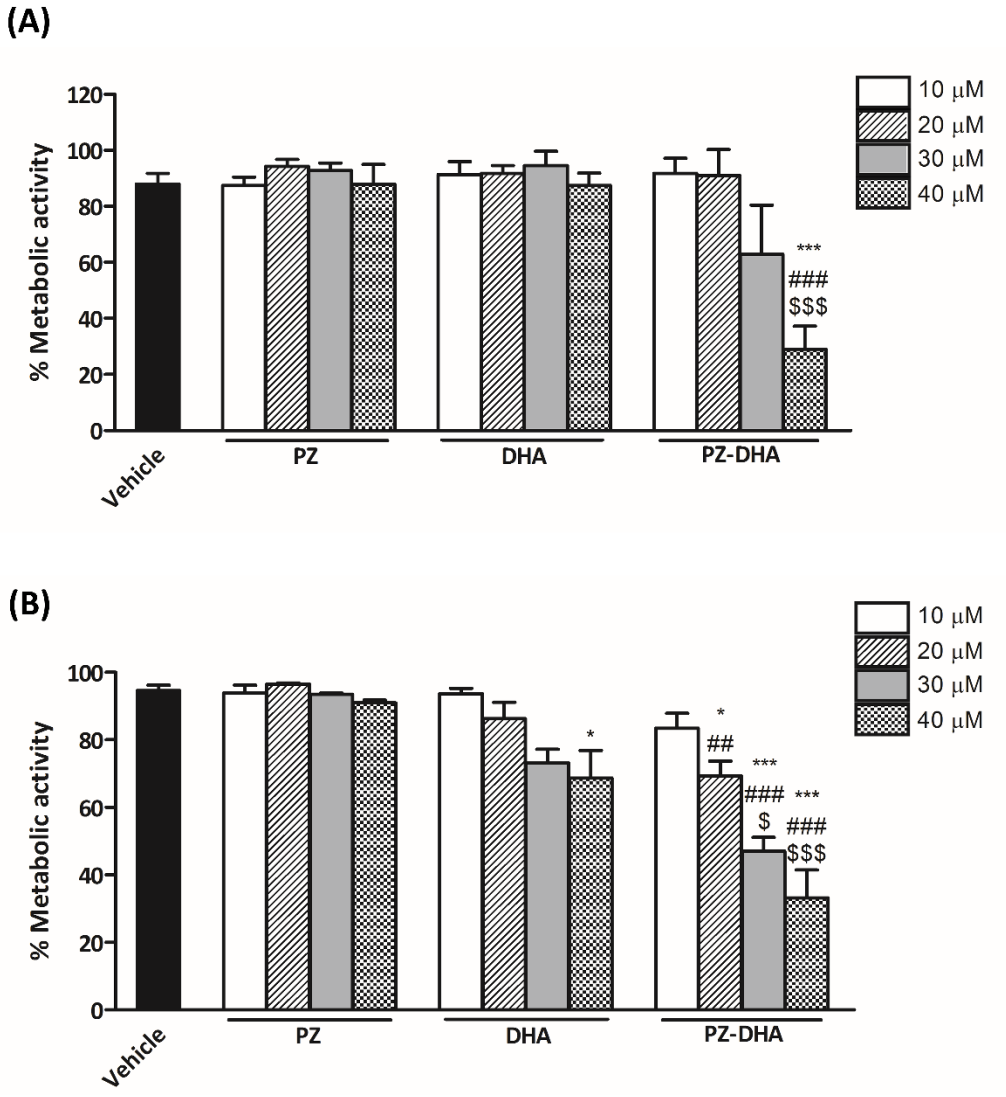


**Figure 6.1. PZ-DHA, at high concentrations, inhibits the metabolic activity of HUVECs and HMVECs *in vitro*.**
**(A)** HUVECs and **(B)** HMVECs were seeded and cultured overnight to promote cell adhesion. Adherent cells were treated with PZ, DHA, PZ-DHA (10 - 40 μM), DMSO vehicle or medium alone and incubated for 72 h at 37°C. At the end of culture, cells were incubated with MTT reagent for 3 h and formazan crystals were collected by centrifugation. Formazan crystals were dissolved in DMSO and absorbance was measured at 570 nm. Data shown are % mean metabolic activity±SEM of three independent experiments. Differences among means of PZ-DHA-treated endothelial cells were compared with respect to vehicle (*), PZ (#) and DHA ($) using ANOVA multiple means comparison method followed by Tukey's post mean comparison test. * and $$p<0.05$, ##$p<0.01$, ***, ### and $$$$p<0.001$.

HMVECs were more sensitive to PZ-DHA at 20 μM, but the polygonal morphology of most of the cells were not altered. In contrast, a high concentration (30 μM) of PZ-DHA altered the morphology of almost all HMVECs and the number of cells in the culture was also reduced (Figure 6.3A). As explained in the section 3.2.1 of chapter 3, a right-ward shift in the 7AAD staining indicates cell death. Neither PZ-DHA nor its parent compounds at 10-30 μM significantly reduced the number of live HUVECs (% mean live PZ-DHA-treated cells ± SEM: 10 μM, 98.9±0.8; 20 μM, 98.9±0.4; 30 μM, 94.1±2.6) ($p$=0.3050) (Figure 6.2B and C). Even though MTT assays suggested a decreased metabolic activity of PZ-DHA-treated HMVECs at 20μM, 7AAD assays did not indicate any cell death. However, a significant reduction in live HMVEC was noted following treatment with 30 μM PZ-DHA, but not PZ or DHA (% mean live cells±SEM: 10 μM, 98.9±0.8; 20 μM, 98.9±0.4; 30 μM, 94.1±2.6) ($p$<0.05) (Figure 6.3B and C). Therefore, further experiments to study the anti-angiogenic activity of PZ-DHA on HUVECs and HMVECs were conducted at 10-20 μM and 10 μM, respectively.

At sub-cytotoxic concentrations, PZ-DHA inhibited the proliferation of both HUVECs and HMVECs, whilst DHA was active only against HUVECs. PZ did not influence the proliferation of HUVECs and HMVECs. Note that the HUVEC proliferation rate was 2.8 times greater than HMVECs. At 10 μM, PZ-DHA decreased HUVEC proliferation by 1.7-fold (mean number of cell divisions±SEM: vehicle, 4.9±0.2; PZ, 4.8±0.3; DHA, 3.1±0.3; PZ-DHA, 2.8±0.2) and the fold decrease was 2.8 when treated with 20 μM (mean number of cell divisions±SEM: vehicle, 4.9±0.2; PZ, 4.4±0.5, DHA, 2.7±0.2, PZ-DHA, 1.7±0.1) ($p$<0.05) (Figure 6.4A and B). PZ-DHA suppressed HMVEC proliferation by 3.4-fold (mean number of cell divisions±SEM: vehicle, 1.7±0.2; PZ, 1.8±0.2; DHA, 1.6±0.2; PZ-DHA, 0.5±0.2) ($p$<0.05) (Figure 6.4C and D). Antiproliferative activity of PZ-DHA for HUVECs was significantly lower than the vehicle control, as well as PZ, but not DHA. Importantly, PZ-DHA almost completely inhibited the proliferation of HMVECs and this activity was significantly lower than the vehicle control, as well as its both parent compounds.

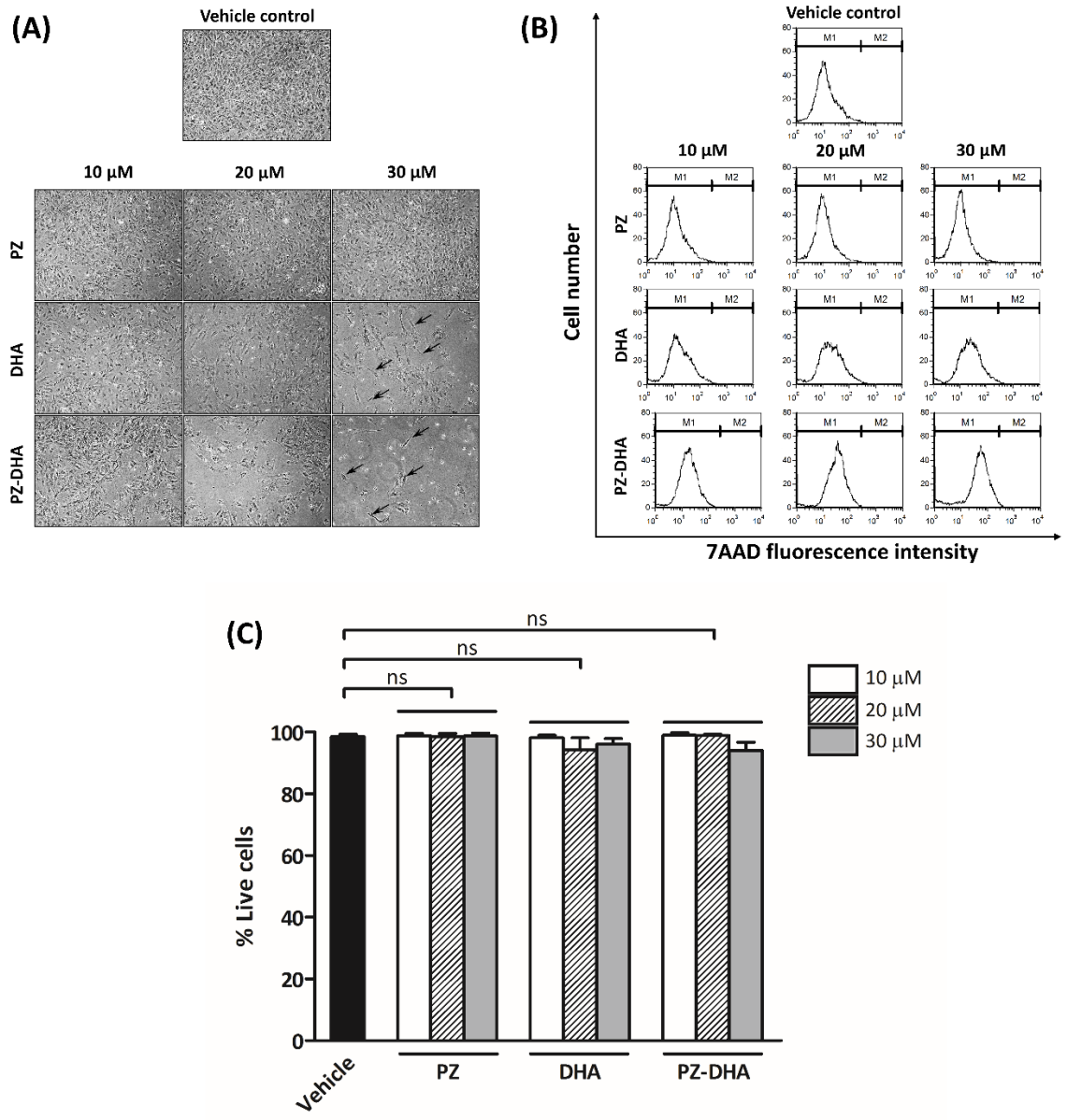


**Figure 6.2. Determination of sub-cytotoxic concentrations of PZ-DHA for HUVECs *in vitro*.**

HUVECs were seeded and treated with 10 µM - 30 µM PZ, DHA, PZ-DHA, vehicle or medium alone and cultured for 72 h at 37°C. **(A)** Cells were photographed using a Nikon eclipse TS 100 phase contrast microscope equipped with Infinity 1 camera at ×200 magnification. Arrows indicate cells that lost the polygonal shape following drug treatment. Cells were then harvested and stained with 7AAD for 5 min at room temperature and the live cell population was identified by reading samples at FL3 detector of the flow cytometer. Data shown are **(B)** representative histograms (M1: live cells, M2: dead cells) and **(C)** mean % live cells±SEM of four experiments conducted independently; ns: not significant.

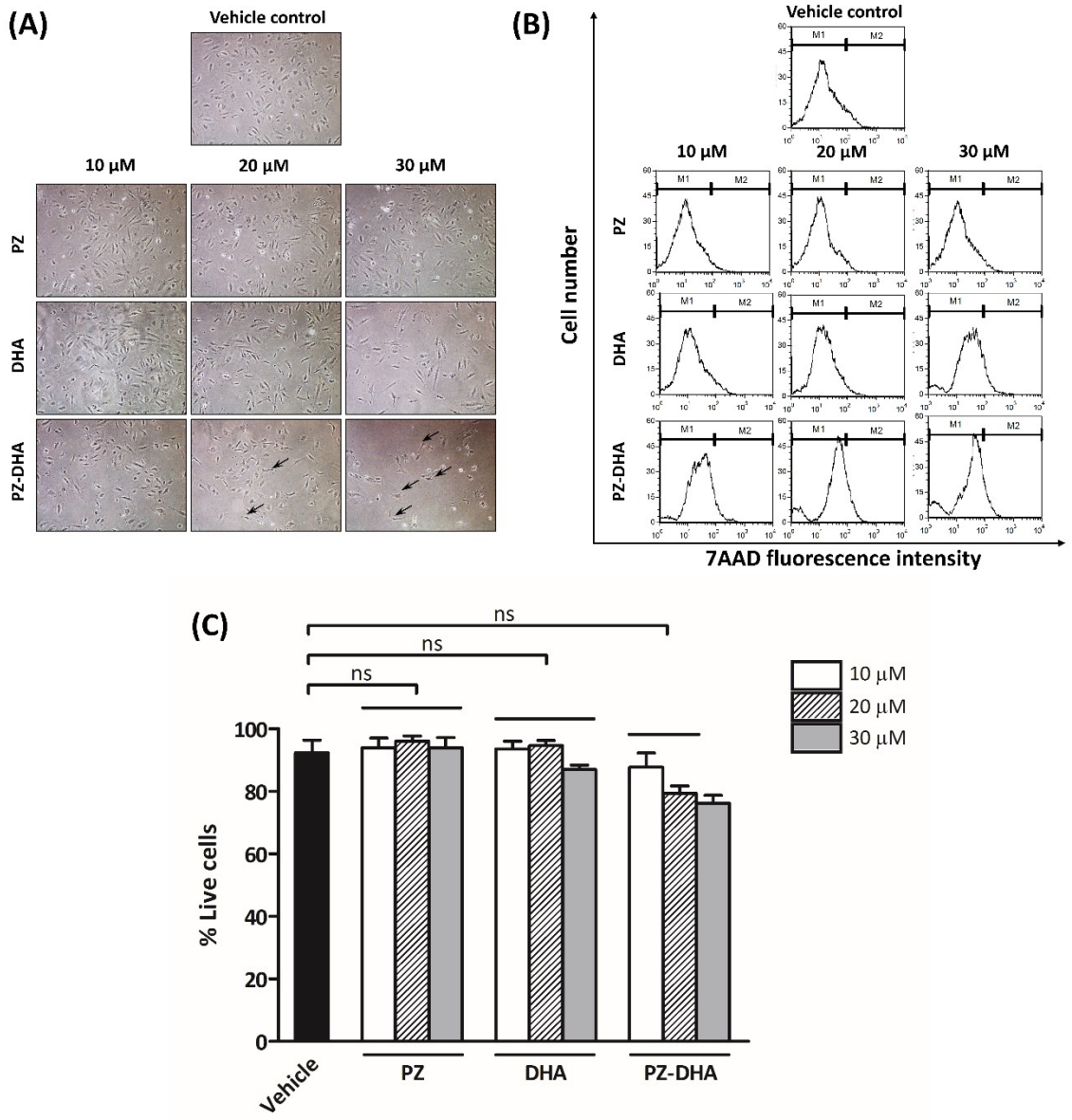


**Figure 6.3. Determination of sub-cytotoxic concentrations of PZ-DHA for HMVECs *in vitro*.**

HMVECs were seeded and treated with 10 µM - 30 µM PZ, DHA, PZ-DHA, vehicle or medium alone and cultured for 72 h at 37°C. **(A)** Cells were photographed using a Nikon eclipse TS 100 phase contrast microscope equipped with Infinity 1 camera at ×200 magnification. Arrows indicate cells that lost the polygonal endothelial cell shape following PZ-DHA treatment. Cells were then harvested and stained with 7AAD for 5 min at room temperature and the live cell population was identified by reading samples at FL3 detector of the flow cytometer. Data shown are **(B)** representative histograms (M1: live cells, M2: dead cells) and **(C)** mean % live cells±SEM of three experiments conducted independently; ns: not significant.

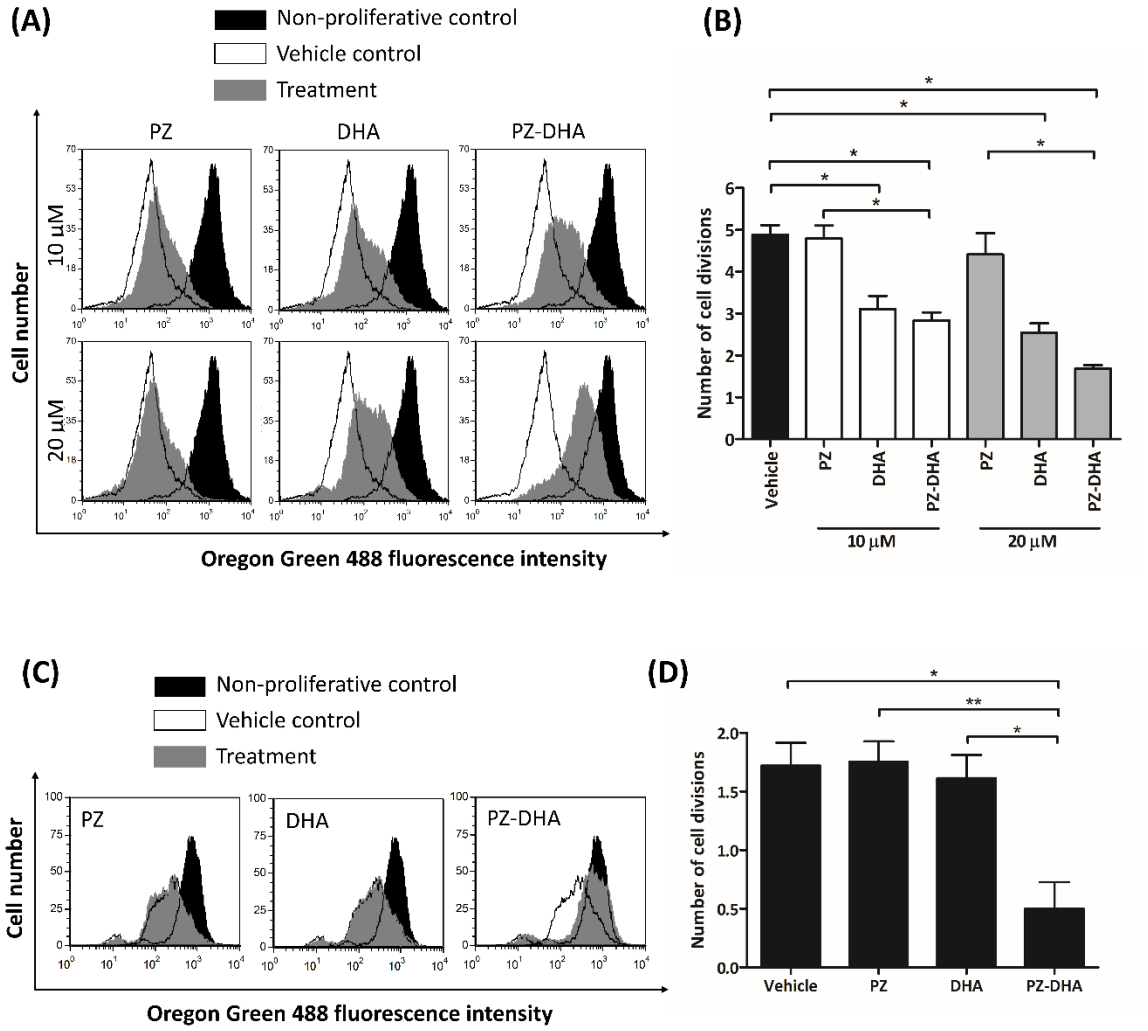


**Figure 6.4. Sub-cytotoxic concentrations of PZ-DHA inhibit the proliferation of HUVECs and HMVECs *in vitro*.**

Endothelial cells were synchronized to $G_0$ phase by culturing cells in serum-free DMEM medium overnight. Synchronized cells were seeded and stained with Oregon Green 488 dye. HUVECs were treated with PZ, DHA, PZ-DHA (10 and 20 µM) or the vehicle and HMVECs were treated with 10 µM drugs or the vehicle and cultured for 72 h at 37°C. At the end of incubation, cells were harvested and analyzed by FL1 detector of the flow cytometer. Data shown are **(A)** representative histograms of HUVECs treated with PZ, DHA or PZ-DHA relative to the vehicle control and non-proliferative control and **(B)** mean number of cell divisions±SEM from three independent experiment. Representative histograms of HMVECs treated with PZ, DHA or PZ-DHA relative to the vehicle control and non-proliferative control and mean number of cell divisions±SEM from three independent experiments are shown in **(C)** and **(D),** respectively. ANOVA multiple mean comparison test was performed and differences among means were compared using Tukey's post mean comparison test; *$p$<0.05, **$p$<0.01.

### 6.2.3 Sub-cytotoxic concentrations of PZ-DHA arrest the replication of HUVECs at $G_0/G_1$ phase

PZ-DHA arrested the HUVEC cell cycle at $G_0/G_1$ while significantly decreasing the number of cells progressing to $G_2$/M phase. PZ-DHA-treated cells accumulated in the $G_0/G_1$ phase, resulting in a 16.6% increase in cell number (mean % number of cells in $G_0/G_1$ phase ± SEM: vehicle, 66.4±3.1; PZ, 67.9±1.8; DHA, 69.1±1.3; PZ-DHA, 83.0±4.8) ($p$<0.05) (Figure 6.5A and B); however, cells in the S phase were not affected (mean % number of cells in S phase±SEM: vehicle, 7.9±0.5; PZ, 7.0±0.9; DHA, 7.6±2.4; PZ-DHA, 7.3±1.7) (Figure 6.5A and B). The significant reduction of number of cells in the $G_2$/M phase suggests that the transition of HUVECs from the S phase to $G_2$ and subsequent progression to the mitotic phase was also inhibited by PZ-DHA (mean % number of cells in $G_2$/M phase±SEM: vehicle, 25.7±2.6; PZ, 25.0±0.5; DHA, 23.2±2.4; PZ-DHA, 9.8±3.4) ($p$<0.05) (Figure 6.5A and B). The effect of PZ-DHA on the expression of cell cycle proteins which regulate the transition of a cell through $G_1$ (cyclin D3 and CDK4) was also tested. PZ-DHA significantly decreased cyclin D3 levels in HUVECs by 27.9% (mean % relative cyclin D3 expression±SEM: vehicle, 103.0±3.0; PZ, 97.9±6.3; DHA, 102.5±2.8; PZ-DHA, 75.1±5.3) ($p$<0.05) (Figure 6.5C). The expression of CDK4 was suppressed by both DHA and PZ-DHA by 47.0% and 72.3%, respectively (mean % relative CDK4 expression±SEM: vehicle, 93.6±6.3; PZ, 75.3±1.6; DHA, 46.6±10.7; PZ-DHA, 21.4±7.4) ($p$<0.05) (Figure 6.5D); however, PZ had no effect on any of the cell cycle regulatory proteins tested.

### 6.2.4 Sub-cytotoxic concentrations of PZ-DHA inhibit Akt signaling in HUVECs

PZ-DHA inhibited the Akt signaling pathway of HUVECs at several levels. At 10 μM, PZ-DHA decreased the phosphorylation of PDK1 at Ser241 in HUVECs (Figure 6.6A). PZ-DHA-induced increase in phosphatase activity was evident by the augmented phosphorylation of PTEN at Ser380 (Figure 6.6B). As a result of the upstream decreased kinase activity and increased phosphatase activity of the pathway, Akt phosphorylation was also inhibited at Ser473 (Figure 6.6C). Activation of two Akt-dependent downstream kinases were also tested. As a result of decreased Akt kinase activity, phosphorylation of mTOR at Ser2448 (Figure 6.6D) and CREB (Figure 6.6E) at Ser133 was also decreased.

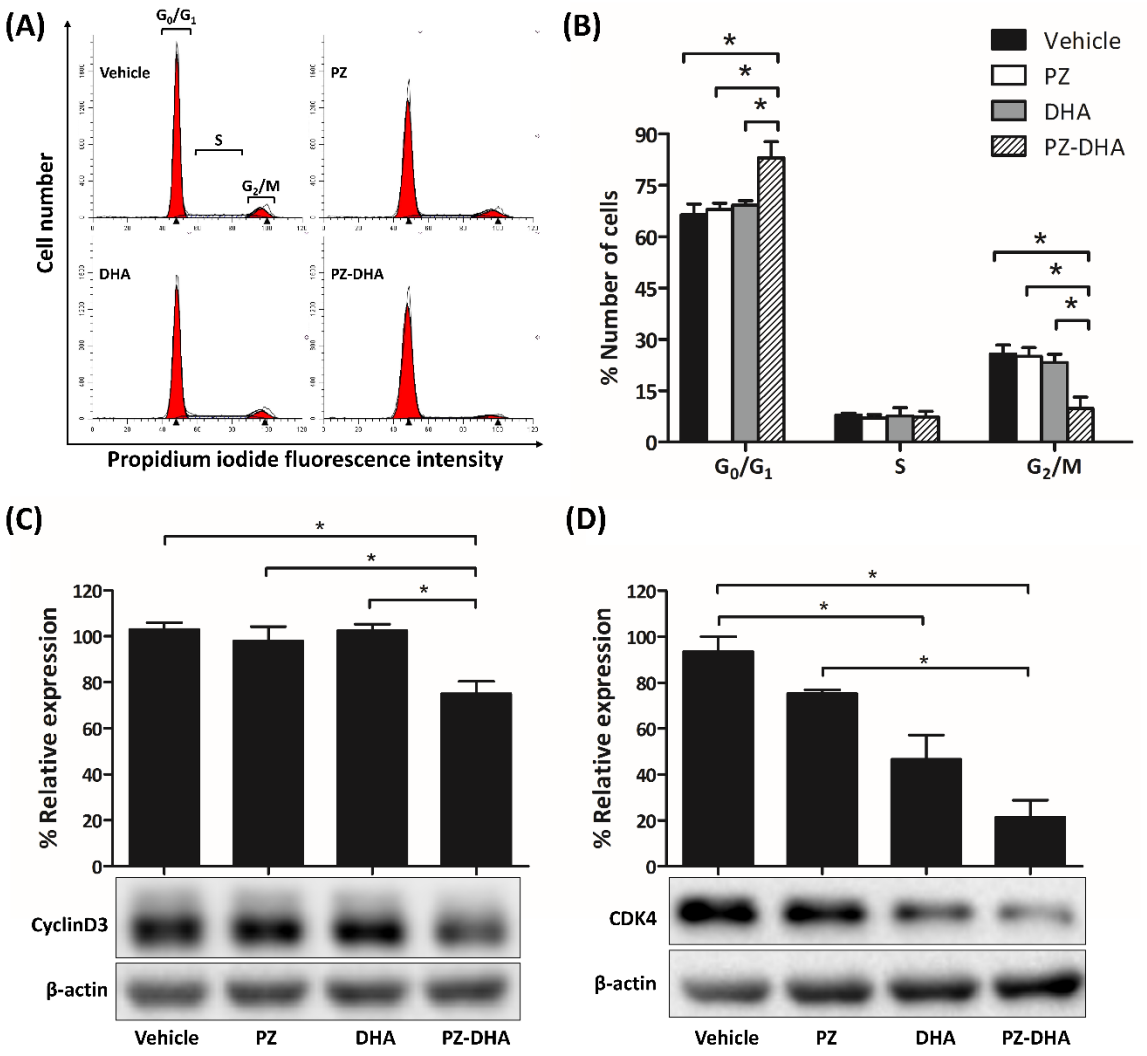


**Figure 6.5. A sub-cytotoxic concentration of PZ-DHA arrests HUVEC replication at $G_0/G_1$ phase.**

HUVECs were synchronized and treated with PZ, DHA, PZ-DHA (10 µM), vehicle or medium alone and cultured for 72 h at 37°C. Cells were harvested and fixed in 70% cold ethanol. Fixed cells were stained with PI in the presence of RNase for analysis by flow cytometry. **(A)** Representative histograms were generated using ModFit software. **(B)** Mean % number±SEM of cells in each phase of the cell cycle was calculated from three independent experiments. HUVECs that were treated with PZ, DHA, PZ-DHA (10 µM), vehicle or medium alone for 72 h were harvested and protein-rich cell lysates were prepared. Relative expression of cyclin D3 and CDK4 were determined using western blot analysis. Data shown are representative blots and mean % relative expression±SEM of **(C)** cyclin D3 and **(D)** CDK4 after three independent experiments. Statistical analysis was performed using one-way ANOVA multiple means comparison method and differences among means were compared using Tukey's post mean comparison method. *$p$<0.05.

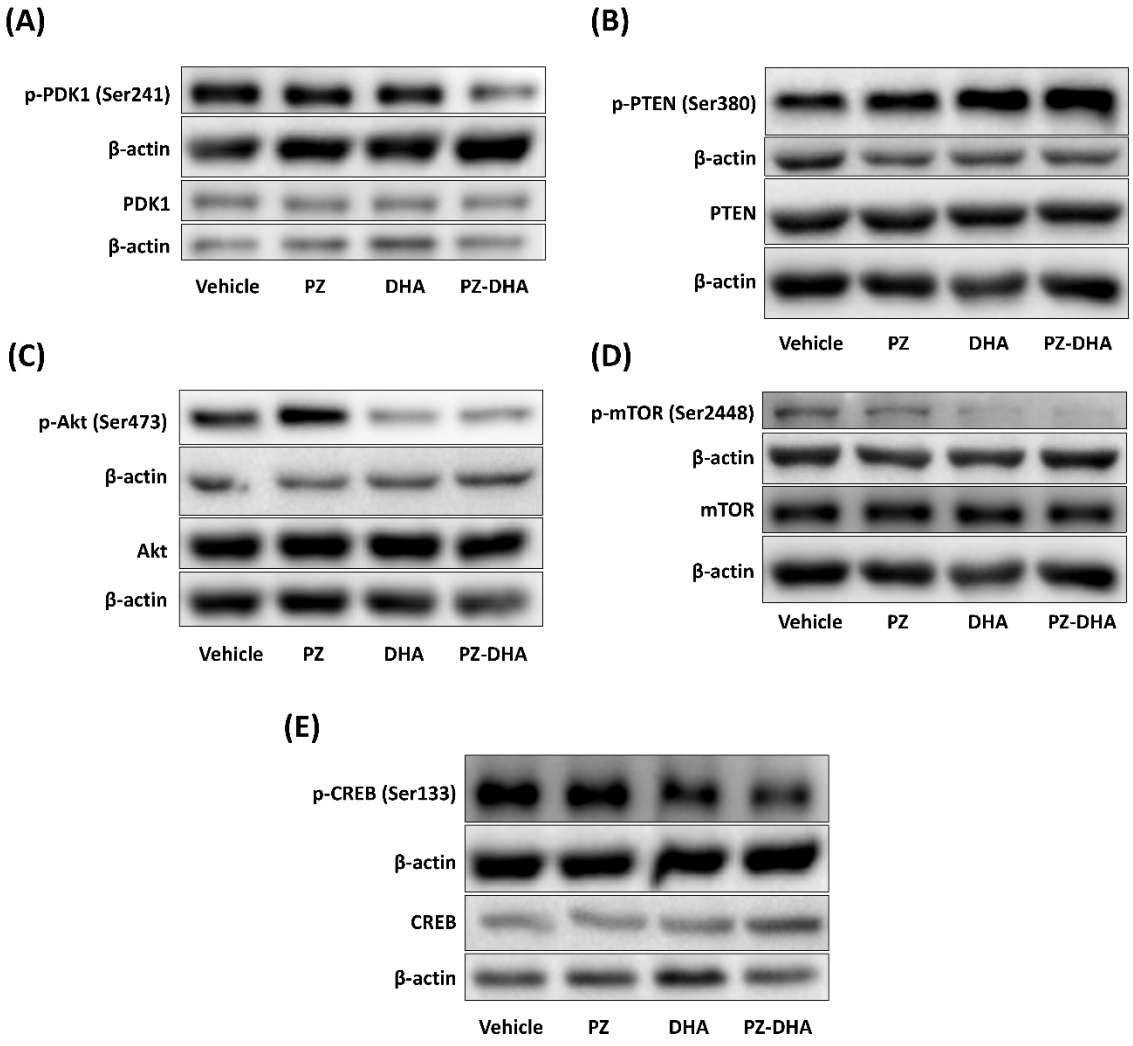


**Figure 6.6. A sub-cytotoxic concentration of PZ-DHA inhibits Akt signaling in HUVECs.**

HUVECs were treated with PZ, DHA, PZ-DHA (10 μM) or vehicle alone and cultured for 72 h. Cells were harvested and protein-rich cell lysates were prepared. Equal amounts of protein (20 μg) were loaded into 10%, 12% or 15% SDS-polyacrylamide gels, as needed, and electrophoresed. Proteins were transferred onto nitrocellulose membranes and blots probed overnight at 4°C with primary antibodies against **(A)** phospho-PDK1 (Ser241)/total-PDK1, **(B)** phospho-PTEN (Ser380)/total-PTEN, **(C)** phospho-Akt (Ser473)/total-Akt, **(D)** phospho-mTOR (Ser2448)/total-mTOR and **(E)** phospho-CREB (Ser133)/total-CREB. Equal protein loading was confirmed by β-actin expression.

### 6.2.5 A sub-cytotoxic concentration of PZ-DHA inhibits the migration of HUVECs

Endothelial cell migration is an essential step of angiogenesis. The effect of PZ-DHA and its parent compounds on the migration of endothelial cells was tested using HUVECs. PZ-DHA significantly reduced the migration of HUVEC by 59.4% in a gap closure assay (mean % migration±SEM: vehicle, 94.9±6.4; PZ, 91.7±6.6; DHA, 57.7±7.5; PZ-DHA, 35.5±7.9) ($p$<0.05) (Figure 6.7A and B). The effect of PZ-DHA on the chemotactic migration of serum starved-HUVEC was then tested using a trans-well cell migration assay. PZ-DHA significantly suppressed the migration of HUVECs by 39.6% and this inhibitory effect was significantly lower than that of its parent compounds (mean % migration±SEM: vehicle, 86.7±7.6; PZ, 70.1±4.0; DHA, 66.2±3.7; P-DHA, 47.2±3.6) ($p$<0.01) (Figure 6.7C and D). The polygonal cellular shape was restored by vehicle-, PZ- and DHA-treated HUVEC following migration; however, the shape of PZ-DHA-treated cells was still distorted after migration (Figure 6.7C).

### 6.2.6 A sub-cytotoxic concentration of PZ-DHA inhibits *in vitro* and *ex vivo* angiogenesis

Before studying the anti-angiogenic activity of PZ-DHA *in vivo*, angiogenesis was modeled and tested *in vitro* and *ex viv*o using human endothelial cells and rat aorta sections, respectively. *In vitro* angiogenesis was scored according to the stage/complexity of the tube formation. PZ-DHA decreased the *in vitro* HUVEC angiogenesis by 6.5-fold (mean angiogenesis score±SEM: vehicle, 4.3±0.7; PZ, 4.0±0.6; DHA, 3.3±0.3; PZ-DHA, 0.7±0.3) ($p$<0.001) (Figure 6.8A and B). PZ-DHA, as well as DHA, significantly attenuated the tube formation by HMVECs by 2.8-fold and 1.8-fold, respectively (mean angiogenesis score±SEM: vehicle, 4.7±0.3; PZ, 3.3±0.3; DHA, 2.6±0.3; PZ-DHA, 1.7±0.3) ($p$<0.01) (Figure 6.8C and D).

PZ-DHA suppressed the sprouting of microvessels from rat aorta endothelium embedded in a Matrigel matrix (Figure 6.9A top panel and B). The statistical significance of the data was not evaluated because the shown data are the mean of two independent experiment; however, a clear reduction in the microvessel sprouting area was observed when the aorta sections were cultured in the presence of PZ-DHA. When the culture period was extended by another three days, endothelial cells that sprouted from the aorta sections

started forming tubules on the Matrigel matrix. However, PZ-DHA-treated cells aligned, but did not differentiate to form tubules (Figure 6.9A bottom panel).

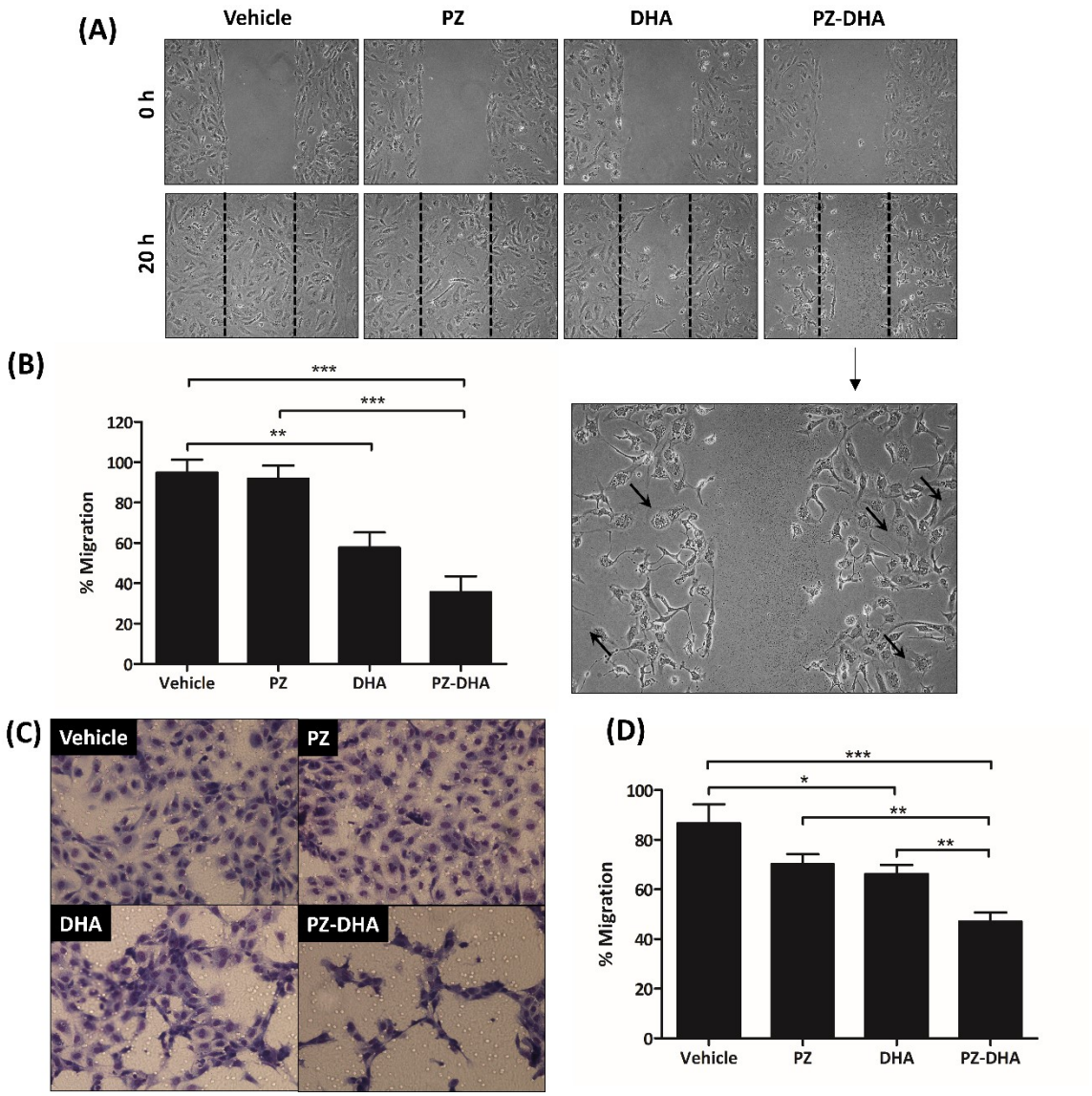


**Figure 6.7. A sub-cytotoxic concentration of PZ-DHA inhibits the migration of HUVECs i*n vitro*.**

HUVECs were seeded in cell culture inserts and incubated with 10 µg/mL mitomycin C for 2 h. Cells were then treated with PZ, DHA, PZ-DHA (10 µM), vehicle or medium alone and cultured for 24 h. Inserts were removed and the number of cells that migrated into the gap was quantified using ImageJ software. Data shown are **(A)** representative pictures of HUVECs in the gap, **(B)** % means migrated HUVECs±SEM from three independent experiments. HUVECs were seeded and treated with PZ, DHA, PZ-DHA (10 µM), vehicle or medium alone and cultured for 24 h. Treated cells were serum-starved and migration toward serum through a porous membrane was determined. Data shown are **(C)** representative pictures of migrated cells and **(D)** mean % migration±SEM of three independent experiments. ANOVA multiple means comparison statistical method was performed and differences among means were compared using Tukey's test; *$p$<0.05, **$p$<0.01, ***$p$<0.001.

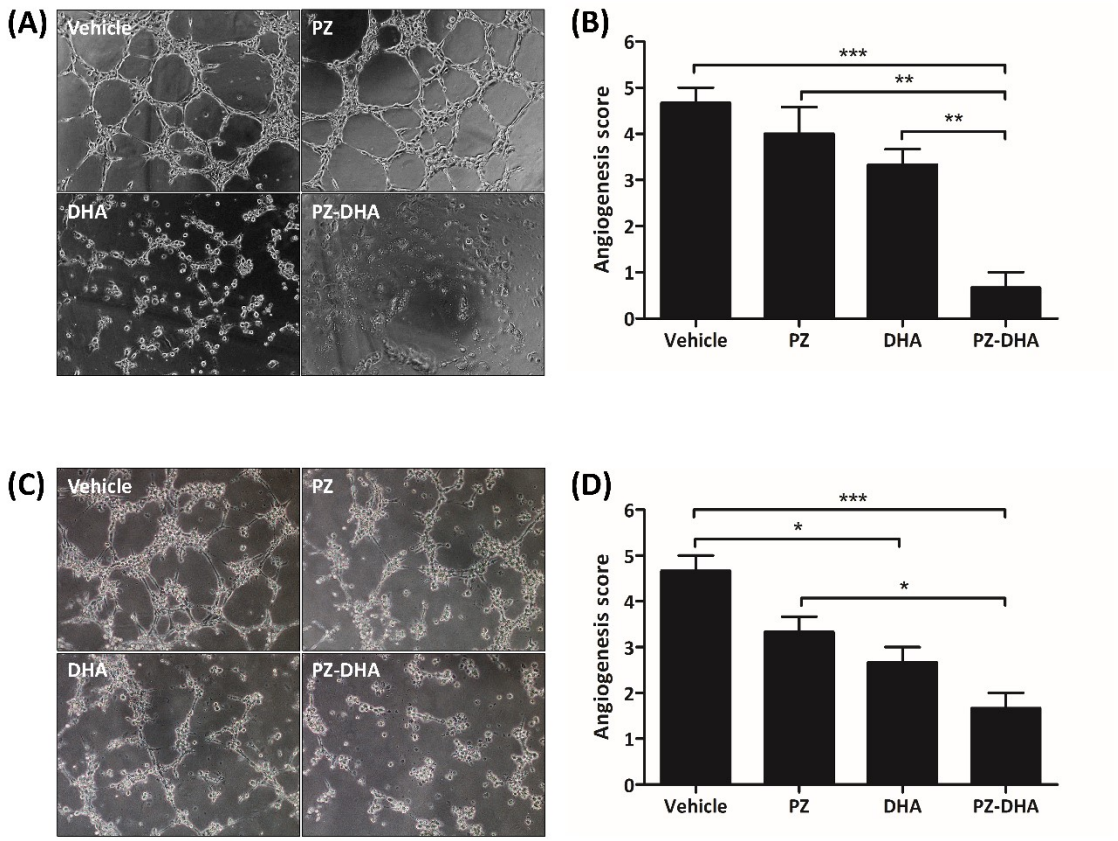


**Figure 6.8. A sub-cytotoxic concentration of PZ-DHA inhibits *in vitro* tube formation by HUVECs and HMVECs.**
HUVECs or HMVECs were treated with PZ, DHA, PZ-DHA (HUVECs: 20 µM and HMVECs: 10 µM), vehicle or medium alone and cultured for 24 h in 6-well plates. Cells were harvested and 7500 cells were resuspended in 50 µL of EGM and seeded onto polymerized ECMatrix. Tube formation by HUVECs and HMVECs was monitored and photographed after 6 h and 4 h, respectively. Images were analyzed and tube formation was quantified according to the complexity of the tube network. Representative images of **(A)** HUVECs and **(C)** HMVECs grown on the ECMatrix and mean angiogenesis score*s*±SEM of **(B)** HUVECs and **(D)** HMVECs calculated from three independent experiments are shown. Statistical analysis was performed using ANOVA multiple means comparison method and differences among means were compared using Tukey's post mean comparison method; **p*<0.05, ***p*<0.01, ****p*<0.001.

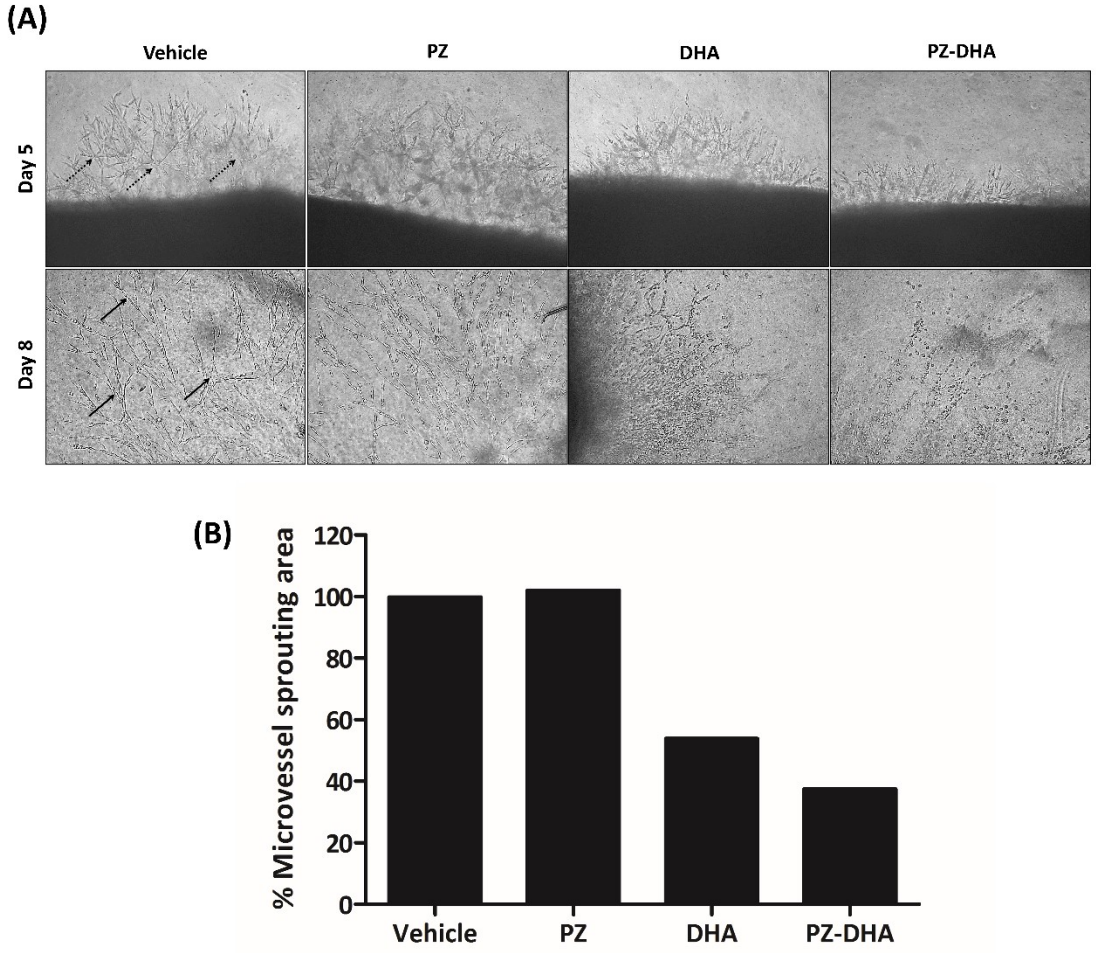


**Figure 6.9. A sub-cytotoxic concentration of PZ-DHA inhibits *ex vivo* angiogenesis from rat aortas.**

Thoracic aortas from adult male Wistar rats were harvested. Inside and outside surface of the aortas were cleaned using sterile saline and aortas were cut into 1×3 mm sections. Sectioned aortas were then placed in a 48-well plate coated with 100 µL growth factor-reduced phenol red-free Matrigel and incubated in a humidified incubator supplied with 5% $CO_2$ at 37°C for 1 h. Aorta sections were covered with another 100 µL Matrigel and incubation was continued for another 30 min. Matrigel was covered with 200 µL EGM-2 supplemented with VEGF and bFGF and the cultures were incubated overnight at 37°C (day 0). On day 1, aorta sections embedded in Matrigel were treated with PZ, DHA, PZ-DHA (20 µM), vehicle, or medium alone and cultured for 8 days. Medium/treatment was replenished on day 4. Development of tubules from aortic endothelium was monitored and photographed on day 5 and 8. **(A)** Sprouting and branching of endothelial cells from the aortas are shown by dashed-arrows in the top panel and tube formation on Matrigel matrix is shown by solid arrows in the bottom panel. **(B)** The surface area covered by sprouted microvessels was calculated using ImageJ software. Data shown are the mean microvessel sprouting area from two independent experiments.

### 6.2.7 Sub-cytotoxic concentrations of PZ-DHA inhibit $VEGF_{165}$-induced small molecular Rho GTPase signaling in HUVECs

Rho GTPase signaling plays a major role in migration, differentiation and subsequent tube formation by endothelial cells (Van Nieuw Amerongen et al., 2003; Yao et al., 2010). Sections 6.2.5 and 6.2.6 showed that PZ-DHA inhibited migration and tube formation by HUVECs grown in a $VEGF_{165}$-supplemented medium. Therefore, the effect of PZ-DHA on basal as well as $VEGF_{165}$-induced small molecular Rho GTPase signaling in HUVECs was studied using western blot analysis. DHA and PZ-DHA, when used at a sub-cytotoxic concentration, significantly inhibited the expression of RhoA in HUVECs by 46.2% and 52.5%, respectively (mean % RhoA expression±SEM: vehicle, 101.0±1.0; 64.8±2.0; DHA, 54.8±12.4; PZ-DHA, 48.5±8.2) ($p$<0.05) (Figure 6.10A). The expression of Cdc42 was also decreased following DHA (by 42.6%) and PZ-DHA (by 46.2%) treatment (mean % Cdc42 expression±SEM: vehicle, 102.2±2.2; 81.2±12.1; DHA, 59.6±0.2; PZ-DHA, 56.0±7.8) ($p$<0.05) (Figure 6.10B); however, the expression of Rac1/2/3 remained unchanged (mean % Rac1/2/3 expression±SEM: vehicle, 95.4±4.6; 103.2±10.5; DHA, 102.0±16.9; PZ-DHA, 95.6±9.7) ($p$= 0.9349) (Figure 6.10C).

$VEGF_{165}$ increased RhoA expression by 30.3%; however, $VEGF_{165}$-induced RhoA over-activation did not reduce in the presence of PZ, DHA, or PZ-DHA (mean % RhoA expression±SEM: vehicle, 93.6±9.0; PZ, 110.9±9.4; DHA, 112.8±6.0; PZ-DHA, 100.2±9.9) ($p$= 0.0576) (Figure 6.10D). A 22.8% increase in Cdc42 expression was noted following $VEGF_{165}$ treatment, which PZ-DHA decreased by 62.1% (mean % Cdc42 expression±SEM: vehicle, 100.4±9.6; PZ, 82.2±14.7; DHA, 61.7±17.0; PZ-DHA, 38.3±3.9) ($p$<0.05) (Figure 6.10E). As a result of $VEGF_{165}$ treatment, Rac1/2/3 expression was also increased by 29.7% and, surprisingly, PZ-DHA significantly decreased $VEGF_{165}$-induced Rac1/2/3 expression by 46.5%, even though basal Rac1/2/3expression was not affected by PZ-DHA (mean % Rac1/2/3 expression±SEM: vehicle, 90.5±10.5; PZ, 71.9±2.5; DHA, 69.8±3.9; PZ-DHA, 43.9±7.7) ($p$<0.05) (Figure 6.10F).

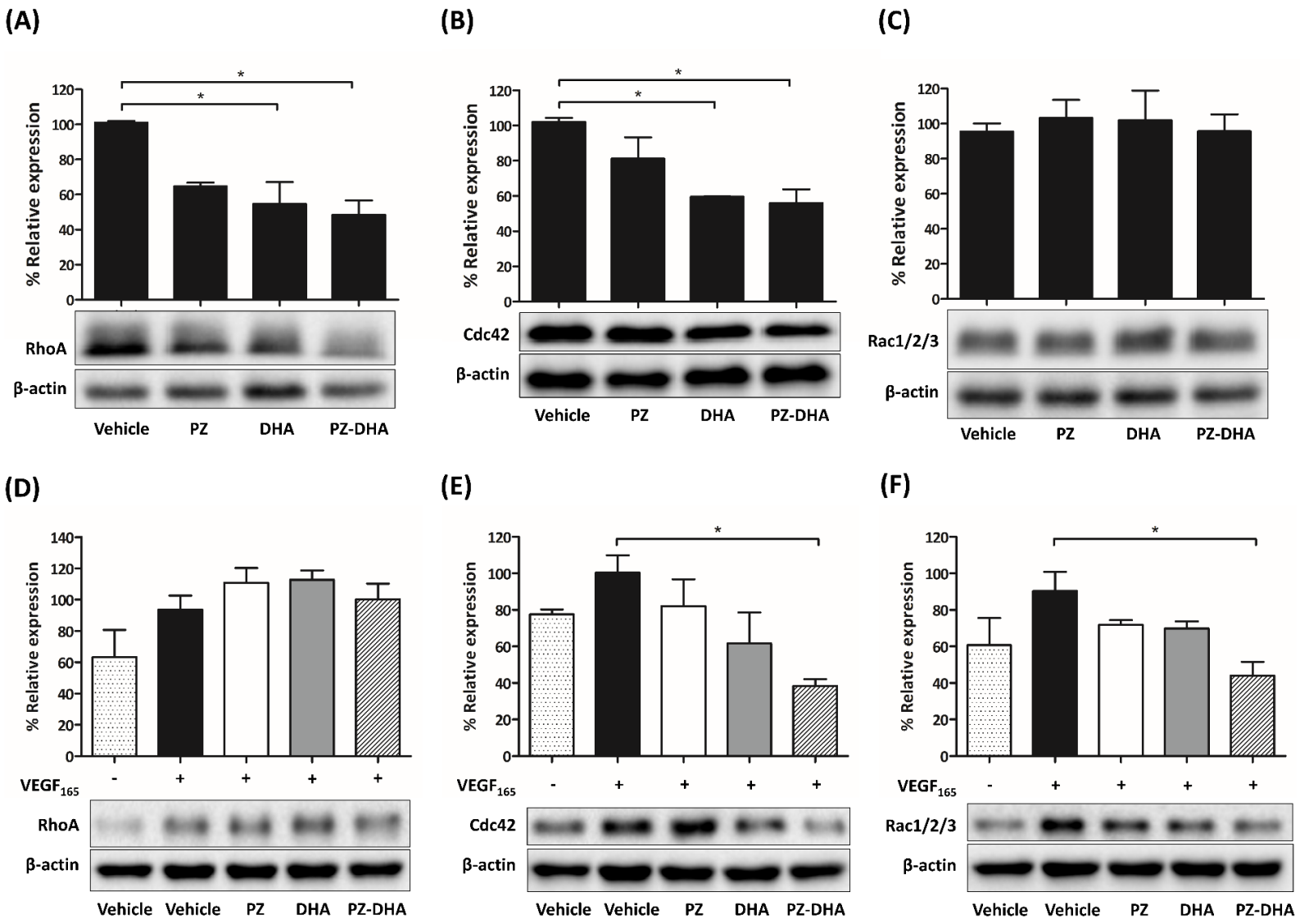
(A)
(B)
(C)
(D)
(E)
(F)
% Relative expression
RhoA
Cdc42
Rac1/2/3
β-actin
VEGF165
Vehicle
PZ
DHA
PZ-DHA
*

**Figure 6.10. A sub-cytotoxic concentration of PZ-DHA inhibits endogenous and VEGF-induced small GTPase signaling in HUVECs.**
The effect of PZ-DHA on endogenous and $VEGF_{165}$-induced expression of small molecular Rho GTPases was determined using western blot analysis. HUVECs were seeded and treated with PZ, DHA, PZ-DHA (10 μM), vehicle or medium alone and cultured in the absence of $VEGF_{165}$ for 72 h. Cells were harvested, lysed and protein concentration in lysates were determined using a Bradford assay and 20 μg of proteins were loaded in to 15% SDS-polyacrylamide gels. Blots were probed with antibodies against **(A)** RhoA, **(B)** Cdc42 and **(C)** Rac1/2/3. Equal protein loading was confirmed by β-actin expression. In a separate experiment, HUVECs that were pre-incubated with/without 10 ng/mL $VEGF_{165}$ were then treated with PZ, DHA, PZ-DHA (10 μM), vehicle or medium alone and cultured in the presence or absence of 5 ng/mL $VEGF_{165}$ for 72 h. Relative expression of $VEGF_{165}$-induced **(D)** RhoA, **(E)** Cdc42 and **(F)** Rac1/2/3 was determined using western blot analysis. Equal protein loading was confirmed by β-actin expression. Data shown are mean % relative expression±SEM from three independent experiments. ANOVA multiple means comparison statistical method was performed and differences among means were compared using Tukey's test; *$p<0.05$.

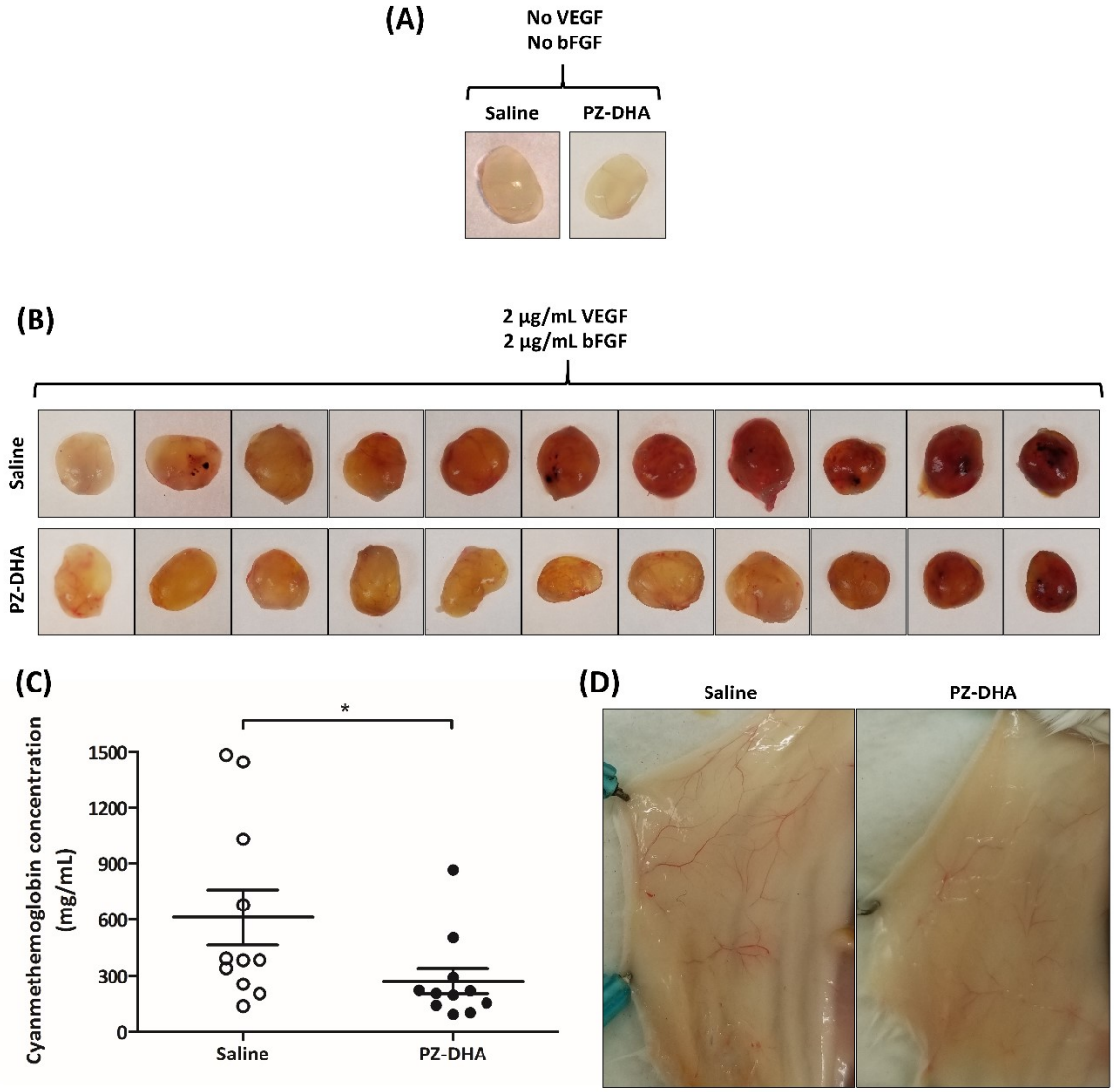


**Figure 6.11. Systemic administration of PZ-DHA suppresses $VEGF_{165}$- and bFGF-induced angiogenesis in Balb/c female mice.**

Phenol red-free Matrigel (300 µL) mixed with/without human $VEGF_{165}$ (2 µg/mL) and bFGF (2 µg/mL) was subcutaneously implanted on both left and right sides along the mid dorsal line of lower posterior area of Balb/c female mice (Day 0). On day 1, mice were randomly assigned into two groups (n=12) and saline or PZ-DHA (100 mg/kg) was administered by intraperitoneal injection. Altogether, 5 doses of saline or PZ-DHA was administered every second day (Day 1, 3, 5, 7 and 9) for 9 days. Mice were euthanized on day 10; Matrigel plugs injected **(A)** without and **(B)** with proangiogenic factors were photographed. **(C)** Matrigel plugs from each mouse were weighed and mean hemoglobin concentration±SEM was determined using cyanmethemoglobin method. Statistical differences between means were compared using Student's t-test; *$p$<0.05. **(D)** Growth of blood vessels on the body wall, toward the Matrigel plugs was also photographed.

### 6.2.8 PZ-DHA inhibits *in vivo* angiogenesis in Balb/c female mice

*In vivo* anti-angiogenic activity of PZ-DHA was investigated using a Matrigel plug assay and Balb/c female mice. VEGF and bFGF induced angiogenesis in Matrigel plugs, which was inhibited by intraperitoneal administration of PZ-DHA (Figure 6.11A and B). PZ-DHA-mediated reduction in blood vessel formation was measured by quantifying hemoglobin concentration in Matrigel plugs. Hemoglobin in Matrigel plugs was converted into a cyanmethemoglobin complex by a reaction with cyanide ions in the Drabkin's reagent. A 2.3-fold reduction in the formation of cyanmethemoglobin complex was noted in Matrigel plugs excised from PZ-DHA-received mice. (mean cyanmethemoglobin concentration (mg/mL)±SEM: saline, 611.9±147.1; PZ-DHA, 270.4±68.6) ($p$<0.05) (Figure 6.11C). Moreover, PZ-DHA-induced reduction in the growth of blood vessels in the body wall (around the Matrigel plugs) was also observed (Figure 6.11D).

## 6.3 Discussion

This chapter is dedicated to investigating the effects of PZ-DHA on different aspects of angiogenesis. The impact of PZ-DHA on endothelial cell proliferation, migration and differentiation in order to form tubules *in vitro* was tested using HUVECs and HMVECs. Thoracic aorta sections harvested from Wistar rats were used to study the *ex vivo* anti-angiogenic activity of PZ-DHA and *in vivo* anti-angiogenic activity was tested using Balb/c mice implanted with Matrigel plugs containing proangiogenic factors.

MTT assays suggested that PZ-DHA suppressed the metabolic activity of HUVECs at 40 μM but not 10 μM - 30 μM. Similarly, 7AAD assays showed that PZ-DHA did not affect HUVEC viability, confirming that PZ-DHA was not toxic to HUVEC at 10 μM - 30 μM (Figure 6.1 and 6.2). In contrast, a concentration-dependent decrease in the metabolic activity of HMVECs was noted in the presence of PZ-DHA (10 μM - 40 μM); however, 7AAD assay confirmed that PZ-DHA was not toxic up to 20 μM concentration, suggesting that the decrease in the metabolic activity may be attributed to a decrease in HMVEC number at 20 μM, and not necessarily to cell death (Figure 6.3). PZ-DHA attenuated the proliferation of HUVECs and HMVECs at sub-cytotoxic concentrations (Figure 6.4) and inhibited the S phase entry of HUVECs as a result of $G_0/G_1$ cell cycle

arrest. PZ-DHA inhibited the expression of cyclin D3 and CDK4, suggesting a decreased formation of cyclin D/CDK4 complex which was consistent with the increased accumulation of HUVECs in $G_0/G_1$ phase (Figure 6.5). DHA downregulated the expression of CDK4 but not the expression of Cyclin D3 or the number of HUVECs passing the G1 checkpoint to enter the S phase. In contrast, Kim et al., 2005 showed that DHA induces $G_0/G_1$ cell cycle arrest, as well as an increase in the sub-$G_1$ peak that suggests an apoptotic effect on proliferating HUVECs (Kim et al., 2005). My findings did not agree with this study, possibly because the study by Kim and colleagues used 40 μM DHA concentration and 24 h post treatment whereas my research was conducted using 10 μM - 20 μM DHA at a 72h time point. Kim et al. (2005) also suggest an increased incorporation of Annexin-V-FITC/PI into HUVEC when treated with DHA, suggesting that their treatment was not sub-cytotoxic. An interplay of cell cycle regulators and pro-apoptotic factors determines the fate of a cell during stress conditions (Pietenpol and Stewart, 2002; Pucci et al., 2000). Therefore, it is possible that the activation of p53 and apoptotic signals played a partial role through the p53-p21 axis in the $G_0/G_1$ cell cycle arrest reported by Kim et al. (2005).

Phosphorylation of Akt affects multiple substrates which lead to cell proliferation (cell cycle regulators), migration through actin reorganization (small molecular RhoGTPases) and angiogenesis in endothelial cells (Ma et al., 2009; Somanath et al., 2006; Yao et al., 2010). Flavonoid-induced inhibitory effects on Akt signaling in endothelial cells and its connection to angiogenesis and cancer progression has been demonstrated by many studies (Fang et al., 2005; Huang et al., 2017; Kim, 2017; Mirossay et al., 2018; Mojzis et al., 2008; Ohga et al., 2009). Effects of DHA and other ω-3 fatty acids on Akt signaling in endothelial cells have been shown in relation to cardiovascular effects (Jump et al., 2012; Yamagata, 2017); however, little is known in relation to cancer progression. To the best of my knowledge, the effects of flavonoid fatty acid derivatives on Akt signaling in endothelial cells have not yet been reported. PZ-DHA inhibited the phosphorylation of PDK1 at Ser241 and increased the phosphatase activity of PTEN by increasing its phosphorylation at Ser380. This upstream negative regulation resulted in the decreased phosphorylation of Akt at Ser473. PZ-DHA also downregulated the phosphorylation of mTOR, which is a Akt downstream effector, suggesting that PZ-DHA-induced anti-

proliferative effects may be regulated through Akt/mTOR signaling. Furthermore, PZ-DHA also inhibited the phosphorylation of CREB at Ser133, suggesting a potential reduction of phosphorylated-CREB nuclear translocation and subsequent activation of VEGF-mediated HUVEC proliferation, migration and tube formation (Figure 6.6).

PZ-DHA-induced anti-migratory effects were shown using gap closure and trans-well cell migration assays (Figure 6.7). Migration assays of HUVECs used 10 μM PZ-DHA, which also significantly inhibited HUVEC proliferation. However, the cell migration in gap closure assay was not impacted by reduced HUVEC proliferation since this was arrested by mitomycin C pre-treatment. It is also highly unlikely that PZ-DHA-induced antiproliferative effects altered HUVEC migration in trans-well cell migration assay because PZ-DHA treatment was limited to 24 h. PZ-DHA inhibited the migration of HUVECs and also inhibited the expression of RhoA and Cdc42, but not Rac1/2/3, suggesting that PZ-DHA inhibited filopodia-driven migration of HUVECs but not lamellipodia formation. This is consistent with the presence of abundant lamellipodia (indicated by arrows in Figure 6.7), but not many filopodia in PZ-DHA-treated HUVECs that migrated on a gelatin-coated surface.

The role of small molecular Rho GTPases in angiogenesis have been studied extensively (Bryan and D'Amore, 2007; Fryer and Field, 2005; van der Meel et al., 2011; Van Nieuw Amerongen et al., 2003). RhoA, Cdc42 and Rac1/2/3 play distinct roles in many steps of angiogenesis such as the integrity of the endothelial cell barrier, basement membrane degradation, endothelial cell proliferation and migration, morphogenesis and capillary formation (van der Meel et al., 2011). Endothelial cell proliferation and cell assembly is regulated by well known cell survival and proliferation pathways such as Akt and MAPK (Gerber et al., 1998; Liu et al., 2006; Wang et al., 2015). Cross-talk of these pathways with each other and other signaling cascades such as Rho GTPase and MMP signaling have been shown in relation to the regulation of angiogenesis at various steps (Boyd et al., 2005; Dimmeler et al., 2000; Mavria et al., 2005). In addition, Ras and Rho family GTPase signaling is also coordinated by divergent and convergent regulatory mechanisms during cell cycle regulation (Bar-Sagi and Hall, 2000). Transition of a cell through $G_1$ phase is mainly regulated by the complexes of D-type cyclins with CDK4 or CDK6 (Dong et al., 2018); these complexes then inactivate Rb by phosphorylation at

serine sites (Ser608, 612, 788, 795) (Rubin, 2013; Weinberg, 1995). Phosphorylation of Rb releases the transcription factor E2F and activates S phase entry of cells (Chellappan et al., 1991; Dimova and Dyson, 2005; Harbour and Dean, 2000). RAS family proteins also play a role in the $G_1$/S cell cycle progression by relieving cells from the inhibitory effects of Rb (Coleman and Olson, 2004; Mittnacht et al., 1997; Peeper et al., 1997). HUVECs used in my cell cycle analysis experiments were serum-starved with the aim of synchronizing them to $G_0$ phase prior to PZ-DHA treatment. A low phosphorylation status of Rb is maintained normally in quiescent cells; therefore, cells that lack Rb activity no longer depend upon RAS-induced Rb inactivation (Coleman and Olson, 2004; Lin et al., 2014). However, Pillai et al. (2010) report that a significant amount of Rb is found in serum starved-HUVECs, suggesting potential RAS activity during $G_1$/S transition (Pillai et al., 2010). Therefore, it is possible that PZ-DHA-induced $G_0/G_1$ arrest of HUVECs may be exerted through inhibition of RAS activity; however, additional work is required to confirm this hypothesis.

Rho, another GTPase family protein, is also involved in the regulation of cell cycle, specially $G_1$/S transition (David et al., 2012). Furthermore, accumulation of $p21^{WAF1/CIP1}$ negatively regulates the $G_1$/S transition by inhibiting CDK activity (Niculescu et al., 1998). Hsu and colleagues suggest an inverse correlation between RhoA and the transcription of $p21^{WAF1/CIP1}$ in HUVECs and mouse cerebral vascular endothelial cells (Hsu et al., 2014). Inhibition of RAS-related Rho expression blocks entry of cells into the S phase through the activation of $p21^{WAF1/CIP1}$ by constitutively expressed RAS, suggesting that Rho and $p21^{WAF1/CIP1}$ are inversely related during cell cycle regulation (Olson et al., 1998). Two other Rho family small molecules, Rac1 and Cdc42, rapidly increase the ubiquitin-independent proteasome-mediated degradation of $p21^{WAF1/CIP1}$ when HUVECs are attached to ECM proteins (Bao et al., 2002). PZ-DHA inhibited the endogenous expression of both RhoA and Cdc42. Additionally, PZ-DHA also attenuated $VEGF_{165}$-induced Cdc42 and Rac1/2/3 expression (Figure 6.10). Taken together, it is apparent that PZ-DHA-induced anti-proliferative activity was exerted through the inhibition of cell cycle regulatory proteins, as well as small molecular Rho GTPase molecules. It is widely accepted that Rho GTPase signaling regulates endothelial cell rearrangement and organization during angiogenesis (Fryer and Field, 2005; Van Nieuw

Amerongen et al., 2003; Soga et al., 2001). Lumen formation during angiogenesis requires early cytoskeletal remodelling and lateral cell–cell contacts, mediated through the Rac1 guanine nucleotide exchange factor DOCK4. $VEGF_{165}$-dependent Rac activation *via* DOCK4 is also necessary for Cdc42 activation and filopodia formation (Abraham et al., 2015). $VEGF_{165}$-simulated RhoA, Cdc42 and Rac1/2/3 expression was noted in HUVECs in the current project, and PZ-DHA down-regulated Cdc42 and Rac1/2/3 but not RhoA (Figure 6.10). However, PZ-DHA significantly decreased tube formation by HUVECs and HMVECs *in vitro*, as well as $VEGF_{165}$-induced sprouting of tubes from rat aortic sections *ex vivo*. This implies that PZ-DHA-induced anti-angiogenic activity was not necessarily mediated through RhoA-dependent mechanisms, but possibly through inhibition of $VEGF_{165}$-stimulated Cdc42 and Rac 1/2/3.

Lastly, anti-angiogenic activity of PZ-DHA was evaluated *in vivo* using the Matrigel plug assay of Balb/c mice. Flavonoids such as quercetin (Pratheeshkumar et al., 2012), apigenin (Bassino et al., 2016) and EGCG (Moyle et al., 2015) demonstrate anti-angiogenic activities through their inhibition of Akt phosphorylation, HIF signaling and expression of cell-cell adhesion molecules. However, some flavonoids such as visnadin, hesperidin and baicalin exert pro-angiogenic activities on microvascular cells by increasing their proliferation, survival and tubulogenesis (Bassino et al., 2016). Therefore, to confirm that PZ-DHA did not have proangiogenic activity *in vivo*, two mice were subcutaneously implanted with pro-angiogenic factor-reduced Matrigel plugs and treated with saline or PZ-DHA by intraperitoneal injection. No blood vessel growth was detected in Matrigel plugs placed in the PZ-DHA-treated mouse or saline-treated mouse, suggesting that PZ-DHA did not promote the synthesis of endogenous pro-angiogenic factors and/or did not exert direct pro-angiogenic activity. PZ-DHA attenuated VEGF- and bFGF-induced angiogenesis *in vivo*, as indicated by significantly decreased hemoglobin content in Matrigel plugs (Figure 6.11). Vessel formation in Matrigel plugs can be used to quantify angiogenesis (Tahergorabi and Khazaei, 2012). Taken together, PZ-DHA-induced *in vitro*, *ex vivo* and *in vivo* anti-angiogenic activity suggests this effect inhibited the hematogenic spread of mammary carcinoma cells, thereby contributing to the anti-metastatic activity of PZ-DHA reported in the chapter 5. This chapter concludes all the data gathered to evaluate the anti-metastatic activity of PZ-DHA during the

project; research limitations and suggested improvements to experiments will be discussed in chapter 7.

# CHAPTER 7 : DISCUSSION

## 7.1 Summary of the major findings of the thesis research

### 7.1.1 Conjugation of DHA to PZ increases the cellular uptake of PZ and stabilization of DHA

PZ-DHA is a novel polyphenol-fatty acid derivative that combines two dietary biomolecules through an ester linkage. The regioselective reaction between the two molecules was catalyzed by CA-LB (Ziaullah and Rupasinghe, 2016; Ziaullah et al., 2013). The goal behind the esterification was to increase the pharmacological activities of both compounds by increasing the cellular intake of PZ and the stability of DHA in a biological system. Cellular uptake of flavonoids has been extensively studied using intestinal epithelial cells such as Caco-2 monocultures and/or Caco-2 co-cultures with HT-29 and TC-7, a clone isolated from late passage of Caco-2 cells which are characterised by higher expression of the glucose transporters (SGLT and GLUT) (Chabane et al., 2009; Jailani and Williamson, 2014; Qiu et al., 2012; Soler et al., 2010). A few studies have also been conducted using liver cells (Wong et al., 2012), kidney cells (Glaeser et al., 2014), endothelial cells (Faria et al., 2010), neuroblastoma cells (Bandaruk et al., 2014), and ovarian cancer cells (Walgren et al., 2000). Most of these cellular uptake assays have been conducted using green tea catechins, quercetin, and quercetin metabolites. Schramm and co-workers report a special flavonoid transport system in bovine and human aortic endothelial cells that mediates rapid uptake of flavonoids (Schramm et al., 1999). García-Villalba et al. (2012) report that the cellular uptake of luteolin (4 hydroxyl groups) is significantly greater than apigenin (3 hydroxyl groups) by JIMT-1 human breast cancer cells and suggest that the % cellular uptake is proportional to the degree of hydroxylation/hydrophilicity of the flavonoid. However, this argument is flawed since the passive diffusion of molecules through the cell membrane occurs through the dissolution in the lipid bi-layer (Grime et al., 2008). In contrast, Grootaert et al. (2016) show that flavonoid aglycones (quercetin and hesperetin) are absorbed better than flavonoid glucosides (rutin and hesperidin) by Caco-2 cells, suggesting that increased hydrophilicity is inversely proportional to the cellular uptake of a flavonoid. This idea is further supported by the necessity for LPH-mediated hydrolysis

of quercetin-3-glucoside to promote intestinal uptake in rats (García-Villalba et al., 2012). This proposed requirement also explains the extremely low uptake of PZ (phloretin-2'-β-D-glucopyranoside) by all cell lines tested in the current thesis research. The cellular uptake of flavonoids and their metabolites has been reported extensively (Spencer et al., 2004). Enzyme-catalyzed acylation has been used as a method of improving the bioavailability of flavonoids (Chebil et al., 2007; Thilakarathna and Rupasinghe, 2013; Viskupič Ová et al., 2009); however, to the best of my knowledge, the validity of this approach has not yet been shown using cultured cells *in vitro*. Nevertheless, the conjugation of DHA with PZ through an esterification reaction was predicted to improve the cellular uptake of PZ by cultured epithelial cells. Using cultured epithelial cells and LC/MS methods, for the first time, my research proves that the esterification of flavonoids with fatty acids improves the cellular uptake of flavonoids. Furthermore, my research showed that the stability of DHA was also enhanced when conjugated to PZ. Taken together, my findings indicate that through these two mechanisms, the intracellular concentration of PZ and DHA was increased by combining them into a single chemical entity.

### 7.1.2 Pharmacokinetics of PZ-DHA

Another objective of this study was to use a mouse model to establish the pharmacokinetic parameters of PZ-DHA. The pharmacokinetics of flavonoids is a complicated area of study. In plants, flavonoids exist as glucosides, except for catechins, and therefore, it is debatable whether flavonoids are better absorbed as aglycones or glucosides. In any case, intestinal absorption of ingested flavonoids is low. When PZ-DHA was administered by intraperitoneal injection, the highest serum concentration reached was 24.4 μM at the 68$^{th}$ minute post administration. PZ-DHA was eliminated from serum at a rate of 0.011 μM/min rate. The biological half-life of PZ-DHA was determined to be 27.3 min. Total PZ-DHA exposure, calculated in terms of the area under the curve of drug concentration vs time curve, was 2168.4 μmol.min/L. It is possible that a fraction of PZ-DHA absorbed into the systemic circulation may also exist in a serum protein-bound form. In general, flavonoids show high affinity for plasma proteins, as well as high distribution into fat tissue (Bolli et al., 2010; Dangles et al., 2001; Zhang et al., 2017). Boulton et al. (1998) showed that 99.1% of quercetin is bound to human plasma

proteins, leaving only 0.9% of quercetin freely available in the plasma. Another study shows that the binding of four flavonoids (orientin, vitexin, cynaroside and quercetin) to plasma proteins ranged from 74-89% (Huang et al., 2013). Flavonoids accumulate in the liver, lungs and kidneys following parenteral or oral administration (Hung et al., 2018; Walle et al., 2007). In my study, PZ-DHA was found in the liver, lungs, kidneys, spleen and brain, suggesting that PZ-DHA was readily distributed throughout the body. Interestingly, the presence of detectable amounts of PZ-DHA in the brain indicate a capacity to cross the BBB, which opens up the possibility of a therapeutic effect on brain tumors. Substances that are administered by intraperitoneal injection are mainly absorbed by the superior and inferior mesenteric veins, which drain into the portal vein (Lukas et al., 1971; Turner et al., 2011). Therefore, following intraperitoneal administration, PZ-DHA must pass through the liver before entering the systemic circulation and, as a result, may undergo hepatic metabolism to generate phase II metabolites, which would also affect the availability of intact PZ-DHA in blood. This was evident by the presence of the PZ-DHA metabolite 4,4',6'-tri-*O*-methyl-phloridzin docosahexaenoate in the liver, kidneys and lungs within 30 min of intraperitoneal administration of PZ-DHA. Two additional conjugation reactions of PZ-DHA occur in the liver; glucuronidation and sulphation. Phloridzin docosahexaenoate-4,4'-di-*O*-sulphide was detected in the liver; however, phloridzin docosahexaenoate-4-*O*-glucuronide and phloridzin docosahexaenoate-4'-*O*-glucuronide were detected only in *in vitro* experiments, suggesting that *in vivo* of these compounds are produced at levels too low to meet the minimum limit for detection or are rapidly degraded in mice. The presence of PZ-DHA and 4,4',6'-tri-*O*-methyl-phloridzin docosahexaenoate in kidneys implies the renal excretion of PZ-DHA as the parent drug and the methylated form.

### 7.1.3 Scheme of ADME of PZ-DHA

The ADME of PZ-DHA following intraperitoneal administration is outlined in Figure 7.1. *Absorption of PZ-DHA*: Following intraperitoneal administration, PZ-DHA is distributed in the peritoneal cavity of Balb/c female mice and readily absorbed by the veins of the mesentery and transported into the liver *via* the superior mesenteric vein and the inferior mesenteric vein. *Distribution of PZ-DHA*: Superior and inferior mesenteric veins (together with the splenic vein) converge, forming the portal vein through which

PZ-DHA in mesenteric vein blood drains into the liver. Then PZ-DHA in the liver is carried to the right atrium of the heart *via* the inferior vena cava and returned to the heart through the route of right atrium of the heart→ right ventricle of the heart→ pulmonary artery→ lungs→ pulmonary veins→ left atrium of the heart. PZ-DHA-containing oxygenated blood then enters the aorta and is pumped throughout the body. Blood vessels supplying the brain originate at the arch of the aorta; hence, PZ-DHA is distributed to the brain *via* left and right carotid arteries. After crossing the BBB, PZ-DHA enters and accumulates in the brain. PZ-DHA is distributed to the lungs *via* bronchial arteries branched from the descending aorta. PZ-DHA is returned to liver *via* hepatic artery branched from descending aorta. The spleen receives PZ-DHA *via* the splenic artery. Some PZ-DHA accumulates in the spleen and some goes to the liver *via* splenic vein. PZ-DHA is distributed to the kidneys *via* renal arteries and accumulates. *Metabolism of PZ-DHA*: PZ-DHA undergoes phase II metabolism in the liver. Methylation of PZ-DHA is catalyzed by methyltransferases to produce 4,4',6'-tri-*O*-methyl-phloridzin docosahexaenoate. Glucuronidation of PZ-DHA is catalyzed by UDP-glucuronosyltransferase to produce phloridzin docosahexaenoate-4-*O*-glucuronide and phloridzin docosahexaenoate-4'-*O*-glucuronide. PZ-DHA is sulphated to generate phloridzin docosahexaenoate-4,4'-di-*O*-sulphide, a conversion that is catalyzed by sulphotransferases. Metabolites may also follow the above-mentioned distribution patterns. PZ-DHA and its metabolites may also enter into bile and circulate through the entero-hepatic circulation; however, this step was not confirmed in the current study. *Excretion of PZ-DHA*: PZ-DHA is excreted *via* the kidneys in its intact form as well as in its methylated form.

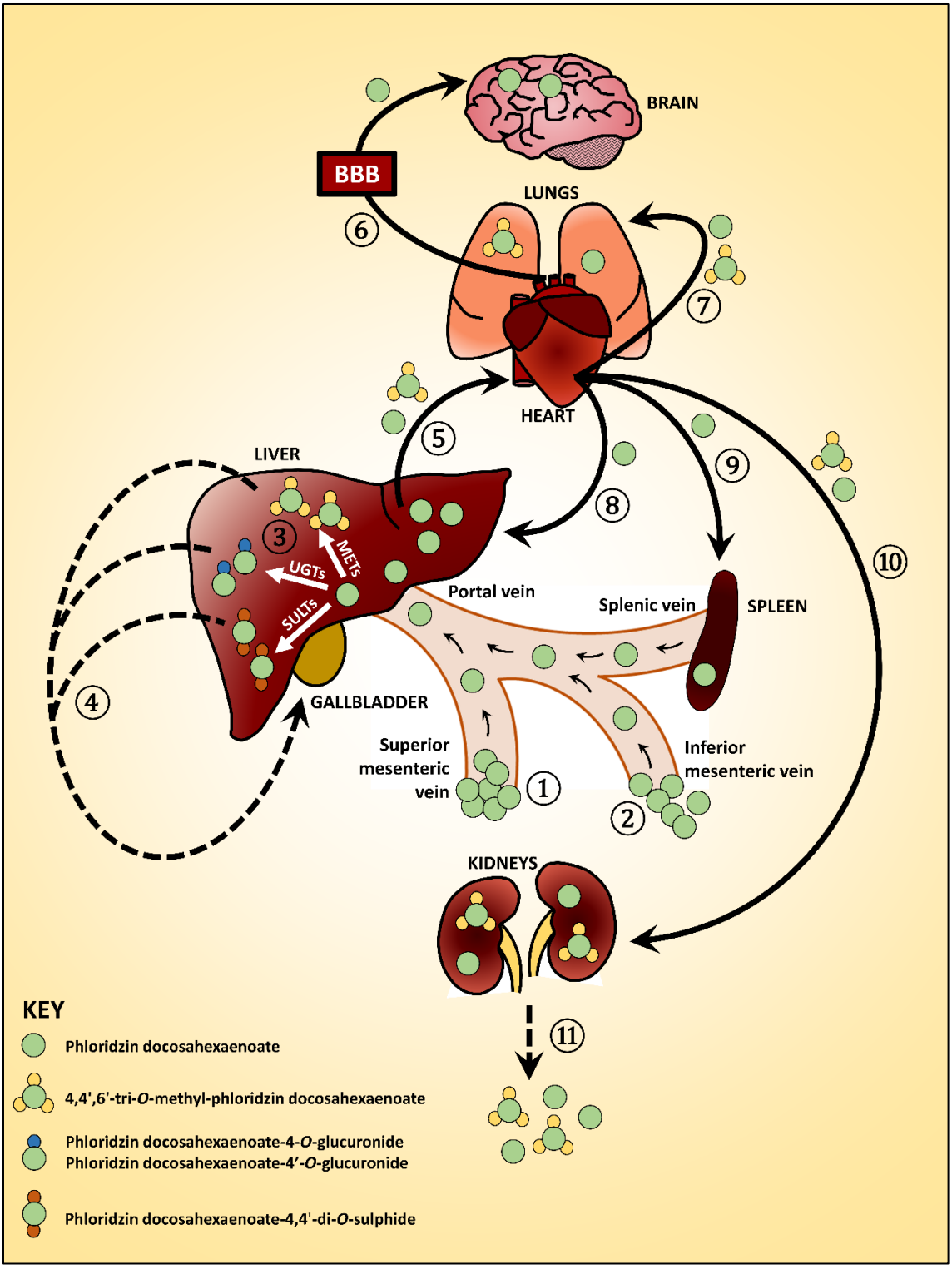
BRAIN
BBB
LUNGS
HEART
LIVER
GALLBLADDER
Portal vein
Splenic vein
SPLEEN
Superior mesenteric vein
Inferior mesenteric vein
KIDNEYS
UGTs
METs
SULTs
1
2
3
4
5
6
7
8
9
10
11
KEY
Phloridzin docosahexaenoate
4,4',6'-tri-O-methyl-phloridzin docosahexaenoate
Phloridzin docosahexaenoate-4-O-glucuronide
Phloridzin docosahexaenoate-4'-O-glucuronide
Phloridzin docosahexaenoate-4,4'-di-O-sulphide

**Figure 7.1. Proposed scheme for the fate of PZ-DHA upon intraperitoneal administration into Balb/c female mice**

Absorption of intraperitoneally administered PZ-DHA *via* ① superior mesenteric vein and ② inferior mesenteric vein; ③ Phase II metabolism of PZ-DHA in the liver; ④ Biliary secretion and entero-hepatic circulation of PZ-DHA and its metabolites; Distribution of PZ-DHA and its metabolites *via* ⑤ inferior vena cava, ⑥ left and right carotid arteries, ⑦ bronchial arteries branched from the descending aorta; ⑧ hepatic artery branched from descending aorta, ⑨ splenic artery, and ⑩ renal arteries branched from descending aorta; ⑪ PZ-DHA may be excreted *via* kidneys. Solid-lined arrows (→) indicate confirmed processes and dashed-line arrows (⇢) indicate suggested potential processes which need to be confirmed in future studies.

**BBB**: blood brain barrier; **METs**: Methyltransferases; **UGTs**: UDP-glucuronosyltransferase; **SULTs**: Sulphotransferases.

### 7.1.4 PZ-DHA is selectively cytotoxic toward breast cancer cells

PZ-DHA inhibited the metabolic activity of triple-negative (MDA-MB-231, MDA-MB-468 and 4T1) and ER+ (MCF-7 and T-47D) mammary carcinoma cells, and caused cell death; however, the viability of non-malignant cells was not affected by PZ-DHA, suggesting a significant selectivity of PZ-DHA-induced cytotoxic effects for malignant cells (sections 4.2.1-4.2.6). Despite of the observed differences in PZ-DHA-induced cytotoxic activities in malignant and non-malignant cells, section 3.2.2 indicates that absorption of PZ-DHA is similar for malignant and non-malignant cells. Studies have shown differences in the structural and biochemical composition of the cell membranes in malignant and non-malignant cells (Alves et al., 2016; Coman and Anderson, 1955). The lipid, protein and saccharide composition of malignant cell membranes is distinctly different from that of non-malignant cells, and these differences affect the association of the plasma membrane with cytoskeletal structures and intra-cellular organelles (Kojima, 1993). Specific changes identified in the plasma membrane of malignant cells include lipid composition and fatty acid composition of phospholipid bi-layer (Canuto et al., 1989; Koizumi et al., 1980; Nihon Seikagakkai. et al., 1985). Therefore, it is possible that after crossing the plasma membrane of non-malignant cells, PZ-DHA binds to the inner leaflet of the phospholipid bi-layer and does not move into the cell interior. This would account for the unchanged Akt pathway activities in MCF-10A cells following PZ-DHA treatment. Intact morphology/cell membrane integrity of MCF-10A seen under the microscope and by Annexin-V/PI staining also indicate that PZ-DHA did not harm non-malignant cells. Malignant cells are more vulnerable to cytotoxic agents due to their loss of DNA damage repair pathways (Kelley et al., 2014; O ’connor, 2015; Willers et al., 2002), increased level of replication stress (Sarni and Kerem, 2017; Zhang et al., 2016) and endogenous DNA damage (O’Connor, 2015; Tubbs and Nussenzweig, 2017). Therefore, the key differences between DNA damage repair mechanisms of malignant and non-malignant cells may have provided non-malignant cells with protection against PZ-DHA-induced DNA damage and cytotoxicity (Fernando, 2014). PZ-DHA also exhibited minimal toxicity toward normal cells in mice. Mice did not show signs of distress or adverse side effects following administration of PZ-DHA and PZ-DHA did not affect liver or kidney function. This implies that PZ-DHA effectively inhibits tumor

growth, metastasis and tumor-associated angiogenesis but does not affect the functions of normal cells.

Even though the viability of both TNBC cells and ER+ breast cancer cells was similarly affected by PZ-DHA, the cellular uptake of PZ-DHA was notably less by ER+ breast cancer cells. ERs belong to the steroid hormone superfamily of nuclear receptors and are mainly located in the cytoplasm of estrogen-sensitive cells (Lee et al., 2012). Upon binding of estrogen to ERs, the estrogen-ER complex is translocated into the nucleus where it acts as a transcription factor by binding to the estrogen response element (Björnström and Sjöberg, 2005; Kumar et al., 2011; Lee et al., 2012). However, studies show that ERs are also located on the surface of estrogen-sensitive cells, where phytoestrogens such as PZ and its aglycone PT may interact with the cell through cell surface ERs (Levin, 2002; Martin et al., 1978; Olson et al., 2006, 2007; Poola et al., 2008; Watson et al., 2005). Kuiper et al. (1998) suggest that the estrogenic potency of phytoestrogens is significant, unlike the limited estrogenic activity of industrial-derived estrogenic chemicals. PZ-DHA-induced cytotoxic activity in MCF-7 cells may therefore be mediated *via* both intra-cellular and cell surface ERs, since the chemical structure of PZ is intact in PZ-DHA. Thus, it is possible that PZ-DHA may not necessarily require entry into the cell to be cytotoxic for MCF-7 cells. Schramm et al. (1999) note that one of the question yet to be addressed is, *"Are the effects of flavonoids on animal cells initiated through their interaction with extracellular targets or intracellular targets?"*. Many studies have been conducted in the past few decades to understand specific extracellular and/or intracellular targets of flavonoids; however, this area of research is still active and has not yet provided a clear answer to this question.

### 7.1.5 Scheme of the molecular mechanisms of PZ-DHA-induced anti-proliferative activity in TNBC cells

The molecular mechanisms of PZ-DHA-induced anti-proliferative activities at a sub-cytotoxic concentration are outlined in Figure 7.2. PZ-DHA inhibits the proliferation of TNBC cells by blockade of PI3K/Akt/mTOR and RAS/RAF/ERK signaling pathways. Binding of growth factors to the extracellular domain of RTK induces dimerization of RTK and leads to the heterologous autophosphorylation of receptor monomers at the

intracellular domain. This results in activation of an intracellular docking site, PI3K is then recruited to the activated docking site and becomes activated. At the second level of the pathway, activated PI3K induces the conversion PIP2 to PIP3, leading to the activation of Akt by phosphorylation at serine and threonine sites (Vara et al., 2004).

PZ-DHA-induced inhibitory effects on Akt signaling are initiated at a higher level of the signaling cascade by the downregulation of PDK1 phosphorylation and the upregulation of PTEN phosphorylation, which inhibits the activation of PIP2 (Georgescu, 2010). Both these events lead to decreased phosphorylation of Akt, which is a serine/threonine kinase proto-oncoprotein with many substrates. Akt-induced down-stream activation of mTOR leads to cell proliferation and survival through development of resistance to apoptosis and chemotherapy-induced cell death (Mahajan and Mahajan, 2012). PZ-DHA inhibited the phosphorylation of mTOR; however, PZ-DHA did not affect the activation of GSK3β. Activation of RTK by binding of an extracellular signaling molecule to its extracellular domain activates the MAPK (ERK) pathway. Following dimerization, activated RTK communicates with membrane-bound RAS through the adaptor protein GRB2 and RAS guanine nucleotide exchange factor protein SOS (Katz et al., 2007). The efficiency of ERK signaling is regulated by the scaffolding protein KSR, kinase suppressor of RAS (Raabe and Rapp, 2002). Activated RAS triggers a phosphorylation cascade involving RAF, MEK and ERK (Mebratu and Tesfaigzi, 2009). PZ-DHA inhibited two proteins of this cascade, RAF and ERK1/2. Phosphorylation of ERK1/2 leads to its activation and subsequent translocation to the nucleus. In the nucleus, ERK activates transcription factors such as ELK which send mitogenic signals that lead to cell proliferation and survival (Lee et al., 2016; Mebratu and Tesfaigzi, 2009). PZ-DHA inhibits Akt and ERK signaling at multiple levels, suggesting that the anti-proliferative effect of PZ-DHA on TNBC cells may be mediated through these two pathways.

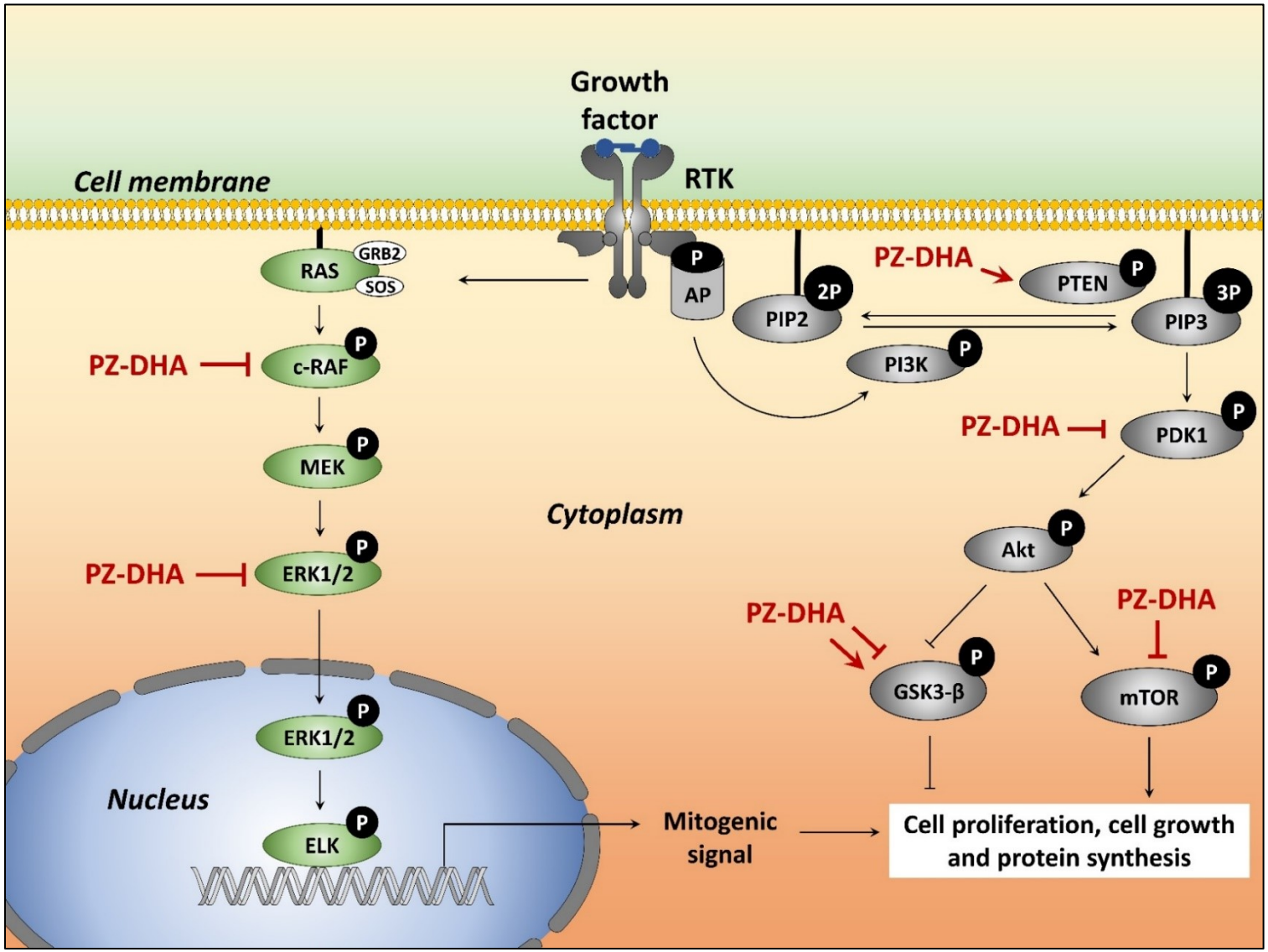
Growth factor
Cell membrane
RTK
RAS
GRB2
SOS
PZ-DHA
c-RAF
MEK
PZ-DHA
ERK1/2
ERK1/2
Nucleus
ELK
P
AP
PIP2
2P
PZ-DHA
PTEN
PIP3
3P
PI3K
PZ-DHA
PDK1
Cytoplasm
Akt
PZ-DHA
GSK3-β
PZ-DHA
mTOR
Mitogenic signal
Cell proliferation, cell growth and protein synthesis

**Figure 7.2. Proposed scheme for PZ-DHA-induced anti-proliferative activities in TNBC cells *in vitro*.**
At sub-cytotoxic concentrations, PZ-DHA suppresses the proliferation of TNBC cells. PZ-DHA inhibits activation of the Akt pathway by inhibiting the phosphorylation of PDK1, Akt and mTOR and inducing the activation of the Akt suppressor, PTEN. In addition, PZ-DHA suppresses the activation of MAPK by inhibiting the phosphorylation of c-RAF and ERK1/2.
**Akt**: protein kinase B; **AP**: activator protein; **c-RAF**: proto-oncogene serine/threonine-protein kinase; **ELK**: Ets-like protein-1; **ERK**: extracellular signal-regulated kinase; **GRB2**: growth factor receptor-bound protein 2; **GSK3-β**: glycogen synthase kinase 3-β; **MEK**: mitogen-activated protein kinase kinase; **mTOR**: mammalian target of rapamycin; **PDK1**: phosphoinositide-dependent kinase-1; **PI3K**: phosphoinositide 3-kinase; **PIP2**: phosphatidylinositol-4,5-bisphosphate; **PIP3**: phosphatidylinositol-3,4,5-trisphosphate; **PTEN**: phosphatase and tensin homolog; **PZ-DHA**: phloridzin docosahexaenoate; **RAS**: small molecular GTPase family proteins; **RTK**: receptor tyrosine kinase; **SOS**: son of sevenless.

### 7.1.6 PZ-DHA inhibits metastasis of TNBC cells

The principle goal of this project was to test the anti-metastatic effects of PZ-DHA using *in vitro* and *in vivo* models of TNBC. PZ-DHA likely inhibited filopodia-driven migration of TNBC cells, as indicated by the down-regulation of Cdc42 but not Rac1/2/3. PZ-DHA did not alter basal levels of Rho GTPase in non-malignant MCF-10A cells; however, TGF-β-induced migration, as well as RhoA and Cdc42 expression were decreased. The phenotypic transformation of epithelial cells at an early stage of metastasis facilitates detachment of cancer cells from a primary tumor and migration (Le Bras et al., 2012; Gavert and Ben-Ze'ev, 2010). Although it is well-accepted that type III EMT triggers the metastatic process (Felipe Lima et al., 2016; Schaeffer et al., 2014; Yang and Weinberg, 2008), recent studies in some model systems show that EMT is not required for metastasis. Fischer et al. (2015) show that metastasis of breast cancer cells into the lungs of triple-transgenic mice carrying polyoma middle-T or Neu oncogenes does not depend on EMT. Furthermore, Zheng et al. (2015) also demonstrate that metastasis of pancreatic cancer cells to the liver and lungs does not require EMT in a mouse model of pancreatic ductal carcinoma with deletion of Snail and Twist, two transcription factors involved in EMT (Zheng et al., 2015). The contradicting observations on the role of EMT and/or MET in metastasis have been discussed widely, leading to the conclusion that multiple hypotheses may exist to explain this complex phenomenon (Jolly et al., 2017b; Wang et al., 2016). As such, EMT and MET are critically important during single-cell dissemination and migration, even though cells do not need to lose cell-cell adhesions completely during collective migration and cluster-based migration (Jolly et al., 2017b). PZ-DHA inhibited the activity of β-catenin, Slug and ZEB-1 in *in vitro* cultures; however, the expression of vimentin was not affected. A characteristic down regulation of E-cadherin and upregulation of vimentin is displayed during EMT (Clark and Vignjevic, 2015). Wong et al. (2014) report that E-cadherin is expressed by cells that are migrating collectively, whereas vimentin is expressed during single-cell migration. Therefore, it is possible that PZ-DHA-induced anti-metastatic activity results from an inhibition of collective breast cancer cell migration rather than single-cell migration. This remains as a hypothesis at this point since effects of PZ-DHA on the expression of E-cadherin and vimentin were not tested *in vivo*; however, it is safe

to conclude that dissemination of cells from the primary tumor site was effectively inhibited by PZ-DHA, as shown by up-regulation of E-cadherin in MDA-MB-231 cell cultures. Both Fisher et al. (2015) and Zheng et al. (2015) show that EMT is a significant contributor to chemoresistance, even though EMT is not required for metastasis. PZ-DHA killed paclitaxel-resistant MDA-MB-231 cells, indicating effectiveness against metastasis and drug-resistant breast cancer cells, most likely because of its ability to impact EMT. Many studies have shown that tumor cell proliferation, metastasis, and distant colony growth are interconnected by a complex network of signaling. In fact, the expression of YB-1 protein by breast cancer cells with activated MAPK signaling inhibits cell proliferation while inducing EMT, which suggests that proliferation is essential for maintaining primary tumor growth to achieve metastatic potential; however, growth inhibition is required for the survival of circulating cancer cells and secondary relapse (Evdokimova et al., 2009). Furthermore, the growth suppressor activity of p16 and p21 promotes metastasis in basal cell carcinoma cells and hamster cheek pouch carcinoma-1 cells, respectively (Thompson et al., 2005; Unden et al., 1996). Hoek et al. (2008) showed that the genetic make-up of human melanoma cells switches between proliferative and invasive states during tumor progression (Hoek et al., 2008). It is therefore apparent that inhibition of tumor growth promotes metastasis by activating alternative signaling pathways. Interestingly, PZ-DHA inhibited primary tumor growth in Balb/c and NOD-SCID mice while also inhibiting the metastasis, which suggests that PZ-DHA is able to act on multiple signaling pathways in an *in vivo* model. Additionally, sections 5.2.7 and 5.2.8 show that the anti-metastatic activity of PZ-DHA does not correlate with the tumor suppression. There is a concern that PZ-DHA may stimulate a neutralizing antibody response in Balb/c mice upon intraperitoneal administration. However, this is unlikely since PZ-DHA is a poor immunogen due to its small size and non-protein nature. Moreover, both parent compounds of PZ-DHA are components of a normal diet and are therefore tolerogenic. In summary, the findings of my research strongly suggest that PZ-DHA inhibits the metastasis of TNBC cells by inhibiting several different factors that contribute to metastasis.

### 7.1.7 Scheme of the molecular mechanisms of PZ-DHA-induced anti-metastatic activity in TNBC cells

The molecular pathways involved in the anti-metastatic effects of PZ-DHA are in Figure 7.3. Even though PZ-DHA did not activate GSK3β through phosphorylation at tyrosine residues, there was inhibition of β-catenin, which implies that PZ-DHA inhibits the cytoplasmic accumulation of β-catenin and possibly its nuclear translocation. PZ-DHA also inhibited Slug and ZEB-1, two transcription factors involved in EMT of TNBC cells. PZ-DHA also reversed the EMT-induced cadherins switch.

PZ-DHA-induced upregulation of E-cadherin indicated restoration of epithelial characteristics that may have been lost during EMT. TGF-β often promotes EMT and metastasis. Furthermore, TGF-β-induced cell migration is mediated through Rho-dependent mechanisms (Raftopoulou and Hall, 2004; Ridley, 2015). PZ-DHA inhibited the TGF-β-induced migration of MDA-MB-231 and MCF-10A cells. PZ-DHA also suppressed RhoA, Cdc42 and Rac1/2/3 overexpression stimulated by TGF-β, suggesting an inhibitory effect on the cell migration that is mediated through actin cytoskeletal changes such as formation of stress fibers, lamellipodia and filopodia. Taken together, my findings suggest that PZ-DHA inhibits the migration and metastasis of TNBC cells mainly by inhibiting EMT and Rho GTPase signaling.

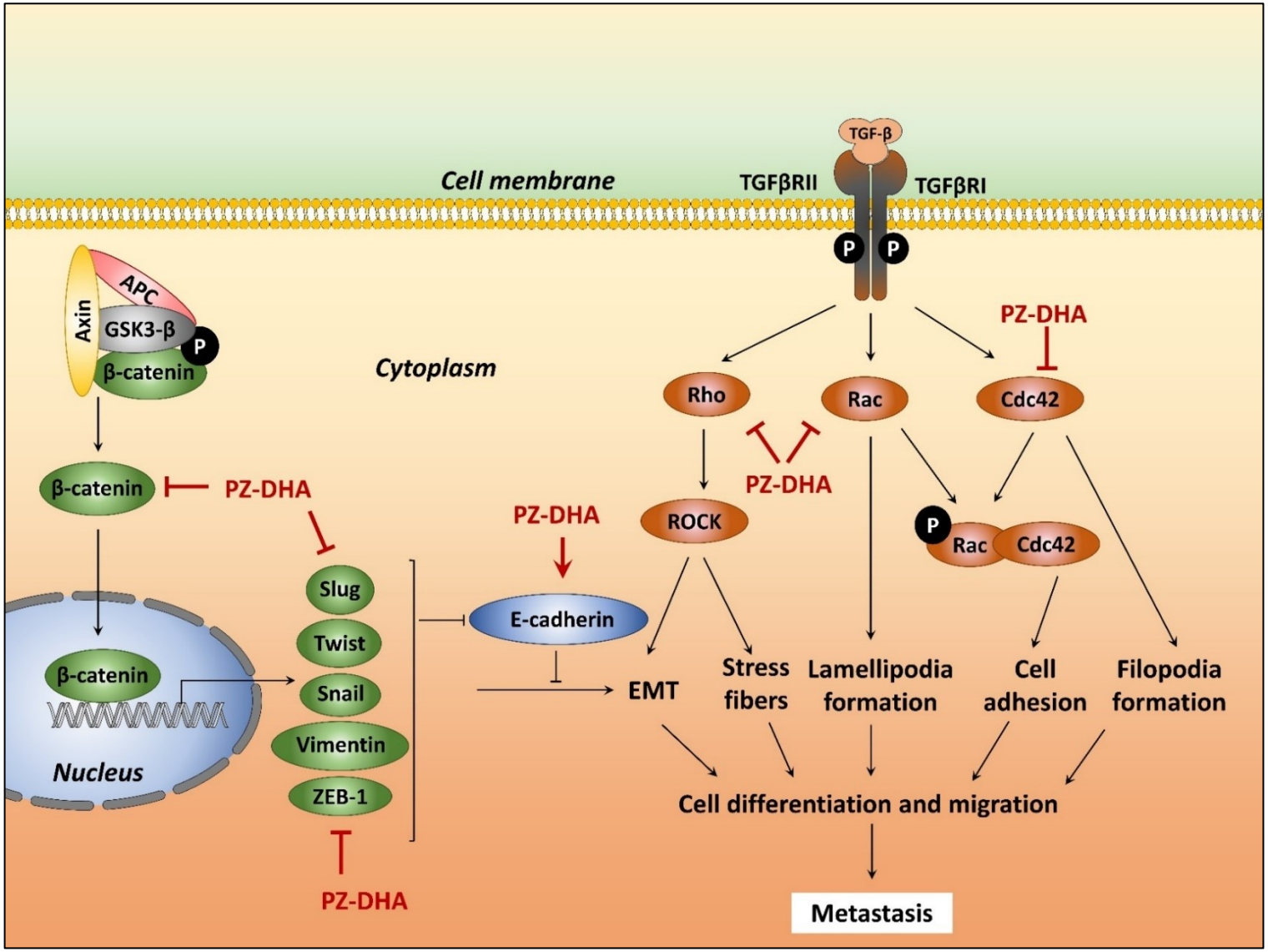
Cell membrane
TGF-β
TGFβRII
TGFβRI
P
P
Axin
APC
GSK3-β
P
β-catenin
Cytoplasm
PZ-DHA
Rho
Rac
Cdc42
β-catenin
PZ-DHA
PZ-DHA
ROCK
PZ-DHA
P
Rac
Cdc42
Slug
Twist
Snail
Vimentin
ZEB-1
E-cadherin
β-catenin
Nucleus
EMT
Stress fibers
Lamellipodia formation
Cell adhesion
Filopodia formation
PZ-DHA
Cell differentiation and migration
Metastasis

**Figure 7.3. Proposed scheme for PZ-DHA-induced anti-metastatic activities in TNBC cells *in vitro*.**
Sub-cytotoxic concentrations of PZ-DHA inhibit migration, invasion and the expression of transcription factors involved in epithelial-to-mesenchymal transition of TNBC cells. PZ-DHA-induced inhibition of the EMT transcription factor β-catenin may contribute to the inhibition of other β-catenin-dependent EMT transcription factors such as Slug, and ZEB-1. This may lead to the upregulation of E-cadherin and inhibition of the EMT process, resulting in a decrease in migration, invasion and metastasis of TNBC cells. Furthermore, PZ-DHA also inhibits TGF-β-induced Cdc42, Rac1/2/3 and RhoA expression, resulting in reduced cell migration, differentiation and EMT.
**APC**: adenomatous polyposis coli; **E-cadherin**: E-type calcium-dependent adhesion; **EMT**: epithelial-to-mesenchymal transition; **GSK3-β**: glycogen synthase kinase 3-β; **PZ-DHA**: phloridzin docosahexaenoate; **Cdc42, Rac1/2/3** and **RhoA**: Rho family small GTPases; **ROCK**: Rho-associated protein kinase; **TGF-β**: transforming growth factor-β; **TGFβRI** and **TGFβII**: transforming growth factor-β receptor I and II; **ZEB1**: zinc finger E-box-binding homeobox 1.

### 7.1.8 PZ-DHA inhibits angiogenesis

Suppression of growth of blood vessels around solid tumors is an effective way of controlling metastasis (Moserle and Casanovas, 2013). PZ-DHA suppressed angiogenesis by inhibiting endothelial cell proliferation, migration, differentiation, and tube formation. At a sub-cytotoxic concentration, PZ-DHA inhibited endothelial cell proliferation by blocking S phase entry, most likely *via* inhibition of Akt signaling. The important role of the PI3K/Akt/mTOR signaling axis in endothelial cell proliferation and survival has been demonstrated in many studies (Gerber et al., 1998; Karar and Maity, 2011). In my experiments, PZ-DHA suppressed the phosphorylation of PDK1 and increased the phosphorylation of PTEN, suggesting an upstream negative regulation of Akt. PZ-DHA also inhibited the phosphorylation of Akt and the inhibitory activity extended to downstream molecules such as mTOR, CREB, and cyclin D3. Sequential inhibition of many signaling molecules throughout the Akt signaling pathway by PZ-DHA suggested a stable and persistent inhibitory effect on Akt signaling. Tumor-associated blood vessels are irregular in shape, highly permeable, and poorly supported by pericytes (Fakhrejahani and Toi, 2012; Raza et al., 2010), resulting in leaky and contorted vasculature that increases interstitial fluid pressure within the tumor, thereby leading to passive migration of cancer cells and poor penetration by chemotherapeutic drugs (Heldin et al., 2004; Lunt et al., 2008; Salnikov et al., 2003). It was initially believed that inhibition of angiogenesis would starve cancer cells to death by blocking their supply of oxygen and nutrients. However, recent cancer research experience suggests that “normalization” of angiogenesis is more effective rather than its inhibition since this approach corrects elevated interstitial fluid pressure, thereby allowing drug penetration and reduction of metastatic spread of cancer cells (Cao, 2016; Goel et al., 2011). A study conducted by Tsuji-Tamura and Ogawa suggested that inhibition of PI3K/Akt/mTOR signaling selectively promotes the abnormal elongation of vascular endothelial cells (Tsuji-Tamura and Ogawa, 2016). Thus, PZ-DHA-mediated inhibition of Akt signaling may contribute to the correction of abnormal vasculature. PZ-DHA-induced anti-proliferative effects were also mediated *via* Rho GTPase signaling. Furthermore, PZ-DHA-mediated inhibition of RhoA- Cdc42- and Rac1/2/3-mediated degradation of $p21^{WAF1/CIP1}$ may have contributed to PZ-DHA-induced $G_1$ cell cycle arrest of endothelial cells. PZ-DHA also

inhibited endothelial cell migration and VEGF-induced expression of small molecular Rho GTPases. The inhibitory effect of PZ-DHA on tube formation by endothelial cells and sprouting of tubules from rat aorta endothelium confirms that PZ-DHA has the capacity to inhibit endothelial cell rearrangement and alignment. Finally, the inhibition of *in vivo* angiogenesis in Balb/c mice by PZ-DHA provided the strongest evidence for PZ-DHA-mediated anti-angiogenic activity.

Inhibition of angiogenesis promised to be an effective approach to suppressing metastasis (Folkman, 1971; Loges et al., 2009). However, following anti-VEGF treatment, tumors often develop resistance. Angiogenesis is strictly controlled by the intricate balance between pro-angiogenic and anti-angiogenic factors; therefore, when VEGF signaling is blocked, tumors tend to activate local adaptation mechanisms that keep angiogenesis active by inducing pro-angiogenic bFGF and PDGF secretion by tumor-associated fibroblasts (Francia et al., 2009; Ribatti, 2016). This results in a sudden surge in tumor metastasis as a result of activation of multiple alternative mechanisms that increase blood flow to and from the tumor (Loges et al., 2009; Moserle and Casanovas, 2013). However, my findings suggest concurrent inhibitory effects of PZ-DHA on metastasis and angiogenesis, which would eliminate this limitation of anti-angiogenic treatment. There might also be several more mechanisms underlying the biological activities of PZ-DHA which need to be further investigated in future experiments.

### 7.1.9 Scheme of the molecular mechanisms of PZ-DHA-induced anti-angiogenic activity

The proposed mechanism of PZ-DHA-induced anti-angiogenic activity is depicted in Figure 7.4. Angiogenesis is a multi-step process that includes endothelial cell proliferation, migration, differentiation and tube formation (Senger and Davis, 2011). PZ-DHA inhibited the angiogenesis process at several steps. PZ-DHA-stimulated phosphorylation of PTEN results in increased phosphatase activity in endothelial cells. A PZ-DHA-mediated decrease in kinase activity of PDK1 together with increased phosphatase activity of PTEN inhibits the phosphorylation of Akt at the serine site, leading to reduced mTOR activation. The activity of the downstream effector of Akt, CREB transcription factor, was also suppressed, which may lead to decreased nuclear

translocation of CREB and subsequent activation of its target genes such as VEGF *via* binding to CRE. PZ-DHA also inhibited the expression of cyclin D3, leading to a $G_1$ cell cycle arrest. This suggests another mechanism for the anti-proliferative activity of PZ-DHA on endothelial cells. S phase entry of endothelial cells was blocked by PZ-DHA-induced inhibition of Rho GTPase-mediated p21 degradation. PZ-DHA inhibited the endogenous RhoA, Cdc42 and VEGF-induced Cdc42 and Rac1/2/3 expression, suggesting that its anti-migratory effects are mediated through the inhibition of small molecular Rho GTPases. Subsequent inhibition of tube formation by blocking VEGF activity and Rho GTPase signaling in addition to reduced endothelial cell proliferation results in decreased angiogenesis.

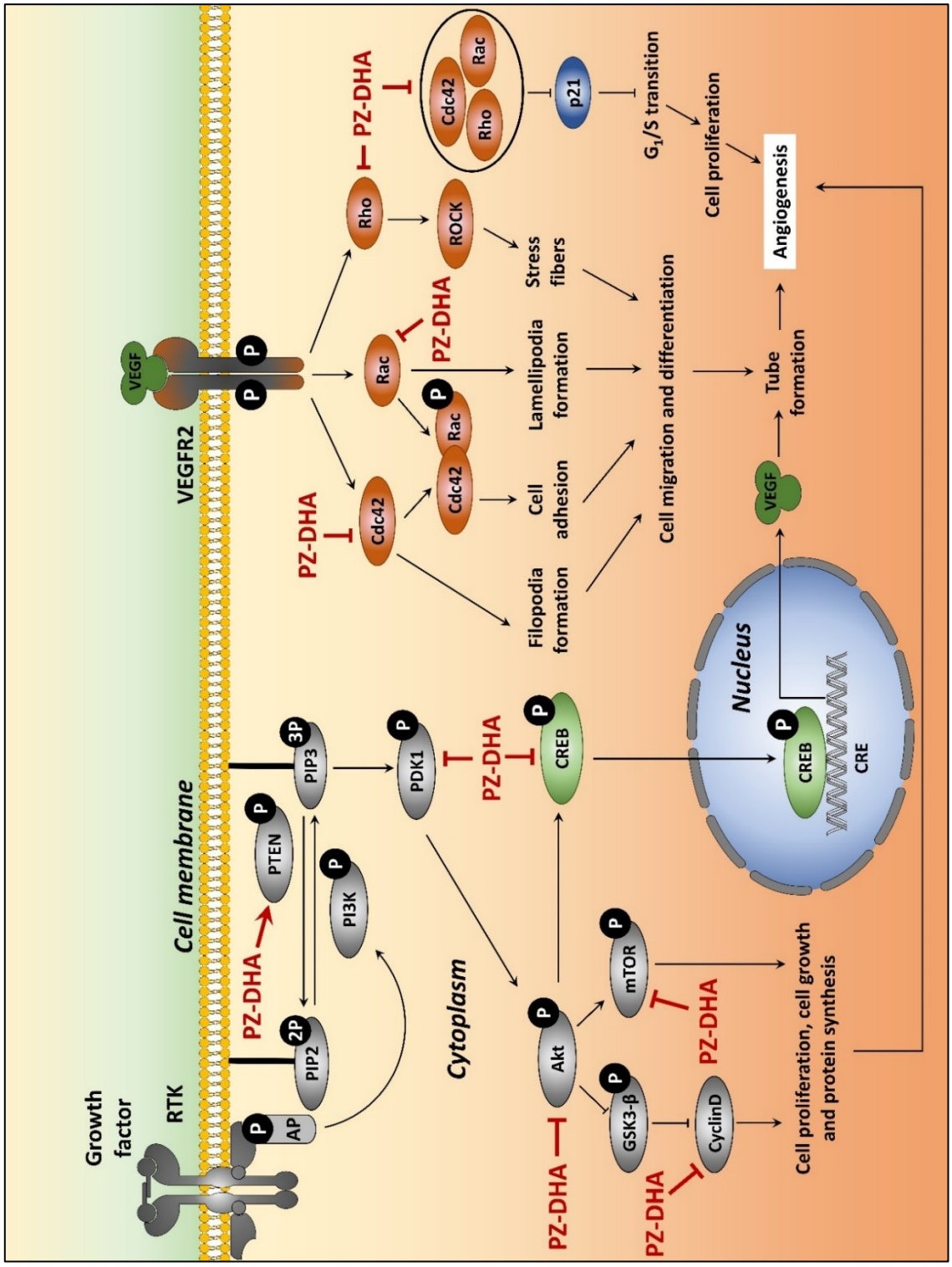


**Figure 7.4. Proposed scheme for the anti-angiogenic activities of PZ-DHA i*n vitro*.**

PZ-DHA inhibits angiogenesis by inhibiting endothelial cell proliferation, migration and tube formation. The anti-proliferative effect of PZ-DHA on endothelial cells are mediated through inhibition of Akt signaling and Rho GTPase driven $G_1$ arrest through the p53-p21 axis. PZ-DHA inhibits endothelial cell migration and differentiation by inhibiting VEGF-induced small molecular Rho GTPase activation.
**Akt**: protein kinase B; **AP**: activator protein; **Cdc42, Rac1/2/3** and **RhoA**: Rho family small GTPases; **CRE**: cAMP (cyclic adenosine monophosphate) response element; **CREB**: cAMP (cyclic adenosine monophosphate) response element binding protein; **GSK3-β**: glycogen synthase kinase 3-β; **mTOR**: mammalian target of rapamycin; **p21**: cyclin-dependent kinase inhibitor 1; **PDK1**: phosphoinositide-dependent kinase-1; **PI3K**: phosphoinositide 3-kinase; **PIP2**: phosphatidylinositol-4,5-bisphosphate; **PIP3**: phosphatidylinositol-3,4,5-trisphosphate; **PTEN**: phosphatase and tensin homolog; **PZ-DHA**: phloridzin docosahexaenoate; **ROCK**: Rho-associated protein kinase; **RTK**: receptor tyrosine kinase; **VEGF**: vascular endothelial growth factor; **VEGFR2**: vascular endothelial growth factor receptor 2.

## 7.2 Limitations of the research

Since PZ-DHA is a novel polyphenol-fatty acid ester derivative, the availability of reports on this compound by other investigators is extremely limited. The cytotoxic activity of PZ-DHA has been previously studied using HepG2 and THP-1 cells (Nair et al., 2014), MDA-MB-231 cells (Fernando et al., 2016), and K562 and Jurkat cells (Arumuggam et al., 2017). However, prior to this study, *in vivo* pharmacological activities of PZ-DHA in a rodent model had been tested only once (Fernando et al., 2016). The current study provides strong justifications to support the anti-metastatic activity of PZ-DHA; however, it must be noted that limitations in study design and experimentation may have skewed some of the research findings. These possible limitations are discussed below.

### 7.2.1 PZ-DHA cellular uptake assays

The goal of combining PZ with DHA through an esterification reaction was to improve cellular uptake of PZ and stability of DHA; in the current project, for the first time, this hypothesis was tested and proven. However, cellular uptake assays were conducted using epithelial cells grown as monolayers; as a result, cells were exposed to test compounds on only from one side of the monolayer, which may underestimate the cellular uptake of PZ-DHA and its parent compounds. Exposure of cultured cells to drugs requires that cells be maintained in humidified, $CO_2$-supplied incubators, which may result in minor, but possibly impactful fluctuations in pH (Friberg et al., 2003; Swietach et al., 2012; Vaidyanathan and Walle, 2003) and oxidative balance (Halliwell, 2003; Yokomizo and Moriwaki, 2006) that may affect the stability/oxidation of drugs as well as cellar functions. This limitation could be addressed by conducting experiments under more controlled conditions, as well as studies in an *in vivo* setting in which pH and oxidative stress are well controlled by homeostatic systems. Cellular uptake assays were conducted by culturing epithelial cells in the presence of PZ-DHA for 72 h. This time point was chosen with the aim of employing the same concentration and time point for subsequent *in vitro* experimentation; however, cellular uptake assays are typically performed at much shorter time points.

### 7.2.2 *In vitro* experiments

The effect of PZ-DHA on the expression of various signaling molecules was tested throughout this project. Except the examination of cyclin, and CDK, and small molecular Rho GTPase expression, phosphorylation was used as an indirect indicator of kinase or phosphatase activity. Phosphorylation is one of the most important post-translational protein modifications and has been widely used in cell biology as a method of measuring enzyme activity (Nishi et al., 2011). Furthermore, phosphorylation events have been considered as an option for targeted therapy of cancer (Ardito et al., 2017; Nishi et al., 2011; Peck, 2006). However, phosphorylation does not always confirm protein activation (Cobb and Goldsmith, 1995); therefore, it would be appropriate to conduct enzyme activation assays to confirm findings from western blot analysis. Furthermore, the studies imply small molecular Rho GTPase expression but do not directly show their activation.

The effect of PZ-DHA on the metabolic activity of cells was tested using either MTT or MTS assays. Mitochondrial succinate dehydrogenase and NADH-dependent oxidoreductases catalyze the reduction of MTT and MTS (Berridge et al., 2005; Lau et al., 2004). However, unlike MTT, the reduction of MTS requires an intermediate electron transporter (e.g.: phenazine methosulfate). Therefore, to minimize any undesirable cytotoxic effects caused by an additional reagent, I decided to switch to the much simpler MTT assay during the later part of the project. Nevertheless, the fact that both assays measure the activity of selected enzymes may have resulted in an underestimation of the overall metabolic activity of the cells.

Since the response of TNBC cells to current chemotherapy is poor, development of resistance and treatment failure is common. Recurrence of TNBC is fueled by the activity of CSCs. The inhibitory action of PZ-DHA on stem cell-like activity was shown using an assay of spheroid formation that used MCF-7 ER+ breast cancer cells, even though MDA-MB-231 cells would be a better choice to study the activity of PZ-DHA on TNBC stem cells. However, the cell-cell interactions of TNBC cells is poor and as a result MDA-MB-231 cells did not form spheroids with distinct margins (Supplementary Figure 8).

The interaction of TNBC cells with endothelial cells was modeled using HUVEC monolayers and PZ-DHA-treated GFP-MDA-MB-231 cells. Western blot analysis showed that PZ-DHA increased E-cadherin expression by MDA-MB-231 cells; however, the expression of E-cadherin was not blocked prior to the adhesion assays, which may have resulted in a confounding effect by aggregated MDA-MB-231 cells.

### 7.2.3 *In vivo* experiments

The effects of PZ-DHA on tumor growth and metastasis was studied in two different mouse models of metastatic TNBC. The use of two different models to evaluate the same aspects bought extra clarity to the research findings; however, these models have some inherent limitations. The growth of a tumor is determined by the proliferative and invasive capacity of the tumor cells, as well as by components of the tumor microenvironment such as fibroblasts, immune cells, blood/lymphatic vasculature, adipose cells, and ECM. (Quail and Joyce, 2013; Wang et al., 2017; Whiteside, 2008). In the syngeneic mouse model in which 4T1 mouse mammary carcinoma cells were transplanted in Balb/c female mice, the cells of the tumor microenvironment, the tumor cells and the host animal are genetically identical; therefore, the role of host-tumor interactions in tumor metastasis will be appropriately evaluated. However, tumors harvested from this model are not necessarily comparable to a human tumor; therefore, conclusions drawn from this model should be interpreted with caution. On the other hand, in the MDA-MB-231 xenograft model in NOD-SCID female mice, the tumor is of human origin; however, the cells that comprise the tumor microenvironment and the TNBC cells are from two different species. Furthermore, this model lacks an immune cell component. Thus, metastasis in this model may not accurately reflect the situation in breast cancer patients. However, when considered together, each model compensates for the limitations of the other. Furthermore, Fleming et al. (2010) suggest that tumor cell implantation into the abdominal/inguinal mammary fat pad (orthotopic implantation) is linked to a greater success in metastatic models compared to the implantation of cells into the thoracic mammary fat pad or flanks (Fleming et al., 2010). Therefore, even though the experimental models are associated with their own limitations, jointly, these studies could be considered informative.

## 7.3 Future directions

### 7.3.1 Additions to the current *in vitro* work

The current study proves an important hypothesis, namely that the combination of fatty acids with flavonoids improves the cellular uptake and stability of both parent compounds. However, this experiment could be greatly improved by introducing better detection methods to the experiment such as the use of radiolabeled-PZ-DHA for cell uptake studies. In addition, Grootaert et al. (2016) introduced a novel flow cytometric method of measuring flavonoid cell uptake following staining with 2-aminoethoxydiphenyl borate, a fluorescent probe (Grootaert et al., 2016). Therefore, the current cellular uptake assays should be confirmed using such improved method, as well as more advanced methods such as the parallel artificial membrane permeability assay (PAPMA) (Masungi et al., 2008). Another possible addition to the current cellular uptake assays would be an investigation of the effects of pH on cell uptake of PZ-DHA, as tumors are known to have an acidic microenvironment (Vallabhajosula et al., 1982). It would also be interesting to check the uptake of PZ-DHA by other adherent and suspension cell lines to determine whether the cell uptake and metabolism is cell line-dependent. Since metabolites increase the pharmacological activity of flavonoids because of increased serum retention time of metabolites (Manach et al., 1998), it would be worth testing the anti-proliferative, anti-metastatic and anti-angiogenic activities of PZ-DHA-metabolites in comparison to PZ-DHA. PZ-DHA down-regulated the expression of β-catenin in MDA-MB-231 cells in a GSK3β-independent mechanism. The literature supports the idea that apple flavonoids-mediated GSK3β regulation in malignant cells follows a different mechanism from non-malignant cells (Antika et al., 2017; Kern et al., 2006); however, this was not confirmed with PZ-DHA. Therefore, the effects of PZ-DHA on GSK3β expression in non-malignant cells such as MCF-10A cells need to be tested. A role of RAS-Rho crosstalk in the $G_1$/S cell cycle arrest has been suggested by previous studies. (Coleman and Olson, 2004; Mittnacht et al., 1997; Peeper et al., 1997). PZ-DHA inhibited the HUVEC proliferation at $G_1$/S; a role of Rho GTPases in relation to cell cycle regulation was also suggested by the current study. Thus, the effect of PZ-DHA on RAS signaling in HUVECs should be investigated.

It is possible that the structural differences in the cell membrane of the malignant and non-malignant cells may play a role in the selective cytotoxic activity of PZ-DHA. Studies show that the interactions between caveolae, lipid rafts and the galectin lattice in the control of cancer cell signalling (de Laurentiis et al., 2007; Patel and Insel, 2009; Shankar et al., 2015). Therefore, potential membrane interactions of PZ-DHA with these cell membrane regions should be investigated.

### 7.3.2 Additions to the current *in vivo* work

The pharmacokinetic experiments that I performed suggested that PZ-DHA undergoes phase II conjugation reactions, and the metabolites and unconjugated PZ-DHA is distributed through out the body. The ultimate goal of this work is to determine the feasibility of formulating PZ-DHA into a form suitable for oral dosing and investigate its behaviour in the body. Before proceeding to these experiments, it is important to understand the fate of PZ-DHA in the enterohepatic circulation, which was not investigated during this project. Furthermore, renal excretion of PZ-DHA was assumed because of the presence of PZ-DHA and its tri-methylated form in the kidneys. This step also remains to be confirmed by assessing PZ-DHA concentration in urine. Experiments also need to be designed to understand the fate of PZ-DHA following oral administration. Oral gavage of PZ-DHA and the subsequent analysis of blood, organs and feces may provide information regarding the feasibility of administering PZ-DHA by the oral route. In order to determine the absolute bioavailability, PZ-DHA administration needs to be performed *via* intravenous route in parallel to the oral administration.

There are a few important areas in which the application of PZ-DHA has not yet been tested. Firstly, it is believed that the surgical removal of a tumor mass results in a substantial reduction in tumor burden. The risk of recurrence due to the residual tumor cells following surgical excision is mainly managed by subsequent chemotherapy and radiation therapy. The sequence of the surgery and chemotherapy/radiation therapy is determined on the basis of tumor invasiveness and its ability to be cleanly resected (Balko et al., 2012; Buchholz et al., 2015; Lee et al., 2011a; Morris et al., 2010; Takano et al., 2015). Secondly, metastasis may be initiated at an early stage in the growth of primary tumors; indeed, mounting recent evidence suggests that dormant metastatic

cancer cells may have become disseminated through the circulation even before the start of preoperative chemo/radiation therapy and/or surgical removal of the tumor (Friberg and Nyström, 2015; Röcken, 2010; Yokota, 2000). Thirdly, Demicheli et al. (2008) noted that the surgical removal of primary tumor may be associated with the risk of surgery-driven metastasis (Demicheli et al., 2008). Since PZ-DHA shows potent and safe anti-metastatic activity *in vivo*, it would be interesting to determine whether PZ-DHA inhibits the *in vivo* metastasis in the above three contexts using a mouse model of metastatic breast cancer in which the primary tumors are resected in a timely fashion.

### 7.3.3 Synergistic effect of PZ-DHA in combination with chemotherapeutic drugs

The search for targeted therapies to treat TNBC is one of the top priorities in breast cancer research. However, the current clinical practice of TNBC treatment is still limited to an appropriate combination of surgery, chemotherapy, and radiation therapy (Yagata et al., 2011). A recent study shows that a combination drug regimen that includes bevacizumab (anti-angiogenic), carboplatin (alkylating agent), and paclitaxel (mitotic inhibitor) improves the overall response rate of TNBC patients with/without metastatic disease (Chalakur-Ramireddy and Pakala, 2018). Pritchard et al. (2013) explains that combination chemotherapy may act in two major ways; first, one drug may simply strengthen the activity of the other drug; second, when combined the two drugs exert a different effect than they would if used separately (Pritchard et al., 2013). The role of flavonoids in concurrent administration with chemotherapy or radiation therapy has been discussed widely (Conklin, 2000; D'Andrea, 2005; Simone et al., 2007). These studies mainly examined the role of pro-oxidant and/or anti-oxidant activity of flavonoids in combination with chemotherapy and/or radiation therapy to enhance the efficacy of treatment and/or to protect the normal cell counterparts from adverse side effects (Ebeid et al., 2016; Kostler et al., 2001; Lamson and Brignall, 1999; Lawenda et al., 2008). The role of quercetin in combination with conventional chemotherapy has been studied extensively (Brito et al., 2015). In addition, Aksamitiene et al. (2012) reported a synergistic effect of luteolin, a flavonoid, when it was combined with nilotinib or 5-fluorouracil, two chemotherapeutic drugs that are used in the treatment of pancreatic cancer. Since PZ-DHA possesses several different biological activities, it would be worth investigating the effects of PZ-DHA in combination with conventional chemotherapeutic

drugs currently used in breast cancer such as doxorubicin, cisplatin and paclitaxel. It is possible that concurrent administration of PZ-DHA with chemotherapeutic agents may inhibit the growth of tumors by accelerating the cytotoxic effects of the chemotherapeutic drugs. PZ-DHA may also sensitize the tumors to chemotherapy by "normalizing" the aberrant vasculature and thereby increasing the penetration of chemotherapeutic drugs into the tumor interior.

### 7.3.4 Efficacy of PZ-DHA on breast cancer stem cell activity

Drug resistance, metastasis, and cancer stem cells are tightly inter-connected aspects of cancer and their collective contribution leads to an extremely aggressive phenotype. The association of cancer stem cells and drug resistance (Phi et al., 2018; Prieto-Vila et al., 2017; Schöning et al., 2017; Vinogradov and Wei, 2012), as well as cancer stem cells and metastasis (Li and Li, 2014; Li et al., 2007; Sampieri and Fodde, 2012; Shiozawa et al., 2013), is supported by a growing body of evidence in literature. The current research shows that PZ-DHA inhibits TNBC metastasis. A preliminary experiment conducted using MCF-7 cells shows that PZ-DHA may also have stem cell suppressor activity. PZ-DHA killed paclitaxel-resistant MDA-MB-231 cells and increased the number of chemo-resistant cells undergoing apoptosis. Taken together, these three findings suggest that cancer stem cell suppressor activity of PZ-DHA may have a significant impact on the metastatic activity and chemoresistance of TNBC cells. However, these hypotheses remain to be investigated in future experiments.

### 7.3.5 Identification of genes involved in the response of breast cancer cells to PZ-DHA treatment as a basis for patient-oriented breast cancer treatment

The complicated dynamic nature of cancer is reflected by the tremendous heterogeneity of solid tumors (Balogh et al., 2011; Dagogo-Jack and Shaw, 2017; Meacham and Morrison, 2013). The heterogeneity that exists between two tumors growing in two patients, but belonging to the same histological subtype is known as intra-tumoral heterogeneity (Bedard et al., 2013; Gerashchenko et al., 2013; Gupta and Somer, 2017). The heterogeneity that exists among the tumor cells of a single patient is known as inter-tumor heterogeneity (Liu et al., 2018; Sutherland and Visvader, 2015). Breast cancer is an extremely heterogeneous disease; therefore, a patient-oriented approach may more

effectively address challenges such as drug resistance and treatment failure (Balogh et al., 2011; Polyak, 2011; Turashvili and Brogi, 2017). Identification of drug-resistance/sensitivity genes will allow for the selection of patients who would most likely benefit from treatment with a particular drug (Garnett et al., 2012). The identification of the genes involved in the response of breast cancer cells to PZ-DHA treatment through a genome-wide RNAi screening approach may provide more precise information on which patients will receive the greatest benefit from PZ-DHA treatment. Identification such genes in future experiments will be very useful going forward.

### 7.3.6 Encapsulation of PZ-DHA in nanoparticles as an approach to targeted drug delivery

Targeted nanoparticle drug delivery is an emerging approach to overcoming biological barriers to cancer chemotherapy (Mudshinge et al., 2011; Singh et al., 2009b; Wilczewska et al., 2012). Even though PZ-DHA shows impressive and safe biological activities both *in vitro* and *in vivo*, the majority of PZ-DHA administered by the intraperitoneal route did not reach the systemic circulation. PZ-DHA is potent in biological systems; however, a higher dose of PZ-DHA is needed to reach an effective concentration at the site of action. Incorporation of flavonoids into nanoparticles has been examined as one possible approach to improving their cellular uptake and bioavailability (Wang et al., 2013). Polylactic-co-glycolic acid (PLGA)-based nanoparticles loaded with quercetin show a 56% increase in the cellular uptake of quercetin by MDA-MB-231 cells and a significant reduction in the viability of the breast cancer cells (Halder et al., 2018). Another study shows PLGA nanoparticles loaded with etoposide or etoposide combined with quercetin caused the $IC_{50}$ of etoposide to decrease by 9-10-fold in MCF-7 breast cancer cells. Furthermore, in rats incorporation of etoposide with quercetin in the nanoparticle improves the bioavailability of etoposide by 2.4-fold when compared to nanoparticle loaded with etoposide alone (Fatma et al., 2016). Oil-based lipid nanoparticles protected encapsulated quercetin, naringenin, and hesperetin from biodegradation and improved the bioaccessibility of these compounds by 56% (Ban et al., 2015). Thus, nanoparticle encapsulation of flavonoids improves their bioavailability by several means. Similarly, incorporation of PZ-DHA into a suitable delivery vehicle such as liposomes, polymeric nanoparticles, micelles or dendrimers may decrease the dose

required to exert maximal biological effects and may also minimize any side effects that might occur due to the overaccumulation of PZ-DHA in body fat.

### 7.4 Significance of the research and concluding remarks

As it has been repeatedly highlighted throughout this thesis, metastatic cancer is a deadly and devastating disease, regardless of the primary tumor site. In particular, TNBC is one of the most aggressive types of breast cancer as recurrence is likely following conventional chemotherapy. Metastatic-TNBC therefore brings two extremely lethal disease conditions together, thereby creating disease that is clinically incurable using current treatment strategies. The overall objective of the current project was to establish pharmacokinetic parameters of a novel polyphenol fatty acid ester derivative and then study its potential to block TNBC metastasis in mice as a first step in possible translation to the clinic.

Here, I tested the efficacy of a novel dietary biomolecule derived-compound known as PZ-DHA against metastatic TNBC. My study utilized *in vitro*, *ex vivo* and *in vivo* models and revealed several major mechanisms by which PZ-DHA inhibits the growth and metastasis of TNBC cells, as well as angiogenesis associated with tumor progression. PZ-DHA suppressed Akt, MAPK, TGF-β, and Rho GTPase signaling pathways in TNBC cells and inhibited TNBC tumor growth and metastasis in mice. Furthermore, PZ-DHA-induced Akt and Rho GTPase signaling was also observed in endothelial cells. The anti-angiogenic activity of PZ-DHA in mice suggested a PZ-DHA-induced reduction in hematogenic spread of TNBC cells. Pharmacokinetic experiments showed that PZ-DHA undergoes phase I and II metabolism and PZ-DHA is readily distributed throughout the body without causing toxic side effects. In addition, the conjugation of PZ with DHA improved the cellular uptake and stability of both compounds.

Findings of this project suggest that metastatic TNBC may be manageable using this novel polyphenol fatty acid ester derivative alone or in combination with other chemotherapeutic drugs. It is still too early to consider a place for PZ-DHA in the clinical setting; however, this research makes a significant contribution to the existing knowledge of the role of dietary biomolecules in the management of metastatic TNBC and reveals the potential of PZ-DHA to inhibit the progression of metastatic TNBC in patients.

## APPENDIX: SUPPLEMENTARY FIGURES

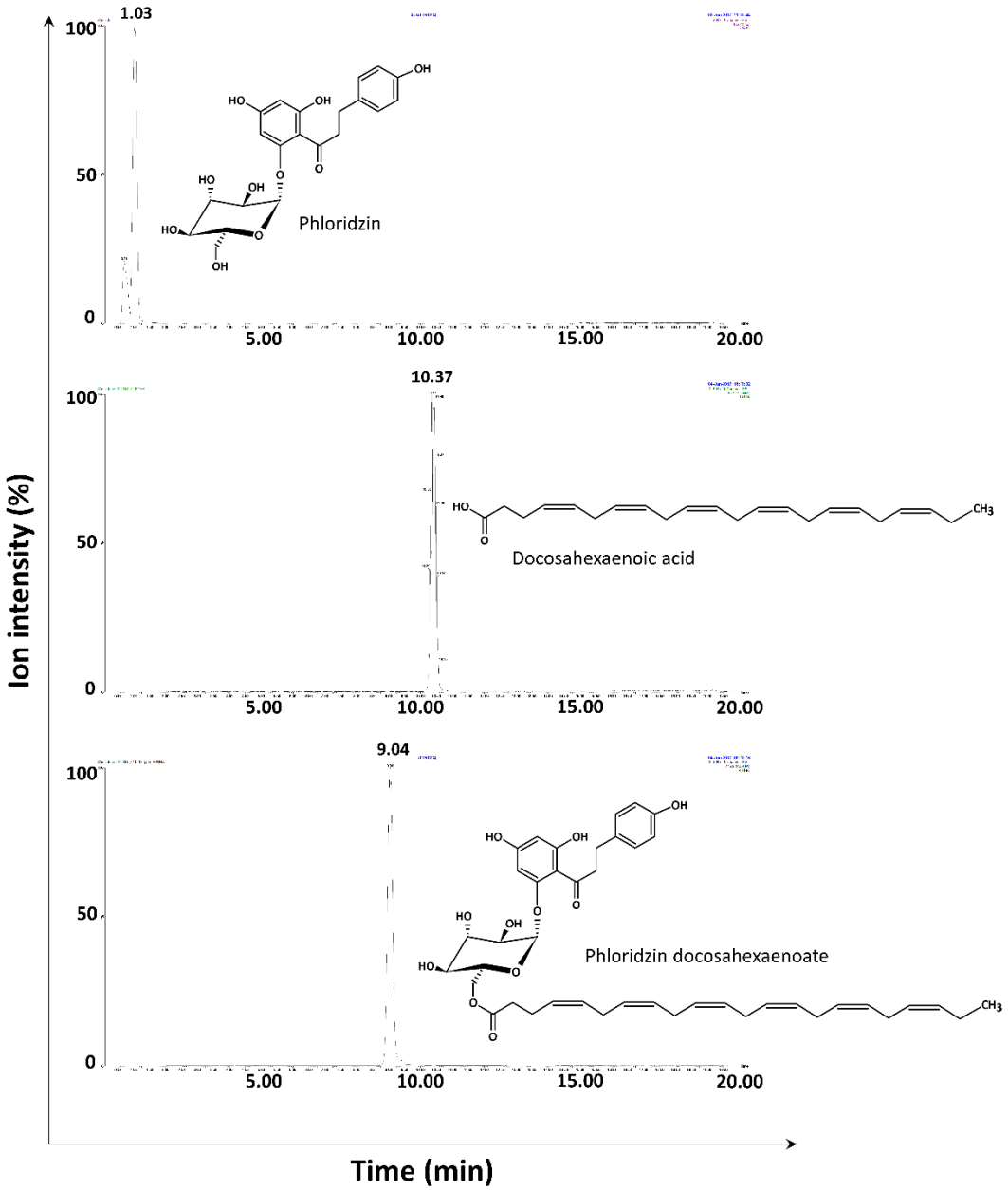


**Supplementary Figure 1. HPLC chromatogram of standard PZ, DHA and PZ-DHA used for *in vitro* and *in vivo* experiments.**

PZ, DHA and PZ-DHA (0.25 mg/mL) standard solutions prepared in methanol were identified using single ion monitoring of UPLC-ESI-MS analysis. PZ, MW=436.413 g/mol, RT=1.03 min; DHA, MW=328.496 g/mol, RT=10.37 min; PZ-DHA: MW=746.88 g/mol, RT=9.04 min.

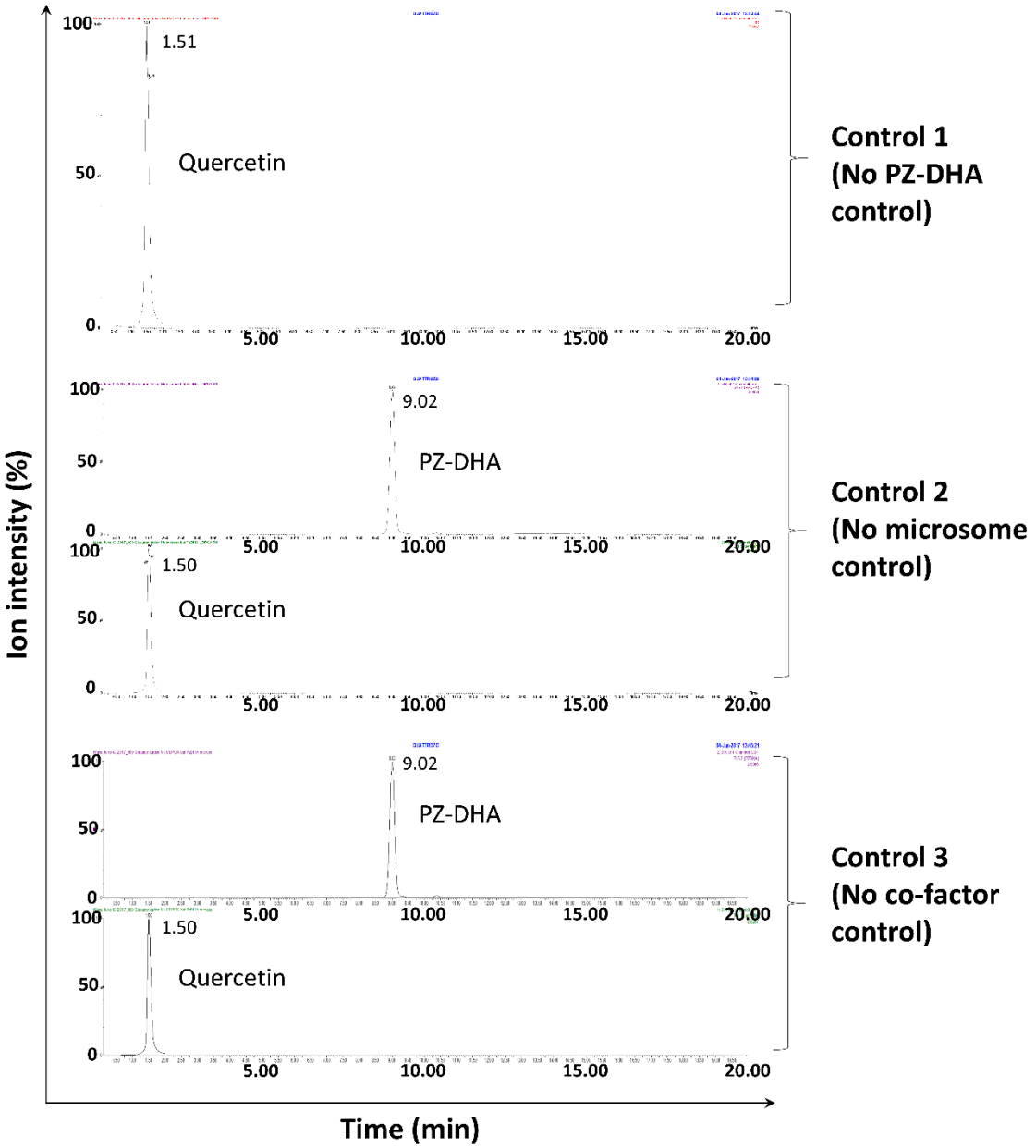


**Supplementary Figure 2. Chromatograms of *in vitro* PZ-DHA phase II metabolite formation control experiments.**

The quercetin was recorded in all control experiments as the internal standard and intact PZ-DHA was recorded in the absence of microsomes and respective cofactors, suggesting that the reactions are microsome-dependent and cofactor-dependent.

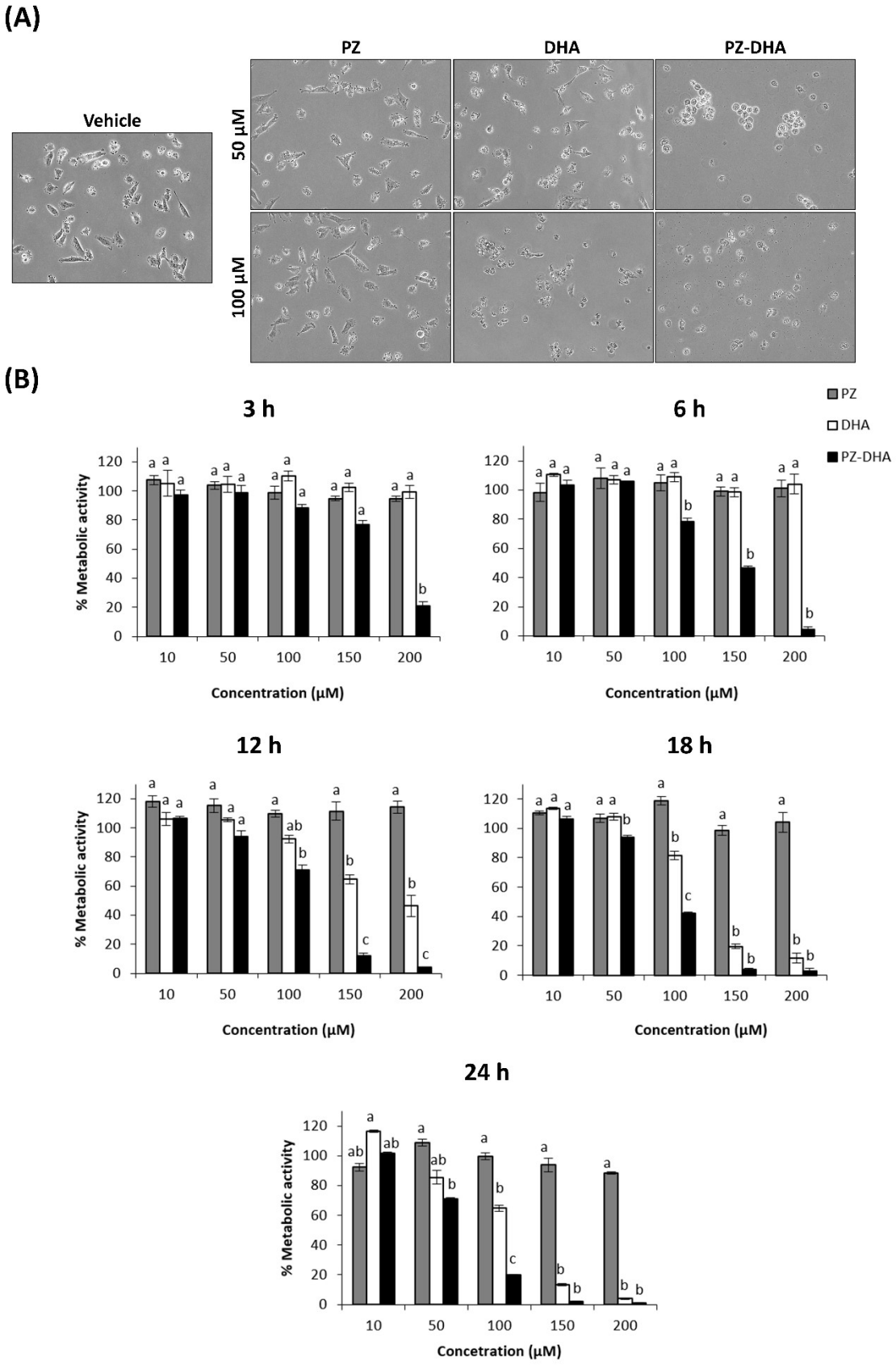
(A)
PZ
DHA
PZ-DHA
Vehicle
50 µM
100 µM
(B)
3 h
6 h
12 h
18 h
24 h
PZ
DHA
PZ-DHA
% Metabolic activity
Concentration (µM)
Concetration (µM)

**Supplementary Figure 3. PZ-DHA inhibits the metabolic activity of MDA-MB-231 human triple- negative breast cancer cells in a concentration- and time-dependent manner (Adapted from my MSc thesis)**

(Fernando, 2014)

**(A)** MDA-MB-231 TNBC cells were seeded and adherent cells were treated with vehicle, 50 μM or 100 μM of PZ, DHA, or PZ-DHA and cultured for 24 h. Following culture, cells were photographed using a Nikon eclipse TS 100 phase contrast microscope equipped with Infinity 1 camera at ×200 magnification. **(B)** MDA-MB-231 cells were treated with PZ, DHA and PZ-DHA and cultured for the indicated time points. At the end of culture, cells were incubated in the presence of MTS/PMS for 3 h and development of the formazan product was determined by measuring the absorbance at 490 nm. Metabolic activity of the cells was calculated using the equation, % relative metabolic activity= $((A_T-A_{TB})/( A_C- A_{CB})) \times 100$, where, $A_T$: absorbance of cells treated with drugs; $A_{TB}$: absorbance of treatment blank; $A_C$: absorbance of cells treated with vehicle control; $A_{CB}$: absorbance of vehicle blank at 24 and 48 h post-treatment compared using one-way ANOVA multiple means comparison method and differences among means were compared using Tukey's multiple means comparison method. Data presented as mean ± SEM are averaged results of three independent experiments performed in quadruplicates. Values with different letters for each concentration level are significantly different at $\alpha = 0.05$ ($p<0.05$).

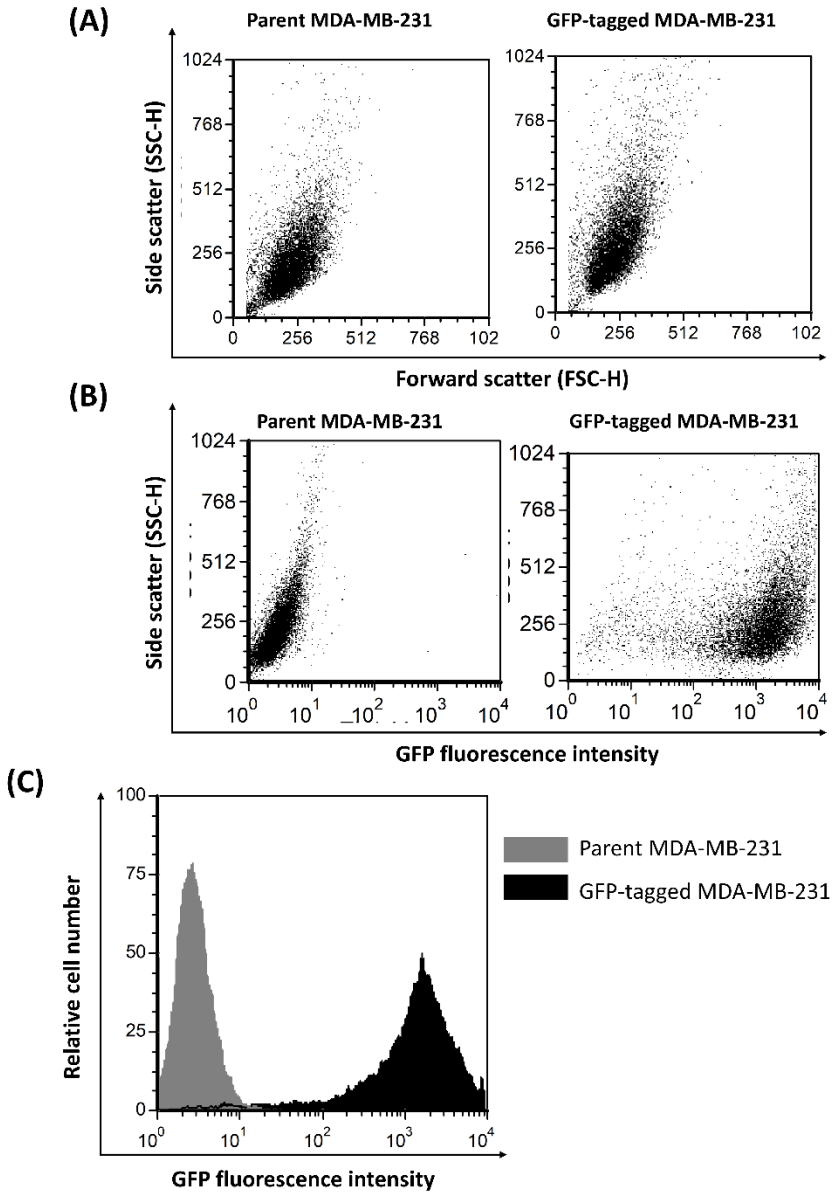


**Supplementary Figure 4. Detection of GFP-tagged MDA-MB-231 cells using flow cytometry.**

Green fluorescence protein (GFP) transfection of MDA-MB-231 cells was confirmed using flow cytometric analysis of parent MDA-MB-231 and GFP-tagged MDA-MB-231 cells. Data shown are **(A)** FSC-H vs SSC-H dot plots and increased GFP fluorescence of MDA-MB-231 on **(B)** SSC-H vs FL1 dot plot and **(C)** histogram of cells acquired by FL1 detector following transfection.

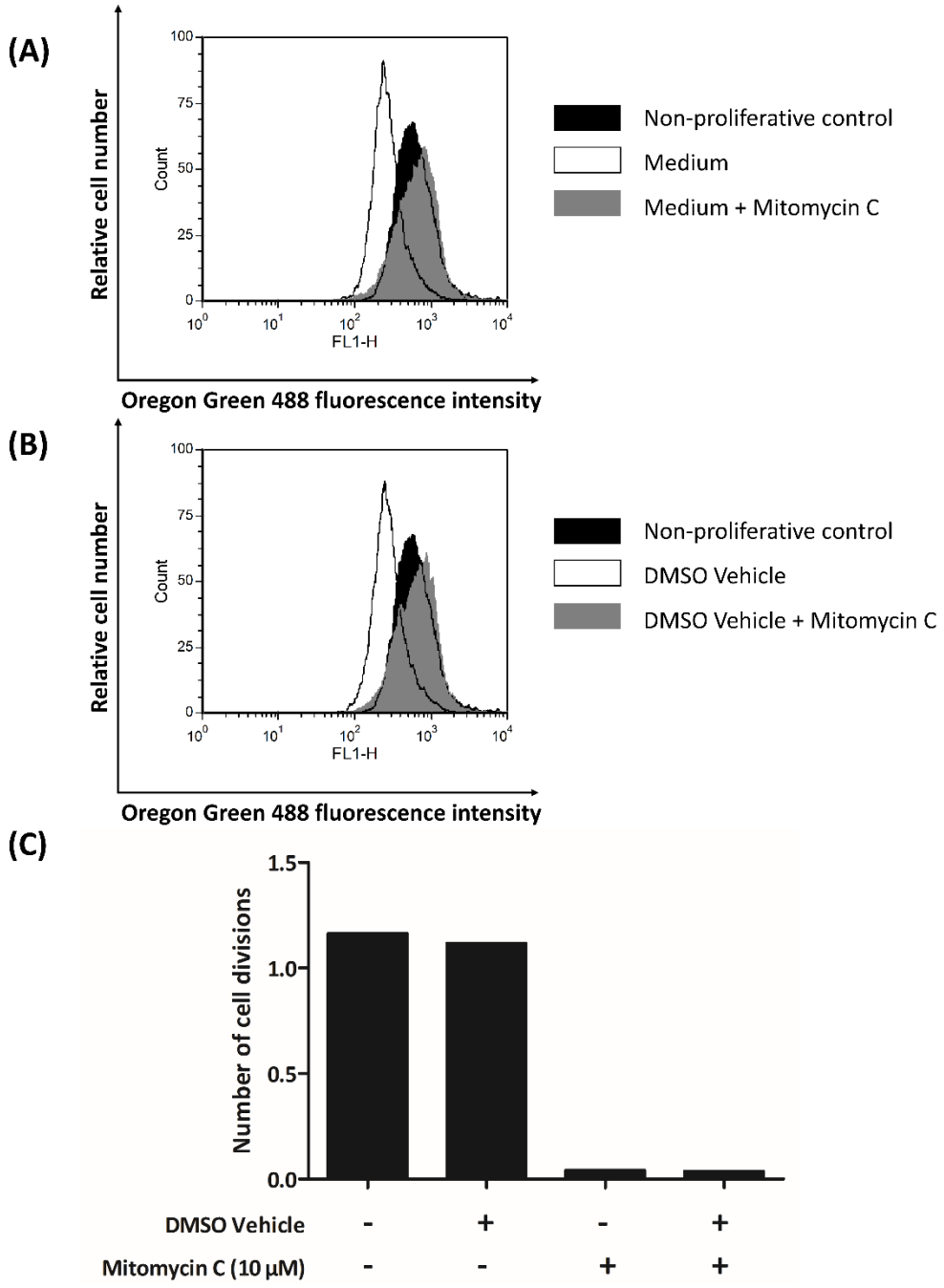


**Supplementary Figure 5. Mitomycin C inhibits the proliferation of MDA-MB-231 cells *in vitro*.**
MDA-MB-231 cells were synchronized to $G_0$ phase by culture in serum-free DMEM overnight. Synchronized cells were seeded and stained with Oregon Green 488 dye, then treated with 10 μM mitomycin C and incubated for 2 h. Cells were then washed and cultured for 48 h. At the end of culture, cells were harvested and analyzed by flow cytometry on FL1. Data shown are representative histograms of cells incubated in the **(A)** absence and **(B)** presence of the DMSO control in comparison to the non-proliferative control and **(C)** number of cell divisions.

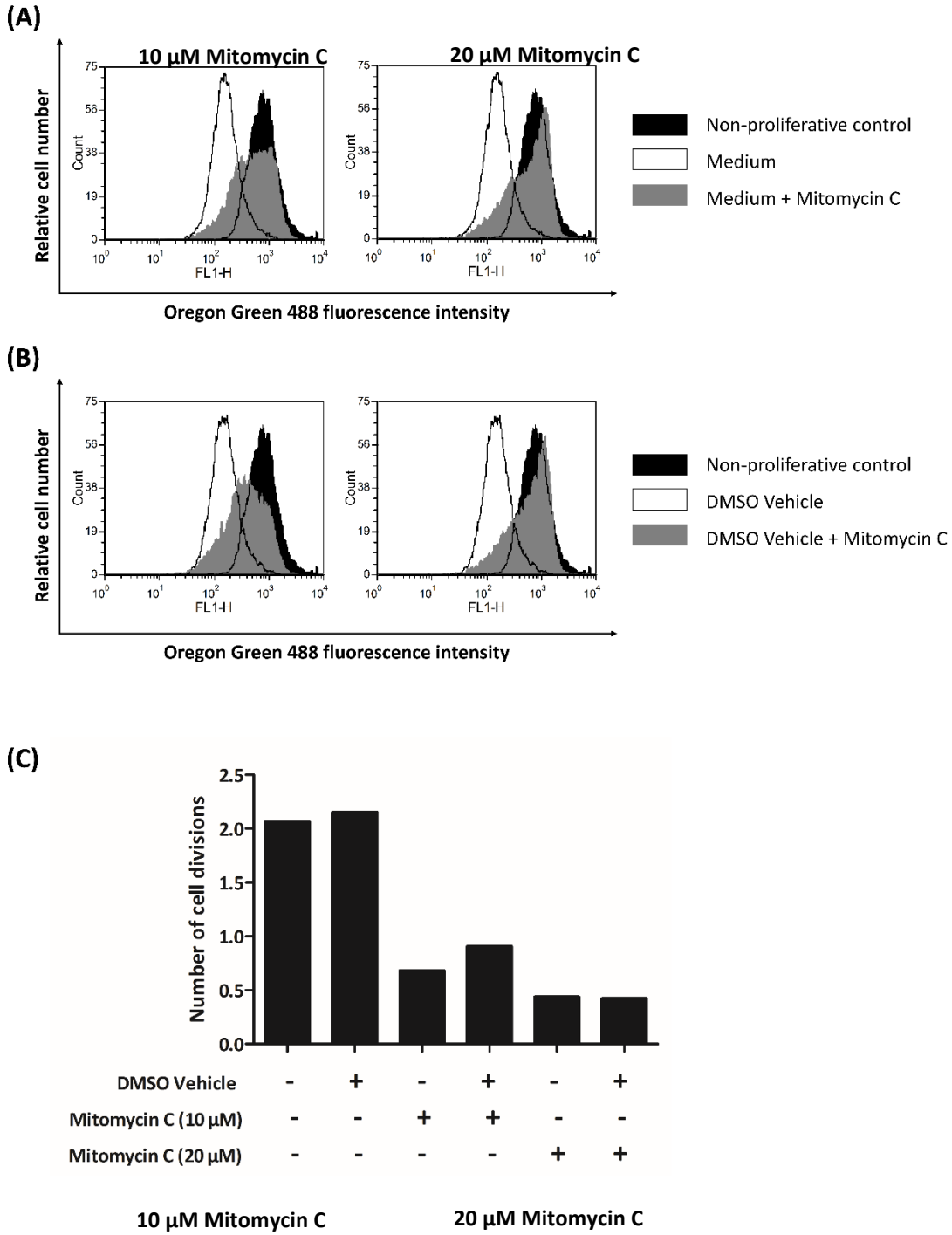


**Supplementary Figure 6. Mitomycin C inhibits the proliferation of 4T1 cells *in vitro*.** 4T1 cells were synchronized to $G_0$ phase by culture in serum-free DMEM overnight. Synchronized cells were seeded and stained with Oregon Green 488 dye, then treated with 10 µM or 20 µM mitomycin C and incubated for 2 h. Cells were then washed and cultured for 48 h. At the end of culture, cells were harvested and analyzed by flow cytometry on FL1. Data shown are representative histograms of cells incubated in the **(A)** absence and **(B)** presence of DMSO control in comparison to the non-proliferative control and **(C)** number of cell divisions.

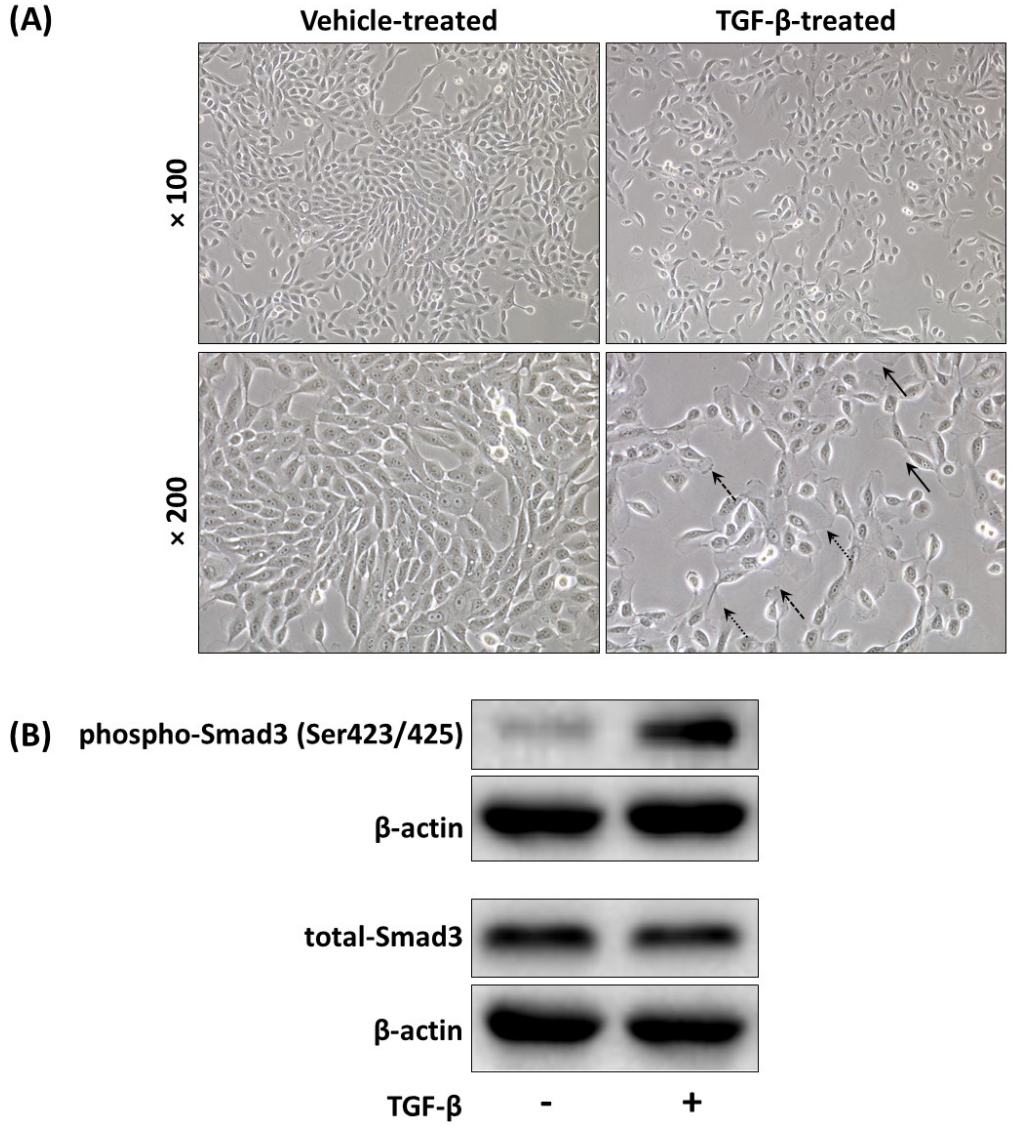


**Supplementary Figure 7. Confirmation of TGF-β signaling in MCF-10A non-malignant mammary epithelial cells.**
**(A)** MCF-10A cells were seeded and cultured in the presence or absence of 10 ng/mL TGF-β, and then TGF-β-induced morphological changes (dashed-arrows: membrane blebs; dotted arrows: lamellipodia; solid arrows: filopodia) were photographed using a Nikon eclipse TS 100 phase contrast microscope equipped with Infinity 1 camera at ×100 and ×200 magnification. **(B)** MCF-10A cells were treated with 10 ng/mL TGF-β for 24 h and the induction of TGF-β-mediated Smad3 phosphorylation at Ser423/425 was detected by western blot analysis. Equal protein loading was confirmed by β-actin expression.

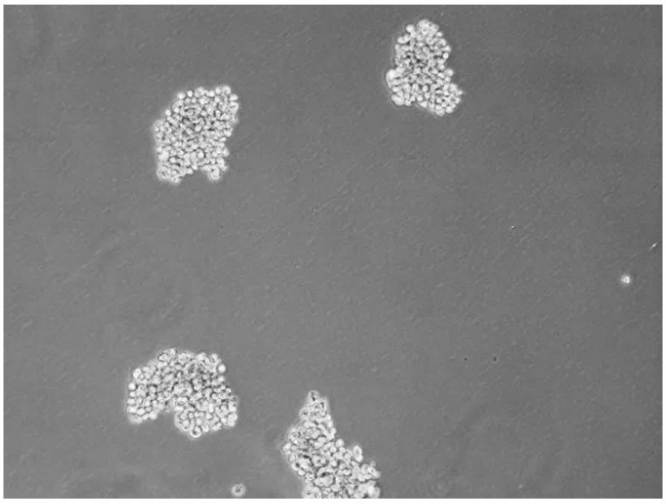

**Supplementary Figure 8. MDA-MB-231 mammospheres lack definite margins.** MDA-MB-231, which are TNBC cells, were grown in ultra-low adherent cell culture plates in spheroid growth medium for 5 days. Medium was replenished every 48 h and mammospheres were photographed using a Nikon eclipse TS 100 phase contrast microscope equipped with Infinity 1 camera at ×200 magnification.

## REFERENCES


Abdal Dayem, A., Choi, H.Y., Yang, G.-M., Kim, K., Saha, S.K., and Cho, S.-G. (2016). The Anti-Cancer Effect of Polyphenols against Breast Cancer and Cancer Stem Cells: Molecular Mechanisms. Nutrients *8*, 581.

Abhinand, C.S., Raju, R., Soumya, S.J., Arya, P.S., and Sudhakaran, P.R. (2016). VEGF-A/VEGFR2 signaling network in endothelial cells relevant to angiogenesis. J. Cell Commun. Signal. *10*, 347–354.

Abid, M.R., Guo, S., Minami, T., Spokes, K.C., Ueki, K., Skurk, C., Walsh, K., and Aird, W.C. (2004). Vascular endothelial growth factor activates PI3K/Akt/forkhead signaling in endothelial cells. Arterioscler. Thromb. Vasc. Biol. *24*, 294–300.

Abourashed, E.A. (2013). Bioavailability of Plant-Derived Antioxidants. Antioxidants *2*, 309–325.

Abraham, S., Scarcia, M., Bagshaw, R.D., McMahon, K., Grant, G., Harvey, T., Yeo, M., Esteves, F.O.G., Thygesen, H.H., Jones, P.F., et al. (2015). A Rac/Cdc42 exchange factor complex promotes formation of lateral filopodia and blood vessel lumen morphogenesis. Nat. Commun. *6*, 7286.

Abu, N., Akhtar, M.N., Yeap, S.K., Lim, K.L., Ho, W.Y., Zulfadli, A.J., Omar, A.R., Sulaiman, M.R., Abdullah, M.P., and Alitheen, N.B. (2014). Flavokawain A Induces Apoptosis in MCF-7 and MDA-MB231 and Inhibits the Metastatic Process In Vitro. PLoS One *9*, e105244.

Abu, N., Mohamed, N.E., Yeap, S.K., Lim, K.L., Akhtar, M.N., Zulfadli, A.J., Kee, B.B., Abdullah, M.P., Omar, A.R., and Alitheen, N.B. (2015). In vivo antitumor and antimetastatic effects of flavokawain B in 4T1 breast cancer cell-challenged mice. Drug Des. Devel. Ther. *9*, 1401–1417.

Adhami, V.M., Syed, D.N., Khan, N., and Mukhtar, H. (2012). Dietary flavonoid fisetin: a novel dual inhibitor of PI3K/Akt and mTOR for prostate cancer management. Biochem. Pharmacol. *84*, 1277–1281.

Ahmed, Z., and Bicknell, R. (2009). Angiogenic Signalling Pathways. In Methods in Molecular Biology, Angiogenesis Protocols, S. Martin, and C. Murray, eds. (Humana Press), pp. 3–24.

Akbar, M., Calderon, F., Wen, Z., and Kim, H.-Y. (2005). Docosahexaenoic acid: a positive modulator of Akt signaling in neuronal survival. Proc. Natl. Acad. Sci. U. S. A. *102*, 10858–10863.

Albini, A., Dell'Eva, R., Vené, R., Ferrari, N., Buhler, D.R., Noonan, D.M., and Fassina, G. (2006). Mechanisms of the antiangiogenic activity by the hop flavonoid xanthohumol: NF-kappaB and Akt as targets. FASEB J. *20*, 527–529.

Alves, A.C., Ribeiro, D., Nunes, C., and Reis, S. (2016). Biophysics in cancer: The relevance of drug-membrane interaction studies. Biochim. Biophys. Acta - Biomembr. *1858*, 2231–2244.

Amawi, H., Ashby, C.R., Tiwari, A.K., and Tiwari, A.K. (2017). Cancer chemoprevention through dietary flavonoids: what's limiting? Chin. J. Cancer *36*, 50.

An, G., Gallegos, J., and Morris, M.E. (2011). The bioflavonoid kaempferol is an Abcg2 substrate and inhibits Abcg2-mediated quercetin efflux. Drug Metab. Dispos. *39*, 426–432.

Anders, C.K., and Carey, L.A. (2009). Biology, metastatic patterns, and treatment of patients with triple-negative breast cancer. Clin. Breast Cancer *9*, S73-81.

André, F., and Zielinski, C.C. (2012). Optimal strategies for the treatment of metastatic triple-negative breast cancer with currently approved agents. Ann. Oncol. *23*, 46–51.

Andreasen, P.A., Egelund, R., and Petersen, H.H. (2000). The plasminogen activation system in tumor growth, invasion, and metastasis. Cell. Mol. Life Sci. *57*, 25–40.

Anothaisintawee, T., Wiratkapun, C., Lerdsitthichai, P., Kasamesup, V., Wongwaisayawan, S., Srinakarin, J., Hirunpat, S., Woodtichartpreecha, P., Boonlikit, S., Teerawattananon, Y., et al. (2013). Risk Factors of Breast Cancer. Asia Pacific J. Public Heal. *25*, 368–387.

Antika, L.D., Lee, E.-J., Kim, Y.-H., Kang, M.-K., Park, S.-H., Kim, D.Y., Oh, H., Choi, Y.-J., and Kang, Y.-H. (2017). Dietary phlorizin enhances osteoblastogenic bone formation through enhancing β-catenin activity via GSK-3β inhibition in a model of senile osteoporosis. J. Nutr. Biochem. *49*, 42–52.

Antonopoulou, I., Varriale, S., Topakas, E., Rova, U., Christakopoulos, P., and Faraco, V. (2016). Enzymatic synthesis of bioactive compounds with high potential for cosmeceutical application. Appl. Microbiol. Biotechnol. *100*, 6519–6543.

Aqil, F., Munagala, R., Jeyabalan, J., and Vadhanam, M. V (2013). Bioavailability of phytochemicals and its enhancement by drug delivery systems. Cancer Lett. *334*, 133–141.

Araki, K., and Miyoshi, Y. (2018). Mechanism of resistance to endocrine therapy in breast cancer: the important role of PI3K/Akt/mTOR in estrogen receptor-positive, HER2-negative breast cancer. Breast Cancer *25*, 392–401.

De Araújo, M.E.M.B., Franco, Y.E.M., Messias, M.C.F., Longato, G.B., Pamphile, J.A., and Carvalho, P.D.O. (2017). Biocatalytic Synthesis of Flavonoid Esters by Lipases and Their Biological Benefits. Planta Med. 7–22.

Arcaro, A., and Guerreiro, A.S. (2007). The phosphoinositide 3-kinase pathway in human cancer: genetic alterations and therapeutic implications. Curr. Genomics *8*, 271–306.

Archer, D.F. (2013). The importance of pharmacokinetic studies in drug development. Contraception *87*, 701–702.

Ardhaoui, M., Falcimaigne, A., Engasser, J.-M., Moussou, P., Pauly, G., and Ghoul, M. (2004). Acylation of natural flavonoids using lipase of Candida antarctica as biocatalyst. J. Mol. Catal. B Enzym. *29*, 63–67.

Ardito, F., Giuliani, M., Perrone, D., Troiano, G., and Lo Muzio, L. (2017). The crucial role of protein phosphorylation in cell signaling and its use as targeted therapy (Review). Int. J. Mol. Med. *40*, 271–280.

Arnold, C., Konkel, A., Fischer, R., and Schunck, W.-H. (2010). Cytochrome P450-dependent metabolism of w-6 and w-3 long-chain polyunsaturated fatty acids. Pharmacol. Reports *62*, 535–547.

Arnold, K.M., Pohlig, R.T., and Sims-Mourtada, J. (2017). Co-activation of Hedgehog and Wnt signaling pathways is associated with poor outcomes in triple negative breast cancer. Oncol. Lett. *14*, 5285–5292.

Arumuggam, N., Melong, N., Too, C.K., Berman, J.N., and Rupasinghe, H.P.V. (2017). Phloridzin docosahexaenoate, a novel flavonoid derivative, suppresses growth and induces apoptosis in T-cell acute lymphoblastic leukemia cells. Am J Cancer Res *7*, 2452–2464.

Bach, A., Bender-Sigel, J., Schrenk, D., Flügel, D., and Kietzmann, T. (2010). The antioxidant quercetin inhibits cellular proliferation via HIF-1-dependent induction of p21WAF. Antioxid. Redox Signal. *13*, 437–448.

Balasubramanian, R., and Zhang, X. (2016). Mechanisms of FGF gradient formation during embryogenesis. Semin. Cell Dev. Biol. *53*, 94–100.

Balko, J.M., Cook, R.S., Vaught, D.B., Kuba, M.G., Miller, T.W., Bhola, N.E., Sanders, M.E., Granja-Ingram, N.M., Smith, J.J., Meszoely, I.M., et al. (2012). Profiling of residual breast cancers after neoadjuvant chemotherapy identifies DUSP4 deficiency as a mechanism of drug resistance. Nat. Med. *18*, 1052–1059.

Balogh, E.P., Ganz, P.A., Murphy, S.B., Nass, S.J., Ferrell, B.R., and Stovall, E. (2011). Patient-centered cancer treatment planning: improving the quality of oncology care. Summary of an Institute of Medicine workshop. Oncologist *16*, 1800–1805.

Ban, C., Park, S.J., Lim, S., Choi, S.J., and Choi, Y.J. (2015). Improving Flavonoid Bioaccessibility using an Edible Oil-Based Lipid Nanoparticle for Oral Delivery. J. Agric. Food Chem. *63*, 5266–5272.

Bandaruk, Y., Mukai, R., and Terao, J. (2014). Cellular uptake of quercetin and luteolin and their effects on monoamine oxidase-A in human neuroblastoma SH-SY5Y cells. Toxicol. Reports *1*, 639–649.

Banyard, J., and Bielenberg, D.R. (2015). The role of EMT and MET in cancer dissemination. Connect. Tissue Res. *56*, 403–413.

Bao, B., Mitrea, C., Wijesinghe, P., Marchetti, L., Girsch, E., Farr, R.L., Boerner, J.L., Mohammad, R., Dyson, G., Terlecky, S.R., et al. (2017). Treating triple negative breast cancer cells with erlotinib plus a select antioxidant overcomes drug resistance by targeting cancer cell heterogeneity. Sci. Rep. *7*, 44125.

Bao, W., Thullberg, M., Zhang, H., Onischenko, A., and Strömblad, S. (2002). Cell attachment to the extracellular matrix induces proteasomal degradation of p21(CIP1) via Cdc42/Rac1 signaling. Mol. Cell. Biol. *22*, 4587–4597.

Bar-Sagi, D., and Hall, A. (2000). Ras and Rho GTPases: a family reunion. Cell *103*, 227–238.

Bassino, E., Antoniotti, S., Gasparri, F., and Munaron, L. (2016). Effects of flavonoid derivatives on human microvascular endothelial cells. Nat. Prod. Res. *30*, 2831–2834.

Batlle, E., and Clevers, H. (2017). Cancer stem cells revisited. Nat. Med. *23*, 1124–1134.

Batra, P., and Sharma, A.K. (2013). Anti-cancer potential of flavonoids: recent trends and future perspectives. 3 Biotech *3*, 439–459.

Bauer, K.S., Cude, K.J., Dixon, S.C., Kruger, E.A., and Figg, W.D. (2000). Carboxyamido-triazole Inhibits Angiogenesis by Blocking the Calcium-Mediated Nitric-Oxide Synthase-Vascular Endothelial Growth Factor Pathway. J. Pharmacol. Exp. Ther. *292*, 31–37.

Beck, C., Schreiber, H., and Rowley, D.A. (2001). Role of TGF-beta in immune-evasion of cancer. Microsc. Res. Tech. *52*, 387–395.

Bedard, P.L., Hansen, A.R., Ratain, M.J., and Siu, L.L. (2013). Tumour heterogeneity in the clinic. Nature *501*, 355–364.

Beenken, A., and Mohammadi, M. (2009). The FGF family: biology, pathophysiology and therapy. Nat. Rev. Drug Discov. *8*, 235–253.

Béliveau, R., Gingras, D., Kruger, E.A., Lamy, S., Sirois, P., Simard, B., Sirois, M.G., Tranqui, L., Baffert, F., Beaulieu, E., et al. (2002). The antiangiogenic agent neovastat (AE-941) inhibits vascular endothelial growth factor-mediated biological effects. Clin. Cancer Res. *8*, 1242–1250.

Benet, L.Z. (1993). The Role of Pharmacokinetics in the Drug Development Process. In Integration of Pharmacokinetics, Pharmacodynamics, and Toxicokinetics in Rational Drug Development, (Boston, MA: Springer US), pp. 115–123.

Bennett, R.N., and Wallsgrove, R.M. (1994). Secondary metabolites in plant defence mechanisms. New Phytol. *127*, 617–633.

Berridge, M. V, Herst, P.M., and Tan, A.S. (2005). Tetrazolium dyes as tools in cell biology: new insights into their cellular reduction. Biotechnol. Annu. Rev. *11*, 127–152.

Bhola, N.E., Balko, J.M., Dugger, T.C., Kuba, M.G., Sánchez, V., Sanders, M., Stanford, J., Cook, R.S., and Arteaga, C.L. (2013). TGF-β inhibition enhances chemotherapy action against triple-negative breast cancer. J. Clin. Invest. *123*, 1348–1358.

Bhowmick, N.A., Ghiassi, M., Bakin, A., Aakre, M., Lundquist, C.A., Engel, M.E., Arteaga, C.L., and Moses, H.L. (2001). Transforming growth factor-beta1 mediates epithelial to mesenchymal transdifferentiation through a RhoA-dependent mechanism. Mol. Biol. Cell *12*, 27–36.

Bhowmick, N.A., Neilson, E.G., and Moses, H.L. (2004). Stromal fibroblasts in cancer initiation and progression. Nature *432*, 332–337.

Bi, H., Li, S., Qu, X., Wang, M., Bai, X., Xu, Z., Ao, X., Jia, Z., Jiang, X., Yang, Y., et al. (2015). DEC1 regulates breast cancer cell proliferation by stabilizing cyclin E protein and delays the progression of cell cycle S phase. Cell Death Dis. *6*, e1891–e1891.

Bielenberg, D.R., and Zetter, B.R. (2015). The Contribution of Angiogenesis to the Process of Metastasis. Cancer J. *21*, 267–273.

Björnström, L., and Sjöberg, M. (2005). Mechanisms of Estrogen Receptor Signaling: Convergence of Genomic and Nongenomic Actions on Target Genes. Mol. Endocrinol. *19*, 833–842.

Blind, R.D., Sablin, E.P., Kuchenbecker, K.M., Chiu, H.-J., Deacon, A.M., Das, D., Fletterick, R.J., and Ingraham, H.A. (2014). The signaling phospholipid PIP3 creates a new interaction surface on the nuclear receptor SF-1. Proc. Natl. Acad. Sci. U. S. A. *111*, 15054–15059.

Boersma, M.G., van der Woude, H., Bogaards, J., Boeren, S., Vervoort, J., Cnubben, N.H.P., van Iersel, M.L.P.S., van Bladeren, P.J., and Rietjens, I.M.C.M. (2002). Regioselectivity of phase II metabolism of luteolin and quercetin by UDP-glucuronosyl transferases. Chem. Res. Toxicol. *15*, 662–670.

Bokkenheuser, V.D., Shackletont, C.H.L., and Winter, J. (1987). Hydrolysis of dietary flavonoid glycosides by strains of intestinal Bacteroides from humans. Biochem. J *248*, 953–956.

Bolli, A., Marino, M., Rimbach, G., Fanali, G., Fasano, M., and Ascenzi, P. (2010). Flavonoid binding to human serum albumin. Biochem. Biophys. Res. Commun. *398*, 444–449.

Borah, N., Gunawardana, S., Torres, H., McDonnell, S., and Van Slambrouck, S. (2017). 5,6,7,3′,4′,5′-Hexamethoxyflavone inhibits growth of triple-negative breast cancer cells via suppression of MAPK and Akt signaling pathways and arresting cell cycle. Int. J. Oncol. *51*, 1685–1693.

Bornstein, P. (2009). Thrombospondins function as regulators of angiogenesis. J. Cell Commun. Signal. *3*, 189–200.

Boucher, Y., Lee, I., and Jain, R.K. (1995). Lack of General Correlation between Interstitial Fluid Pressure and Oxygen Partial Pressure in Solid Tumors. Microvasc. Res. *50*, 175–182.

Bourgaud, F., Gravot, A., Milesi, S., and Gontier, E. (2001). Production of plant secondary metabolites: a historical perspective. Plant Sci. *161*, 839–851.

Bower, J.J., Vance, L.D., Psioda, M., Smith-Roe, S.L., Simpson, D.A., Ibrahim, J.G., Hoadley, K.A., Perou, C.M., and Kaufmann, W.K. (2017). Patterns of cell cycle checkpoint deregulation associated with intrinsic molecular subtypes of human breast cancer cells. Npj Breast Cancer *3*, 1–9.

Boyd, P.J., Doyle, J., Gee, E., Pallan, S., and Haas, T.L. (2005). MAPK signaling regulates endothelial cell assembly into networks and expression of MT1-MMP and MMP-2. Am. J. Physiol. Physiol. *288*, C659–C668.

Brabletz, T., Kalluri, R., Nieto, M.A., and Weinberg, R.A. (2018). EMT in cancer. Nat. Rev. Cancer *18*, 128–134.

Brand, A., Bauer, N.G., Hallott, A., Goldbaum, O., Ghebremeskel, K., Reifen, R., and Richter-Landsberg, C. (2010). Membrane lipid modification by polyunsaturated fatty acids sensitizes oligodendroglial OLN-93 cells against oxidative stress and promotes up-regulation of heme oxygenase-1 (HSP32). J. Neurochem. *113*, 465–476.

Le Bras, G.F., Taubenslag, K.J., and Andl, C.D. (2012). The regulation of cell-cell adhesion during epithelial-mesenchymal transition, motility and tumor progression. Cell Adh. Migr. *6*, 365–373.

Brater, D.C. (2002). Measurement of renal function during drug development. Br. J. Clin. Pharmacol. *54*, 87–95.

Brito, A., Ribeiro, M., Abrantes, A., Pires, A., Teixo, R., Tralhao, J., and Botelho, M. (2015). Quercetin in Cancer Treatment, Alone or in Combination with Conventional Therapeutics? Curr. Med. Chem. *22*, 3025–3039.

Broadley, K.N., Aquino, A.M., Woodward, S.C., Buckley-Sturrock, A., Sato, Y., Rifkin, D.B., and Davidson, J.M. (1989). Monospecific antibodies implicate basic fibroblast growth factor in normal wound repair. Lab. Invest. *61*, 571–575.

Brooks, P.C. (1996). Cell adhesion molecules in angiogenesis. Cancer Metastasis Rev. *15*, 187–194.

Brownson, D.M., Azios, N.G., Fuqua, B.K., Dharmawardhane, S.F., and Mabry, T.J. (2002). Flavonoid Effects Relevant to Cancer. J. Nutr. *132*, 3482S–3489S.

Bryan, B.A., and D'Amore, P.A. (2007). What tangled webs they weave: Rho-GTPase control of angiogenesis. Cell. Mol. Life Sci. *64*, 2053–2065.

Buchholz, T.A., Mittendorf, E.A., and Hunt, K.K. (2015). Surgical Considerations After Neoadjuvant Chemotherapy: Breast Conservation Therapy. JNCI Monogr. *2015*, 11–14.

Buckley, J.D., and Howe, P.R.C. (2010). Long-Chain Omega-3 Polyunsaturated Fatty Acids May Be Beneficial for Reducing Obesity—A Review. Nutrients *2*, 1212–1230.

Burbelo, P., Wellstein, A., and Pestell, R.G. (2004). Altered Rho GTPase Signaling Pathways in Breast Cancer Cells. Breast Cancer Res. Treat. *84*, 43–48.

Burney, I.A., and Al-Moundhri, M.S. (2008). Major Advances in the Treatment of Cancer: What does a Non-Oncologist need to know? Sultan Qaboos Univ. Med. J. *8*, 137–148.

de Caestecker, M.P., Piek, E., and Roberts, A.B. (2000). Role of Transforming Growth Factor-beta Signaling in Cancer. J. Natl. Cancer Inst. *92*, 1388–1402.

Caldon, E., Daly, R.J., Sutherland, R.L., and Musgrove, E.A. (2006). Cell Cycle Control in Breast Cancer Cells. J. Cell. Biochem. J. Cell. Biochem *97*, 261–274.

Callahan, R., and Hurvitz, S. (2011). Human epidermal growth factor receptor-2-positive breast cancer: Current management of early, advanced, and recurrent disease. Curr. Opin. Obstet. Gynecol. *23*, 37–43.

Campos-Vega, R., and Oomah, B.D. (2013). Chemistry and classification of phytochemicals. In Handbook of Plant Food Phytochemicals, (Oxford: John Wiley & Sons Ltd), pp. 5–48.

Campuzano, S., Pedrero, M., and Pingarrón, J.M. (2017). Non-Invasive Breast Cancer Diagnosis through Electrochemical Biosensing at Different Molecular Levels. Sensors *17*, 1–23.

Canadian Cancer Statistics (2017a). Canadian Cancer Statistics. Can. Cancer Soc.

Canadian Cancer Statistics (2017b). Canadian Cancer Society's Advisory Committee on Cancer Statistics. (2017). Toronto, ON: Canadian Cancer Society.

Cancer Genome Atlas Network (2012). Comprehensive molecular portraits of human breast tumours. Nature *490*, 61–70.

Canuto, R.A., Biocca, M.E., Muzio, G., and Dianzani, M.U. (1989). Fatty acid composition of phospholipids in mitochondria and microsomes during diethylnitrosamine carcinogenesis in rat liver. Cell Biochem. Funct. *7*, 11–19.

Cao, Y. (2016). Future options of anti-angiogenic cancer therapy. Chin. J. Cancer *35*, 21.

Carey, L.A., Dees, E.C., Sawyer, L., Gatti, L., Moore, D.T., Collichio, F., Ollila, D.W., Sartor, C.I., Graham, M.L., and Perou, C.M. (2007). The Triple Negative Paradox: Primary Tumor Chemosensitivity of Breast Cancer Subtypes. Hum. Canacer Biol. *13*, 2329–2334.

Casamayor, A., Morrice, N.A., and Alessi, D.R. (1999). Phosphorylation of Ser-241 is essential for the activity of 3-phosphoinositide-dependent protein kinase-1: identification of five sites of phosphorylation in vivo. Biochem. J. *342*, 287–292.

Castañeda-Gill, J.M., and Vishwanatha, J.K. (2016). Antiangiogenic mechanisms and factors in breast cancer treatment. J. Carcinog. *15*, 1.

Cerezo, A.B., Winterbone, M.S., Moyle, C.W.A., Needs, P.W., and Kroon, P.A. (2015). Molecular structure-function relationship of dietary polyphenols for inhibiting VEGF-induced VEGFR-2 activity. Mol. Nutr. Food Res. *59*, 2119–2131.

Chabane, M.N., Ahmad, A. Al, Peluso, J., Muller, C.D., and Ubeaud-Séquier, G. (2009). Quercetin and naringenin transport across human intestinal Caco-2 cells. J. Pharm. Pharmacol. *61*, 1473–1483.

Chaffer, C.L., and Weinberg, R.A. (2011). A Perspective on Cancer Cell Metastasis. Science (80-. ). *331*, 1559–1564.

Chalakur-Ramireddy, N.K.R., and Pakala, S.B. (2018). Combined drug therapeutic strategies for the effective treatment of Triple Negative Breast Cancer. Biosci. Rep. *38*, 1–14.

Chalhoub, N., and Baker, S.J. (2009). PTEN and the PI3-kinase pathway in cancer. Annu. Rev. Pathol. *4*, 127–150.

Chambers, A.F., Groom, A.C., and MacDonald, I.C. (2002). Metastasis: Dissemination and growth of cancer cells in metastatic sites. Nat. Rev. Cancer *2*, 563–572.

Chang, J.C. (2016). Cancer stem cells. Medicine (Baltimore). *95*, S20–S25.

Chang, R., Zhang, P., and You, J. (2016). Post-translational modifications of EMT transcriptional factors in cancer metastasis. Open Life Sci. *11*, 237–243.

Chang, Y., Chi, C., and Wang, J. (2009). Reactive Oxygen Species Production Is Involved in Quercetin-Induced Apoptosis in Human Hepatoma Cells Reactive Oxygen Species Production Is Involved in Quercetin-Induced Apoptosis in Human Hepatoma Cells. Nutr. Cancer *55*, 201–209.

Chap, C., and Patel, J. (2011). A decade of progress in cancer research. BMC Cancer *11*, 498.

Chebil, L., Humeau, C., Falcimaigne, A., Engasser, J.-M., and Ghoul, M. (2006). Enzymatic acylation of flavonoids. Process Biochem. *41*, 2237–2251.

Chebil, L., Anthoni, J., Humeau, C., Gerardin, C., Engasser, J.-M., and Ghoul, M. (2007). Enzymatic Acylation of Flavonoids: Effect of the Nature of the Substrate, Origin of Lipase, and Operating Conditions on Conversion Yield and Regioselectivity. J. Agric. Food Chem. *55*, 9496–9502.

Chellappan, S.P., Hiebert, S., Mudryj, M., Horowitz, J.M., and Nevins, J.R. (1991). The E2F transcription factor is a cellular target for the RB protein. Cell *65*, 1053–1061.

Chen, H., and Liu, R.H. (2018). Potential Mechanisms of Action of Dietary Phytochemicals for Cancer Prevention by Targeting Cellular Signaling Transduction Pathways. J. Agric. Food Chem. *66*, 3260–3276.

Chen, J., Chang, H., Peng, X., Gu, Y., Yi, L., Zhang, Q., Zhu, J., and Mi, M. (2016). 3,6-dihydroxyflavone suppresses the epithelial-mesenchymal transition in breast cancer cells by inhibiting the Notch signaling pathway. Sci. Rep. *6*, 28858.

Chen, K., Huang, Y., and Chen, J. (2013). Understanding and targeting cancer stem cells: therapeutic implications and challenges. Acta Pharmacol. Sin. *34*, 732–740.

Chen, X., Lowe, M., Herliczek, T., Hall, M.J., Danes, C., Lawrence, D.A., and Keyomarsi, K. (2000). Protection of Normal Proliferating Cells Against Chemotherapy by Staurosporine-Mediated, Selective, and Reversible G1 Arrest. J. Natl. Cancer Inst. *92*, 1999–2008.

Chiang, G.G., and Abraham, R.T. (2005). Phosphorylation of mammalian target of rapamycin (mTOR) at Ser-2448 is mediated by p70S6 kinase. J. Biol. Chem. *280*, 25485–25490.

Chiang, L.-C., Ng, L.T., Lin, I.-C., Kuo, P.-L., and Lin, C.-C. (2006). Anti-proliferative effect of apigenin and its apoptotic induction in human Hep G2 cells. Cancer Lett. *237*, 207–214.

Chiang, S.P.H., Cabrera, R.M., and Segall, J.E. (2016). Tumor cell intravasation. Am. J. Physiol. Cell Physiol. *311*, C1–C14.

Cho, R.J., Huang, M., Campbell, M.J., Dong, H., Steinmetz, L., Sapinoso, L., Hampton, G., Elledge, S.J., Davis, R.W., and Lockhart, D.J. (2001). Transcriptional regulation and function during the human cell cycle. Nat. Genet. *27*, 48–54.

Choi, S.U., Ryu, S.Y., Yoon, S.K., Jung, N.P., Park, S.H., Kim, K.H., Choi, E.J., and Lee, C.O. (1999). Effects of flavonoids on the growth and cell cycle of cancer cells. Anticancer Res. *19*, 5229–5233.

Choi, Y.K., Woo, S.-M., Cho, S.-G., Moon, H.E., Yun, Y.J., Kim, J.W., Noh, D.-Y., Jang, B.H., Shin, Y.C., Kim, J.-H., et al. (2013). Brain-metastatic triple-negative breast cancer cells regain growth ability by altering gene expression patterns. Cancer Genomics Proteomics *10*, 265–275.

Christinger, H.W., Fuh, G., de Vos, A.M., and Wiesmann, C. (2004). The crystal structure of placental growth factor in complex with domain 2 of vascular endothelial growth factor receptor-1. J. Biol. Chem. *279*, 10382–10388.

Christopoulos, P.F., Msaouel, P., and Koutsilieris, M. (2015). The role of the insulin-like growth factor-1 system in breast cancer. Mol. Cancer *14*, 43.

Chu, X., Bleasby, K., Chan, G.H., Nunes, I., and Evers, R. (2016). The Complexities of Interpreting Reversible Elevated Serum Creatinine Levels in Drug Development: Does a Correlation with Inhibition of Renal Transporters Exist? Drug Metab. Dispos. *44*, 1498–1509.

Chua, Y.L., Dufour, E., Dassa, E.P., Rustin, P., Jacobs, H.T., Taylor, C.T., and Hagen, T. (2010). Stabilization of Hypoxia-inducible Factor-1α Protein in Hypoxia Occurs Independently of Mitochondrial Reactive Oxygen Species Production. J. Biol. Chem. *285*, 31277–31284.

Clark, A.G., and Vignjevic, D.M. (2015). Modes of cancer cell invasion and the role of the microenvironment. Curr. Opin. Cell Biol. *36*, 13–22.

Cobb, M.H., and Goldsmith, E.J. (1995). How MAP kinases are regulated. J. Biol. Chem. *270*, 14843–14846.

Coleman, M.L., and Olson, M.F. (2004). Ras and Rho GTPases in G1-phase cell-cycle regulation. Nat. Rev. Mol. Cell Biol. *5*, 355–366.

Coman, D.R., and Anderson, T.F. (1955). A Structural Difference between the Surfaces of Normal. Cancer Res. *15*, 541–543.

Compagni, A., Wilgenbus, P., Impagnatiello, M.A., Cotten, M., and Christofori, G. (2000). Fibroblast growth factors are required for efficient tumor angiogenesis. Cancer Res. *60*, 7163–7169.

Conklin, K.A. (2000). Dietary antioxidants during cancer chemotherapy: impact on chemotherapeutic effectiveness and development of side effects. Nutr. Cancer *37*, 1–18.

Crespy, V., Aprikian, O., Morand, C., Besson, C., Manach, C., Demigné, C., and Rémésy, C. (2001). Bioavailability of Phloretin and Phloridzin in Rats. J. Nutr. *131*, 3227–3230.

Cybulski, C., Kluźniak, W., Huzarski, T., Wokołorczyk, D., Kashyap, A., Jakubowska, A., Szwiec, M., Byrski, T., Dębniak, T., Górski, B., et al. (2015). Clinical outcomes in women with breast cancer and a PALB2 mutation: a prospective cohort analysis. Lancet. Oncol. *16*, 638–644.

D'Andrea, G.M. (2005). Use of Antioxidants During Chemotherapy and Radiotherapy Should Be Avoided. CA. Cancer J. Clin. *55*, 319–321.

D'Eliseo, D., and Velotti, F. (2016). Omega-3 Fatty Acids and Cancer Cell Cytotoxicity: Implications for Multi-Targeted Cancer Therapy. J. Clin. Med. *5*, 15.

D 'angelo, G., Strumant, I., Martialt, J., Weiner, R.I., and Prusiner, S.B. (1995). Activation of mitogen-activated protein kinases by vascular endothelial growth factor and basic fibroblast growth factor in capillary endothelial cells is inhibited by the antiangiogenic factor 16-kDa N-terminal fragment of prolactin. Cell Biol. *92*, 6374–6378.

Dagogo-Jack, I., and Shaw, A.T. (2017). Tumour heterogeneity and resistance to cancer therapies. Nat. Rev. Clin. Oncol. *15*, 81–94.

Dang, D., and Peng, Y. (2013). Roles of p53 and p16 in triple-negative breast cancer. Breast Cancer Manag. *2*, 537–544.

Dangles, O., Dufour, C., Manach, C., Morand, C., and Remesy, C. (2001). Binding of flavonoids to plasma proteins. Methods Enzymol. *335*, 319–333.

David, M., Petit, D., and Bertoglio, J. (2012). Cell cycle regulation of Rho signaling pathways. Cell Cycle *11*, 3003–3010.

Davion, S., Sullivan, M., Rohan, S., and Siziopikou, K.P. (2012). p53 Expression in Triple Negative Breast Carcinomas: Evidence of Age-Related and Racial Differences *. J. Cancer Ther. *3*, 649–654.

Day, A.J., Cañada, F.J., Díaz, J.C., Kroon, P.A., Mclauchlan, R., Faulds, C.B., Plumb, G.W., Morgan, M.R., and Williamson, G. (2000a). Dietary flavonoid and isoflavone glycosides are hydrolysed by the lactase site of lactase phlorizin hydrolase. FEBS Lett. *468*, 166–170.

Day, A.J., Bao, Y., Morgan, M.R.., and Williamson, G. (2000b). Conjugation position of quercetin glucuronides and effect on biological activity. Free Radic. Biol. Med. *29*, 1234–1243.

Day, M.L., Zhao, X., Vallorosi, C.J., Putzi, M., Powell, C.T., Lin, C., and Day, K.C. (1999). E-cadherin mediates aggregation-dependent survival of prostate and mammary epithelial cells through the retinoblastoma cell cycle control pathway. J. Biol. Chem. *274*, 9656–9664.

Dell'Eva, R., Pfeffer, U., Indraccolo, S., Albini, A., and Noonan, D. (2002). Inhibition of tumor angiogenesis by angiostatin: from recombinant protein to gene therapy. Endothelium *9*, 3–10.

Demicheli, R., Retsky, M.W., Hrushesky, W.J.M., Baum, M., and Gukas, I.D. (2008). The effects of surgery on tumor growth: a century of investigations. Ann. Oncol. *19*, 1821–1828.

Demo, S.D., Kikuchi, A., Peters, K.G., MacNicol, A.M., Muslin, A.J., and Williams, L.T. (1994). Signaling molecules that mediate the actions of FGF. Princess Takamatsu Symp. *24*, 243–249.

Dennis, P.A., Kastan, M.B., Savarese, D., Hsieh, C., Stewart, F., Canman, C., Kastan, M., Reed, J., Roussel, M., O'Connor, R., et al. (1998). Cellular survival pathways and resistance to cancer therapy. Drug Resist. Updat. *1*, 301–309.

Dent, S.F. (2009). The role of VEGF in triple-negative breast cancer: where do we go from here? Ann. Oncol. *20*, 1615–1617.

Dent, R., Hanna, W.M., Trudeau, M., Rawlinson, E., Sun, P., and Narod, S.A. (2009). Pattern of metastatic spread in triple-negative breast cancer. Breast Cancer Res. Treat. *115*, 423–428.

Derynck, R., Akhurst, R.J., and Balmain, A. (2001). Erratum: TGF-β signaling in tumor suppression and cancer progression. Nat. Genet. *29*, 117–129.

Dey, N., Barwick, B.G., Moreno, C.S., Ordanic-Kodani, M., Chen, Z., Oprea-Ilies, G., Tang, W., Catzavelos, C., Kerstann, K.F., Sledge, G.W., et al. (2013). Wnt signaling in triple negative breast cancer is associated with metastasis. BMC Cancer *13*, 537.

Dey, N., De, P., and Leyland-Jones, B. (2017). PI3K-AKT-mTOR inhibitors in breast cancers: From tumor cell signaling to clinical trials. Pharmacol. Ther. *175*, 91–106.

Dimmeler, S., Zeiher, A.M., and Cardiology, M. (2000). Akt Takes Center Stage in Angiogenesis Signaling. Circ Res *86*, 4–5.

Dimova, D.K., and Dyson, N.J. (2005). The E2F transcriptional network: old acquaintances with new faces. Oncogene *24*, 2810–2826.

Ding, V.W., Chen, R.H., and McCormick, F. (2000). Differential regulation of glycogen synthase kinase 3beta by insulin and Wnt signaling. J. Biol. Chem. *275*, 32475–32481.

Ding, Z., Liang, J., Li, J., Lu, Y., Ariyaratna, V., Lu, Z., Davies, M.A., Westwick, J.K., and Mills, G.B. (2010). Physical Association of PDK1 with AKT1 Is Sufficient for Pathway Activation Independent of Membrane Localization and Phosphatidylinositol 3 Kinase. PLoS One *5*, e9910.

Diniz, C., Suliburska, J., and Ferreira, I.M.P.L.V.O. (2017). New insights into the antiangiogenic and proangiogenic properties of dietary polyphenols. Mol. Nutr. Food Res. *61*, 1600912.

Dippel, V., Milde-Langosch, K., Wicklein, D., Schumacher, U., Altevogt, P., Oliveira-Ferrer, L., Jänicke, F., and Schröder, C. (2013). Influence of L1-CAM expression of breast cancer cells on adhesion to endothelial cells. J. Cancer Res. Clin. Oncol. *139*, 107–121.

Dominguez-Sola, D., Ying, C.Y., Grandori, C., Ruggiero, L., Chen, B., Li, M., Galloway, D.A., Gu, W., Gautier, J., and Dalla-Favera, R. (2007). Non-transcriptional control of DNA replication by c-Myc. Nature *448*, 445–451.

Dong, P., Zhang, C., Parker, B.-T., You, L., and Mathey-Prevot, B. (2018). Cyclin D/CDK4/6 activity controls G1 length in mammalian cells. PLoS One *13*, e0185637.

Doo, T., and Maskarinec, G. (2014). Polyphenols and Breast Cancer Prevention. In Polyphenols in Human Health and Disease, (Elsevier), pp. 1331–1340.

Dormond-Meuwly, A., Roulin, D., Dufour, M., Benoit, M., Demartines, N., and Dormond, O. (2011). The inhibition of MAPK potentiates the anti-angiogenic efficacy of mTOR inhibitors. Biochem. Biophys. Res. Commun. *407*, 714–719.

Doucette, C.D., Hilchie, A.L., Liwski, R., and Hoskin, D.W. (2013). Piperine, a dietary phytochemical, inhibits angiogenesis. J. Nutr. Biochem. *24*, 231–239.

Dudka, A.A., Sweet, S.M.M., and Heath, J.K. (2010). Signal transducers and activators of transcription-3 binding to the fibroblast growth factor receptor is activated by receptor amplification. Cancer Res. *70*, 3391–3401.

Duivenvoorden, W.C., Hirte, H.W., and Singh, G. (1999). Transforming growth factor beta1 acts as an inducer of matrix metalloproteinase expression and activity in human bone-metastasizing cancer cells. Clin. Exp. Metastasis *17*, 27–34.

Duttaroy, A., and Basak, S. (2012). Docosahexaenoic acid and angiogenesis: a role in early placentation. Clin. Lipidol. ISSN *7*, 303–312.

Eason, C.T., Bonner, F.W., and Parke, D. V. (1990). The importance of pharmacokinetic and receptor studies in drug safety evaluation. Regul. Toxicol. Pharmacol. *11*, 288–307.

Easton, D.F., Pharoah, P.D.P., Antoniou, A.C., Tischkowitz, M., Tavtigian, S. V., Nathanson, K.L., Devilee, P., Meindl, A., Couch, F.J., Southey, M., et al. (2015). Gene-Panel Sequencing and the Prediction of Breast-Cancer Risk. N. Engl. J. Med. *372*, 2243–2257.

Ebeid, S.A., Abd El Moneim, N.A., El-Benhawy, S.A., Hussain, N.G., and Hussain, M.I. (2016). Assessment of the radioprotective effect of propolis in breast cancer patients undergoing radiotherapy. New perspective for an old honey bee product. J. Radiat. Res. Appl. Sci. *9*, 431–440.

Ebi, H., Costa, C., Faber, A.C., Nishtala, M., Kotani, H., Juric, D., Della Pelle, P., Song, Y., Yano, S., Mino-Kenudson, M., et al. (2013). PI3K regulates MEK/ERK signaling in breast cancer via the Rac-GEF, P-Rex1. Proc. Natl. Acad. Sci. U. S. A. *110*, 21124–21129.

Edlund, S., Landström, M., Heldin, C.-H., and Aspenström, P. (2002). Transforming growth factor-beta-induced mobilization of actin cytoskeleton requires signaling by small GTPases Cdc42 and RhoA. Mol. Biol. Cell *13*, 902–914.

Elmore, S. (2007). Apoptosis: a review of programmed cell death. Toxicol. Pathol. *35*, 495–516.

Elumalai, P., Arunkumar, R., Benson, C.S., Sharmila, G., and Arunakaran, J. (2014). Nimbolide inhibits IGF-I-mediated PI3K/Akt and MAPK signalling in human breast cancer cell lines (MCF-7 and MDA-MB-231). Cell Biochem. Funct. *32*, 476–484.

Epriliati, I., and Ginjom, I.R. (2012). Bioavailability of Phytochemicals. In Phytochemicals – A Global Perspective of Their Role in Nutrition and Health, V. Rao, ed. (InTech), pp. 401–428.

Eroles, P., Bosch, A., Pérez-Fidalgo, J.A., and Lluch, A. (2012). Molecular biology in breast cancer: intrinsic subtypes and signaling pathways. Cancer Treat. Rev. *38*, 698–707.

Esmaeili, V., Shahverdi, A.H., Moghadasian, M.H., and Alizadeh, A.R. (2015). Dietary fatty acids affect semen quality: a review. Andrology *3*, 450–461.

Evdokimova, V., Tognon, C., Ng, T., and Sorensen, P.H.B. (2009). Reduced proliferation and enhanced migration: Two sides of the same coin? Molecular mechanisms of metastatic progression by YB-1. Cell Cycle *8*, 2901–2906.

Fabian, C.J., Kimler, B.F., Phillips, T.A., Nydegger, J.L., Kreutzjans, A.L., Carlson, S.E., Hidaka, B.H., Metheny, T., Zalles, C.M., Mills, G.B., et al. (2015a). Modulation of Breast Cancer Risk Biomarkers by High-Dose Omega-3 Fatty Acids: Phase II Pilot Study in Postmenopausal Women. Cancer Prev. Res. (Phila). *8*, 922–931.

Fabian, C.J., Kimler, B.F., and Hursting, S.D. (2015b). Omega-3 fatty acids for breast cancer prevention and survivorship. Breast Cancer Res. *17*, 62.

Fabris, V.T., Sahores, A., Vanzulli, S.I., Colombo, L., Molinolo, A.A., Lanari, C., and Lamb, C.A. (2010). Inoculated mammary carcinoma-associated fibroblasts: contribution to hormone independent tumor growth. BMC Cancer *10*, 293.

Fakhrejahani, E., and Toi, M. (2012). Tumor angiogenesis: pericytes and maturation are not to be ignored. J. Oncol. *2012*, 261750.

Falcon, B.L., Chintharlapalli, S., Uhlik, M.T., and Pytowski, B. (2016). Antagonist antibodies to vascular endothelial growth factor receptor 2 (VEGFR-2) as anti-angiogenic agents. Pharmacol. Ther. *164*, 204–225.

Fang, J., Xia, C., Cao, Z., Zheng, J.Z., Reed, E., and Jiang, B.-H. (2005). Apigenin inhibits VEGF and HIF-1 expression via PI3K/AKT/p70S6K1 and HDM2/p53 pathways. FASEB J. *19*, 342–353.

Fang, X., Yu, S.X., Lu, Y., Bast, R.C., Woodgett, J.R., and Mills, G.B. (2000). Phosphorylation and inactivation of glycogen synthase kinase 3 by protein kinase A. Proc. Natl. Acad. Sci. *97*, 11960–11965.

Faria, A., Pestana, D., Teixeira, D., Azevedo, J., Freitas, V., Mateus, N., and Calhau, C. (2010). Flavonoid transport across RBE4 cells: A blood-brain barrier model. Cell. Mol. Biol. Lett. *15*, 234–241.

Faria, A., Mateus, N., and Ao Calhau, C. (2012). Flavonoid transport across blood-brain barrier: Implication for their direct neuroprotective actions. Nutr. Aging *1*, 89–97.

Faria, A., Meireles, M., Fernandes, I., Santos-Buelga, C., Gonzalez-Manzano, S., Dueñas, M., de Freitas, V., Mateus, N., and Calhau, C. (2014). Flavonoid metabolites transport across a human BBB model. Food Chem. *149*, 190–196.

Fasolo, D., Bassani, V.L., and Teixeira, H.F. (2009). Development of topical nanoemulsions containing quercetin and 3-O-methylquercetin. Pharmazie *64*, 726–730.

Fatma, S., Talegaonkar, S., Iqbal, Z., Panda, A.K., Negi, L.M., Goswami, D.G., and Tariq, M. (2016). Novel flavonoid-based biodegradable nanoparticles for effective oral delivery of etoposide by P-glycoprotein modulation: an in vitro, ex vivo and in vivo investigations. Drug Deliv *23*, 1071–7544.

Fearnley, G.W., Smith, G.A., Abdul-Zani, I., Yuldasheva, N., Mughal, N.A., Homer-Vanniasinkam, S., Kearney, M.T., Zachary, I.C., Tomlinson, D.C., Harrison, M.A., et al. (2016). VEGF-A isoforms program differential VEGFR2 signal transduction, trafficking and proteolysis. Biol. Open *5*, 571–583.

Fedele, M., Cerchia, L., and Chiappetta, G. (2017). The Epithelial-to-Mesenchymal Transition in Breast Cancer: Focus on Basal-Like Carcinomas. Cancers (Basel). *9*, 134.

Felipe Lima, J., Nofech-Mozes, S., Bayani, J., and Bartlett, J. (2016). EMT in Breast Carcinoma—A Review. J. Clin. Med. *5*, 65.

Fer, M., Corcos, L., Dréano, Y., Plée-Gautier, E., Salaün, J.-P., Berthou, F., and Amet, Y. (2008a). Cytochromes P450 from family 4 are the main omega hydroxylating enzymes in humans: CYP4F3B is the prominent player in PUFA metabolism. J. Lipid Res. *49*, 2379–2389.

Fer, M., Dréano, Y., Lucas, D., Corcos, L., Salaün, J.-P., Berthou, F., and Amet, Y. (2008b). Metabolism of eicosapentaenoic and docosahexaenoic acids by recombinant human cytochromes P450. Arch. Biochem. Biophys. *471*, 116–125.

Fernández, P.L., Jares, P., Rey, M.J., Campo, E., and Cardesa, A. (1998). Cell cycle regulators and their abnormalities in breast cancer. J Clin Pathol Mol Pathol *51*, 305–309.

Fernando, W. (2014). Efficacy and safety of docosahexaenoic acid acylated phloridzin for treating triple negative breast cancer. Dalhousie University.

Fernando, W., Rupasinghe, H.P.V., and Hoskin, D.W. (2015). Regulation of Hypoxia-inducible Factor-1α and Vascular Endothelial Growth Factor Signaling by Plant Flavonoids. Mini Rev. Med. Chem. *15*, 479–489.

Fernando, W., Coombs, M.R.P., Hoskin, D.W., and Rupasinghe, H.P.V. (2016). Docosahexaenoic acid-acylated phloridzin, a novel polyphenol fatty acid ester derivative, is cytotoxic to breast cancer cells. Carcinogenesis *37*, 1004–1013.

Ferrara, N. (2001). Role of vascular endothelial growth factor in regulation of physiological angiogenesis. Am. J. Physiol. Physiol. *280*, C1358–C1366.

Finger, E.C., and Giaccia, A.J. (2010). Hypoxia, inflammation, and the tumor microenvironment in metastatic disease. Cancer Metastasis Rev. *29*, 285–293.

Fink, B.N., Steck, S.E., Wolff, M.S., Britton, J.A., Kabat, G.C., Schroeder, J.C., Teitelbaum, S.L., Neugut, A.I., and Gammon, M.D. (2006). Dietary Flavonoid Intake and Breast Cancer Risk among Women on Long Island. Am. J. Epidemiol. *165*, 514–523.

Fink, B.N., Steck, S.E., Wolff, M.S., Britton, J.A., Kabat, G.C., Gaudet, M.M., Abrahamson, P.E., Bell, P., Schroeder, J.C., Teitelbaum, S.L., et al. (2007). Dietary flavonoid intake and breast cancer survival among women on Long Island. Cancer Epidemiol. Biomarkers Prev. *16*, 2285–2292.

Finn, R.S., Dering, J., Conklin, D., Kalous, O., Cohen, D.J., Desai, A.J., Ginther, C., Atefi, M., Chen, I., Fowst, C., et al. (2009). PD 0332991, a selective cyclin D kinase 4/6 inhibitor, preferentially inhibits proliferation of luminal estrogen receptor-positive human breast cancer cell lines in vitro. Breast Cancer Res. *11*, R77.

Finn, R.S., Crown, J.P., Lang, I., Boer, K., Bondarenko, I.M., Kulyk, S.O., Ettl, J., Patel, R., Pinter, T., Schmidt, M., et al. (2015). The cyclin-dependent kinase 4/6 inhibitor palbociclib in combination with letrozole versus letrozole alone as first-line treatment of oestrogen receptor-positive, HER2-negative, advanced breast cancer (PALOMA-1/TRIO-18): a randomised phase 2 study. Lancet Oncol. *16*, 25–35.

Fischer, K.R., Durrans, A., Lee, S., Sheng, J., Li, F., Wong, S.T.C., Choi, H., El Rayes, T., Ryu, S., Troeger, J., et al. (2015). Epithelial-to-mesenchymal transition is not required for lung metastasis but contributes to chemoresistance. Nature *527*, 472–476.

Fitzmaurice, C., Dicker, D., Pain, A., Hamavid, H., Moradi-Lakeh, M., MacIntyre, M.F., Allen, C., Hansen, G., Woodbrook, R., Wolfe, C., et al. (2015). The Global Burden of Cancer 2013. JAMA Oncol. *1*, 505–527.

Fleming, J.M., Miller, T.C., Meyer, M.J., Ginsburg, E., and Vonderhaar, B.K. (2010). Local regulation of human breast xenograft models. J. Cell. Physiol. *224*, 795–806.

Folkman, J. (1971). Tumor Angiogenesis: Therapeutic Implications. N. Engl. J. Med. *285*, 1182–1186.

Folkman, J. (1990). What Is the Evidence That Tumors Are Angiogenesis Dependent? J. Natl. Cancer Inst. *82*, 4–6.

Folkman, J. (2002). Role of angiogenesis in tumor growth and metastasis. Semin. Oncol. *29*, 15–18.

Folkman, J., Cole, P., and Zimmerman, S. (1966). Tumor behavior in isolated perfused organs: in vitro growth and metastases of biopsy material in rabbit thyroid and canine intestinal segment. Ann. Surg. *164*, 491–502.

Foulkes, W.D., Smith, I.E., and Reis-Filho, J.S. (2010). Triple-Negative Breast Cancer. N. Engl. J. Med. *363*, 1938–1948.

von Fournier, D., Hoeffken, W., and Friedrich, M. (1989). Natural Growth Rate of Primary Breast Cancer and its Metastases. In Breast Diseases, (Berlin, Heidelberg: Springer Berlin Heidelberg), pp. 78–96.

Francia, G., Emmenegger, U., and Kerbel, R.S. (2009). Tumor-Associated Fibroblasts as "Trojan Horse" Mediators of Resistance to Anti-VEGF Therapy. Cancer Cell *15*, 3–5.

Friberg, S., and Nyström, A. (2015). Cancer Metastases: Early Dissemination and Late Recurrences. Cancer Growth Metastasis *8*, 43–49.

Friberg, E.G., Čunderlíková, B., Pettersen, E.O., and Moan, J. (2003). pH effects on the cellular uptake of four photosensitizing drugs evaluated for use in photodynamic therapy of cancer. Cancer Lett. *195*, 73–80.

Fruman, D.A. (2010). Regulatory Subunits of Class IA PI3K. In Current Topics in Microbiology and Immunology, pp. 225–244.

Fruman, D.A., Chiu, H., Hopkins, B.D., Bagrodia, S., Cantley, L.C., and Abraham, R.T. (2017). The PI3K Pathway in Human Disease. Cell *170*, 605–635.

Fryer, B.H., and Field, J. (2005). Rho, Rac, Pak and angiogenesis: old roles and newly identified responsibilities in endothelial cells. Cancer Lett. *229*, 13–23.

Fukumoto, S. (2008). Actions and mode of actions of FGF19 subfamily members. Endocr. J. *55*, 23–31.

Furdui, C.M., Lew, E.D., Schlessinger, J., and Anderson, K.S. (2006). Autophosphorylation of FGFR1 Kinase Is Mediated by a Sequential and Precisely Ordered Reaction. Mol. Cell *21*, 711–717.

Gallo, D., Zannoni, G.F., De Stefano, I., Mosca, M., Ferlini, C., Mantuano, E., and Scambia, G. (2008). Soy Phytochemicals Decrease Nonsmall Cell Lung Cancer Growth In Female Athymic Mice. J. Nutr. *138*, 1360–1364.

Ganesan, R., Mallets, E., and Gomez-Cambronero, J. (2016). The transcription factors Slug (SNAI2) and Snail (SNAI1) regulate phospholipase D (PLD) promoter in opposite ways towards cancer cell invasion. Mol. Oncol. *10*, 663–676.

Gao, D., Du, J., Cong, L., and Liu, Q. (2008). Risk Factors for Initial Lung Metastasis from Breast Invasive Ductal Carcinoma in Stages I-III of Operable Patients. Jpn. J. Clin. Oncol. *39*, 97–104.

García-Villalba, R., Carrasco-Pancorbo, A., Oliveras-Ferraros, C., Menéndez, J.A., Segura-Carretero, A., and Fernández-Gutiérrez, A. (2012). Uptake and metabolism of olive oil polyphenols in human breast cancer cells using nano-liquid chromatography coupled to electrospray ionization–time of flight-mass spectrometry. J. Chromatogr. B *898*, 69–77.

Garnett, M.J., Edelman, E.J., Heidorn, S.J., Greenman, C.D., Dastur, A., Lau, K.W., Greninger, P., Thompson, I.R., Luo, X., Soares, J., et al. (2012). Systematic identification of genomic markers of drug sensitivity in cancer cells. Nature *483*, 570–575.

Gavert, N., and Ben-Ze'ev, A. (2010). Coordinating changes in cell adhesion and phenotype during EMT-like processes in cancer. F1000 Biol. Rep. *2*, 86–89.

George, V.C., Dellaire, G., and Rupasinghe, H.P.V. (2017). Plant flavonoids in cancer chemoprevention: role in genome stability. J. Nutr. Biochem. *45*, 1–14.

Georgescu, M.-M. (2010). PTEN Tumor Suppressor Network in PI3K-Akt Pathway Control. Genes Cancer *1*, 1170–1177.

Gerashchenko, T.S., Denisov, E. V., Litviakov, N. V., Zavyalova, M. V., Vtorushin, S. V., Tsyganov, M.M., Perelmuter, V.M., and Cherdyntseva, N. V. (2013). Intratumor heterogeneity: Nature and biological significance. Biochem. *78*, 1201–1215.

Gerber, H.P., McMurtrey, A., Kowalski, J., Yan, M., Keyt, B.A., Dixit, V., and Ferrara, N. (1998). Vascular endothelial growth factor regulates endothelial cell survival through the phosphatidylinositol 3'-kinase/Akt signal transduction pathway. Requirement for Flk-1/KDR activation. J. Biol. Chem. *273*, 30336–30343.

Germa, C., Miller, M., Mukhopadhyay, P., Hewes, B., Caponigro, G., Scherer, S.J., and Hirawat, S. (2017). Discovery and development of novel therapies in advanced breast cancer: rapid development of ribociclib. Ann. Oncol. *28*, 2021–2024.

Gialeli, C., Theocharis, A.D., and Karamanos, N.K. (2011). Roles of matrix metalloproteinases in cancer progression and their pharmacological targeting. FEBS J. *278*, 16–27.

Gingras, D., Lamy, S., and Béliveau, R. (2000). Tyrosine phosphorylation of the vascular endothelial-growth-factor receptor-2 (VEGFR-2) is modulated by Rho proteins. Biochem. J. *348 Pt 2*, 273–280.

Giulianelli, S., Cerliani, J.P., Lamb, C.A., Fabris, V.T., Bottino, M.C., Gorostiaga, M.A., Novaro, V., Góngora, A., Baldi, A., Molinolo, A., et al. (2008). Carcinoma-associated fibroblasts activate progesterone receptors and induce hormone independent mammary tumor growth: A role for the FGF-2/FGFR-2 axis. Int. J. Cancer *123*, 2518–2531.

Glaeser, H., Bujok, K., Schmidt, I., Fromm, M.F., and Mandery, K. (2014). Organic anion transporting polypeptides and organic cation transporter 1 contribute to the cellular uptake of the flavonoid quercetin. Naunyn. Schmiedebergs. Arch. Pharmacol. *387*, 883–891.

Glatz, J.F.C., and van der Vusse, G.J. (1996). Cellular fatty acid-binding proteins: Their function and physiological significance. Prog. Lipid Res. *35*, 243–282.

Goel, S., Duda, D.G., Xu, L., Munn, L.L., Boucher, Y., Fukumura, D., and Jain, R.K. (2011). Normalization of the vasculature for treatment of cancer and other diseases. Physiol. Rev. *91*, 1071–1121.

Goldhirsch, a, Wood, W.C., Coates, a S., Gelber, R.D., Thürlimann, B., and Senn, H.-J. (2011). Strategies for subtypes--dealing with the diversity of breast cancer: highlights of the St. Gallen International Expert Consensus on the Primary Therapy of Early Breast Cancer 2011. Ann. Oncol. *22*, 1736–1747.

Gooch, J.L., Van Den Berg, C.L., and Yee, D. (1999). Insulin-like growth factor (IGF)-I rescues breast cancer cells from chemotherapy-induced cell death--proliferative and anti-apoptotic effects. Breast Cancer Res. Treat. *56*, 1–10.

Gopinathan, G., Milagre, C., Pearce, O.M.T., Reynolds, L.E., Hodivala-Dilke, K., Leinster, D.A., Zhong, H., Hollingsworth, R.E., Thompson, R., Whiteford, J.R., et al. (2015). Interleukin-6 Stimulates Defective Angiogenesis. Cancer Res. *75*, 3098–3107.

Góth, M.I., Hubina, E., Raptis, S., Nagy, G.M., and Tóth, B.E. (2003). Physiological and pathological angiogenesis in the endocrine system. Microsc. Res. Tech. *60*, 98–106.

Granado-Serrano, A.B., Martin, M.A., Bravo, L., Goya, L., and Ramos, S. (2006). Quercetin Induces Apoptosis via Caspase Activation, Regulation of Bcl-2, and Inhibition of PI-3-Kinase/Akt and ERK Pathways in a Human Hepatoma Cell Line (HepG2). J. Nutr. *136*, 2715–2721.

Greenhalgh, D.G., Sprugel, K.H., Murray, M.J., and Ross, R. (1990). PDGF and FGF stimulate wound healing in the genetically diabetic mouse. Am. J. Pathol. *136*, 1235–1246.

Greenshields, A.L., Doucette, C.D., Sutton, K.M., Madera, L., Annan, H., Yaffe, P.B., Knickle, A.F., Dong, Z., and Hoskin, D.W. (2015). Piperine inhibits the growth and motility of triple-negative breast cancer cells. Cancer Lett. *357*, 129–140.

Greenshields, A.L., Shepherd, T.G., and Hoskin, D.W. (2017). Contribution of reactive oxygen species to ovarian cancer cell growth arrest and killing by the anti-malarial drug artesunate. Mol. Carcinog. *56*, 75–93.

Griffin, J.P., Posner, J., and Barker, G.R. (2013). The textbook of pharmaceutical medicine (Wiley-Blackwell).

Grime, J.M.A., Edwards, M.A., Rudd, N.C., and Unwin, P.R. (2008). Quantitative visualization of passive transport across bilayer lipid membranes. Proc. Natl. Acad. Sci. U. S. A. *105*, 14277–14282.

Grootaert, C., Gonzales, G.B., Vissenaekens, H., Van de Wiele, T., Raes, K., Smagghe, G., and Van Camp, J. (2016). Flow Cytometric Method for the Detection of Flavonoids in Cell Lines. J. Biomol. Screen. *21*, 858–865.

Gross, J.M., and Yee, D. (2002). How does the estrogen receptor work? Breast Cancer Res. *4*, 62.

Guhr, G., and Lachance, P.A. Role of Phytochemicals in Chronic Disease Prevention. In Nutraceuticals, (Trumbull, Connecticut, USA: Food & Nutrition Press, Inc.), pp. 311–364.

Guilluy, C., Garcia-Mata, R., and Burridge, K. (2011). Rho protein crosstalk: another social network? Trends Cell Biol. *21*, 718–726.

Gunsoy, N.B., Garcia-Closas, M., and Moss, S.M. (2014). Estimating breast cancer mortality reduction and overdiagnosis due to screening for different strategies in the United Kingdom. Br. J. Cancer *110*, 2412–2419.

Gupta, R.G., and Somer, R.A. (2017). Intratumor Heterogeneity: Novel Approaches for Resolving Genomic Architecture and Clonal Evolution. Mol. Cancer Res. *15*, 1127–1137.

Häcker, G. (2000). The morphology of apoptosis. Cell Tissue Res. *301*, 5–17.

Hadari, Y.R., Gotoh, N., Kouhara, H., Lax, I., and Schlessinger, J. (2001). Critical role for the docking-protein FRS2 alpha in FGF receptor-mediated signal transduction pathways. Proc. Natl. Acad. Sci. U. S. A. *98*, 8578–8583.

Hadjiagapiou, C., and Spector, A.A. (1987). Docosahexaenoic acid metabolism and effect on prostacyclin production in endothelial cells. Arch. Biochem. Biophys. *253*, 1–12.

Hahnen, E., Hauke, J., Engel, C., Neidhardt, G., Rhiem, K., and Schmutzler, R.K. (2017). Germline Mutations in Triple-Negative Breast Cancer. Breast Care (Basel). *12*, 15–19.

Halder, A., Mukherjee, P., Ghosh, S., Mandal, S., Chatterji, U., and Mukherjee, A. (2018). Smart PLGA nanoparticles loaded with Quercetin: Cellular uptake and in-vitro anticancer study. Mater. Today Proc. *5*, 9698–9705.

Halliwell, B. (2003). Oxidative stress in cell culture: an under-appreciated problem? FEBS Lett. *540*, 3–6.

Hanahan, D., and Weinberg, R.A. (2000). The hallmarks of cancer. Cell *100*, 57–70.

Hanahan, D., and Weinberg, R.A. (2011). Hallmarks of Cancer: The Next Generation. Cell *144*, 646–674.

Hanna, S., and El-Sibai, M. (2013). Signaling networks of Rho GTPases in cell motility. Cell. Signal. *25*, 1955–1961.

Harbour, J.W., and Dean, D.C. (2000). The Rb/E2F pathway: expanding roles and emerging paradigms. Genes Dev. *14*, 2393–2409.

Hartigan, J.A., Xiong, W.-C., and Johnson, G.V.W. (2001). Glycogen Synthase Kinase 3β Is Tyrosine Phosphorylated by PYK2. Biochem. Biophys. Res. Commun. *284*, 485–489.

Hashemzaei, M., Delarami Far, A., Yari, A., Heravi, R.E., Tabrizian, K., Taghdisi, S.M., Sadegh, S.E., Tsarouhas, K., Kouretas, D., Tzanakakis, G., et al. (2017). Anticancer and apoptosis-inducing effects of quercetin in vitro and in vivo. Oncol. Rep. *38*, 819–828.

Hassan, M., Sallam, H., and Hassan, Z. (2011). The Role of Pharmacokinetics and Pharmacodynamics in Early Drug Development with reference to the Cyclin-dependent Kinase (Cdk) Inhibitor - Roscovitine. Sultan Qaboos Univ. Med. J. *11*, 165–178.

Hasson, S.P., Rubinek, T., Ryvo, L., and Wolf, I. (2013). Endocrine resistance in breast cancer: focus on the phosphatidylinositol 3-kinase/akt/mammalian target of rapamycin signaling pathway. Breast Care (Basel). *8*, 248–255.

Hay, N., and Sonenberg, N. (2004). Upstream and downstream of mTOR. Genes Dev. *18*, 1926–1945.

Hazan, R.B., Qiao, R., Keren, R., Badano, I., and Suyama, K. (2004). Cadherin switch in tumor progression. Ann. N. Y. Acad. Sci. *1014*, 155–163.

Heerboth, S., Housman, G., Leary, M., Longacre, M., Byler, S., Lapinska, K., Willbanks, A., and Sarkar, S. (2015). EMT and tumor metastasis. Clin. Transl. Med. *4*, 6.

Heldin, C.-H., Rubin, K., Pietras, K., and Östman, A. (2004). High interstitial fluid pressure — an obstacle in cancer therapy. Nat. Rev. Cancer *4*, 806–813.

Heloterä, H., and Alitalo, K. (2007). The VEGF family, the inside story. Cell *130*, 591–592.

Hendriks, J.J.A., Alblas, J., van der Pol, S.M.A., van Tol, E.A.F., Dijkstra, C.D., and de Vries, H.E. (2004). Flavonoids influence monocytic GTPase activity and are protective in experimental allergic encephalitis. J. Exp. Med. *200*, 1667–1672.

Heneman, K. (2008). Nutrition and health info sheet. ANR Publ. *8313*, 1–4.

Hidaka, B.H., Li, S., Harvey, K.E., Carlson, S.E., Sullivan, D.K., Kimler, B.F., Zalles, C.M., and Fabian, C.J. (2015). Omega-3 and omega-6 Fatty acids in blood and breast tissue of high-risk women and association with atypical cytomorphology. Cancer Prev. Res. (Phila). *8*, 359–364.

Ho, L., Ferruzzi, M.G., Janle, E.M., Wang, J., Gong, B., Chen, T.-Y., Lobo, J., Cooper, B., Wu, Q.L., Talcott, S.T., et al. (2013). Identification of brain-targeted bioactive dietary quercetin-3- *O* -glucuronide as a novel intervention for Alzheimer's disease. FASEB J. *27*, 769–781.

Hoek, K.S., Eichhoff, O.M., Schlegel, N.C., Döbbeling, U., Kobert, N., Schaerer, L., Hemmi, S., and Dummer, R. (2008). In vivo switching of human melanoma cells between proliferative and invasive states. Cancer Res. *68*, 650–656.

Hogan, B.L.M., Blessing, M., Winnier, G.E., Suzuki, N., and Jonest, C.M. (1994). Growth factors in development: the role of TGF-B related polypeptide signalling molecules in embryogenesis. Development *53*, 53–60.

Holgado-Madruga, M., Moscatello, D.K., Emlet, D.R., Dieterich, R., Wong, A.J., and Lax, I. (1997). Grb2-associated binder-1 mediates phosphatidylinositol 3-kinase activation and the promotion of cell survival by nerve growth factor. Proc. Natl. Acad. Sci. U. S. A. *94*, 12419–12424.

Holmes, D.I.R., and Zachary, I. (2005). The vascular endothelial growth factor (VEGF) family: angiogenic factors in health and disease. Genome Biol. *6*, 209.

Holst, B., and Williamson, G. (2008). Nutrients and phytochemicals: from bioavailability to bioefficacy beyond antioxidants. Curr. Opin. Biotechnol. *19*, 73–82.

Hou, A., Toh, L.X., Gan, K.H., Lee, K.J.R., Manser, E., and Tong, L. (2013). Rho GTPases and Regulation of Cell Migration and Polarization in Human Corneal Epithelial Cells. PLoS One *8*, e77107.

Howe, L.R., Watanabe, O., Leonard, J., Brown, A.M.C., Perou, C.M., Naber, S., and Kuperwasser, C. (2003). Twist is up-regulated in response to Wnt1 and inhibits mouse mammary cell differentiation. Cancer Res. *63*, 1906–1913.

Howe, P., Buckley, J., Murphy, K., Pettman, T., Milte, C., Coates, A., Howe, P.R.C., Buckley, J.D., Murphy, K.J., Pettman, T., et al. (2014). Relationship between Erythrocyte Omega-3 Content and Obesity Is Gender Dependent. Nutrients *6*, 1850–1860.

Hrvatsko prirodoslovno društvo. Biološka sekcija., N., ŠTAJCAR, D., and BAŠIĆ, I. (2009). Propolis and its flavonoid compounds cause cytotoxicity on human urinary bladder transitional cell carcinoma in primary culture. Period. Biol. *111*, 113–121.

Hsu, J.-W., Yasmin-Karim, S., King, M.R., Wojciechowski, J.C., Mickelsen, D., Blair, M.L., Ting, H.-J., Ma, W.-L., and Lee, Y.-F. (2011). Suppression of prostate cancer cell rolling and adhesion to endothelium by 1α,25-dihydroxyvitamin D3. Am. J. Pathol. *178*, 872–880.

Hsu, Y.-H., Chang, C.-C., Yang, N.-J., Lee, Y.-H., and Juan, S.-H. (2014). RhoA-Mediated Inhibition of Vascular Endothelial Cell Mobility: Positive Feedback Through Reduced Cytosolic p21 and p27. J. Cell. Physiol. *229*, 1455–1465.

Hsu, Y.L., Kuo, P.L., Tzeng, W.S., and Lin, C.C. (2006). Chalcone inhibits the proliferation of human breast cancer cell by blocking cell cycle progression and inducing apoptosis. Food Chem. Toxicol. *44*, 704–713.

Huang, Z., and Bao, S.-D. (2004). Roles of main pro- and anti-angiogenic factors in tumor angiogenesis. World J. Gastroenterol. *10*, 463–470.

Huang, C.-Y., Hsiao, J.-K., Lu, Y.-Z., Lee, T.-C., and Yu, L.C.-H. (2011). Anti-apoptotic PI3K/Akt signaling by sodium/glucose transporter 1 reduces epithelial barrier damage and bacterial translocation in intestinal ischemia. Lab. Investig. *91*, 294–309.

Huang, J., Bae, J.-O., Tsai, J.P., Kadenhe-Chiweshe, A., Papa, J., Lee, A., Zeng, S., Kornfeld, Z.N., Ullner, P., Zaghloul, N., et al. (2009). Angiopoietin-1/Tie-2 activation contributes to vascular survival and tumor growth during VEGF blockade. Int. J. Oncol. *34*, 79–87.

Huang, S., Zhu, X., Huang, W., He, Y., Pang, L., Lan, X., Shui, X., Chen, Y., Chen, C., and Lei, W. (2017). Quercetin Inhibits Pulmonary Arterial Endothelial Cell Transdifferentiation Possibly by Akt and Erk1/2 Pathways. Biomed Res. Int. *2017*, 1–8.

Huang, Y., Chen, H., He, F., Zhang, Z.-R., Zheng, L., Liu, Y., Lan, Y.-Y., Liao, S.-G., Li, Y.-J., and Wang, Y.-L. (2013). Simultaneous determination of human plasma protein binding of bioactive flavonoids in Polygonum orientale by equilibrium dialysis combined with UPLC–MS/MS. J. Pharm. Anal. *3*, 376–381.

Hubbard, S.R., and Miller, W.T. (2007). Receptor tyrosine kinases: mechanisms of activation and signaling. Curr. Opin. Cell Biol. *19*, 117–123.

Hudis, C.A., and Gianni, L. (2011). Triple-Negative Breast Cancer: An Unmet Medical Need. Oncologist *16*, 1–11.

Hui, C., Qi, X., Qianyong, Z., Xiaoli, P., Jundong, Z., and Mantian, M. (2013). Flavonoids, flavonoid subclasses and breast cancer risk: a meta-analysis of epidemiologic studies. PLoS One *8*, e54318.

Hui, L., Zheng, Y., Yan, Y., Bargonetti, J., and Foster, D.A. (2006). Mutant p53 in MDA-MB-231 breast cancer cells is stabilized by elevated phospholipase D activity and contributes to survival signals generated by phospholipase D. Oncogene *25*, 7305–7310.

Hung, W.-L., Chang, W.-S., Lu, W.-C., Wei, G.-J., Wang, Y., Ho, C.-T., and Hwang, L.S. (2018). Pharmacokinetics, bioavailability, tissue distribution and excretion of tangeretin in rat. J. Food Drug Anal. *26*, 849–857.

Hunter, K.W., Crawford, N.P., and Alsarraj, J. (2008). Mechanisms of metastasis. Breast Cancer Res. *10*, 1–10.

Hynes, R.O. (2003). Metastatic Potential: Generic Predisposition of the Primary Tumor or Rare, Metastatic Variants—Or Both? Cell *113*, 821–823.

Innis, S.M. (2007). Dietary (n-3) Fatty Acids and Brain Development. J. Nutr. *137*, 855–859.

Innis, S.M. (2014). Omega-3 Fatty Acid Biochemistry: Perspectives from Human Nutrition. Mil. Med. *17982*, 82–87.

Ishisaka, A., Mukai, R., Terao, J., Shibata, N., and Kawai, Y. (2014). Specific localization of quercetin-3-O-glucuronide in human brain. Arch. Biochem. Biophys. *557*, 11–17.

Ismail, A., Bannenberg, G., Rice, H.B., Schutt, E., and MacKay, D. (2016). Oxidation in EPA- and DHA-rich oils: an overview. Lipid Technol. *28*, 55–59.

Israels, E.D., and Israels, L.G. (2000). The Cell Cycle. Oncologist *5*, 510–513.

Itoh, N., and Ornitz, D.M. (2011). Fibroblast growth factors: from molecular evolution to roles in development, metabolism and disease. J. Biochem. *149*, 121–130.

Iyengar, N.M., Hudis, C.A., and Gucalp, A. (2013). Omega-3 Fatty Acids for Prevention of Breast Cancer: an Update and the State of the Science. Curr. Breast Cancer Rep. *5*, 247–254.

Jahroudi, N., and Greenberger, J.S. (1995). The role of endothelial cells in tumor invasion and metastasis. J. Neurooncol. *23*, 99–108.

Jailani, F., and Williamson, G. (2014). Effect of edible oils on quercetin, kaempferol and galangin transport and conjugation in the intestinal Caco-2/HT29-MTX co-culture model. Food Funct. *5*, 653.

Jancova, P., and Siller, M. (2012). Phase II Drug Metabolism. In Topics on Drug Metabolism, J. Paxton, ed. (InTech), pp. 1–27.

Jancova, P., Anzenbacher, P., and Anzenbacherova, E. (2010). Phase II drug metabolizing enzymes. Biomed Pap Med Fac Univ Palacky Olomouc Czech Repub *154*, 103–116.

Jansen, S., Gosens, R., Wieland, T., and Schmidt, M. (2018). Paving the Rho in cancer metastasis: Rho GTPases and beyond. Pharmacol. Ther. *183*, 1–21.

Javerzat, S., Auguste, P., and Bikfalvi, A. (2002). The role of fibroblast growth factors in vascular development. Trends Mol. Med. *8*, 483–489.

Jendraschak, E., and Sage, E.H. (1996). Regulation of angiogenesis by SPARC and angiostatin: implications for tumor cell biology. Semin. Cancer Biol. *7*, 139–146.

Jenzer Bern, H., and Sadeghi Bern, L. (2016). Phytochemicals: Sources and biological functions. J. Pharmacogn. Phytochem. JPP *339*, 339–341.

Jeon, J.S., Zervantonakis, I.K., Chung, S., Kamm, R.D., and Charest, J.L. (2013). In Vitro Model of Tumor Cell Extravasation. PLoS One *8*, e56910.

Jiang, W., and Hu, M. (2012). Mutual interactions between flavonoids and enzymatic and transporter elements responsible for flavonoid disposition via phase II metabolic pathways. RSC Adv. *2*, 7948–7963.

Jimenez, C., Hernandez, C., Pimentel, B., and Carrera, A.C. (2002). The p85 regulatory subunit controls sequential activation of phosphoinositide 3-kinase by Tyr kinases and Ras. J. Biol. Chem. *277*, 41556–41562.

Jin, X., and Mu, P. (2015). Targeting Breast Cancer Metastasis. Breast Cancer (Auckl). *9*, 23–34.

Jin, H., Lee, W.S., Eun, S.Y., Jung, J.H., Park, H.-S., Kim, G., Choi, Y.H., Ryu, C.H., Jung, J.M., Hong, S.C., et al. (2014). Morin, a flavonoid from Moraceae, suppresses growth and invasion of the highly metastatic breast cancer cell line MDA-MB-231 partly through suppression of the Akt pathway. Int. J. Oncol. *45*, 1629–1637.

Jin, L., Han, B., Siegel, E., Cui, Y., Giuliano, A., and Cui, X. (2018). Breast cancer lung metastasis: Molecular biology and therapeutic implications. Cancer Biol. Ther. *0*, 1–11.

Johnson, M.D., Jennings, M.T., Gold, L.I., and Moses, H.L. (1993). Transforming growth factor-beta in neural embryogenesis and neoplasia. Hum. Pathol. *24*, 457–462.

Jolly, M.K., Boareto, M., Debeb, B.G., Aceto, N., Farach-Carson, M.C., Woodward, W.A., and Levine, H. (2017a). Inflammatory breast cancer: a model for investigating cluster-based dissemination. Npj Breast Cancer *3*, 21.

Jolly, M.K., Ware, K.E., Gilja, S., Somarelli, J.A., and Levine, H. (2017b). EMT and MET: necessary or permissive for metastasis? Mol. Oncol. *11*, 755–769.

Jopling, H.M., Odell, A.F., Hooper, N.M., Zachary, I.C., Walker, J.H., and Ponnambalam, S. (2009). Rab GTPase regulation of VEGFR2 trafficking and signaling in endothelial cells. Arterioscler. Thromb. Vasc. Biol. *29*, 1119–1124.

Jovanović, B., Beeler, J.S., Pickup, M.W., Chytil, A., Gorska, A.E., Ashby, W.J., Lehmann, B.D., Zijlstra, A., Pietenpol, J.A., and Moses, H.L. (2014). Transforming growth factor beta receptor type III is a tumor promoter in mesenchymal-stem like triple negative breast cancer. Breast Cancer Res. *16*, R69.

Jump, D.B., Depner, C.M., and Tripathy, S. (2012). Omega-3 fatty acid supplementation and cardiovascular disease. J. Lipid Res. *53*, 2525–2545.

Juntilla, M.M., and Koretzky, G.A. (2008). Critical roles of the PI3K/Akt signaling pathway in T cell development. Immunol. Lett. *116*, 104–110.

Jussila, L., and Alitalo, K. (2002). Vascular Growth Factors and Lymphangiogenesis. Physiol. Rev. *82*, 673–700.

Kalluri, R., and Weinberg, R.A. (2009). The basics of epithelial-mesenchymal transition. J. Clin. Invest. *119*, 1420–1428.

Kang, Y., Siegel, P.M., Shu, W., Drobnjak, M., Kakonen, S.M., Cordón-Cardo, C., Guise, T.A., and Massagué, J. (2003). A multigenic program mediating breast cancer metastasis to bone. Cancer Cell *3*, 537–549.

Kang, Y., He, W., Tulley, S., Gupta, G.P., Serganova, I., Chen, C.-R., Manova-Todorova, K., Blasberg, R., Gerald, W.L., and Massague, J. (2005). Breast cancer bone metastasis mediated by the Smad tumor suppressor pathway. Proc. Natl. Acad. Sci. *102*, 13909–13914.

Karar, J., and Maity, A. (2011). PI3K/AKT/mTOR Pathway in Angiogenesis. Front. Mol. Neurosci. *4*, 51.

Katsoura, M.H., Polydera, A.C., Tsironis, L., Tselepis, A.D., and Stamatis, H. (2006). Use of ionic liquids as media for the biocatalytic preparation of flavonoid derivatives with antioxidant potency. J. Biotechnol. *123*, 491–503.

Katsuno, Y., Lamouille, S., and Derynck, R. (2013). TGF-β signaling and epithelial–mesenchymal transition in cancer progression. Curr. Opin. Oncol. *25*, 76–84.

Katz, M., Amit, I., and Yarden, Y. (2007). Regulation of MAPKs by growth factors and receptor tyrosine kinases. Biochim. Biophys. Acta *1773*, 1161–1176.

Kelley, M.R., Logsdon, D., and Fishel, M.L. (2014). Targeting DNA repair pathways for cancer treatment: what's new? Future Oncol. *10*, 1215–1237.

Kelly, P., Ma, Z., Baidas, S., Moroose, R., Shah, N., Dagan, R., Mamounas, E., and Rineer, J. (2017). Patterns of Progression in Metastatic Estrogen Receptor Positive Breast Cancer: An Argument for Local Therapy. Int. J. Breast Cancer *2017*, 1–7.

Kendall, R.L., Rutledge, R.Z., Mao, X., Tebben, A.J., Hungate, R.W., and Thomas, K.A. (1999). Vascular endothelial growth factor receptor KDR tyrosine kinase activity is increased by autophosphorylation of two activation loop tyrosine residues. J. Biol. Chem. *274*, 6453–6460.

Kennecke, H., Yerushalmi, R., Woods, R., Cheang, M.C.U., Voduc, D., Speers, C.H., Nielsen, T.O., and Gelmon, K. (2010). Metastatic behavior of breast cancer subtypes. J. Clin. Oncol. *28*, 3271–3277.

Kennedy, B.K., and Lamming, D.W. (2016). The Mechanistic Target of Rapamycin: The Grand ConducTOR of Metabolism and Aging. Cell Metab. *23*, 990–1003.

Kern, M., Pahlke, G., Ngiewih, Y., and Marko, D. (2006). Modulation of Key Elements of the Wnt Pathway by Apple Polyphenols. J. Agric. Food Chem. *54*, 7041–7046.

Kessenbrock, K., Plaks, V., and Werb, Z. (2010). Matrix metalloproteinases: regulators of the tumor microenvironment. Cell *141*, 52–67.

Khalifa, J., Duprez-Paumier, R., Filleron, T., Lacroix Triki, M., Jouve, E., Dalenc, F., and Massabeau, C. (2016). Outcome of pN0 Triple-Negative Breast Cancer with or without Lymph Node Irradiation: A Single Institution Experience. Breast J. *22*, 510–519.

Khan, B.A., Akhtar, N., Khan, H., and De Andrade Braga, V. (2013a). Development, characterization and antioxidant activity of polysorbate based O/W emulsion containing polyphenols derived from Hippophae rhamnoides and Cassia fistula. Brazilian J. Pharm. Sci. *49*.

Khan, K.H., Yap, T.A., Yan, L., and Cunningham, D. (2013b). Targeting the PI3K-AKT-mTOR signaling network in cancer. Chin. J. Cancer *32*, 253–265.

Kiiski, J.I., Pelttari, L.M., Khan, S., Freysteinsdottir, E.S., Reynisdottir, I., Hart, S.N., Shimelis, H., Vilske, S., Kallioniemi, A., Schleutker, J., et al. (2014). Exome sequencing identifies FANCM as a susceptibility gene for triple-negative breast cancer. Proc. Natl. Acad. Sci. U. S. A. *111*, 15172–15177.

Kim, G.D. (2017). Myricetin Inhibits Angiogenesis by Inducing Apoptosis and Suppressing PI3K/Akt/mTOR Signaling in Endothelial Cells. J. Cancer Prev. *22*, 219–227.

Kim, M.H. (2003). Flavonoids inhibit VEGF/bFGF-induced angiogenesis in vitro by inhibiting the matrix-degrading proteases. J. Cell. Biochem. *89*, 529–538.

Kim, H.J., Vosseler, C.A., Weber, P.C., and Erl, W. (2005). Docosahexaenoic acid induces apoptosis in proliferating human endothelial cells. J. Cell. Physiol. *204*, 881–888.

Kim, J.-H., Lee, E.-O., Lee, H.-J., Ku, J.-S., Lee, M.-H., Yang, D.-C., and Kim, S.-H. (2007). Caspase Activation and Extracellular Signal-Regulated Kinase / Akt Inhibition Were Involved in Luteolin-Induced Apoptosis in Lewis Lung carcinoma cells. *611*, 597–611.

Kim, N., Jeong, S., Jing, K., Shin, S., Kim, S., Heo, J.-Y., Kweon, G.-R., Park, S.-K., Wu, T., Park, J.-I., et al. (2015). Docosahexaenoic Acid Induces Cell Death in Human Non-Small Cell Lung Cancer Cells by Repressing mTOR via AMPK Activation and PI3K/Akt Inhibition. Biomed Res. Int. *2015*, 239764.

Kim, W.R., Flamm, S.L., Di Bisceglie, A.M., and Bodenheimer, H.C. (2008). Serum activity of alanine aminotransferase (ALT) as an indicator of health and disease. Hepatology *47*, 1363–1370.

Kim, Y.-S., Yi, B.-R., Kim, N.-H., and Choi, K.-C. (2014). Role of the epithelial–mesenchymal transition and its effects on embryonic stem cells. Exp. Mol. Med. *46*, e108–e108.

Kimbung, S., Loman, N., and Hedenfalk, I. (2015). Clinical and molecular complexity of breast cancer metastases. Semin. Cancer Biol. *35*, 85–95.

Kingston, B., and Johnston, S. (2016). Novel Treatments in Breast Cancer. Clin. Med. Insights Ther. *8*, CMT.S18492.

Klagsbrunl, M., and Moses, M.A. (1999). Molecular angiogenesis. Chem. Biol. *6*, R217-24.

Knoll, T., Grobholz, R., Alken, P., Michel, M.S., Trojan, L., and Thomas, D. (2004). Expression of pro-angiogenic growth factors VEGF, EGF and bFGF and their topographical relation to neovascularisation in prostate cancer. Urol. Res. *32*, 97–103.

Koch, S., and Claesson-Welsh, L. (2012). Signal transduction by vascular endothelial growth factor receptors. Cold Spring Harb. Perspect. Med. *2*, a006502.

Koirala, N., Pandey, R.P., Parajuli, P., Jung, H.J., and Sohng, J.K. (2014). Methylation and subsequent glycosylation of 7,8-dihydroxyflavone. J. Biotechnol. *184*, 128–137.

Koirala, N., Thuan, N.H., Ghimire, G.P., Jung, H.J., Oh, T.-J., and Sohng, J.K. (2015). Metabolic engineering of Escherichia coli for the production of isoflavonoid-7- O -methoxides and their biological activities. Biotechnol. Appl. Biochem. *10*, 1452.

Koirala, N., Thuan, N.H., Ghimire, G.P., Thang, D. Van, and Sohng, J.K. (2016). Methylation of flavonoids: Chemical structures, bioactivities, progress and perspectives for biotechnological production. Enzyme Microb. Technol. *86*, 103–116.

Koizumi, K., Tamiya-Koizumi, K., Fujii, T., Okuda, J., and Kojima, K. (1980). Comparative study of the phospholipid composition of plasma membranes isolated from rat primary hepatomas induced by 3'-methyl-4-dimethylaminoazobenzene and from normal growing rat livers. Cancer Res. *40*, 909–913.

Kojima, K. (1993). Molecular aspects of the plasma membrane in tumor cells. Nagoya J. Med. Sci *56*, 1–18.

Königsberg, R., Pfeiler, G., Klement, T., Hammerschmid, N., Brunner, A., Zeillinger, R., Singer, C., and Dittrich, C. (2012). Tumor characteristics and recurrence patterns in triple negative breast cancer: A comparison between younger (<65) and elderly (≥65) patients. Eur. J. Cancer *48*, 2962–2968.

Kostler, W.J., Hejna, M., Wenzel, C., and Zielinski, C.C. (2001). Oral Mucositis Complicating Chemotherapy and/or Radiotherapy: Options for Prevention and Treatment. CA. Cancer J. Clin. *51*, 290–315.

Kozłowska, A., and Szostak-Wegierek, D. (2014). Flavonoids--food sources and health benefits. Rocz. Panstw. Zakl. Hig. *65*, 79–85.

Kuhnle, G., Spencer, J.P.E., Schroeter, H., Shenoy, B., Debnam, E.S., Srai, S.K.S., Rice-Evans, C., and Hahn, U. (2000). Epicatechin and Catechin are O-Methylated and Glucuronidated in the Small Intestine. Biochem. Biophys. Res. Commun. *277*, 507–512.

Kumar, A., Collins, H.M., Scholefield, J.H., and Watson, S.A. (2000). Increased type-IV collagenase (MMP-2 and MMP-9) activity following preoperative radiotherapy in rectal cancer. Br. J. Cancer *82*, 960–965.

Kumar, R., Zakharov, M.N., Khan, S.H., Miki, R., Jang, H., Toraldo, G., Singh, R., Bhasin, S., and Jasuja, R. (2011). The dynamic structure of the estrogen receptor. J. Amino Acids *2011*, 812540.

Kumar Mukhopadhyay, M., Banerjee, P., and Nath, D. (2012). Phytochemicals – biomolecules for prevention and treatment of human diseases-a review. Int. J. Sci. Eng. Res. *3*, 1–32.

Kuo, C.-Y., Zupkó, I., Chang, F.-R., Hunyadi, A., Wu, C.-C., Weng, T.-S., and Wang, H.-C. (2016). Dietary flavonoid derivatives enhance chemotherapeutic effect by inhibiting the DNA damage response pathway. Toxicol. Appl. Pharmacol. *311*, 99–105.

Kurz, H. Physiology of angiogenesis. J. Neurooncol. *50*, 17–35.

Lai, L., Fu, Q., Liu, Y., Jiang, K., Guo, Q., Chen, Q., Yan, B., Wang, Q., and Shen, J. (2012). Piperine suppresses tumor growth and metastasis in vitro and in vivo in a 4T1 murine breast cancer model. Acta Pharmacol. Sin. *33*, 523–530.

Lai, W.-W., Hsu, S.-C., Chueh, F.-S., Chen, Y.-Y., Yang, J.-S., Lin, J.-P., Lien, J.-C., Tsai, C.-H., and Chung, J.-G. (2013). Quercetin inhibits migration and invasion of SAS human oral cancer cells through inhibition of NF-κB and matrix metalloproteinase-2/-9 signaling pathways. Anticancer Res. *33*, 1941–1950.

Lamalice, L., Le Boeuf, F., and Huot, J. (2007). Endothelial Cell Migration During Angiogenesis. Circ. Res. *100*, 782–794.

Lamson, D.W., and Brignall, M.S. (1999). Antioxidants in Cancer Therapy; Their Actions and Interactions With Oncologic Therapies. Altern. Med. Rev. x Altern Med Rev *44*, 304–329.

Lamy, S., Gingras, D., and Béliveau, R. (2002). Green tea catechins inhibit vascular endothelial growth factor receptor phosphorylation. Cancer Res. *62*, 381–385.

Lau, C.B.S., Ho, C.Y., Kim, C.F., Leung, K.N., Fung, K.P., Tse, T.F., Chan, H.H.L., and Chow, M.S.S. (2004). Cytotoxic activities of Coriolus versicolor (Yunzhi) extract on human leukemia and lymphoma cells by induction of apoptosis. Life Sci. *75*, 797–808.

de Laurentiis, A., Donovan, L., and Arcaro, A. (2007). Lipid rafts and caveolae in signaling by growth factor receptors. Open Biochem. J. *1*, 12–32.

Lawenda, B.D., Kelly, K.M., Ladas, E.J., Sagar, S.M., Vickers, A., and Blumberg, J.B. (2008). Should supplemental antioxidant administration be avoided during chemotherapy and radiation therapy? J. Natl. Cancer Inst. *100*, 773–783.

Lawler, J. (2002). Thrombospondin-1 as an endogenous inhibitor of angiogenesis and tumor growth. J. Cell. Mol. Med. *6*, 1–12.

Lawler, P.R., and Lawler, J. (2012). Molecular Basis for the Regulation of Angiogenesis by Thrombospondin-1 and -2. Cold Spring Harb. Perspect. Med. *2*, a006627–a006627.

Lebrun, J.-J. (2012). The Dual Role of TGF β in Human Cancer: From Tumor Suppression to Cancer Metastasis. ISRN Mol. Biol. *2012*, 1–28.

Lee, J.L., and Streuli, C.H. (2014). Integrins and epithelial cell polarity. J. Cell Sci. *127*, 3217–3225.

Lee, C.-J., Hsu, L.-S., Yue, C.-H., Lin, H., Chiu, Y.-W., Lin, Y.-Y., Huang, C.-Y., Hung, M.-C., and Liu, J.-Y. (2016). MZF-1/Elk-1 interaction domain as therapeutic target for protein kinase Cα-based triple-negative breast cancer cells. Oncotarget *7*, 59845–59859.

Lee, C.W., Song, M.J., Park, S.T., Ki, E.Y., Lee, S.J., Lee, K.H., Ryu, K.S., Park, J.S., and Hur, S.Y. (2011a). Residual tumor after the salvage surgery is the major risk factors for primary treatment failure in malignant ovarian germ cell tumors: A retrospective study of single institution. World J. Surg. Oncol. *9*, 123.

Lee, H.-R., Kim, T.-H., and Choi, K.-C. (2012). Functions and physiological roles of two types of estrogen receptors, ERα and ERβ, identified by estrogen receptor knockout mouse. Lab. Anim. Res. *28*, 71–76.

Lee, H., Kizito, S.A., Weese, S.J., Craig-Schmidt, M.C., Lee, Y., Wei, C.-I., and An, H. (2003). Analysis of Headspace Volatile and Oxidized Volatile Compounds in DHA-enriched Fish Oil on Accelerated Oxidative Storage. Food Chem. Toxicol. *68*, 2169–2177.

Lee, H., Kang, C., Jung, E., Kim, J.-S., and Kim, E. (2011b). Antimetastatic activity of polyphenol-rich extract of Ecklonia cava through the inhibition of the Akt pathway in A549 human lung cancer cells. Food Chem. *127*, 1229–1236.

Leight, J.L., Wozniak, M.A., Chen, S., Lynch, M.L., and Chen, C.S. (2012). Matrix rigidity regulates a switch between TGF-β1–induced apoptosis and epithelial–mesenchymal transition. Mol. Biol. Cell *23*, 781–791.

Leitzmann, C. (2016). Characteristics and Health Benefits of Phytochemicals. Forsch. Komplementmed. *23*, 69–74.

León-González, A.J., Auger, C., and Schini-Kerth, V.B. (2015). Pro-oxidant activity of polyphenols and its implication on cancer chemoprevention and chemotherapy. Biochem. Pharmacol. *98*, 371–380.

Levin, E.R. (2002). Cellular functions of plasma membrane estrogen receptors. Steroids *67*, 471–475.

Lewis, D. (2003). Human Cytochromes P450 Associated with the Phase 1 Metabolism of Drugs and other Xenobiotics: A Compilation of Substrates and Inhibitors of the CYP1, CYP2 and CYP3 Families. Curr. Med. Chem. *10*, 1955–1972.

Li, S., and Li, Q. (2014). Cancer stem cells and tumor metastasis. Int. J. Oncol. *44*, 1806–1812.

Li, C.-Y., Wang, L.-X., Dong, S.-S., Hong, Y., Zhou, X.-H., Zheng, W.-W., and Zheng, C. (2018). Phlorizin Exerts Direct Protective Effects on Palmitic Acid (PA)-Induced Endothelial Dysfunction by Activating the PI3K/AKT/eNOS Signaling Pathway and Increasing the Levels of Nitric Oxide (NO). Med. Sci. Monit. Basic Res. *24*, 1–9.

Li, F., Tiede, B., Massagué, J., and Kang, Y. (2007). Beyond tumorigenesis: cancer stem cells in metastasis. Cell Res. *17*, 3–14.

Li, F., Li, C., Zhang, H., Lu, Z., Li, Z., You, Q., Lu, N., and Guo, Q. (2012). VI-14, a novel flavonoid derivative, inhibits migration and invasion of human breast cancer cells. Toxicol. Appl. Pharmacol. *261*, 217–226.

Lien, W.M., and Ackerman, N.B. (1970). The blood supply of experimental liver metastases. II. A microcirculatory study of the normal and tumor vessels of the liver with the use of perfused silicone rubber. Surgery *68*, 334–340.

Limdi, J.K., and Hyde, G.M. (2003). Evaluation of abnormal liver function tests. Postgrad. Med. J. *79*, 307–312.

Lin, S.-P., Chiu, F.-Y., Wang, Y., Yen, M.-L., Kao, S.-Y., and Hung, S.-C. (2014). RB maintains quiescence and prevents premature senescence through upregulation of DNMT1 in mesenchymal stromal cells. Stem Cell Reports *3*, 975–986.

Lin, Y.-S., Tsai, P.-H., Kandaswami, C.C., Cheng, C.-H., Ke, F.-C., Lee, P.-P., Hwang, J.-J., and Lee, M.-T. (2011). Effects of dietary flavonoids, luteolin, and quercetin on the reversal of epithelial–mesenchymal transition in A431 epidermal cancer cells. Cancer Sci *102*, 1829–1839.

Lirdprapamongkol, K., Sakurai, H., Abdelhamed, S., Yokoyama, S., Maruyama, T., Athikomkulchai, S., Viriyaroj, A., Awale, S., Yagita, H., Ruchirawat, S., et al. (2013). A flavonoid chrysin suppresses hypoxic survival and metastatic growth of mouse breast cancer cells. Oncol. Rep. *30*, 2357–2364.

Liu, R.H. (2003). Health benefits of fruit and vegetables are from additive and synergistic combinations of phytochemicals. Am. J. Clin. Nutr. *78*, 517S–520S.

Liu, B., Ezeogu, L., Zellmer, L., Yu, B., Xu, N., and Joshua Liao, D. (2015a). Protecting the normal in order to better kill the cancer. Cancer Med. *4*, 1394–1403.

Liu, F., Gu, L.-N., Shan, B.-E., Geng, C.-Z., and Sang, M.-X. (2016). Biomarkers for EMT and MET in breast cancer: An update. Oncol. Lett. *12*, 4869–4876.

Liu, H., Lv, L., and Yang, K. (2015b). Chemotherapy targeting cancer stem cells. Am. J. Cancer Res. *5*, 880–893.

Liu, J., Dang, H., and Wang, X.W. (2018). The significance of intertumor and intratumor heterogeneity in liver cancer. Exp. Mol. Med. *50*, e416.

Liu, W., Shen, S.-M., Zhao, X.-Y., and Chen, G.-Q. (2012). Targeted genes and interacting proteins of hypoxia inducible factor-1. Int. J. Biochem. Mol. Biol. *3*, 165–178.

Liu, Y., Hu, M., Rein, M.J., Barron, D., Williamson, G., Bladeren, P.J. van, and Rietjens, I.M.C.M. (2002). Absorption and metabolism of flavonoids in the caco-2 cell culture model and a perused rat intestinal model. Drug Metab. Dispos. *30*, 370–377.

Liu, Z.-J., Xiao, M., Balint, K., Soma, A., Pinnix, C.C., Capobianco, A.J., Velazquez, O.C., and Herlyn, M. (2006). Inhibition of endothelial cell proliferation by Notch1 signaling is mediated by repressing MAPK and PI3K/Akt pathways and requires MAML1. FASEB J. *20*, 1009–1011.

Lobo, N.A., Shimono, Y., Qian, D., and Clarke, M.F. (2007). The Biology of Cancer Stem Cells. Annu. Rev. Cell Dev. Biol. *23*, 675–699.

Loges, S., Mazzone, M., Hohensinner, P., and Carmeliet, P. (2009). Silencing or Fueling Metastasis with VEGF Inhibitors: Antiangiogenesis Revisited. Cancer Cell *15*, 167–170.

Lohela, M., Bry, M., Tammela, T., and Alitalo, K. (2009). VEGFs and receptors involved in angiogenesis versus lymphangiogenesis. Curr. Opin. Cell Biol. *21*, 154–165.

Long, X., Fan, M., Bigsby, R.M., and Nephew, K.P. (2008). Apigenin inhibits antiestrogen-resistant breast cancer cell growth through estrogen receptor-alpha-dependent and estrogen receptor-alpha-independent mechanisms. Mol. Cancer Ther. *7*, 2096–2108.

Lonic, A., Barry, E.F., Quach, C., Kobe, B., Saunders, N., and Guthridge, M.A. (2008). Fibroblast growth factor receptor 2 phosphorylation on serine 779 couples to 14-3-3 and regulates cell survival and proliferation. Mol. Cell. Biol. *28*, 3372–3385.

Lukas, G., Brindle, S.D., and Greengard, P. (1971). The route of absorption of intraperitoneally administered compounds. Tnn J. Pharmacol. Exp. Ther. *178*, 562–566.

Lumachi, F., Brunello, A., Maruzzo, M., Basso, U., and Basso, S.M.M. (2013). Treatment of estrogen receptor-positive breast cancer. Curr. Med. Chem. *20*, 596–604.

Lunt, S.J., Fyles, A., Hill, R.P., and Milosevic, M. (2008). Interstitial fluid pressure in tumors: therapeutic barrier and biomarker of angiogenesis. Futur. Oncol. *4*, 793–802.

Luo, Z., Murray, B.S., Yusoff, A., Morgan, M.R.A., Povey, M.J.W., and Day, A.J. (2011). Particle-Stabilizing Effects of Flavonoids at the Oil−Water Interface. J. Agric. Food Chem. *59*, 2636–2645.

Lux, M., Janni, W., Hartkopf, A., Nabieva, N., Taran, F.-A., Overkamp, F., Kolberg, H.-C., Hadji, P., Tesch, H., Ettl, J., et al. (2017). Update Breast Cancer 2017 – Implementation of Novel Therapies. Geburtshilfe Frauenheilkd. *77*, 1281–1290.

Ma, J., Sawai, H., Ochi, N., Matsuo, Y., Xu, D., Yasuda, A., Takahashi, H., Wakasugi, T., and Takeyama, H. (2009). PTEN regulate angiogenesis through PI3K/Akt/VEGF signaling pathway in human pancreatic cancer cells. Mol. Cell. Biochem. *331*, 161–171.

Ma, R., Feng, Y., Lin, S., Chen, J., Lin, H., Liang, X., Zheng, H., and Cai, X. (2015). Mechanisms involved in breast cancer liver metastasis. J. Transl. Med. *13*, 64.

MacGowan, A.P. (2001). Role of Pharmacokinetics and Pharmacodynamics: Does the Dose Matter? Clin. Infect. Dis. *33*, S238–S239.

Mader, J.S., Smyth, D., Marshall, J., and Hoskin, D.W. (2006). Bovine lactoferricin inhibits basic fibroblast growth factor- and vascular endothelial growth factor165-induced angiogenesis by competing for heparin-like binding sites on endothelial cells. Am. J. Pathol. *169*, 1753–1766.

Mahajan, K., and Mahajan, N.P. (2012). PI3K-independent AKT activation in cancers: a treasure trove for novel therapeutics. J. Cell. Physiol. *227*, 3178–3184.

Malinda, K.M. (2009). In Vivo Matrigel Migration and Angiogenesis Assay. (Humana Press), pp. 287–294.

Manach, C., Morand, C., Crespy, V., Demigné, C., Texier, O., Régérat, F., and Rémésy, C. (1998). Quercetin is recovered in human plasma as conjugated derivatives which retain antioxidant properties. FEBS Lett. *426*, 331–336.

Marjon, P.L., Bobrovnikova-Marjon, E. V, and Abcouwer, S.F. (2004). Expression of the pro-angiogenic factors vascular endothelial growth factor and interleukin-8/CXCL8 by human breast carcinomas is responsive to nutrient deprivation and endoplasmic reticulum stress. Mol. Cancer *3*, 4.

Martin, P.M., Horwitz, K.B., Ryan, D.S., and Mcguire, W.L. (1978). Phytoestrogen Interaction with Estrogen Receptors in Human Breast Cancer Cells*. Endocrinology *103*, 1860–1867.

Martínez-Pérez, C., Ward, C., Turnbull, A.K., Mullen, P., Cook, G., Meehan, J., Jarman, E.J., Thomson, P.I.T., Campbell, C.J., McPhail, D., et al. (2016). Antitumour activity of the novel flavonoid Oncamex in preclinical breast cancer models. Br. J. Cancer *114*, 905–916.

Mason, R.P., and Sherratt, S.C.R. (2017). Omega-3 fatty acid fish oil dietary supplements contain saturated fats and oxidized lipids that may interfere with their intended biological benefits. Biochem. Biophys. Res. Commun. *483*, 425–429.

Masungi, C., Mensch, J., Van Dijck, A., Borremans, C., Willems, B., Mackie, C., Noppe, M., and Brewster, M.E. (2008). Parallel artificial membrane permeability assay (PAMPA) combined with a 10-day multiscreen Caco-2 cell culture as a tool for assessing new drug candidates. Pharmazie *63*, 194–199.

Matesanz, N., Park, G., McAllister, H., Leahey, B., Devine, A., McVeigh, G., Gardiner, T.A., and McDonald, D.M. (2009). Omega-3 Fatty Acids Modulate Angiogenesis Through the Regulation of Nitric Oxide and Superoxide Anion Production in Retinal Microvascular Endothelial Cells (RMEC). Invest. Ophthalmol. Vis. Sci. *50*, 2957–2957.

Matsuo, A.Y.O., Gallagher, E.P., Trute, M., Stapleton, P.L., Levado, R., and Schlenk, D. (2008). Characterization of Phase I biotransformation enzymes in coho salmon (Oncorhynchus kisutch). Comp. Biochem. Physiol. C. Toxicol. Pharmacol. *147*, 78–84.

Matsuo, M., Sasaki, N., Saga, K., and Kaneko, T. (2005). Cytotoxicity of Flavonoids toward Cultured Normal Human Cells. Biol. Pharm. Bull. *28*, 253–259.

Mavria, G., Vercoulen, Y., Yeo, M., Paterson, H., Karasarides, M., Marais, R., Bird, D., and Marshall, C.J. (2005). ERK-MAPK signaling opposes Rho-kinase to promote endothelial cell survival and sprouting during angiogenesis. Cancer Cell *9*, 33–44.

Mayer, E.L. (2015). Targeting Breast Cancer with CDK Inhibitors. Curr. Oncol. Rep. *17*, 20.

McDonald, D.M., and Baluk, P. (2002). Significance of blood vessel leakiness in cancer. Cancer Res. *62*, 5381–5385.

McMahon, G. (2000). VEGF receptor signaling in tumor angiogenesis. Oncologist *5 Suppl 1*, 3–10.

Meacham, C.E., and Morrison, S.J. (2013). Tumour heterogeneity and cancer cell plasticity. Nature *501*, 328–337.

Mebratu, Y., and Tesfaigzi, Y. (2009). How ERK1/2 activation controls cell proliferation and cell death: Is subcellular localization the answer? Cell Cycle *8*, 1168–1175.

Medina, M., and Wandosell, F. (2011). Deconstructing GSK-3: The Fine Regulation of Its Activity. Int. J. Alzheimers. Dis. *2011*, 479249.

van der Meel, R., Symons, M.H., Kudernatsch, R., Kok, R.J., Schiffelers, R.M., Storm, G., Gallagher, W.M., and Byrne, A.T. (2011). The VEGF/Rho GTPase signalling pathway: A promising target for anti-angiogenic/anti-invasion therapy. Drug Discov. Today *16*, 219–228.

Mellou, F., Loutrari, H., Stamatis, H., Roussos, C., and Kolisis, F.N. (2006). Enzymatic esterification of flavonoids with unsaturated fatty acids: Effect of the novel esters on vascular endothelial growth factor release from K562 cells. Process Biochem. *41*, 2029–2034.

Meloche, S. (1995). Cell cycle reentry of mammalian fibroblasts is accompanied by the sustained activation of P44mapk and P42mapk isoforms in the G1 phase and their inactivation at the G1/s transition. J. Cell. Physiol. *163*, 577–588.

Melzer, C., Hass, R., von der Ohe, J., Lehnert, H., and Ungefroren, H. (2017). The role of TGF-β and its crosstalk with RAC1/RAC1b signaling in breast and pancreas carcinoma. Cell Commun. Signal. *15*, 19.

Mester, J., and Redeuilh, G. (2008). Proliferation of breast cancer cells: regulation, mediators, targets for therapy. Anticancer. Agents Med. Chem. *8*, 872–885.

Miettinen, P.J., Ebner, R., Lopez, A.R., and Derynck, R. (1994). TGF-beta induced transdifferentiation of mammary epithelial cells to mesenchymal cells: involvement of type I receptors. J. Cell Biol. *127*, 2021–2036.

Millan, F.A., Denhez, F., Kondaiah, P., and Akhurst, R.J. (1991). Embryonic gene expression patterns of TGF beta 1, beta 2 and beta 3 suggest different developmental functions in vivo. Development *111*, 1.

Mine, S., Fujisaki, T., Kawahara, C., Tabata, T., Iida, T., Yasuda, M., Yoneda, T., and Tanaka, Y. (2003). Hepatocyte growth factor enhances adhesion of breast cancer cells to endothelial cells in vitro through up-regulation of CD44. Exp. Cell Res. *288*, 189–197.

Mirochnik, Y., Kwiatek, A., and Volpert, O. V (2008). Thrombospondin and apoptosis: molecular mechanisms and use for design of complementation treatments. Curr. Drug Targets *9*, 851–862.

Mirossay, L., Varinská, L., and Mojžiš, J. (2018). Antiangiogenic effect of flavonoids and chalcones: An update. Int. J. Mol. Sci. *19*, 27.

Mirzoeva, S., Kim, N.D., Chiu, K., Franzen, C.A., Bergan, R.C., and Pelling, J.C. (2008). Inhibition of HIF-1 alpha and VEGF expression by the chemopreventive bioflavonoid apigenin is accompanied by Akt inhibition in human prostate carcinoma PC3-M cells. Mol. Carcinog. *47*, 686–700.

Mittnacht, S., Paterson, H., Olson, M.F., and Marshall, C.J. (1997). Ras signalling is required for inactivation of the tumour suppressor pRb cell-cycle control protein. Curr. Biol. *7*, 219–221.

Modzelewska, A., Pettit, C., Achanta, G., Davidson, N.E., Huang, P., and Khan, S.R. (2006). Anticancer activities of novel chalcone and bis-chalcone derivatives. Bioorg. Med. Chem. *14*, 3491–3495.

Mohammadi, M., Honegger, A.M., Rotin, D., Fischer, R., Bellot, F., Li, W., Dionne, C.A., Jaye, M., Rubinstein, M., and Schlessinger, J. (1991). A tyrosine-phosphorylated carboxy-terminal peptide of the fibroblast growth factor receptor (Flg) is a binding site for the SH2 domain of phospholipase C-gamma 1. Mol. Cell. Biol. *11*, 5068–5078.

Mohammadi, M., Dikic, I., Sorokin, A., Burgess, W.H., Jaye, M., and Schlessinger, J. (1996). Identification of six novel autophosphorylation sites on fibroblast growth factor receptor 1 and elucidation of their importance in receptor activation and signal transduction. Mol. Cell. Biol. *16*, 977–989.

Mojzis, J., Varinska, L., Mojzisova, G., Kostova, I., and Mirossay, L. (2008). Antiangiogenic effects of flavonoids and chalcones. Pharmacol. Res. *57*, 259–265.

Morris, G.J., Robinson, P.A., Lo, S., Samuel, T.A., Sheikh, A.A., Jordan Iii, W.E., Thomas, L.C., Kiel, K., and Peters, C.A. (2010). Residual Disease After Neoadjuvant Chemotherapy for Breast Cancer. Semin. Oncol. *37*, 1–10.

Morrison, D.K. (2001). KSR: a MAPK scaffold of the Ras pathway? J. Cell Sci. *114*, 1609–1612.

Moserle, L., and Casanovas, O. (2013). Anti-angiogenesis and metastasis: a tumour and stromal cell alliance. J. Intern. Med. *273*, 128–137.

Moustakas, A., and Heldin, P. (2014). TGFβ and matrix-regulated epithelial to mesenchymal transition. Biochim. Biophys. Acta - Gen. Subj. *1840*, 2621–2634.

Moyle, C.W.A., Cerezo, A.B., Winterbone, M.S., Hollands, W.J., Alexeev, Y., Needs, P.W., and Kroon, P.A. (2015). Potent inhibition of VEGFR-2 activation by tight binding of green tea epigallocatechin gallate and apple procyanidins to VEGF: Relevance to angiogenesis. Mol. Nutr. Food Res. *59*, 401–412.

Mudshinge, S.R., Deore, A.B., Patil, S., and Bhalgat, C.M. (2011). Nanoparticles: Emerging carriers for drug delivery. Saudi Pharm. J. *19*, 129–141.

Munin, A., and Edwards-Lévy, F. (2011). Encapsulation of Natural Polyphenolic Compounds; a Review. Pharmaceutics *3*, 793–829.

Murakami, M., and Simons, M. (2008). Fibroblast growth factor regulation of neovascularization. Curr. Opin. Hematol. *15*, 215–220.

Mustafa, D.A.M., Dekker, L.J., Stingl, C., Kremer, A., Stoop, M., Sillevis Smitt, P.A.E., Kros, J.M., and Luider, T.M. (2012). A proteome comparison between physiological angiogenesis and angiogenesis in glioblastoma. Mol. Cell. Proteomics *11*, 1–9.

Nagy, J.A., Chang, S.-H., Dvorak, A.M., and Dvorak, H.F. (2009). Why are tumour blood vessels abnormal and why is it important to know? Br. J. Cancer *100*, 865–869.

Nair, S.V.G., Ziaullah, and Rupasinghe, H.P.V. (2014). Fatty acid esters of phloridzin induce apoptosis of human liver cancer cells through altered gene expression. PLoS One *9*, e107149.

Narita, T., Kawakami-Kimura, N., Matsuura, N., Funahashi, H., and Kannagi, R. (1996). Adhesion of human breast cancer cells to vascular endothelium mediated by Sialyl Lewisx/E-selectin. Breast Cancer *3*, 19–23.

Narod, S.A., Iqbal, J., and Miller, A.B. (2015). Why have breast cancer mortality rates declined? J. Cancer Policy *5*, 8–17.

Nebert, D.W., Wikvall, K., and Miller, W.L. (2013). Human cytochromes P450 in health and disease. Philos. Trans. R. Soc. Lond. B. Biol. Sci. *368*, 20120431.

Nehra, D., Le, H.D., Fallon, E.M., Carlson, S.J., Woods, D., White, Y.A., Pan, A.H., Guo, L., Rodig, S.J., Tilly, J.L., et al. (2012). Prolonging the female reproductive lifespan and improving egg quality with dietary omega-3 fatty acids. Aging Cell *11*, 1046–1054.

Nelson, J.A., and Falk, R.E. (1993). The efficacy of phloridzin and phloretin on tumor cell growth. Anticancer Res. *13*, 2287–2292.

Nemeth, K., Plumb, G.W., Berrin, J.-G., Juge, N., Jacob, R., Naim, H.Y., Williamson, G., Swallow, D.M., and Kroon, P.A. (2003). Deglycosylation by small intestinal epithelial cell ?-glucosidases is a critical step in the absorption and metabolism of dietary flavonoid glycosides in humans. Eur. J. Nutr. *42*, 29–42.

New, D.C., Wu, K., Kwok, A.W.S., and Wong, Y.H. (2007). G protein-coupled receptor-induced Akt activity in cellular proliferation and apoptosis. FEBS J. *274*, 6025–6036.

Nguyen, L.T., Lee, Y.-H., Sharma, A.R., Park, J.-B., Jagga, S., Sharma, G., Lee, S.-S., and Nam, J.-S. (2017). Quercetin induces apoptosis and cell cycle arrest in triple-negative breast cancer cells through modulation of Foxo3a activity. Korean J. Physiol. Pharmacol. *21*, 205–213.

Ni, F., Gong, Y., Li, L., Abdolmaleky, H.M., and Zhou, J.-R. (2012). Flavonoid Ampelopsin Inhibits the Growth and Metastasis of Prostate Cancer In Vitro and in Mice. PLoS One *7*, e38802.

Nicolini, A., Ferrari, P., Kotlarova, L., Rossi, G., and Biava, P.M. (2015). The PI3K-AKt-mTOR Pathway and New Tools to Prevent Acquired Hormone Resistance in Breast Cancer. Curr. Pharm. Biotechnol. *16*, 804–815.

Niculescu, A.B., Chen, X., Smeets, M., Hengst, L., Prives, C., and Reed, S.I. (1998). Effects of p21(Cip1/Waf1) at both the G1/S and the G2/M cell cycle transitions: pRb is a critical determinant in blocking DNA replication and in preventing endoreduplication. Mol. Cell. Biol. *18*, 629–643.

Nieto, M.A., Huang, R.Y.-J., Jackson, R.A., and Thiery, J.P. (2016). EMT: 2016. Cell *166*, 21–45.

Van Nieuw Amerongen, G.P., Koolwijk, P., Versteilen, A., and Van Hinsbergh, V.W.M. (2003). Involvement of RhoA/Rho Kinase Signaling in VEGF-Induced Endothelial Cell Migration and Angiogenesis In Vitro. Arter. Thromb Vasc Biol *23*, 211–217.

Nihon Seikagakkai., K., Koizumi, K., Ishihara, H., and Kojima, K. (1985). The Journal of biochemistry. J. Biochem. *97*, 773–779.

Nishi, H., Hashimoto, K., and Panchenko, A.R. (2011). Phosphorylation in Protein-Protein Binding: Effect on Stability and Function. Structure *19*, 1807–1815.

Nishida, N., Yano, H., Nishida, T., Kamura, T., and Kojiro, M. (2006). Angiogenesis in cancer. Vasc. Health Risk Manag. *2*, 213–219.

Nooter, K., and Stoter, G. (1996). Molecular Mechanisms of Multidrug Resistance in Cancer Chemotherapy. Pathol. - Res. Pract. *192*, 768–780.

Nowak, D.G., Amin, E.M., Rennel, E.S., Hoareau-Aveilla, C., Gammons, M., Damodoran, G., Hagiwara, M., Harper, S.J., Woolard, J., Ladomery, M.R., et al. (2010). Regulation of vascular endothelial growth factor (VEGF) splicing from pro-angiogenic to anti-angiogenic isoforms: a novel therapeutic strategy for angiogenesis. J. Biol. Chem. *285*, 5532–5540.

Nuti, E., Bassani, B., Camodeca, C., Rosalia, L., Cantelmo, A., Gallo, C., Baci, D., Bruno, A., Orlandini, E., Nencetti, S., et al. (2017). Synthesis and antiangiogenic activity study of new hop chalcone Xanthohumol analogues. Eur. J. Med. Chem. *138*, 890–899.

O'Connor, M.J. (2015). Targeting the DNA Damage Response in Cancer. Mol. Cell *60*, 547–560.

O'Farrell, P.H. (2001). Triggering the all-or-nothing switch into mitosis. Trends Cell Biol. *11*, 512–519.

O'Reilly, M.S., Boehm, T., Shing, Y., Fukai, N., Vasios, G., Lane, W.S., Flynn, E., Birkhead, J.R., Olsen, B.R., and Folkman, J. (1997). Endostatin: An Endogenous Inhibitor of Angiogenesis and Tumor Growth. Cell *88*, 277–285.

O 'connor, M.J. (2015). Targeting the DNA Damage Response in Cancer. Mol. Cell *60*, 547–560.

Obakan-Yerlikaya, P., Arisan, E.D., Coker-Gurkan, A., and Palavan-Unsal, N. (2017). Breast Cancer and Flavonoids as Treatment Strategy. In Breast Cancer - From Biology to Medicine, (InTech), pp. 305–326.

Oda, T., Miyao, N., Takahashi, A., Yanase, M., Masumori, N., Itoh, N., Tamakawa, M., and Tsukamoto, T. (2001). Growth rates of primary and metastatic lesions of renal cell carcinoma. Int. J. Urol. *8*, 473–477.

Ogata, H., Kikuchi, Y., Natori, K., Shiraga, N., Kobayashi, M., Magoshi, S., Saito, F., Osaku, T., Kanazawa, S., Kubota, Y., et al. (2015). Liver Metastasis of a Triple-Negative Breast Cancer and Complete Remission for 5 Years After Treatment With Combined Bevacizumab/Paclitaxel/Carboplatin: Case Report and Review of the Literature. Medicine (Baltimore). *94*, e1756.

Ohga, N., Hida, K., Hida, Y., Muraki, C., Tsuchiya, K., Matsuda, K., Ohiro, Y., Totsuka, Y., and Shindoh, M. (2009). Inhibitory effects of epigallocatechin-3 gallate, a polyphenol in green tea, on tumor-associated endothelial cells and endothelial progenitor cells. Cancer Sci *100*, 1963–1970.

Oladipupo, S.S., Smith, C., Santeford, A., Park, C., Sene, A., Wiley, L.A., Osei-Owusu, P., Hsu, J., Zapata, N., Liu, F., et al. (2014). Endothelial cell FGF signaling is required for injury response but not for vascular homeostasis. Dev. Biol. *111*, 13379–13384.

Oliveira, E.J., Watson, D.G., and Grant, M.H. (2002). Metabolism of quercetin and kaempferol by rat hepatocytes and the identification of flavonoid glycosides in human plasma. Xenobiotica *32*, 279–287.

de Oliveira, C., Weir, S., Rangrej, J., Krahn, M.D., Mittmann, N., Hoch, J.S., Chan, K.K.W., and Peacock, S. (2018). The economic burden of cancer care in Canada: a population-based cost study. C. Open *6*, E1–E10.

De Oliveira, E.B., Humeau, C., Chebil, L., Maia, E.R., Dehez, F., Maigret, B., Ghoul, M., and Engasser, J.-M. (2009). A molecular modelling study to rationalize the regioselectivity in acylation of flavonoid glycosides catalyzed by Candida antarctica lipase B. J. Mol. Catal. B Enzym. *59*, 96–105.

Olson, M.F., and Sahai, E. (2009). The actin cytoskeleton in cancer cell motility. Clin. Exp. Metastasis *26*, 273–287.

Olson, M.F., Paterson, H.F., and Marshall, C.J. (1998). Signals from Ras and Rho GTPases interact to regulate expression of p21Waf1/Cip1. Nature *394*, 295–299.

Olson, M.L., Kargacin, M.E., Honeyman, T.W., Ward, C.A., and Kargacin, G.J. (2006). Effects of phytoestrogens on sarcoplasmic/endoplasmic reticulum calcium ATPase 2a and Ca2+ uptake into cardiac sarcoplasmic reticulum. J. Pharmacol. Exp. Ther. *316*, 628–635.

Olson, M.L., Kargacin, M.E., Ward, C.A., and Kargacin, G.J. (2007). Effects of phloretin and phloridzin on Ca2+ handling, the action potential, and ion currents in rat ventricular myocytes. J. Pharmacol. Exp. Ther. *321*, 921–929.

Olsson, A.-K., Dimberg, A., Kreuger, J., and Claesson-Welsh, L. (2006). VEGF receptor signalling ? in control of vascular function. Nat. Rev. Mol. Cell Biol. *7*, 359–371.

Omiecinski, C.J., Vanden Heuvel, J.P., Perdew, G.H., and Peters, J.M. (2011). Xenobiotic Metabolism, Disposition, and Regulation by Receptors: From Biochemical Phenomenon to Predictors of Major Toxicities. Toxicol. Sci. *120*, S49–S75.

Ong, S.H., Guy, G.R., Hadari, Y.R., Laks, S., Gotoh, N., Schlessinger, J., and Lax, I. (2000). FRS2 proteins recruit intracellular signaling pathways by binding to diverse targets on fibroblast growth factor and nerve growth factor receptors. Mol. Cell. Biol. *20*, 979–989.

Ornitz, D.M., and Itoh, N. (2015). The Fibroblast Growth Factor signaling pathway. Wiley Interdiscip. Rev. Dev. Biol. *4*, 215–266.

Ovcaricek, T., Frkovic, S.G., Matos, E., Mozina, B., and Borstnar, S. (2011). Triple negative breast cancer - prognostic factors and survival. Radiol. Oncol. *45*, 46–52.

Ozben, T. (2006). Mechanisms and strategies to overcome multiple drug resistance in cancer. FEBS Lett. *580*, 2903–2909.

Padua, D., and Massagué, J. (2009). Roles of TGFβ in metastasis. Cell Res. *19*, 89–102.

Paduch, R. (2016). The role of lymphangiogenesis and angiogenesis in tumor metastasis. Cell. Oncol. (Dordr). *39*, 397–410.

Paget, S. (1889). The distribution of secondary growths in cancer of the breast. Lancet *133*, 571–573.

Pal, S.K., and Mortimer, J. (2009). Triple-negative breast cancer: Novel therapies and new directions. Maturitas *63*, 269–274.

Palazzolo, G., Horvath, P., and Zenobi-Wong, M. (2012). The Flavonoid Isoquercitrin Promotes Neurite Elongation by Reducing RhoA Activity. PLoS One *7*, e49979.

Pang, M.-F., Georgoudaki, A.-M., Lambut, L., Johansson, J., Tabor, V., Hagikura, K., Jin, Y., Jansson, M., Alexander, J.S., Nelson, C.M., et al. (2016). TGF-β1-induced EMT promotes targeted migration of breast cancer cells through the lymphatic system by the activation of CCR7/CCL21-mediated chemotaxis. Oncogene *35*, 748–760.

Pang, X., Yi, T., Yi, Z., Cho, S.G., Qu, W., Pinkaew, D., Fujise, K., and Liu, M. (2009). Morelloflavone, a biflavonoid, inhibits tumor angiogenesis by targeting rho GTPases and extracellular signal-regulated kinase signaling pathways. Cancer Res. *69*, 518–525.

Papageorgis, P. (2015). TGFβ Signaling in Tumor Initiation, Epithelial-to-Mesenchymal Transition, and Metastasis. J. Oncol. *2015*, 587193.

Papetti, M., and Herman, I.M. (2002). Mechanisms of normal and tumor-derived angiogenesis. Am. J. Physiol. - Cell Physiol. *282*, C947–C970.

Park, H.G., Lawrence, P., Engel, M.G., Kothapalli, K., and Brenna, J.T. (2016). Metabolic fate of docosahexaenoic acid (DHA; 22:6n-3) in human cells: direct retroconversion of DHA to eicosapentaenoic acid (20:5n-3) dominates over elongation to tetracosahexaenoic acid (24:6n-3). FEBS Lett. *590*, 3188–3194.

Park, J.E., Keller, G.A., and Ferrara, N. (1993). The vascular endothelial growth factor (VEGF) isoforms: differential deposition into the subepithelial extracellular matrix and bioactivity of extracellular matrix-bound VEGF. Mol. Biol. Cell *4*, 1317–1326.

Parks, C.A., Brett, N.R., Agellon, S., Lavery, P., Vanstone, C.A., Maguire, J.L., Rauch, F., and Weiler, H.A. (2017). DHA and EPA in red blood cell membranes are associated with dietary intakes of omega-3-rich fish in healthy children. Prostaglandins, Leukot. Essent. Fat. Acids *124*, 11–16.

Parri, M., and Chiarugi, P. (2010). Rac and Rho GTPases in cancer cell motility control. Cell Commun. Signal. *8*, 23.

Patel, H.H., and Insel, P.A. (2009). Lipid rafts and caveolae and their role in compartmentation of redox signaling. Antioxid. Redox Signal. *11*, 1357–1372.

dela Paz, N.G., Melchior, B., and Frangos, J.A. (2013). Early VEGFR2 activation in response to flow is VEGF-dependent and mediated by MMP activity. Biochem. Biophys. Res. Commun. *434*, 641–646.

Pećina-Slaus, N. (2003). Tumor suppressor gene E-cadherin and its role in normal and malignant cells. Cancer Cell Int. *3*, 17.

Peck, S.C. (2006). Analysis of protein phosphorylation: methods and strategies for studying kinases and substrates. Plant J. *45*, 512–522.

Peeper, D.S., Upton, T.M., Ladha, M.H., Neuman, E., Zalvide, J., Bernards, R., DeCaprio, J.A., and Ewen, M.E. (1997). Ras signalling linked to the cell-cycle machinery by the retinoblastoma protein. Nature *386*, 177–181.

Peitzsch, C., Tyutyunnykova, A., Pantel, K., and Dubrovska, A. (2017). Cancer stem cells: The root of tumor recurrence and metastases. Semin. Cancer Biol. *44*, 10–24.

Perrot-Applanat, M. (2012). VEGF isoforms. Cell Adh. Migr. *6*, 526–527.

Peterson, J., Lagiou, P., Samoli, E., Lagiou, A., Katsouyanni, K., La Vecchia, C., Dwyer, J., and Trichopoulos, D. (2003). Flavonoid intake and breast cancer risk: a case--control study in Greece. Br. J. Cancer *89*, 1255–1259.

Petri, N., Tannergren, C., Holst, B., Mellon, F.A., Bao, Y., Plumb, G.W., Bacon, J., O'Leary, K.A., Kroon, P.A., Knutson, L., et al. (2003). Absorption/metabolism of sulforaphane and quercetin, and regulation of phase II enzymes, in human jejunum in vivo. Drug Metab. Dispos. *31*, 805–813.

Phan, M.A.T., Paterson, J., Bucknall, M., and Arcot, J. (2016). Interactions between phytochemicals from fruits and vegetables: Effects on bioactivities and bioavailability. Crit. Rev. Food Sci. Nutr. 1–20.

Phi, L.T.H., Sari, I.N., Yang, Y.-G., Lee, S.-H., Jun, N., Kim, K.S., Lee, Y.K., and Kwon, H.Y. (2018). Cancer Stem Cells (CSCs) in Drug Resistance and their Therapeutic Implications in Cancer Treatment. Stem Cells Int. *2018*, 1–16.

Philpott, N.J., Turner, a J., Scopes, J., Westby, M., Marsh, J.C., Gordon-Smith, E.C., Dalgleish, a G., and Gibson, F.M. (1996). The use of 7-amino actinomycin D in identifying apoptosis: simplicity of use and broad spectrum of application compared with other techniques. Blood *87*, 2244–2251.

Piantelli, M., Rossi, C., Iezzi, M., La Sorda, R., Iacobelli, S., Alberti, S., and Natali, P.G. (2006). Flavonoids inhibit melanoma lung metastasis by impairing tumor cells endothelium interactions. J. Cell. Physiol. *207*, 23–29.

Pickup, M., Novitskiy, S., and Moses, H.L. (2013). The roles of TGFβ in the tumour microenvironment. Nat. Rev. Cancer *13*, 788–799.

Pietenpol, J.A., and Stewart, Z.A. (2002). Cell cycle checkpoint signaling: cell cycle arrest versus apoptosis. Toxicology *181–182*, 475–481.

Di Pietro, A., Conseil, G., Pérez-Victoria, J.M., Dayan, G., Baubichon-Cortay, H., Trompier, D., Steinfels, E., Jault, J.M., de Wet, H., Maitrejean, M., et al. (2002). Modulation by flavonoids of cell multidrug resistance mediated by P-glycoprotein and related ABC transporters. Cell. Mol. Life Sci. *59*, 307–322.

Pikulski, M., and Brodbelt, J.S. (2003). Differentiation of Flavonoid Glycoside Isomers by Using Metal Complexation and Electrospray Ionization Mass Spectrometry. J Am Soc Mass Spectrom *14*, 1437–1453.

Pillai, S., Kovacs, M., and Chellappan, S. (2010). Regulation of vascular endothelial growth factor receptors by Rb and E2F1: role of acetylation. Cancer Res. *70*, 4931–4940.

Pistelli, M., Pagliacci, A., Battelli, N., Santinelli, A., Biscotti, T., Ballatore, Z., Berardi, R., and Cascinu, S. (2013). Prognostic factors in early-stage triple-negative breast cancer: lessons and limits from clinical practice. Anticancer Res. *33*, 2737–2742.

Pogash, T.J., El-Bayoumy, K., Amin, S., Gowda, K., de Cicco, R.L., Barton, M., Su, Y., Russo, I.H., Himmelberger, J.A., Slifker, M., et al. (2015). Oxidized derivative of docosahexaenoic acid preferentially inhibit cell proliferation in triple negative over luminal breast cancer cells. In Vitro Cell. Dev. Biol. Anim. *51*, 121–127.

Polyak, K. (2011). Heterogeneity in breast cancer. J. Clin. Invest. *121*, 3786–3788.

Poojari, Y., and Clarson, S.J. (2009). Lipase catalyzed synthesis of silicone polyesters. Chem. Commun. *0*, 6834.

Poola, I., Abraham, J., Liu, A., Marshalleck, J.J., and Dewitty, R.L. (2008). The Cell Surface Estrogen Receptor, G Protein- Coupled Receptor 30 (GPR30), is Markedly Down Regulated During Breast Tumorigenesis. Breast Cancer (Auckl). *1*, 65–78.

Pópulo, H., Lopes, J.M., and Soares, P. (2012). The mTOR signalling pathway in human cancer. Int. J. Mol. Sci. *13*, 1886–1918.

Porter, A.P., Papaioannou, A., and Malliri, A. (2016). Deregulation of Rho GTPases in cancer. Small GTPases *7*, 123–138.

Pratheeshkumar, P., Budhraja, A., Son, Y.-O., Wang, X., Zhang, Z., Ding, S., Wang, L., Hitron, A., Lee, J.-C., Xu, M., et al. (2012). Quercetin inhibits angiogenesis mediated human prostate tumor growth by targeting VEGFR- 2 regulated AKT/mTOR/P70S6K signaling pathways. PLoS One *7*, e47516.

Pratt, D.S., and Kaplan, M.M. (2000). Evaluation of Abnormal Liver-Enzyme Results in Asymptomatic Patients. N. Engl. J. Med. *342*, 1266–1271.

Prieto-Vila, M., Takahashi, R., Usuba, W., Kohama, I., and Ochiya, T. (2017). Drug Resistance Driven by Cancer Stem Cells and Their Niche. Int. J. Mol. Sci. *18*, 2574.

Pritchard, J.R., Bruno, P.M., Gilbert, L.A., Capron, K.L., Lauffenburger, D.A., and Hemann, M.T. (2013). Defining principles of combination drug mechanisms of action. Proc. Natl. Acad. Sci. U. S. A. *110*, E170-9.

Pucci, B., Kasten, M., and Giordano, A. (2000). Cell cycle and apoptosis. Neoplasia *2*, 291–299.

Qiu, J., Kitamura, Y., Miyata, Y., Tamaru, S., Tanaka, K., Tanaka, T., and Matsui, T. (2012). Transepithelial Transport of Theasinensins through Caco-2 Cell Monolayers and Their Absorption in Sprague–Dawley Rats after Oral Administration. J. Agric. Food Chem. *60*, 8036–8043.

Quail, D.F., and Joyce, J.A. (2013). Microenvironmental regulation of tumor progression and metastasis. Nat. Med. *19*, 1423–1437.

Querques, G., Forte, R., and Souied, E.H. (2011). Retina and omega-3. J. Nutr. Metab. *2011*, 748361.

Raabe, T., and Rapp, U.R. (2002). KSR-A Regulator and Scaffold Protein of the MAPK Pathway. Sci. Signal. *136*, 28.

Rabbani, S.A., and Mazar, A.P. (2001). The role of the plasminogen activation system in angiogenesis and metastasis. Surg. Oncol. Clin. N. Am. *10*, 393–415.

Raftopoulou, M., and Hall, A. (2004). Cell migration: Rho GTPases lead the way. Dev. Biol. *265*, 23–32.

Rahman, M.M., Veigas, J.M., Williams, P.J., and Fernandes, G. (2013). DHA is a more potent inhibitor of breast cancer metastasis to bone and related osteolysis than EPA. Breast Cancer Res. Treat. *141*, 341–352.

Rahman, M.S., Alam, M.B., Choi, Y.H., and Yoo, J.C. (2017). Anticancer activity and antioxidant potential of Aponogeton undulatus against Ehrlich ascites carcinoma cells in Swiss albino mice. Oncol. Lett. *14*, 3169–3176.

Rampurwala, M., Wisinski, K.B., and O'Regan, R. (2016). Role of the androgen receptor in triple-negative breast cancer. Clin. Adv. Hematol. Oncol. *14*, 186–193.

Rao, A. V, and Ali, A. (2007). Biologically active phytochemicals in human health: Lycopene. Int. J. Food Prop. *10*, 279–288.

Ravishankar, D., Watson, K.A., Greco, F., and Osborn, H.M.I. (2016). Novel synthesised flavone derivatives provide significant insight into the structural features required for enhanced anti-proliferative activity. RSC Adv. *6*, 64544–64556.

Raza, A., Franklin, M.J., and Dudek, A.Z. (2010). Pericytes and vessel maturation during tumor angiogenesis and metastasis. Am. J. Hematol. *85*, 593–598.

Rhodes, L. V., Tilghman, S.L., Boue, S.M., Wang, S., Khalili, H., Muir, S.E., Bratton, M.R., Zhang, Q., Wang, G., Burow, M.E., et al. (2012). Glyceollins as novel targeted therapeutic for the treatment of triple-negative breast cancer. Oncol. Lett. *3*, 163–171.

Ribatti, D. (2016). Tumor refractoriness to anti-VEGF therapy. Oncotarget *7*, 46668–46677.

Riddick, D.S., Ding, X., Wolf, C.R., Porter, T.D., Pandey, A. V, Zhang, Q.-Y., Gu, J., Finn, R.D., Ronseaux, S., McLaughlin, L.A., et al. (2013). NADPH-cytochrome P450 oxidoreductase: roles in physiology, pharmacology, and toxicology. Drug Metab. Dispos. *41*, 12–23.

Ridley, A.J. (2015). Rho GTPase signalling in cell migration. Curr. Opin. Cell Biol. *36*, 103–112.

Ring, B.Z., and Ross, D.T. (2005). Predicting the sites of metastases. Genome Biol. *6*, 241.

Rivenbark, A.G., O'Connor, S.M., and Coleman, W.B. (2013). Molecular and Cellular Heterogeneity in Breast Cancer: Challenges for Personalized Medicine. Am. J. Pathol. *183*, 1113–1124.

Rizk, M., Zou, L., Savic, R., and Dooley, K. (2017). Importance of Drug Pharmacokinetics at the Site of Action. Clin. Transl. Sci. *10*, 133–142.

Robinson, S. (1993). Principles of Chemotherapy. Eur. J. Cancer Care (Engl). *2*, 55–65.

Röcken, M. (2010). Early tumor dissemination, but late metastasis: insights into tumor dormancy. J. Clin. Invest. *120*, 1800–1803.

Romanel, A., Jensen, L.J., Cardelli, L., and Csikász-Nagy, A. (2012). Transcriptional Regulation Is a Major Controller of Cell Cycle Transition Dynamics. PLoS One *7*, e29716.

Romanouskaya, T. V., and Grinev, V. V. (2009). Cytotoxic Effect of Flavonoids on Leukemia Cells and Normal Cells of Human Blood. Bull. Exp. Biol. Med. *148*, 57–59.

Roodman, G.D. (2004). Mechanisms of Bone Metastasis. N. Engl. J. Med. *350*, 1655–1664.

Rose, D.P., Connolly, J.M., and Coleman, M. (1996). Effect of omega-3 fatty acids on the progression of metastases after the surgical excision of human breast cancer cell solid tumors growing in nude mice. Clin. Cancer Res. *2*, 1751–1756.

Rossette, M.C., Moraes, D.C., Sacramento, E.K., Romano-Silva, M.A., Carvalho, J.L., Gomes, D.A., Caldas, H., Friedman, E., Bastos-Rodrigues, L., and De Marco, L. (2017). The *In Vitro* and *In Vivo* Antiangiogenic Effects of Flavokawain B. Phyther. Res. *31*, 1607–1613.

Rubin, S.M. (2013). Deciphering the retinoblastoma protein phosphorylation code. Trends Biochem. Sci. *38*, 12–19.

Ruiz, P.A., and Haller, D. (2006). Functional diversity of flavonoids in the inhibition of the proinflammatory NF-kappaB, IRF, and Akt signaling pathways in murine intestinal epithelial cells. J. Nutr. *136*, 664–671.

Rundhaug, J.E. (2005). Matrix metalloproteinases and angiogenesis. J. Cell. Mol. Med. *9*, 267–285.

Rupasinghe, H.P.V., and Yasmin, A. (2010). Inhibition of oxidation of aqueous emulsions of Omega-3 fatty acids and fish oil by phloretin and phloridzin. Molecules *15*, 251–257.

Rupasinghe, H.P.V., Thilakarathna, S.H., and Nair, S.V.G. (2012). Polyphenols: Chemistry, Dietary Sources and Health Benefits. In Polyphenols: Chemistry, Dietary Sources and Health Benefits, X.Y. and L.L. J. Sun, K. N. Prasad, A. Ismail, B. Yang, ed. (Nova Science Publishers, Inc. Hauppauge, NY, USA), pp. 333–368.

Sak, K. (2012). Chemotherapy and dietary phytochemical agents. Chemother. Res. Pract. *2012*, 282570.

Sak, K. (2014). Cytotoxicity of dietary flavonoids on different human cancer types. Pharmacogn. Rev. *8*, 122–146.

Salem, J.H., Humeau, C., Chevalot, I., Harscoat-Schiavo, C., Vanderesse, R., Blanchard, F., and Fick, M. (2010). Effect of acyl donor chain length on isoquercitrin acylation and biological activities of corresponding esters. Process Biochem. *45*, 382–389.

Salnikov, A. V., Iversen, V. V., Koisti, M., Sundberg, C., Johansson, L., Stuhr, L.B., Sjöquist, M., Ahlström, H., Reed, R.K., and Rubin, K. (2003). Lowering of tumor interstitial fluid pressure specifically augments efficacy of chemotherapy. FASEB J. *17*, 1756–1758.

Sampieri, K., and Fodde, R. (2012). Cancer stem cells and metastasis. Semin. Cancer Biol. *22*, 187–193.

Santuario-Facio, S.K., Cardona-Huerta, S., Perez-Paramo, Y.X., Trevino, V., Hernandez-Cabrera, F., Rojas-Martinez, A., Uscanga-Perales, G., Martinez-Rodriguez, J.L., Martinez-Jacobo, L., Padilla-Rivas, G., et al. (2017). A New Gene Expression Signature for Triple Negative Breast Cancer Using Frozen Fresh Tissue before Neoadjuvant Chemotherapy. Mol. Med. *23*, 101.

Sarabipour, S., and Hristova, K. (2016). Mechanism of FGF receptor dimerization and activation. Nat. Commun. *7*, 10262.

Sarni, D., and Kerem, B. (2017). Oncogene-Induced Replication Stress Drives Genome Instability and Tumorigenesis. Int. J. Mol. Sci. *19*, 1–10.

Schaeffer, D., Somarelli, J.A., Hanna, G., Palmer, G.M., and Garcia-Blanco, M.A. (2014). Cellular migration and invasion uncoupled: increased migration is not an inexorable consequence of epithelial-to-mesenchymal transition. Mol. Cell. Biol. *34*, 3486–3499.

Schmid, I., Krall, W.J., Uittenbogaart, C.H., Braun, J., and Giorgi, J. V (1992). Dead cell discrimination with 7-amino-actinomycin D in combination with dual color immunofluorescence in single laser flow cytometry. Cytometry *13*, 204–208.

Schöning, J.P., Monteiro, M., and Gu, W. (2017). Drug resistance and cancer stem cells: the shared but distinct roles of hypoxia-inducible factors HIF1α and HIF2α. Clin. Exp. Pharmacol. Physiol. *44*, 153–161.

van Schoor, G., Moss, S.M., Otten, J.D.M., Donders, R., Paap, E., den Heeten, G.J., Holland, R., Broeders, M.J.M., and Verbeek, A.L.M. (2011). Increasingly strong reduction in breast cancer mortality due to screening. Br. J. Cancer *104*, 910–914.

Schramm, D.D., Collins, H.E., and German, J.B. (1999). Flavonoid transport by mammalian endothelial cells. J. Nutr. Biochem. *10*, 193–197.

Scully, O.J., Bay, B.-H., Yip, G., and Yu, Y. (2012). Breast cancer metastasis. Cancer Genomics Proteomics *9*, 311–320.

Seaman, S., Stevens, J., Yang, M.Y., Logsdon, D., Graff-Cherry, C., and St Croix, B. (2007). Genes that distinguish physiological and pathological angiogenesis. Cancer Cell *11*, 539–554.

Seger, R., and Krebs, E.G. (1995). The MAPK signaling cascade. FASEB J. *9*, 726–735.

Sekhon-Loodu, S., Ziaullah, and Rupasinghe, H.P.V. (2015). Docosahexaenoic acid ester of phloridzin inhibit lipopolysaccharide-induced inflammation in THP-1 differentiated macrophages. Int. Immunopharmacol. *25*, 199–206.

Sekine, S., Kubo, K., Tadokoro, T., and Saito, M. (2007). Effect of Docosahexaenoic Acid Ingestion on Temporal Change in Urinary Excretion of Mercapturic Acid in ODS Rats. J. Clin. Biochem. Nutr. *41*, 184–190.

Senger, D.R., and Davis, G.E. (2011). Angiogenesis. Cold Spring Harb. Perspect. Biol. *3*, 1–19.

Serrano-Gomez, S.J., Maziveyi, M., and Alahari, S.K. (2016). Regulation of epithelial-mesenchymal transition through epigenetic and post-translational modifications. Mol. Cancer *15*, 18.

Sesink, A.L.A., O'Leary, K.A., and Hollman, P.C.H. (2001). Quercetin Glucuronides but Not Glucosides Are Present in Human Plasma after Consumption of Quercetin-3-Glucoside or Quercetin-4′-Glucoside. J. Nutr. *131*, 1938–1941.

Seyfried, T.N., and Huysentruyt, L.C. (2013). On the origin of cancer metastasis. Crit. Rev. Oncog. *18*, 43–73.

Shankar, J., Boscher, C., and Nabi, I.R. (2015). Caveolin-1, galectin-3 and lipid raft domains in cancer cell signalling. Essays Biochem. *57*, 189–201.

Sharpe, R., Pearson, A., Herrera-Abreu, M.T., Johnson, D., Mackay, A., Welti, J.C., Natrajan, R., Reynolds, A.R., Reis-Filho, J.S., Ashworth, A., et al. (2011). FGFR signaling promotes the growth of triple-negative and basal-like breast cancer cell lines both in vitro and in vivo. Clin. Cancer Res. *17*, 5275–5286.

Shibuya, M. (2006). Vascular endothelial growth factor receptor-1 (VEGFR-1/Flt-1): a dual regulator for angiogenesis. Angiogenesis *9*, 225–230.

Shibuya, M. (2010). Tyrosine Kinase Receptor Flt/VEGFR Family: Its Characterization Related to Angiogenesis and Cancer. Genes Cancer *1*, 1119–1123.

Shibuya, M. (2011). Vascular Endothelial Growth Factor (VEGF) and Its Receptor (VEGFR) Signaling in Angiogenesis: A Crucial Target for Anti- and Pro-Angiogenic Therapies. Genes Cancer *2*, 1097–1105.

Shiga, K., Hara, M., Nagasaki, T., Sato, T., Takahashi, H., and Takeyama, H. (2015). Cancer-Associated Fibroblasts: Their Characteristics and Their Roles in Tumor Growth. Cancers (Basel). *7*, 2443–2458.

Shimada, H., Nilsson, C., Noda, Y., Kim, H., Lundström, T., and Yajima, T. (2017). Effects of Food on the Pharmacokinetics of Omega-3-Carboxylic Acids in Healthy Japanese Male Subjects: A Phase , Randomized, Open-label, Three-period, Crossover Trial. J Atheroscler Thromb *24*, 980–987.

Shin, S., Jing, K., Jeong, S., Kim, N., Song, K.-S., Heo, J.-Y., Park, J.-H., Seo, K.-S., Han, J., Park, J.-I., et al. (2013). The omega-3 polyunsaturated fatty acid DHA induces simultaneous apoptosis and autophagy via mitochondrial ROS-mediated Akt-mTOR signaling in prostate cancer cells expressing mutant p53. Biomed Res. Int. *2013*, 568671.

Shin, S.K., Kim, J.H., Lee, J.H., Son, Y.H., Lee, M.W., Kim, H.J., Noh, S.A., Kim, K.P., Kim, I.-G., and Lee, M.J. (2017). Docosahexaenoic acid-mediated protein aggregates may reduce proteasome activity and delay myotube degradation during muscle atrophy in vitro. Exp. Mol. Med. *49*.

Shiozawa, Y., Nie, B., Pienta, K.J., Morgan, T.M., and Taichman, R.S. (2013). Cancer stem cells and their role in metastasis. Pharmacol. Ther. *138*, 285–293.

Sighoko, D., Hunt, B.R., Irizarry, B., Watson, K., Ansell, D., and Murphy, A.M. (2018). Disparity in breast cancer mortality by age and geography in 10 racially diverse US cities. Cancer Epidemiol. *53*, 178–183.

Siletz, A., Schnabel, M., Kniazeva, E., Schumacher, A.J., Shin, S., Jeruss, J.S., and Shea, L.D. (2013). Dynamic Transcription Factor Networks in Epithelial-Mesenchymal Transition in Breast Cancer Models. PLoS One *8*, e57180.

Simón, D., Benitez, M.J., Gimenez-Cassina, A., Garrido, J.J., Bhat, R. V., Díaz-Nido, J., and Wandosell, F. (2008). Pharmacological inhibition of GSK-3 is not strictly correlated with a decrease in tyrosine phosphorylation of residues 216/279. J. Neurosci. Res. *86*, 668–674.

Simone, C.B., Simone, N.L., and Simone, V. (2007). Antioxidants and other nutrients do not interfere with chemotherapy or radiation therapy and can increase kill and increase survival, part 1. Altern. Ther. Health Med. *13*, 22–28.

Singh, H., Milner, C.S., Aguilar Hernandez, M.M., Patel, N., and Brindle, N.P.J. (2009a). Vascular endothelial growth factor activates the Tie family of receptor tyrosine kinases. Cell. Signal. *21*, 1346–1350.

Singh, R., Lillard, J.W., and Jr. (2009b). Nanoparticle-based targeted drug delivery. Exp. Mol. Pathol. *86*, 215–223.

Sirkisoon, S.R., Carpenter, R.L., Rimkus, T., Miller, L., Metheny-Barlow, L., and Lo, H.-W. (2016). EGFR and HER2 signaling in breast cancer brain metastasis. Front. Biosci. (Elite Ed). *8*, 245–263.

Sleeman, J.P., Nazarenko, I., and Thiele, W. (2011). Do all roads lead to Rome? Routes to metastasis development. Int. J. Cancer *128*, 2511–2526.

Smid, M., Wang, Y., Zhang, Y., Sieuwerts, A.M., Yu, J., Klijn, J.G.M., Foekens, J.A., and Martens, J.W.M. (2008). Subtypes of breast cancer show preferential site of relapse. Cancer Res. *68*, 3108–3114.

Smith, G.A., Fearnley, G.W., Tomlinson, D.C., Harrison, M.A., and Ponnambalam, S. (2015). The cellular response to vascular endothelial growth factors requires co-ordinated signal transduction, trafficking and proteolysis. Biosci. Rep. *35*, 1–15.

Smith, M.L., Murphy, K., Doucette, C.D., Greenshields, A.L., and Hoskin, D.W. (2016). The Dietary Flavonoid Fisetin Causes Cell Cycle Arrest, Caspase-Dependent Apoptosis, and Enhanced Cytotoxicity of Chemotherapeutic Drugs in Triple-Negative Breast Cancer Cells. J. Cell. Biochem. *117*, 1913–1925.

Soga, N., Namba, N., McAllister, S., Cornelius, L., Teitelbaum, S.L., Dowdy, S.F., Kawamura, J., and Hruska, K.A. (2001). Rho Family GTPases Regulate VEGF-Stimulated Endothelial Cell Motility. Exp. Cell Res. *269*, 73–87.

Soler, A., Romero, M.P., Macià, A., Saha, S., Furniss, C.S.M., Kroon, P.A., and Motilva, M.J. (2010). Digestion stability and evaluation of the metabolism and transport of olive oil phenols in the human small-intestinal epithelial Caco-2/TC7 cell line. Food Chem. *119*, 703–714.

Solomon, V.R., and Lee, H. (2012). Anti-breast cancer activity of heteroaryl chalcone derivatives. Biomed. Pharmacother. *66*, 213–220.

Somanath, P.R., Razorenova, O. V, Chen, J., and Byzova, T. V (2006). Akt1 in endothelial cell and angiogenesis. Cell Cycle *5*, 512–518.

Song, H., Hedayati, M., Hobbs, R.F., Shao, C., Bruchertseifer, F., Morgenstern, A., Deweese, T.L., and Sgouros, G. (2013). Targeting aberrant DNA double-strand break repair in triple-negative breast cancer with alpha-particle emitter radiolabeled anti-EGFR antibody. Mol. Cancer Ther. *12*, 2043–2054.

Song, J.-L., Chen, C., Yuan, J.-P., and Sun, S.-R. (2016). Progress in the clinical detection of heterogeneity in breast cancer. Cancer Med. *5*, 3475–3488.

Soni, A., Ren, Z., Hameed, O., Chanda, D., Morgan, C.J., Siegal, G.P., and Wei, S. (2015). Breast Cancer Subtypes Predispose the Site of Distant Metastases. Am. J. Clin. Pathol. *143*, 471–478.

Soumya, S.J., Athira, A.P., Binu, S., and Sudhakaran, P.R. (2016). mTOR as a Modulator of Metabolite Sensing Relevant to Angiogenesis. In Molecules to Medicine with MTOR, (Elsevier), pp. 229–243.

Spencer, J.P.., Abd El Mohsen, M.M., and Rice-Evans, C. (2004). Cellular uptake and metabolism of flavonoids and their metabolites: implications for their bioactivity. Arch. Biochem. Biophys. *423*, 148–161.

Srivastava, S., Somasagara, R.R., Hegde, M., Nishana, M., Tadi, S.K., Srivastava, M., Choudhary, B., and Raghavan, S.C. (2016). Quercetin, a Natural Flavonoid Interacts with DNA, Arrests Cell Cycle and Causes Tumor Regression by Activating Mitochondrial Pathway of Apoptosis. Sci. Rep. *6*, 24049.

Stacker, S.A., and Achen, M.G. (2013). The VEGF signaling pathway in cancer: the road ahead. Chin. J. Cancer *32*, 297–302.

Stankovic, S., Konjevic, G., Gopcevic, K., Jovic, V., Inic, M., and Jurisic, V. (2010). Activity of MMP-2 and MMP-9 in sera of breast cancer patients. Pathol. - Res. Pract. *206*, 241–247.

Stauffer, C.E., and Zeffren, E. (1970). Concerning the Mechanism of Ester Hydrolysis by Proteases. J. Biol. Chem. *245*, 3282–3284.

Stetler-Stevenson, W.G. (1999). Matrix metalloproteinases in angiogenesis: a moving target for therapeutic intervention. J. Clin. Invest. *103*, 1237–1241.

Suhardja, A., and Hoffman, H. (2003). Role of growth factors and their receptors in proliferation of microvascular endothelial cells. Microsc. Res. Tech. *60*, 70–75.

Sun, C.Q., Johnson, K.D., Wong, H., and Foo, L.Y. (2017). Biotransformation of Flavonoid Conjugates with Fatty Acids and Evaluations of Their Functionalities. Front. Pharmacol. *8*, 759.

Sun, T., Chen, Q.Y., Wu, L.J., Yao, X.M., and Sun, X.J. (2012). Antitumor and antimetastatic activities of grape skin polyphenols in a murine model of breast cancer. Food Chem. Toxicol. *50*, 3462–3467.

Suphioglu, C., De Mel, D., Kumar, L., Sadli, N., Freestone, D., Michalczyk, A., Sinclair, A., and Ackland, M.L. (2010). The omega-3 fatty acid, DHA, decreases neuronal cell death in association with altered zinc transport. FEBS Lett. *584*, 612–618.

Surh, Y.-J. (2003). Cancer chemoprevention with dietary phytochemicals. Nat. Rev. Cancer *3*, 768–780.

Sutherland, K.D., and Visvader, J.E. (2015). Cellular Mechanisms Underlying Intertumoral Heterogeneity. Trends in Cancer *1*, 15–23.

Swietach, P., Hulikova, A., Patiar, S., Vaughan-Jones, R.D., and Harris, A.L. (2012). Importance of Intracellular pH in Determining the Uptake and Efficacy of the Weakly Basic Chemotherapeutic Drug, Doxorubicin. PLoS One *7*, e35949.

Synnott, N.C., Murray, A., McGowan, P.M., Kiely, M., Kiely, P.A., O'Donovan, N., O'Connor, D.P., Gallagher, W.M., Crown, J., and Duffy, M.J. (2017). Mutant p53: a novel target for the treatment of patients with triple-negative breast cancer? Int. J. Cancer *140*, 234–246.

Tahergorabi, Z., and Khazaei, M. (2012). A review on angiogenesis and its assays. Iran. J. Basic Med. Sci. *15*, 1110–1126.

Takano, H., Tsuchikawa, T., Nakamura, T., Okamura, K., Shichinohe, T., and Hirano, S. (2015). Potential risk of residual cancer cells in the surgical treatment of initially unresectable pancreatic carcinoma after chemoradiotherapy. World J. Surg. Oncol. *13*, 209.

Tan, G.-J., Peng, Z.-K., Lu, J.-P., and Tang, F.-Q. (2013). Cathepsins mediate tumor metastasis. World J. Biol. Chem. *4*, 91–101.

Tang, D., Wu, D., Hirao, A., Lahti, J.M., Liu, L., Mazza, B., Kidd, V.J., Mak, T.W., and Ingram, A.J. (2002). ERK activation mediates cell cycle arrest and apoptosis after DNA damage independently of p53. J. Biol. Chem. *277*, 12710–12717.

Tennakoon, A.H., Izawa, T., Kuwamura, M., and Yamate, J. (2015). Pathogenesis of Type 2 Epithelial to Mesenchymal Transition (EMT) in Renal and Hepatic Fibrosis. J. Clin. Med. *5*, 1–16.

Thiery, J.P., and Lim, C.T. (2013). Tumor Dissemination: An EMT Affair. Cancer Cell *23*, 272–273.

Thilakarathna, S.H., and Rupasinghe, H.P.V. (2013). Flavonoid bioavailability and attempts for bioavailability enhancement. Nutrients *5*, 3367–3387.

Thompson, E.W., Newgreen, D.F., Tarin, D., Hu, M.G., Katsurano, M., Sasaki, A., and Hu, G. (2005). Carcinoma invasion and metastasis: a role for epithelial-mesenchymal transition? Cancer Res. *65*, 5991–5; discussion 5995.

Tojkander, S., Gateva, G., and Lappalainen, P. (2012). Actin stress fibers--assembly, dynamics and biological roles. J. Cell Sci. *125*, 1855–1864.

Tolcher, A.W. (2001). Novel compounds in the therapy of breast cancer: opportunities for integration with docetaxel. Oncologist *6*, 40–44.

Tonini, T., Rossi, F., and Claudio, P.P. (2003). Molecular basis of angiogenesis and cancer. Oncogene *22*, 6549–6556.

Trecate, G., Sinues, P.M.-L., and Orlandi, R. (2016). Noninvasive strategies for breast cancer early detection. Futur. Oncol. *12*, 1395–1411.

Triantafyllou, A., Liakos, P., Tsakalof, A., Chachami, G., Paraskeva, E., Molyvdas, P.-A., Georgatsou, E., Simos, G., and Bonanou, S. (2007). The flavonoid quercetin induces hypoxia-inducible factor-1alpha (HIF-1alpha) and inhibits cell proliferation by depleting intracellular iron. Free Radic. Res. *41*, 342–356.

Tsai, J.H., and Yang, J. (2013). Epithelial-mesenchymal plasticity in carcinoma metastasis. Genes Dev. *27*, 2192–2206.

Tseng, L.M., Hsu, N.C., Chen, S.C., Lu, Y.S., Lin, C.H., Chang, D.Y., Li, H., Lin, Y.C., Chang, H.K., Chao, T.C., et al. (2013). Distant metastasis in triple-negative breast cancer. Neoplasma *60*, 290–294.

Tsuji-Tamura, K., and Ogawa, M. (2016). Inhibition of the PI3K-Akt and mTORC1 signaling pathways promotes the elongation of vascular endothelial cells. J. Cell Sci. *129*, 1165–1178.

Tubbs, A., and Nussenzweig, A. (2017). Endogenous DNA Damage as a Source of Genomic Instability in Cancer. Cell *168*, 644–656.

Turashvili, G., and Brogi, E. (2017). Tumor Heterogeneity in Breast Cancer. Front. Med. *4*, 227.

Turner, N., Moretti, E., Siclari, O., Migliaccio, I., Santarpia, L., D'Incalci, M., Piccolo, S., Veronesi, A., Zambelli, A., Del Sal, G., et al. (2013). Targeting triple negative breast cancer: Is p53 the answer? Cancer Treat. Rev. *39*, 541–550.

Turner, P. V, Brabb, T., Pekow, C., and Vasbinder, M.A. (2011). Administration of substances to laboratory animals: routes of administration and factors to consider. J. Am. Assoc. Lab. Anim. Sci. *50*, 600–613.

Ullrich, A., and Schlessinger, J. (1990). Signal transduction by receptors with tyrosine kinase activity. Cell *61*, 203–212.

Unden, A.B., Holmberg, E., Lundh-Rozell, B., Stähle-Bäckdahl, M., Zaphiropoulos, P.G., Toftgård, R., and Vorechovsky, I. (1996). Mutations in the human homologue of Drosophila patched (PTCH) in basal cell carcinomas and the Gorlin syndrome: different in vivo mechanisms of PTCH inactivation. Cancer Res. *56*, 4562–4565.

Ungefroren, H., Sebens, S., Giehl, K., Helm, O., Groth, S., Faendrich, F., Roecken, C., Sipos, B., Lehnert, H., Gieseler, F., et al. (2014). Rac1b negatively regulates TGF-β1-induced cell motility in pancreatic ductal epithelial cells by suppressing Smad signalling. Oncotarget *5*, 277–290.

Upadhyay, S., and Dixit, M. (2015). Role of Polyphenols and Other Phytochemicals on Molecular Signaling. Oxid. Med. Cell. Longev. *2015*, 1–15.

Vaidyanathan, J.B., and Walle, T. (2003). Cellular Uptake and Efflux of the Tea Flavonoid (−)- Epicatechin-3-gallate in the Human Intestinal Cell Line Caco-2. J. Pharmacol. Exp. Ther. *307*, 745–752.

Valastyan, S., and Weinberg, R.A. (2011). Tumor Metastasis: Molecular Insights and Evolving Paradigms. Cell *147*, 275–292.

Vallabhajosula, S.R., Harwig, J.F., and Wolf, W. (1982). Effect of pH on tumor cell uptake of radiogallium in vitro and in vivo. Eur. J. Nucl. Med. *7*, 462–468.

VanRollins, M., Baker, R.C., Sprecher, H.W., and Murphy, R.C. (1984). Oxidation of Docosahexaenoic Acid by Rat Liver Microsome. J. Biol. Chem. *259*, 5776–5783.

Vara, J.Á.F., Casado, E., de Castro, J., Cejas, P., Belda-Iniesta, C., and González-Barón, M. (2004). PI3K/Akt signalling pathway and cancer. Cancer Treat. Rev. *30*, 193–204.

Varinska, L., van Wijhe, M., Belleri, M., Mitola, S., Perjesi, P., Presta, M., Koolwijk, P., Ivanova, L., and Mojzis, J. (2012). Anti-angiogenic activity of the flavonoid precursor 4-hydroxychalcone. Eur. J. Pharmacol. *691*, 125–133.

Vasickova, L., Stavek, P., and Suchanek, P. (2011). Possible effect of DHA intake on body weight reduction and lipid metabolism in obese children. Neuro Endocrinol. Lett. *32 Suppl 2*, 64–67.

Vázquez, R.N., Camargo, A.B., Marchevsky, E.J., and Luco, J.M. (2014). Molecular factors influencing the affinity of flavonoid compounds on P-glycoprotein efflux transporter. Curr. Comput. Aided. Drug Des. *10*, 250–258.

Vidya Priyadarsini, R., Senthil Murugan, R., Maitreyi, S., Ramalingam, K., Karunagaran, D., and Nagini, S. (2010). The flavonoid quercetin induces cell cycle arrest and mitochondria-mediated apoptosis in human cervical cancer (HeLa) cells through p53 induction and NF-κB inhibition. Eur. J. Pharmacol. *649*, 84–91.

Vinogradov, S., and Wei, X. (2012). Cancer stem cells and drug resistance: the potential of nanomedicine. Nanomedicine (Lond). *7*, 597–615.

Viskupič Ová, J., Ondrejovič, M., Turdík, E.Š., and Viskupicˇová, J. (2009). The potential and practical applications of acylated flavonoids. Pharmazie *64*, 355–360.

Viskupicova, J., Ondrejovic, M., and Maliar, T. (2012). Enzyme-Mediated Preparation of Flavonoid Esters and Their Applications. In Biochemistry, D. Ekinci, ed. (InTech), pp. 263–286.

Viskupičová, J., Ondrejovič, M., and Šturdík, E. (2008). Bioavailability and metabolism of flavonoids. J. Food Nutr. Res. *47*, 151–162.

Voduc, K.D., Cheang, M.C.U., Tyldesley, S., Gelmon, K., Nielsen, T.O., and Kennecke, H. (2010). Breast cancer subtypes and the risk of local and regional relapse. J. Clin. Oncol. *28*, 1684–1691.

Vollmer, C.M., Ribas, A., Butterfield, L.H., Dissette, V.B., Andrews, K.J., Eilber, F.C., Montejo, L.D., Chen, A.Y., Hu, B., Glaspy, J.A., et al. (1999). p53 Selective and Nonselective Replication of an E1B-deleted Adenovirus in Hepatocellular Carcinoma. Cancer Res. *59*, 4369–4374.

Voudouri, K., Berdiaki, A., Tzardi, M., Tzanakakis, G.N., and Nikitovic, D. (2015). Insulin-like growth factor and epidermal growth factor signaling in breast cancer cell growth: focus on endocrine resistant disease. Anal. Cell. Pathol. (Amst). *2015*, 975495.

Waikar, S.S., and Bonventre, J. V (2009). Creatinine kinetics and the definition of acute kidney injury. J. Am. Soc. Nephrol. *20*, 672–679.

Walgren, R.A., Karnaky, K.J., Lindenmayer, G.E., Walle, T., and Miller, D. (2000). Efflux of dietary flavonoid quercetin 4'-beta-glucoside across human intestinal Caco-2 cell monolayers by apical multidrug resistance-associated protein-2. J. Pharmacol. Exp. Ther. *294*, 830–836.

Walle, T. (2004). Absorption and metabolism of flavonoids. Free Radic. Biol. Med. *36*, 829–837.

Walle, T. (2009). Methylation of dietary flavones increases their metabolic stability and chemopreventive effects. Int. J. Mol. Sci. *10*, 5002–5019.

Walle, T., Ta, N., Kawamori, T., Wen, X., Tsuji, P.A., and Walle, U.K. (2007). Cancer chemopreventive properties of orally bioavailable flavonoids—Methylated versus unmethylated flavones. Biochem. Pharmacol. *73*, 1288–1296.

Wang, G.L., Jiang, B.H., Rue, E.A., and Semenza, G.L. (1995). Hypoxia-inducible factor 1 is a basic-helix-loop-helix-PAS heterodimer regulated by cellular O2 tension. Proc. Natl. Acad. Sci. U. S. A. *92*, 5510–5514.

Wang, J., Chung, M.H., Xue, B., Ma, H., Ma, C., and Hattori, M. (2010a). Estrogenic and antiestrogenic activities of phloridzin. Biol. Pharm. Bull. *33*, 592–597.

Wang, J., Wei, Q., Wang, X., Tang, S., Liu, H., Zhang, F., Mohammed, M.K., Huang, J., Guo, D., Lu, M., et al. (2016). Transition to resistance: An unexpected role of the EMT in cancer chemoresistance. Genes Dis. *3*, 3–6.

Wang, L., Ling, Y., Chen, Y., Li, C.-L., Feng, F., You, Q.-D., Lu, N., and Guo, Q.-L. (2010b). Flavonoid baicalein suppresses adhesion, migration and invasion of MDA-MB-231 human breast cancer cells. Cancer Lett. *297*, 42–48.

Wang, M., Zhao, J., Zhang, L., Wei, F., Lian, Y., Wu, Y., Gong, Z., Zhang, S., Zhou, J., Cao, K., et al. (2017). Role of tumor microenvironment in tumorigenesis. J. Cancer *8*, 761–773.

Wang, Q.R., Yao, X.Q., Wen, G., Fan, Q., Li, Y.-J., Fu, X.Q., Li, C.K., and Sun, X.G. (2011). Apigenin suppresses the growth of colorectal cancer xenografts via phosphorylation and up-regulated FADD expression. Oncol. Lett. *2*, 43–47.

Wang, S., Zhang, J., Meiwan, C., and Wang, Y. (2013). Delivering flavonoids into solid tumors using nanotechnologies. Expert Opin. Drug Deliv. *10*, 1411–1428.

Wang, S., Su, R., Nie, S., Sun, M., Zhang, J., Wu, D., and Moustaid-Moussa, N. (2014a). Application of nanotechnology in improving bioavailability and bioactivity of diet-derived phytochemicals. J. Nutr. Biochem. *25*, 363–376.

Wang, S., Amato, K.R., Song, W., Youngblood, V., Lee, K., Boothby, M., Brantley-Sieders, D.M., and Chen, J. (2015). Regulation of endothelial cell proliferation and vascular assembly through distinct mTORC2 signaling pathways. Mol. Cell. Biol. *35*, 1299–1313.

Wang, Y., Gapstur, S.M., Gaudet, M.M., Peterson, J.J., Dwyer, J.T., and McCullough, M.L. (2014b). Evidence for an Association of Dietary Flavonoid Intake with Breast Cancer Risk by Estrogen Receptor Status Is Limited. J. Nutr. *144*, 1603–1611.

Warnakulasuriya, S.N., Ziaullah, and Rupasinghe, H.P.V. (2014). Long chain fatty acid acylated derivatives of quercetin-3-o-glucoside as antioxidants to prevent lipid oxidation. Biomolecules *4*, 980–993.

Waterman, P.G. (2007). Roles for Secondary Metabolites in Plants. (Wiley-Blackwell), pp. 255–275.

Watson, C.S., Bulayeva, N.N., Wozniak, A.L., and Finnerty, C.C. (2005). Signaling from the membrane via membrane estrogen receptor-α: Estrogens, xenoestrogens, and phytoestrogens. Steroids *70*, 364–371.

Weedon-Fekjær, H., Romundstad, P.R., and Vatten, L.J. (2014). Modern mammography screening and breast cancer mortality: population study. BMJ *348*, g3701.

Weinberg, R.A. (1995). The Retinoblastoma Protein and Cell Cycle Control Review. Cell *81*, 323–330.

Weinstein, I.B., and Case, K. (2008). The history of Cancer Research: introducing an AACR Centennial series. Cancer Res. *68*, 6861–6862.

Wen, X., and Walle, T. (2006). Methylated Flavonoids Have Greatly Improved Intestinal Absorption and Metabolic Stability. Drug Metab. Dispos. *34*, 1786–1792.

Weng, C.-J., Yen, G.-C., Weng, C.-J., and Yen, G.-C. (2012). Flavonoids, a ubiquitous dietary phenolic subclass, exert extensive in vitro anti-invasive and in vivo anti-metastatic activities. Cancer Metastasis Rev *31*, 323–351.

Westermarck, J., and Kahari, V. (1999). Regulation of matrix metalloproteinase expression in tumor invasion. FASEB J. *13*, 781–792.

Whiteside, T.L. (2008). The tumor microenvironment and its role in promoting tumor growth. Oncogene *27*, 5904–5912.

WHO (2018). World Health Organization | Cancer fact sheet. WHO.

Widmann, C., Gibson, S., Jarpe, M.B., and Johnson, G.L. (1999). Mitogen-Activated Protein Kinase: Conservation of a Three-Kinase Module From Yeast to Human. Physiol. Rev. *79*, 143–180.

Wilczewska, A.Z., Niemirowicz, K., Markiewicz, K.H., and Car, H. (2012). Nanoparticles as drug delivery systems. Pharmacol. Reports *64*, 1020–1037.

Willers, H., Xia, F., and Powell, S.N. (2002). Recombinational DNA Repair in Cancer and Normal Cells: The Challenge of Functional Analysis. J. Biomed. Biotechnol. *2*, 86–93.

Withana, N.P., Blum, G., Sameni, M., Slaney, C., Anbalagan, A., Olive, M.B., Bidwell, B.N., Edgington, L., Wang, L., Moin, K., et al. (2012). Cathepsin B Inhibition Limits Bone Metastasis in Breast Cancer. Cancer Res. *72*, 1199–1209.

Wong, C.C., Akiyama, Y., Abe, T., Lippiat, J.D., Orfila, C., and Williamson, G. (2012). Carrier-mediated transport of quercetin conjugates: Involvement of organic anion transporters and organic anion transporting polypeptides. Biochem. Pharmacol. *84*, 564–570.

Woo, R.A., and Poon, R.Y.C. (2003). Cyclin-dependent kinases and S phase control in mammalian cells. Cell Cycle *2*, 316–324.

Wu, M.Y., and Hill, C.S. (2009). Tgf-beta superfamily signaling in embryonic development and homeostasis. Dev. Cell *16*, 329–343.

Wu, C., You, J., Fu, J., Wang, X., and Zhang, Y. (2016a). Phosphatidylinositol 3-Kinase/Akt Mediates Integrin Signaling To Control RNA Polymerase I Transcriptional Activity. Mol. Cell. Biol. *36*, 1555–1568.

Wu, K.-H., Ho, C.-T., Chen, Z.-F., Chen, L.-C., Whang-Peng, J., Lin, T.-N., and Ho, Y.-S. (2018). The apple polyphenol phloretin inhibits breast cancer cell migration and proliferation via inhibition of signals by type 2 glucose transporter. J. Food Drug Anal. *26*, 221–231.

Wu, Y., Sarkissyan, M., and Vadgama, J. V (2016b). Epithelial-Mesenchymal Transition and Breast Cancer. J. Clin. Med. *5*.

Xiao, J. (2017). Dietary Flavonoid Aglycones and Their Glycosides: Which Show Better Biological Significance? Crit. Rev. Food Sci. Nutr. *57*, 1874–1905.

Xiao, Z.-P., Peng, Z.-Y., Peng, M.-J., Yan, W.-B., Ouyang, Y.-Z., and Zhu, H.-L. (2011). Flavonoids health benefits and their molecular mechanism. Mini Rev. Med. Chem. *11*, 169–177.

Xie, J., Wang, X., and Proud, C.G. (2016). mTOR inhibitors in cancer therapy. F1000Research *5*.

Xu, X., and Dai, H. (2012). Type 2 epithelial mesenchymal transition in vivo: truth or pitfalls? Chin. Med. J. (Engl). *125*, 3312–3317.

Xu, Y., Xin, Y., Diao, Y., Lu, C., Fu, J., Luo, L., and Yin, Z. (2011). Synergistic effects of apigenin and paclitaxel on apoptosis of cancer cells. PLoS One *6*, e29169.

Yadegarynia, S., Pham, A., Ng, A., Nguyen, D., Lialiutska, T., Bortolazzo, A., Sivryuk, V., Bremer, M., and White, J.B. (2012). Profiling flavonoid cytotoxicity in human breast cancer cell lines: determination of structure-function relationships. Nat. Prod. Commun. *7*, 1295–1304.

Yagata, H., Kajiura, Y., and Yamauchi, H. (2011). Current strategy for triple-negative breast cancer: appropriate combination of surgery, radiation, and chemotherapy. Breast Cancer *18*, 165–173.

Yalaza, M., İnan, A., and Bozer, M. (2016). Male Breast Cancer. J. Breast Heal. *12*, 1–8.

Yamagata, K. (2017). Docosahexaenoic acid regulates vascular endothelial cell function and prevents cardiovascular disease. Lipids Health Dis. *16*, 118.

Yamamoto, T., Ebisuya, M., Ashida, F., Okamoto, K., Yonehara, S., and Nishida, E. (2006). Continuous ERK activation downregulates antiproliferative genes throughout G1 phase to allow cell-cycle progression. Curr. Biol. *16*, 1171–1182.

Yan, W.-J., Ma, X.-C., Gao, X.-Y., Xue, X.-H., and Zhang, S.-Q. (2016). Latest research progress in the correlation between baicalein and breast cancer invasion and metastasis. Mol. Clin. Oncol. *4*, 472–476.

Yancopoulos, G.D., Davis, S., Gale, N.W., Rudge, J.S., Wiegand, S.J., and Holash, J. (2000). Vascular-specific growth factors and blood vessel formation. Nat. 2000 4076801.

Yang, J., and Weinberg, R.A. (2008). Epithelial-Mesenchymal Transition: At the Crossroads of Development and Tumor Metastasis. Dev. Cell *14*, 818–829.

Yang, Y., and Yee, D. (2012). Targeting Insulin and Insulin-Like Growth Factor Signaling in Breast Cancer. J. Mammary Gland Biol. Neoplasia *17*, 251–261.

Yang, D., Wang, X.-Y., and Lee, J.H. (2015a). Effects of flavonoids on physical and oxidative stability of soybean oil O/W emulsions. Food Sci. Biotechnol. *24*, 851–858.

Yang, X., Liaw, L., Prudovsky, I., Brooks, P.C., Vary, C., Oxburgh, L., and Friesel, R. (2015b). Fibroblast growth factor signaling in the vasculature. Curr. Atheroscler. Rep. *17*, 509.

Yao, D., Dai, C., and Peng, S. (2011a). Mechanism of the mesenchymal-epithelial transition and its relationship with metastatic tumor formation. Mol. Cancer Res. *9*, 1608–1620.

Yao, L., Romero, M.J., Toque, H.A., Yang, G., Caldwell, R.B., and Caldwell, R.W. (2010). The role of RhoA/Rho kinase pathway in endothelial dysfunction. J. Cardiovasc. Dis. Res. *1*, 165–170.

Yao, N., Chen, C.-Y., Wu, C.-Y., Motonishi, K., Kung, H.-J., and Lam, K.S. (2011b). Novel flavonoids with antiproliferative activities against breast cancer cells. J. Med. Chem. *54*, 4339–4349.

Yerushalmi, R., Gelmon, K.A., Leung, S., Gao, D., Cheang, M., Pollak, M., Turashvili, G., Gilks, B.C., and Kennecke, H. (2012). Insulin-like growth factor receptor (IGF-1R) in breast cancer subtypes. Breast Cancer Res. Treat. *132*, 131–142.

Yin, Y., Sui, C., Meng, F., Ma, P., and Jiang, Y. (2017). The omega-3 polyunsaturated fatty acid docosahexaenoic acid inhibits proliferation and progression of non-small cell lung cancer cells through the reactive oxygen species-mediated inactivation of the PI3K /Akt pathway. Lipids Health Dis. *16*, 87.

Yokomizo, A., and Moriwaki, M. (2006). Effects of Uptake of Flavonoids on Oxidative Stress Induced by Hydrogen Peroxide in Human Intestinal Caco-2 Cells. Biosci. Biotech. Biochem *70*, 1317–1324.

Yokota, J. (2000). Tumor progression and metastasis. Carcinogenesis *21*, 497–503.

Youdim, K.A., Dobbie, M.S., Kuhnle, G., Proteggente, A.R., Abbott, N.J., and Rice-Evans, C. (2003). Interaction between flavonoids and the blood–brain barrier: in vitro studies. J. Neurochem *85*, 180–192.

Yuan, J.P., Wang, L.W., Qu, A.P., Chen, J.M., Xiang, Q.M., Chen, C., Sun, S.-R., Pang, D.-W., Liu, J., and Li, Y. (2015). Quantum Dots-Based Quantitative and In Situ Multiple Imaging on Ki67 and Cytokeratin to Improve Ki67 Assessment in Breast Cancer. PLoS One *10*, e0122734.

Yun, Y.-R., Won, J.E., Jeon, E., Lee, S., Kang, W., Jo, H., Jang, J.-H., Shin, U.S., and Kim, H.-W. (2010). Fibroblast growth factors: biology, function, and application for tissue regeneration. J. Tissue Eng. *2010*, 218142.

Zanger, U.M., and Schwab, M. (2013). Cytochrome P450 enzymes in drug metabolism: Regulation of gene expression, enzyme activities, and impact of genetic variation. Pharmacol. Ther. *138*, 103–141.

Zanger, U.M., Turpeinen, M., Klein, K., and Schwab, M. (2008). Functional pharmacogenetics/genomics of human cytochromes P450 involved in drug biotransformation. Anal. Bioanal. Chem. *392*, 1093–1108.

Zeisberg, M., and Neilson, E.G. (2009). Biomarkers for epithelial-mesenchymal transitions. J. Clin. Invest. *119*, 1429–1437.

Zenger, K., Agnolet, S., Schneider, B., and Kraus, B. (2015). Biotransformation of Flavokawains A, B, and C, Chalcones from Kava ( *Piper methysticum* ), by Human Liver Microsomes. J. Agric. Food Chem. *63*, 6376–6385.

Zetter, B.R. (1998). Angiogenesis and tumor metastasis. Annu. Rev. Med. *49*, 407–424.

Zhang, W., and Liu, H.T. (2002). MAPK signal pathways in the regulation of cell proliferation in mammalian cells. Cell Res. *12*, 9–18.

Zhang, F., Phiel, C.J., Spece, L., Gurvich, N., and Klein, P.S. (2003). Inhibitory phosphorylation of glycogen synthase kinase-3 (GSK-3) in response to lithium. Evidence for autoregulation of GSK-3. J. Biol. Chem. *278*, 33067–33077.

Zhang, G., Panigrahy, D., Mahakian, L.M., Yang, J., Liu, J.-Y., Stephen Lee, K.S., Wettersten, H.I., Ulu, A., Hu, X., Tam, S., et al. (2013). Epoxy metabolites of docosahexaenoic acid (DHA) inhibit angiogenesis, tumor growth, and metastasis. Proc. Natl. Acad. Sci. U. S. A. *110*, 6530–6535.

Zhang, J., Dai, Q., Park, D., and Deng, X. (2016). Targeting DNA Replication Stress for Cancer Therapy. Genes (Basel). *7*, 1–16.

Zhang, L., Pu, Z., Wang, J., Zhang, Z., Hu, D., and Wang, J. (2014). Baicalin inhibits hypoxia-induced pulmonary artery smooth muscle cell proliferation via the AKT/HIF-1α/p27-associated pathway. Int. J. Mol. Sci. *15*, 8153–8168.

Zhang, L., Ren, T., Wang, Z., Wang, R., and Chang, J. (2017). Comparative study of the binding of 3 flavonoids to the fat mass and obesity-associated protein by spectroscopy and molecular modeling. J. Mol. Recognit. *30*, e2606.

Zhang, X., Ibrahimi, O.A., Olsen, S.K., Umemori, H., Mohammadi, M., and Ornitz, D.M. (2006). Receptor specificity of the fibroblast growth factor family. The complete mammalian FGF family. J. Biol. Chem. *281*, 15694–15700.

Zhang, X., Nie, D., and Chakrabarty, S. (2010). Growth factors in tumor microenvironment. Front. Biosci. (Landmark Ed. *15*, 151–165.

Zhang, Y.-J., Gan, R.-Y., Li, S., Zhou, Y., Li, A.-N., Xu, D.-P., and Li, H.-B. (2015a). Antioxidant Phytochemicals for the Prevention and Treatment of Chronic Diseases. Molecules *20*, 21138–21156.

Zhang, Y., Warren, M.S., Zhang, X., Diamond, S., Williams, B., Punwani, N., Huang, J., Huang, Y., and Yeleswaram, S. (2015b). Impact on creatinine renal clearance by the interplay of multiple renal transporters: a case study with INCB039110. Drug Metab. Dispos. *43*, 485–489.

Zhao, J., Davis, L.C., and Verpoorte, R. (2005). Elicitor signal transduction leading to production of plant secondary metabolites. Biotechnol. Adv. *23*, 283–333.

Zhao, R., Xiang, N., Domann, F.E., and Zhong, W. (2009). Effects of selenite and genistein on G2/M cell cycle arrest and apoptosis in human prostate cancer cells. Nutr. Cancer *61*, 397–407.

Zhao, X., Wang, Q., Yang, S., Chen, C., Li, X., Liu, J., Zou, Z., and Cai, D. (2016). Quercetin inhibits angiogenesis by targeting calcineurin in the xenograft model of human breast cancer. Eur. J. Pharmacol. *781*, 60–68.

Zheng, J.-S., Hu, X.-J., Zhao, Y.-M., Yang, J., and Li, D. (2013). Intake of fish and marine n-3 polyunsaturated fatty acids and risk of breast cancer: meta-analysis of data from 21 independent prospective cohort studies. BMJ *346*, 1–10.

Zheng, X., Carstens, J.L., Kim, J., Scheible, M., Kaye, J., Sugimoto, H., Wu, C.-C., LeBleu, V.S., and Kalluri, R. (2015). Epithelial-to-mesenchymal transition is dispensable for metastasis but induces chemoresistance in pancreatic cancer. Nature *527*, 525–530.

Zhou, R., Xu, L., Ye, M., Liao, M., Du, H., and Chen, H. (2014). Formononetin inhibits migration and invasion of MDA-MB-231 and 4T1 breast cancer cells by suppressing MMP-2 and MMP-9 through PI3K/AKT signaling pathways. Horm. Metab. Res. *46*, 753–760.

Zhu, C., Qi, X., Chen, Y., Sun, B., Dai, Y., and Gu, Y. (2011). PI3K/Akt and MAPK/ERK1/2 signaling pathways are involved in IGF-1-induced VEGF-C upregulation in breast cancer. J. Cancer Res. Clin. Oncol. *137*, 1587–1594.

Zhu, J., Zhang, H., Zhu, Z., Zhang, Q., Ma, X., Cui, Z., and Yao, T. (2015). Effects and mechanism of flavonoids from Astragalus complanatus on breast cancer growth. Naunyn. Schmiedebergs. Arch. Pharmacol. *388*, 965–972.

Ziaullah, and Rupasinghe, H.P.V. (2016). Sonochemical enzyme-catalyzed regioselective acylation of flavonoid glycosides. Bioorg. Chem. *65*, 17–25.

Ziaullah, Bhullar, K.S., Warnakulasuriya, S.N., and Rupasinghe, H.P.V. (2013). Biocatalytic synthesis, structural elucidation, antioxidant capacity and tyrosinase inhibition activity of long chain fatty acid acylated derivatives of phloridzin and isoquercitrin. Bioorg. Med. Chem. *21*, 684–692.

Ziegler, U., and Groscurth, P. (2004). Morphological Features of Cell Death. Physiology *19*, 124–128.

van Zijl, F., Krupitza, G., and Mikulits, W. (2011). Initial steps of metastasis: cell invasion and endothelial transmigration. Mutat. Res. *728*, 23–34.

Zorzi, G.K., Caregnato, F., Moreira, J.C.F., Teixeira, H.F., and Carvalho, E.L.S. (2016). Antioxidant Effect of Nanoemulsions Containing Extract of Achyrocline satureioides (Lam) D.C.—Asteraceae. AAPS PharmSciTech *17*, 844–850.

**OXFORD UNIVERSITY PRESS LICENSE**
**TERMS AND CONDITIONS**

Jun 30, 2018

This Agreement between Dalhousie University -- HP Vasantha Rupasinghe ("You") and Oxford University Press ("Oxford University Press") consists of your license details and the terms and conditions provided by Oxford University Press and Copyright Clearance Center.

| | |
|---|---|
| License Number | 4377720329239 |
| License date | Jun 28, 2018 |
| Licensed content publisher | Oxford University Press |
| Licensed content publication | Carcinogenesis |
| Licensed content title | Docosahexaenoic acid-acylated phloridzin, a novel polyphenol fatty acid ester derivative, is cytotoxic to breast cancer cells |
| Licensed content author | Fernando, Wasundara; Coombs, Melanie R.Power |
| Licensed content date | Aug 17, 2016 |
| Type of Use | Thesis/Dissertation |
| Institution name | |
| Title of your work | Thesis |
| Publisher of your work | Dalhousie University |
| Expected publication date | Aug 2018 |
| Permissions cost | 0.00 CAD |
| Value added tax | 0.00 CAD |
| Total | 0.00 CAD |
| Title | Thesis |
| Instructor name | HP Vasantha Rupasinghe |
| Institution name | Dalhousie University |
| Expected presentation date | Aug 2018 |
| Order reference number | Wasu2018Thesis |
| Portions | The six figures and extracts of the text in the thesis format. |
| Requestor Location | Dalhousie University<br>50 Pictou Road<br>Room 219 Cox Building<br><br>TRURO, NS B2N 5E3<br>Canada<br>Attn: Vasantha Rupasinghe |
| Publisher Tax ID | GB125506730 |
| Customer VAT ID | UMCanada |
| Billing Type | Invoice |
| Billing Address | Dalhousie University<br>50 Pictou Road<br>Room 219 Cox Building<br><br>TRURO, NS B2N 5E3<br>Canada<br>Attn: Vasantha Rupasinghe |
| Total | 0.00 CAD |